The role of DEL1 in chondrocyte expansion and mechanotransduction : an investigative study.

Ala Qusous

School of Life Sciences

THE ROLE OF DEL1 IN CHONDROCYTE EXPANSION AND MECHANOTRANSDUCTION – AN INVESTIGATIVE STUDY.

ALA QUSOUS

A thesis submitted in partial fulfilment of he requirements of the University of Westminster for the degree of Doctor of Philosophy

September 2009

Statement of Originality

The accompanying thesis submitted for the degree of Doctor of Philosophy is entitled “The role of DEL1 in chondrocyte expansion and mechanotransduction – an investigative study”. This thesis is based on the work conducted by the author in the Department of Human Health Sciences, University of Westminster during the period between September 2005 and September 2009. All the work recorded in this thesis is original unless otherwise acknowledged in the text or by references.

This work has not been submitted for another degree in this or any other University.

Table of Contents

Table of Figures iv
List of Tables vii
Abbreviations: viii
Acknowledgements xi
Dedications xii
Abstract xiii
1 Introduction 1
1.1 Cartilage and Chondrocytes 2
1.1.1 Structure of Cartilage 2
1.1.2 Chondrocytes and chondrocytic phenotype 6
1.2 Osteoarthritis 12
1.3 In vitro Expansion of chondrocytes 14
1.4 Mechanotransduction and Calcium Homeostasis 18
1.5 Volume Regulation and 2D Expansion 20
1.6 Actin Cytoskeletal Organisation 23
1.7 DEL1 and Integrin Signalling 26
1.7.1 Integrin Signalling 27
1.7.2 Developmental Endothelial Locus 1 (DEL1) 28
1.8 Aims 30
2 Materials and methods 31
2.1 Materials 32
2.1.1 Tissue Culture 32
2.1.2 Molecular Biology 33
2.1.3 Actin Cytoskeleton studies 34
2.1.4 Antibodies used in protein identification experiments 34
2.1.5 Fluorophores 35
2.1.6 Pharmacological and inhibitory reagents 36
2.2 Culture Media and Experimental Salines 37
2.3 Chondrocyte isolation and culture 38
2.4 Expression Profiling of Expanded Chondrocytes 40
2.4.1 RNA extraction, Reverse transcription and Polymerase Chain Reaction (PCR) 40
2.4.2 Gel Densitometery Optimisation 44
2.4.3 GAPD suitability as an internal PCR positive control 44
2.5 Confocal Microscopy 48
2.6 siRNA design 50
2.7 siRNA and transfection 55
2.7.1 Optimisation of MTT viability assay 55
2.7.2 Transfection and transfection efficiency quantification 57
2.7.3 Uptake and localisation of siRNA 62
2.8 Actin organisation 64
2.9 Volume, cellular dimensions and Sphericity of chondrocytes 68
2.9.1 Optimisation of Imaris Isosurface Feature using beads 68

2.9.2 Chondrocyte Cell Dimesion and Volume Acquisition 70
2.9.3 RVI experiments 72
2.10 Calcium imaging 73
2.11 Chondrocyte Attachment Assay 77
2.12 Cellular protein isolation and analysis 78
2.12.1 Intracellular cell signal proteins 78
2.12.2 Extracellular DEL1 protein isolation 78
2.12.3 SDS-PAGE 79
2.12.4 Western Blot 80
2.12 Statistical Analysis 82
3 Experimental Chapter: The influence of chondrocyte expansion on phenotype, morphology and dedifferentiation. 83
3.1 Chapter introduction 84
Aims of Experimental Chapter 86
3.2 Results 88
3.2.1 Expansion and Growth Rates 88
3.2.2 Morphology, shape and volume of freshly isolated and expanded chondrocytes 93
3.2.3 Phenotype and expression profiling of cultured chondrocytes 99
3.2.4 The regulation of actin cytoskeletal organisation upon 2D culture 102
3.3 Chapter Discussion 107
4 Experimental Chapter: The mechanotransduction properties of 2D cultured chondrocytes. 113
4.1 Chapter Introduction 114
4.1.1 RVI 114
4.1.2 Calcium Signalling 115
Aims of Experimental Chapter 116
4.2 Results 117
4.2.1 Regulatory volume increase (RVI) in freshly isolated and 2D expanded chondrocytes 117
4.2.2 Calcium mechanotransduction and Homeostasis 122
4.3 Chapter Discussion 133
5 Experimental Chapter: The role of DEL1 in 2D chondrocytes expansion 140
5.1 Chapter introduction 141
Aims of Experimental Chapter 143
5.2 Results 144
5.2.1 The expression level of DEL1 in response to 2D culture of chondrocytes 144
5.2.2 DEL1 knockdown using RNAi technology 149
5.2.3 The role of DEL1 knockdown on chondrocytic phenotype, morphology and mechanotransduction 152
5.3 Chapter Discussion 170
6 Experimental Chapter: The molecular signalling pathway of DEL1 in chondrocytes. 175
6.1 Chapter Introduction 176
Aims of Experimental Chapter 178
6.2 Results 179

6.2.1 The role of DEL1 on Akt activation signalling 179
6.2.2 The expression and role of Twist in 2D expansion of chondrocytes 183
6.2.3 The dependency of Twist expression on DEL1 level in 2D culture of chondrocytes 185
6.2.4 The feedback effect of Twist and SOX9 on DEL1 expression .. 189
6.3 Chapter Discussion 199
7 Discussion, Conclusion and Future Work 203
7.1 Quantification of changes in phenotypic markers in response to 2D culture 204
7.2 The role of DEL1 in the regulation of chondrocyte phenotype 207
7.3 Summary and concluding remarks 209
8 References and bibliography 214

Table of Figures

Figure 1.1: Schematic diagram of the structure of the extracellular matrix (ECM). 5
Figure 1.2: Representative image of bovine articular cartilage..... 9
Figure 1.3: Morphology of freshly isolated and 2D-cultured chondrocytes..... 17
Figure 1.4: Representative Diagram of transporters involved in RVI..... 22
Figure 1.5: Actin organisation of freshly isolated and 2D-cultured chondrocytes 25
Figure 2.1: The linear relationship between the band intensity and size vs. the amount of DNA present..... 45
Figure 2.2: The level of expression of Glyceraldehyde 3-phosphate dehydrogenase (GAPD) during culture 46
Figure 2.3: A representative image of an ethidium bromide-stained DNA gel ... 47
Figure 2.4: The natural anti-viral mechanism that led to the discovery of RNAi. 51
Figure 2.5: Linear relationship between the absorbance of reduced MTT crystals and the total cell number. 56
Figure 2.6: Transfection efficiency of freshly isolated chondrocytes (P0)..... 59
Figure 2.7: Transfection efficiency monolayer expanded chondrocytes after 9 days in culture (P1) 60
Figure 2.8: Transfection efficiency monolayer expanded chondrocytes after 14 days in culture (P2). 61
Figure 2.9: Confocal Z-stack series of images of chondrocytes after 48 hours of transfection with 10nM FAM-labelled negative control siRNA (green) and 3μl/ml of HiPerfect. 63
Figure 2.10 Representative diagram of fluorescence of actin-phalloidin-alexa 488 complexes across standardised cellular dimensions..... 66
Figure 2.11: Representative mean fluorescence of phalloidin-alexa 488 across standardised cell diameter 2D cultured chondrocytes. 67
Figure 2.12: Apparent volume of beads analysed using Imaris 6.3.1 using 10-90% threshold. 69
Figure 2.13: Illustrative diagram of isosurface objects created using Imaris (Bitplane) at 10% and 60% threshold. 71
Figure 2.14: The effects of fluid flow on calcium signalling..... 75
Figure 2.15: Effects of Ionomycin and negative control DMSO solution on $[Ca^{2+}]_i$ in freshly isolated chondrocytes. 76
Figure 3.1: Growth curve of bovine articular chondrocyte upon in vitro culture. 90
Figure 3.2: Viability assay in response to in vitro 2D culture. 91
Figure 3.3: Morphology of freshly isolated and 2D cultured chondrocytes as seen under confocal microscopy. 96

Figure 3.4: Cellular dimensions and sphericity of chondrocytes as quantified using Imaris Isosurface Surpass utility. 97
Figure 3.5 The expression profiling of chondrocytes before and throughout culture 101
Figure 3.6: Actin organisation in freshly isolated and 2D cultured chondrocytes as seen with confocal microscopy. 103
Figure 3.7: The number of actin striation units across the cell cytoplasm of freshly isolated and 2D cultured chondrocytes, ... 104
Figure 3.8: Percentage of cortical and filamentous actin structures in freshly isolated and 2D cultured chondrocytes. 106
Figure 3.9: Model of the significant changes ($p<0.05$) in phenotypic markers in response to 2D culture. 112
Figure 4.1: The capacity of freshly isolated and 2D expanded chondrocytes to exhibit RVI in response to hyperosmotic conditions. 118
Figure 4.2: Box plot of 2D expanded chondrocytes against percentage volume recovery at time 20 minutes. 120
Figure 4.3: The effect of REV5901 loading on freshly isolated and 2D cultured chondrocytes. 123
Figure 4.4: Effect of extracellular calcium removal on REV5901-induced calcium rise in freshly isolated and 2D cultured chondrocytes. 125
Figure 4.5: $[Ca^{2+}]_i$ rise inhibition profiling in freshly isolated and 2D cultured chondrocytes. 128
Figure 4.6: Changes in $[Ca^{2+}]_I$ in response to REV5901 loading in the presence of pharmacological inhibitors to G-protein downstream elements. 130
Figure 4.7: Representative diagram of currently known intracellular calcium signalling pathways. 139
Figure 5.1: Changes in the expression of DEL1 in chondrocytes upon 2D culture. 146
Figure 5.2: Changes in DEL1 and collagen expression ratio within the first 9 days of 2D culture. 147
Figure 5.3: Western blot image of chondrocyte supernatant assayed for DEL1 protein. 148
Figure 5.4: The transience inhibition effect of anti-DEL1 siRNA transfection on DEL1 mRNA levels. 150
Figure 5.5: Percentage attachment of freshly isolated and 2D cultured chondrocytes. 155
Figure 5.6: Percentage attachment of chondrocytes against time in control and Del(-)/P1 chondrocytes. 156
Figure 5.7: Changes in chondrocyte morphology and cellular dimension in response to long-term DEL1 knockdown. 160
Figure 5.8: Changes in chondrocyte expression battery in response to DEL1 knockdown. 162
Figure 5.9: Actin organisation upon DEL1 knockdown 164
Figure 5.10: RVI in DEL1(-)/P1 chondrocytes in response to hyperosmotic challenge. 166
Figure 5.11: Contribution of store-mediated calcium release to REV5901-induced calcium rise. 168

Figure 5.12: The sensitivity of DEL1(-) chondrocytes to calcium channel inhibitors. 169
Figure 6.1: Changes in Akt phosphorylation and activity upon 2D culture. 180
Figure 6.2: The effect of DEL1 knockdown on the phosphorylation and activity of Akt. 182
Figure 6.3: The level of Twist expression in freshly isolated and 2D cultured chondrocytes. 184
Figure 6.4: The effect of DEL1 knockdown on the expression of Twist in P1 chondrocytes. 186
Figure 6.5: The effect of pharmacological inhibition of β-catenin on Twist expression. 188
Figure 6.6: The effect of BMP2 treatment on the expression of SOX9, Twist and DEL1. 191
Figure 6.7: Changes in the expression of collagen molecules in response to BMP2 treatment in P3 chondrocytes. 192
Figure 6.8: Twist expression upon knockdown using anti-Twist siRNA. 194
Figure 6.9: Changes in Expression of collagens in P3 chondrocytes in response to Twist knockdown using anti-Twist siRNA. 197
Figure 6.10: The effect of Twist knockdown on the expression of DEL1 and SOX9. 198
Figure 6.11: The proposed pathway of action of DEL1. 202
Figure 7.1: New Analysis tool for the study of filamentous actin organisation. 213

List of Tables

Table 1.1: Summary of the properties of the zones of mature articular cartilage. 10
Table 1.2: The effect of various stimuli on the regulation of ECM in chondrocytes. 11
Table 1.3: Summary of chondrocytic phenotypes in relation to the types of collagen synthesised. 16
Table 2.1: Tissue culture reagents. 32
Table 2.2: Reagents used in molecular biology studies. 33
Table 2.3: Reagents used to study the actin cytoskeleton. 34
Table 2.4: Reagents used to study the actin cytoskeleton. 34
Table 2.5 Fluorophores used. 35
Table 2.6: Pharmacological agents used in calcium signalling determination. 36
Table 2.7: Sequences of PCR primer pairs 42
Table 2.8: Steps involved in Polymerase Chain Reaction (PCR) amplification. 43
Table 2.9: Fluorophores used in confocal microscopy for imaging and cell volume calculation. 49
Table 2.10: Criteria of the rational siRNA design 53
Table 2.11: Sequences of siRNA sequences used in knockdown experiments. 54
Table 3.1: Range of seeding densities used in the literature for in vitro expansion of chondrocytes. 87
Table 3.2: Summary of culture properties of chondrocytes cultured at literature-based seeding densities. 92
Table 3.3: Cell volume changes in freshly isolated and 2D cultured chondrocytes as acquired by Imaris and calculated mathematically. 98
Table 4.1: Volume regulatory properties of freshly isolated and 2D cultured chondrocytes. 121
Table 4.2: Impact of loading of various solutions on $[Ca^{2+}]_i$ levels. 132
Table 5.1: Growth rate properties of P1 and DEL1(-)/P1 chondrocytes. 151
Table 5.2: Summary of attachment properties of freshly isolated and 2D cultured chondrocytes. 157
Table 5.3: Summary of changes observed upon DEL1 knockdown and possible mode of action. 174
Table 7.1: Summary of the properties of differentiated, mesodifferentiated and dedifferentiated chondrocytes as defined using key markers of phenotype. 212

Abbreviations:

$[Ca^{2+}]_i$:	intracellular calcium
$[Na^{+}]_e$:	Extracellular sodium
2D:	Two-Dimensional
3D:	Three-Dimensional
Akt:	v-Akt murine thymoma viral oncogene homolog 1
AM:	Acetyloxymethyl
BMP-6:	Bone Morphogenetic Protein – 6
bp:	base pair
BPS:	Basic Physiological Saline
CD:	Cluster of differentiation
cDNA:	complementary Deoxyribonucleic Acid
CLSM:	Confocal Laser Scanning Microscope
col1:col2:	Ratio of collagen I to collagen II
DAG:	Diacylglycerol
DEL1:	Developmental Endothelial Locus 1
DEPC:	Diethylpyrocarbonate
DMEM:	Dulbecco's Modified Eagle Medium
DMSO:	Dimethyl Sulphoxide
dNTP:	deoxyribonucleotides
ds:	double stranded
dsRNA:	Double stranded Ribonucleic Acid
DZ:	Deep Zone
ECM:	Extracellular Matrix
EDIL:	EGF-like repeats and discoidin I-like domains
EDTA:	ethylenediaminetetraacetic acid
EGF:	Endothelial Growth Factor
EGTA:	ethylene glycol tetraacetic acid
NCX:	Epithelial Sodium Channel
FAM:	5'-carboxyfluorescein

FCS: Foetal Calf Serum

FnR: Fibronectin Receptor

GAG: Glycosaminoglycan

GAPD: Glyceraldehyde 3-phosphate dehydrogenase

GC: Guanine-Cytosine

GPCR: G-protein Coupled Receptor

HD: High Density

$(I-I_B).A$: Difference between Intensity and Background multiplied by Area

IP3: Inositol triphosphate

LB: Latrunculin B

LD: Low Density

MD: Intermediate Density

mOsm: Milliosmole/Kg H_2O

MACI: Matrix-induced autologous chondrocyte implantation

mRNA: messenger Ribonucleic Acid

MSC: Mesenchymal Stem Cells

MTT: 3-(4,5-Dimethylthiazol-2-yl)-2,5-diphenyltetrazolium bromide

MZ: Mid Zone

NCBI: National Centre for Biotechnology Information

NHE: Na^+/H^+ antiporter

NKCC1: Sodium/potassium/chloride transporter member 1

nt: nucleotide

OA: Osteoarthritis

P/S: Penicillin Streptomycin Solution

PBS: Phosphate Buffer Saline

PCR: Polymerase Chain Reaction

PGs: Proteoglycans

PCR: Polymerase Chain Reaction

PI5K: Phosphatidylinositol 5-kinase

PIP2: Phosphatidylinositol (4,5)-biphosphate

PIP3: Phosphatidylinositol (3,4,5)-triphosphate

PKC:	Protein Kinase C
PLCβ3:	Phosspholipase C Beta 3
REV5901:	Alpha-pentyl-3-(2-quinolinylmethoxy)-benzene-methanol
RGD:	Arginine-Glycine-Aspartic acid
RISC:	RNA-induced Silencing Complex
RNAi:	Ribonucleic Acid Interference
RNase A:	Ribonuclease A
RT-:	Reverse Transcriptase
RVD:	Regulatory Volume Decrease
RVI:	Regulatory Volume Increase
SACC:	Stretch-activated Cation Channel
SDS:	sodium dodecyl sulphate
siRNA:	Small Interfering Ribonucleic Acid
SLC12A2:	Solute Carrier Family 12 Member 2, (NKCC1)
SLC16A3:	Monocarboxylic acid transporter member 3
SOX9:	Sex determining region Y-box 9
StU:	Striation Unit
SZ:	Superficial Zone
t½:	Half the time required for chondrocytes to recover 100% volume
TBE:	Tris-Borate-EDTA
TBS:	Tris-Buffered Saline
TBS/T:	Tris-Buffered Saline containing Tween
TE:	Tris-EDTA
TGF-β:	Transforming Growth Factor Beta
Tm:	Mid temperature
U73122:	1-[6-[[(17β)-3-methoxyestra-1,3,5(10)-trien-17-yl]amino]hexyl]-1H-pyrrole-2,5-dione
VSAC:	Volume-sensitive anion channel

Acknowledgements

I would like to acknowledge my director of studies Dr Mark J P Kerrigan for his exceptional support and assistance in what must have been the longest five years of his academic career. Thank You, Dr Kerrigan and sorry about the drama. My eternal gratitude goes out to Mr Andrew Stanton for his financial and moral support.

Special thanks to Prof Tajalli Keshavarz who welcomed me with open arms first as a MSc postgraduate, later as a PhD student and most recently as my supervisor. My lifelong gratitude goes to the Cavendish Campus and the School of Biosciences for having awarded me a fee waiver to pursue my career. Many thanks to Prof Simon Jarvis, Prof Frank Hucklebridge, Prof Jane Lewis, Dr Sanjiv Rughooputh, Dr Pamela Greenwell, Ms Jennifer Mackenzie, Ms Vanita Amin and all the members of staff at the School of Life Sciences.

I would like to acknowledge all my friends and colleagues at the University of Westminster over the years both in Osteoarthritis Research Laboratory and otherwise. In chronological order to name but a few, Mr Headley Williams and Mrs Anna Wingate (my first friend in the UK), Mrs Corinne Geewan who shadowed me in my early months, Mrs Claire Cove for the ‘bestest’ lunches and tea breaks, Ms Hanna Everitt, Ellie Parker, Yanitsa Nedelcheva and Magdalena Kaneva.

Finally special thanks to my dear friends: Marcel Thanassack, Scavo Parker, Nicky Fernandez Reiss, Auntie Sofie, Faisal Atmeh, Azza Shoaibi, Hazem Jabaji, Bonnie Bell, Russell McLean, Melinda Molnar, Nertila Beshi, Regan Andrew, Ewelina Skowronek and every at T&G Covent Garden and Ku Bar for the best fun!

Dedications

I would like to dedicate this thesis to my dear Mother, my best friend, the greatest mother and the strongest woman in the world.

I also dedicate this work to Dr Noor Qusous and The Badra's.

In living memory of Stephen Robert Parker.

Abstract

Matrix-induced autologous chondrocyte implantation offers a potential cure for joint disease and is currently challenged by loss of differentiated phenotype upon culture. To investigate the mechanism of dedifferentiation, chondrocytes were cultured at low density ($1x10^4$cell/cm^2) and subcultured on days 9 (P1), 14 (P2) and 21 (P3). A loss of a differentiated phenotype was observed in P1 with a reduction in sphericity from 0.72±0.02 to 0.52±0.03. Changes in cellular dimensions in response to 2D culture were additionally recorded with an increase and decrease in cell length and depth, respectively, yielding an increase in cell volume from 474.72±32.08 to 725.20±35.55μm^3. Furthermore, the effect of 2D culture-induced dedifferentiation on mechanotransduction was investigated in response to a hyperosmotic challenge whereby regulatory volume increase (RVI) was only observed in 2D cultured chondrocytes with linear volume recovery rates in P1 and biphasic RVI in P2 and P3. Similarly, a REV5901-induced intracellular calcium rise via PLCβ and PKC was shown to be sensitive to extracellular sodium ($[Na^+]_e$) in freshly isolated and Gd^{3+} in 2D cultured chondrocytes. A 2.70±0.63-fold increase in type I collagen (col1) expression was observed in P1 chondrocytes, whereas a 1.58±0.43-fold increase in type II collagen (col2) was followed by a decline to baseline levels upon further culture. A transient rise in the chondrocytic transcription factor Sox9 and Developmental Endothelial Locus 1 (DEL1) was observed in P1 chondrocytes, suggesting the existence of a third phenotype termed 'mesodifferentiated*' and a potential role for DEL1 in chondrocyte dedifferentiation. DEL1 knockdown by RNA interference (RNAi) promoted a differentiated phenotype as characterised by a decrease in cell volume, reduced col1 expression, inhibition of RVI and elevated sensitivity to $[Na^+]_e$. DEL1 knockdown was shown to inhibit P1-associated Akt phosphorylation and the expression of the dedifferentiation transcription factor Twist, additionally reduced in the presence of R-Etodolac. The induction of Sox9 expression using Bone Morphogenetic Protein 2 and Twist knockdown using RNAi enhanced the expression of DEL1, suggesting DEL1 regulation of dedifferentiation by a feedback signal previously unreported.

* Greek, from mesos, *middle*

1 Introduction

Osteoarthritis (OA) is a common joint disease that leads to disability with six million working days lost in the UK and a total estimated cost totalling £5.5 billion (Peach *et al.*, 2005). An emerging treatment for OA is cartilage replacement where cartilage explants are removed from patients, the chondrocytes isolated and then subsequently grown in 2D (expansion) monolayer culture medium *in vitro* (Giannoni *et al.*, 2005; Sgaglione, 2005; Tallheden *et al.*, 2005). An important factor when working with articular cartilage is the regulation of the cell phenotype whereby as a result of monolayer culture, chondrocytes undergo dedifferentiation and acquire a fibroblast-like phenotype (Benya & Shaffer, 1982b). Changes in cell shape, actin reorganisation, regulatory volume increase (RVI), calcium homeostasis, and key genes expression was investigated in response to 2d culture to further our understanding of dedifferentiation.

1.1 Cartilage and Chondrocytes

1.1.1 Structure of Cartilage

Articular Cartilage is a dense connective tissue which provides a scaffold for bone deposition and smooth surfaces for the movement of articulating bones (Stockwell, 1978; Buckwalter & Mankin, 1998; Gray, 2000). Cartilage, in conjunction with synovial fluid, provides protection against both compressive and dynamic loading as a consequence of joint use by dissipating the weight over a larger surface area (Stockwell, 1971b, c; Gray, 2000). Cartilage has a glassy appearance with a white colour (Stockwell, 1979; Hall, 1998b). Cartilage is comprised of an extracellular matrix (ECM) synthesised by the only resident cell type chondrocytes, which account for ~10% of the tissue volume as measured in adult human hip cartilage (Stockwell, 1971a; Byers *et al.*, 1977). In response to physio-chemical environment, chondrocytes maintain a balance of anabolism and catabolism of a limited number of ECM macromolecules thus

maintaining and adapting the ECM to the forces against it (Holmes *et al.*, 1988; Urban, 1994; Archer & Francis-West, 2003; Lin *et al.*, 2006).

The ECM of articular cartilage is comprised principally of collagen type II, which is the most abundant form of collagen in healthy adult cartilage (Matyas *et al.*, 1995; Nalin *et al.*, 1995), and proteoglycan (PG). PGs contribute to the ability of cartilage to resist compression (Urban, 1994) and are composed of chains of Glucosaminoglycans (GAG; mainly chondroitin sulphate and keratan sulphate) attached to aggrecan core protein (Hughes, 1997). PGs are further interlinked by a backbone of hyaluronic acid, which is in turn bound to cluster of differentiation 44 (CD44) on the chondrocyte cell membrane, forming clusters in the order of $5x10^4$ to $5x10^5$ kDa (Figure 1.1). Due to the negative charge on their carboxyl and sulphonic groups, PGs have a high affinity to cations (mainly, sodium and to a less extent potassium and calcium) and therefore contribute to a relatively higher ionic strength of cartilage (310-370 mOsm) compared to that of other body fluids (Stockwell, 1991b; Urban, 1994; Wilkins *et al.*, 2000).

Type II Collagen is a homotrimeric protein with a characteristic Gly-X-Y repeat forming right handed helical fibres fibres, 30-200nm in diameter. Collagen type I is expressed in smaller quantities throughout cartilage and more abundantly in bone-cartilage surface (Roberts, 1985) forming a heterotrimeric helix. Conversely, Type IX collagen is a highly glycosylated non fibular protein that interlinks type II collagen fibres, thereby forming a complex mesh that 'traps' chondrocytes and prevents maximal hydration of PGs (Stockwell, 1991a; Eyre *et al.*, 2002). This mesh is able to tolerate high pressures that arise during load bearing, sometimes as high as 0.2MPa in the adult human hip (Hodge, 1986).

As well as structural proteins, cartilage comprises of other proteins involved in the regulation of the ECM. Fibronectin, Anchorin and Cartilage Oligomeric

Proteins (COMP) are involved in linking extracellular fibres to the chondrocyte cell surface and are thus implicated in the maintenance and repair of ECM (Roberts, 1985). COMP interacts with type II collagen by its third epithelial growth factor (EGF) repeat (Tan *et al.*, 2009) where mutations can cause osteochondrodysplasias pseudoachondroplasia (Song *et al.*, 2003; Tufan *et al.*, 2007), thereby suggesting a role for COMP in cartilage development.

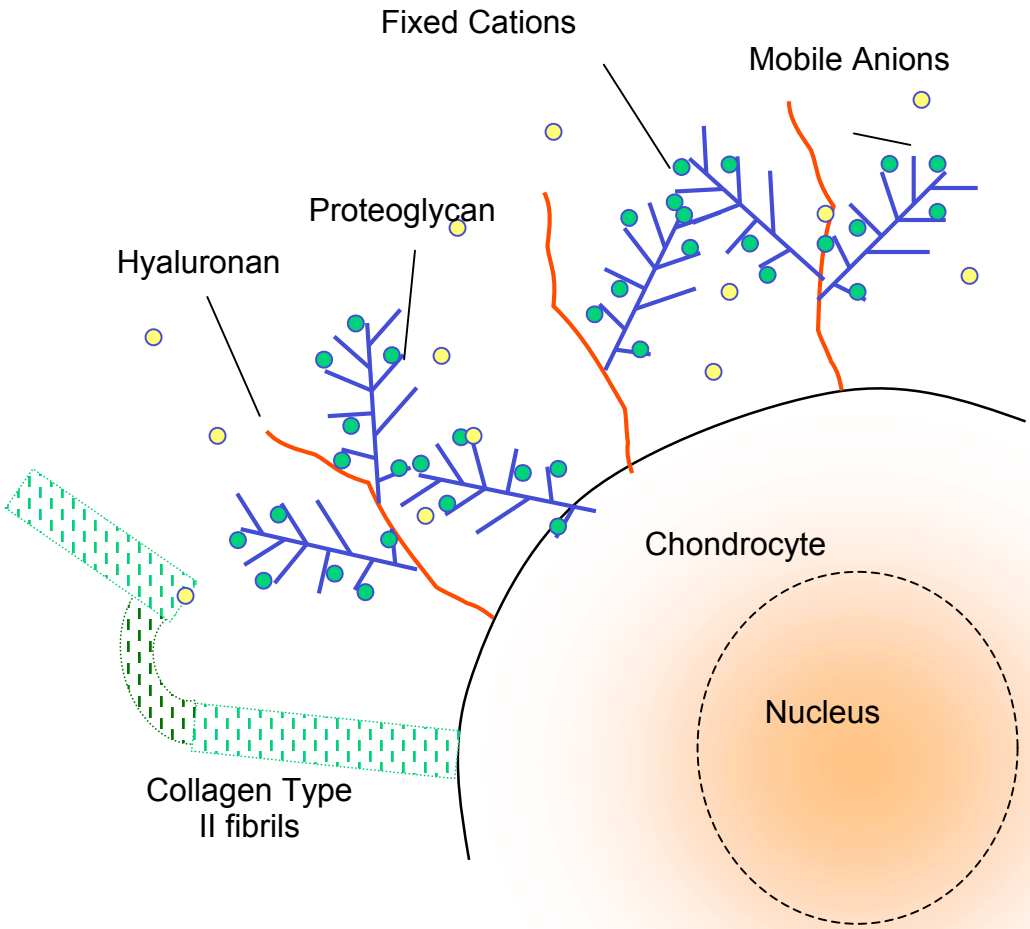

Figure 1.1: Schematic diagram of the structure of the extracellular matrix (ECM).

The extracellular matrix (ECM) of cartilage is mainly composed of proteoglycans (PGs) and collagen fibrils. PGs branch from hyaluronan molecules that extend from the chondrocyte cell surface. Negatively charged glycosaminoglucan chains of PGs attract cations and cause water retention in the tissue. Collagen Type II fibrils are interlinked by collagen Type IX fibrils and together they form a mesh that traps PGs. Adapted from Urban, 1994.

1.1.2 Chondrocytes and chondrocytic phenotype

Chondrocytes are the only resident cells found in cartilage at a density of up to 10,000 chondrocytes/mm^3 in human adult femoral head cartilage and are responsible for the maintenance of the cartilage ECM (Stockwell, 1971). During embryogenesis, chondrocyte are extensively distributed within the foetus and are responsible for the longitudinal bone growth within the epiphyseal growth plate (Hall & Miyake, 1992; Archer & Francis-West, 2003). Chondrocytes differentiate from colony-forming unit-fibroblast, and later mesenchymal stem cells (MSC) which appear as condensations between 10-12 days postcoitum and initially express collagen type I prior to differentiation into foetal chondrocytes (Lui *et al.*, 1995).

In vivo, three distinct chondrocytic phenotypes have been observed in healthy tissue; foetal in embryonic tissue, hypertrophic in immature, and differentiated in mature cartilage. During embryogenesis, mesenchymal stem cells differentiate into foetal chondrocytes, which are arranged in two distinct zones termed reserve and proliferative zones (Ryan & Sandell, 1990). Chondrocytes in the reserve zone possess a volume of $1500\pm240\mu m^3$, are uniform yet compactly arranged, and occur singly or in pairs (Melrose *et al.*, 2008). Conversely, chondrocytes in the proliferative zone are flat and well divided into longitudinal columns with exclusive mitotic activity (Ballock & O'Keefe, 2003). Foetal chondrocytes switch to the expression of chondrocyte specific type II collagen (Ryan & Sandell, 1990; Sandell *et al.*, 1991) in addition to type IX and XI collagens, while levels of type I collagen expression are significantly inhibited (Luo *et al.*, 1995).

During postnatal bone growth, foetal chondrocytes in growth plates proceed through a differentiation pathway characterised by cellular enlargement (chondrocyte hypertrophy) and resulting in terminal differentiation (Drissi *et al.*, 2005). Hypertrophic chondrocytes increase in volume by a factor ~10x

compared to foetal chondrocytes reaching a volume of 17,500±425μm^3 (Bohme *et al.*, 1995; Ng *et al.*, 1997; DeLise *et al.*, 2000), primarily as a result of water imbibition (Buckwalter *et al.*, 1986), and express high levels of collagen X, the role of which is to facilitate calcium deposition within the matrix (Alvarez *et al.*, 2001).

Differentiated (mature) chondrocytes synthesise and maintain the ECM, and are therefore 'maturationally arrested' and do not exhibit proliferation potential (Sailor *et al.*, 1996; Buckwalter & Mankin, 1998; Drissi *et al.*, 2005). As cartilage is avascular in nature, chondrocytes operate and maintain low oxygen tension to outgrow fibroblasts, and rely on nutrients obtained from the articular surface by diffusion (Rajpurohit *et al.*, 1996) as well as signals obtained by the extracellular ionic environment and ECM interactions (Stockwell, 1991a). Chondrocytes produce PGs and types II, III, IX and XI collagens, degrading the ECM by the secretion of collagenases and gelatinases and inhibit blood vessel invasion by synthesis of tissue inhibitor metalloproteinases (Stockwell, 1991a).

A cross section of mature cartilage (Figure 1.2) highlights the presence of four zones; superficial zone (SZ), middle zone (MZ), deep zone (DZ) and calcified zone (Stockwell, 1991a). In the SZ, collagen fibres are densely packed around flattened chondrocytes, ellipsoid in shape and are approximately 2-3μm in diameter with a volume of 454±18μm^3, whereas In the MZ, chondrocytes are spherical (sometimes found in pairs) with a lightly larger volume of 553±15μm^3 and are embedded in randomly arranged collagen fibres forming a 'Basket Weave' structure (Table 1.1). The DZ is characterised by columns of ellipsoid cells possessing a volume of 805±79μm^3 distributed between radially oriented collagen fibres that extend into the calcified zone (Stockwell, 1991a; Hall, 1998b).

The transcription factor SOX9 is a key regulator of chondrocyte differentiation in both mesenchymal stem cells and foetal chondrocytes (Ng *et al.*, 1997; DeLise *et al.*, 2000) and the expression level remains elevated in differentiated chondrocytes accounting to 20% of the expression of Glyceraldehyde 3-phosphate dehydrogenase (GAPD) (Haag *et al.*, 2008). The expression of various chondrocyte-specific genes including type II collagen is tightly regulated by chondrocyte-specific SOX9 transcription factor (de Crombrugghe *et al.*, 2000) and mutations in SOX9 lead to skeletal malformation syndromes including campomelic dysplasia (Sock *et al.*, 2003).

Chondrocytes are able to 'sense' and respond to external factors and regulate matrix synthesis to the forces and stimuli perceived, some of which will be introduced in following sections (Table 1.2).

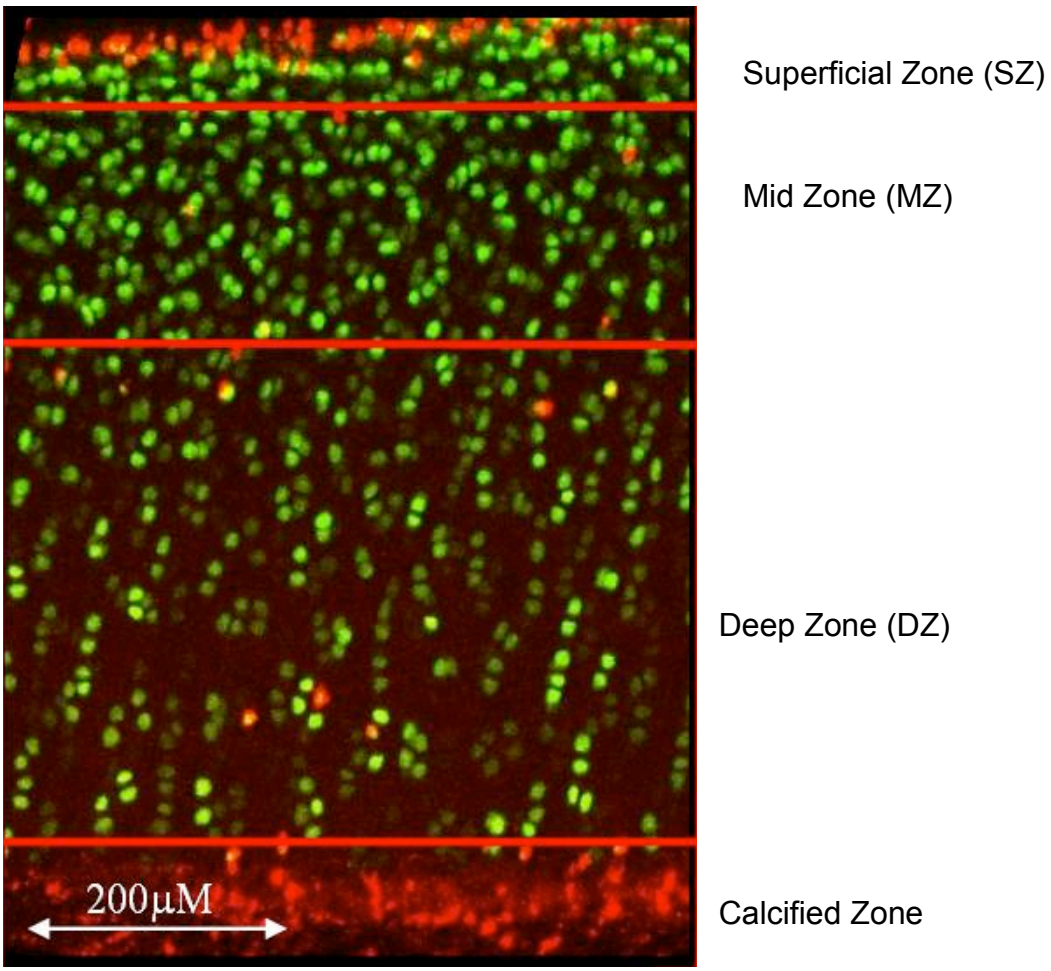

Figure 1.2: Representative image of bovine articular cartilage.

Cartilage explant from bovine metacarpal and metatarsal pharyngeal joints were isolated asceptically and loaded with 5μM calcein-AM (green) and propidium iodide (red) and subsequently imaged using confocal laser scanning microscopy. Chondrocytes in Superficial Zone are aligned parallel to the cartilage surface, whereas in the Mid Zone and Deep Zone, chondrocytes are found in pairs or in columnar stacks of 4 perpendicular to the articular surface, respectively. Image acquired by Dr Mark J. P. Kerrigan, adapted with permission.

Table 1.1: Summary of the properties of the zones of mature articular cartilage.

Chondrocytes in the three zones of cartilage appear to possess distinctly different characteristics. Chondrocytes in the Superficial Zone (SZ) are embedded in tangentially arranged collagen fibres whereas in the Mid Zone (MZ), chondrocytes are larger in diameter and thus volume, found in pairs and embedded in a 'basketweave' structure of collagens. In the Deep Zone (DZ), however, chondrocytes are still larger than in the MZ and arranged in collagen fibres with an orientation perpendicular to the articular surface {Hall, 1998; Urban, 1994; Maroudas, 1980; Bush and Hall, 2001).

Zone	Chondrocyte morphology	Volume (μm^3)	Cellular Density (%)	Collagen orientiation	Osmolarity (mOsm)
SZ	Single, ellipsoid	454±18	17%	Tangential, tight fibrils mainly aligned with tangential stress	310 – 370
MZ	Single or in pairs, ovoid	553±15	53%	Radial random 'basketweave'	-
DZ	Small groups, short columns of 2-6 cells	805±79	30%	Perpindicular to articular surface	370 - 480

Table 1.2: The effect of various stimuli on the regulation of ECM in chondrocytes.

Chondrocytes are able to respond to chemical and mechanical stimuli by the regulation of the Extracelullar Matrix. In response to Vitamin D3, ascorbic acid or mechanical loading there was an upregulation of aggrecan synthesis, whereas incubation with Interleukin 1β or in hypo-osmotic condtions suppressed the expression of collagen and proteoglycans.

Regulator	Effect	References
Vitamin D3	Stimulation of proteoglycan synthesis	Harmand *et al.*, 1984; Horton *et al.*, 1991
Ascorbic Acid	Expression of type X collagen	Hering *et al.*, 1994
Thyroid hormone	Increase in alkaline phophatase synthesis	Williams *et al.*, 1998
Mechanical loading	Stimulation of aggrecan synthesis	Buschmann *et al.*, 1996; Valhmu *et al.*, 1998
Interleukin 1β	Suppression of collagen and proteoglycan synthesis	Ikebe *et al.*, 1988; Tyler & Benton, 1988; Yaron *et al.*, 1989
Hypo-osmotic conditions	Suppression of matrix synthesis	Hopewell & Urban, 2003

1.2 Osteoarthritis

Osteoarthritis (OA; or more accurately yet less commonly referred to as Osteoarthrosis) is a common joint disease that leads to disability. In the UK, 7 million people are diagnosed with OA (Arthritis Research Campaign website), and 206 million working days were lost in 1999-2000 with a total estimated cost of £5.5 billion (Peach *et al.*, 2005). Symptoms of OA include pain, stiffness and in severe cases loss of joint function (Bulstrode, 2002).

Cartilage can be damaged by bone remodelling or trauma (Roos *et al.*, 1998), metabolic diseases (haemochromatosis and Ochnronosis), accumulation of toxins in the synonvium, alteration in load bearing in people suffering from obesity (Anderson & Felson, 1988) or anatomical abnormalities (Roos *et al.*, 1998; Mototani *et al.*, 2005). This is followed by attempted cartilage repair which leads to cartilage “fibrillation” (Stockwell, 1991a), subchondral cyst formation, bone outgrowth, hyperplasia of the synovium and sclerosis of subchondral bone (Stevens & Lowe, 2000).

In OA, there is an increase in cartilage hydration attributed to the degradation of collagen structures and thus the increased swelling capacity of PGs (Stockwell, 1991b). Tissue hydration causes an increase in the bioavailability of diffusible factors, including cytokines and nutrients, and subsequent changes in ionic environment. An increase in OA chondrocyte cell volume was also observed and an article reported that it was due to passive swelling in the over-hydrated tissue (Bush & Hall, 2005).

On the cellular level, OA chondrocytes escape the maturation arrest (tightly regulated by Transforming Growth Factor Beta; TGF-β) and undergo a

hypertrophic-like Bone Morphogenetic Protein (BMP) dependent maturation (Ballock *et al.*, 1993; Serra *et al.*, 1999; Grimsrud *et al.*, 2001; Li *et al.*, 2006) whilst expressing high levels of types X, III, IIA and VI collagen (Schmid *et al.*, 1991; Aigner *et al.*, 1995; Soder *et al.*, 2002; Gebhard *et al.*, 2003) and abnormal levels of versican, a chondroitin sulphate proteoglycan (Martin *et al.*, 2001). Moreover, there is also an upregulation of inflammatory mediators including IL-1β, IL-4, TNFα, Nitric Oxide (LeGrand *et al.*, 2001), and matrix metalloproteinases (Tetlow *et al.*, 2001; Fernandes *et al.*, 2002).

Osteoarthritis is managed using painkillers (Paracetamol), non-steroidal anti-inflammatory drugs (NSAIDs; aspirin, Ibuprofen and, to a less degree, selective COX-2 inhibitors including Celecoxib) and/or corticosteroid treatment (Prednisone; on the website of the National Health Service). More recent developments in OA therapy include MabThera, a chimeric human monoclonal antibody against CD20 (Tsiakalos *et al.*, 2008; Nakou *et al.*, 2009), and other similar biotechnological drugs against TNFα and IL-1 (Koumakis *et al.*, 2009; Mertens & Singh, 2009). Nevertheless, the aetiology and mechanism of disease progression is still largely unknown and the only treatment to OA is joint arthroplasty.

1.3 In vitro Expansion of chondrocytes

An emerging treatment for OA is cartilage replacement (Giannoni *et al.*, 2005; Sgaglione, 2005; Tallheden *et al.*, 2005) whereby cartilage explants are removed from patients and chondrocytes isolated, and subsequently grown ('expanded') in 2D monolayer culture medium *in vitro* until a suitable density is reached. Chondrocytes can then be re-introduced into the patient *via* a 3D support (Chen *et al.*, 2003; Kino-oka *et al.*, 2005). The focus of this technology is to provide a viable cartilage replacement, specific to an individual patient, and thus improve the treatment of OA although there are technological limitations to this therapy.

Regulation of the chondrocyte phenotype is an important factor when working with articular cartilage (Drissi *et al.*, 2005). As previously discussed, chondrocytes *in situ* exhibit a 'differentiated' phenotype whereby chondrocytes appear rounded (Figure 1.3A) and express aggrecan and elevated levels of ratios of collagen type II to collagen type I expression (Benya *et al.*, 1981; Benya & Shaffer, 1982a). Conversely, as a result of monolayer culture, chondrocytes exhibit what is termed 'dedifferentiated phenotype' acquring fibroblast-like morphology (Figure 1.3B) and low ratio of expression of type II collagen to type I collagen (Benya & Shaffer, 1982b; Stokes *et al.*, 2001; Table 1.3).

Dedifferentiated phenotype is also characterised by the expression of Cathepsin B (Benya *et al.*, 1981; Benya & Shaffer, 1982a; Baici *et al.*, 1988b) and Twist (Stokes *et al.*, 2002), a transcription factor that forms complexes with a wide range of transcription factors (Reinhold *et al.*, 2006). In chondrocytes, the expression of Twist *via* β-catenin-dependent pathway strongly inhibited SOX9-mediated differentiated phenotype (Reinhold *et al.*, 2006). Moreover, Twist interacts with transcription factor 3 leading to expression of CD44 (Nusse,

2005), a collagen receptor upregulated in 2D-cultured chondrocytes (Stokes *et al.*, 2002).

Trying to 'recapture' the chondrocytic differentiated phenotype following expansion has been under intensive research. It has been shown that it was possible to maintain the chondrocyte phenotype by growing chondrocytes in 3D supports composed of type II collagen, agarose or alginate (Nehrer *et al.,* 1997; Beekman *et al.*, 1997; Benz *et al.*, 2002b; Miot *et al.*, 2005a). Supplementation with TGFβ1 or BMP6 induced the upregulation of chondrocyte-specific genes including type II collagen, SOX9 and aggrecan (Zhou *et al.*, 2008; Sung *et al.*, 2009; van der Windt *et al.*, 2009). Similarly, the application of cyclic hydrostatic pressure has been shown to induce the expression of GAG and type II collagen whilst downregulating type I collagen (Heyland *et al.*, 2006; Kawanishi *et al.*, 2007). Finally, treatment with actin depolymerising drugs including cytochalasin D have been shown to induce the re-expression of type II collagen and upregulation of PGs synthesis (Newman & Watt, 1988; Benz *et al.*, 2002a; Miot *et al.*, 2005b).

The success of the recapture methodologies was found to be influenced by the passage number where introduction of chondrocytes cultured for 3-12 days into 3D high-density culture induced a recovery of phenotype (Shakibaei, 1998, Schulze-Tanzil *et al.*, 2002). Upon further culture, however, chondrocyte phenotype recovery was abolished, suggesting the existence of irreverisibly dedifferentiated chondrocytes in later passages (Haisch *et al.*, 2006).

Table 1.3: Summary of chondrocytic phenotypes in relation to the types of collagen synthesised.

The types of collagen synthesised in the extracellular matrix is highly dependent on the chondrocytic phenotype. In vivo, foetal chondrocytes express elevated levels of type III collagen, hypertrophic chondrocytes are characterised by the expression of type X collagen and differentiated adult chondrocytes by the expression of predominantly type II collagen. In Osteoarthritic tissue however, chondrocytes express elevated levels of type X and VI collagen and upon 2D culture chondrocytes upregulated the expression of type I collagen.

Phenotype	Collagen	References
Foetal	Type III	Hayes *et al.*, 2001
Differentiated	Type II, III, IX, XI	Benya & Shaffer, 1982b; Benya *et al.*, 1988; Hauselmann *et al.*, 1994; Hauselmann *et al.*, 1996
Dedifferentiated (Fibroblastic)	Type I, III	Benya & Shaffer, 1982b; Baici *et al.*, 1988a; Liu *et al.*, 1998; Zwicky & Baici, 2000
Hypertrophic	Type X	(Aigner & McKenna, 2002)
Osteoarthritic	Type II, III, X, VI	Aigner *et al.*, 1995; Soder *et al.*, 2002; Gebhard *et al.*, 2003

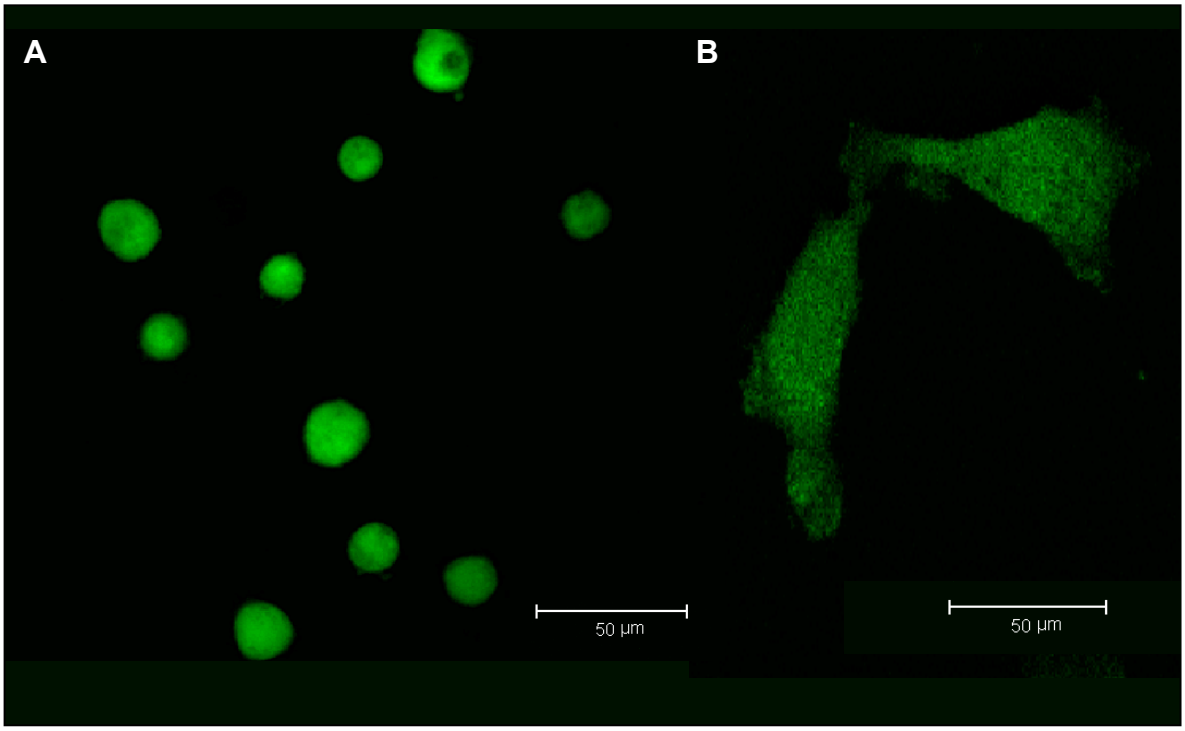

Figure 1.3: Morphology of freshly isolated and 2D-cultured chondrocytes

Freshly isolated and 2D-cultured chondrocytes were incubated with 5µM calcein-AM for 30 minutes and imaged using confocal microscopy (Panels A and B, respectively). Freshly isolated chondrocytes (Panels A) possessed a round shape, whereas following 21 days in monolayer culture, 2D-cultured chondrocytes (Panels B) appeared 'fibroblastic' with an irregular 'flat' morphology.

1.4 Mechanotransduction and Calcium Homeostasis

As previously mentioned, chondrocytes residing in articular cartilage are subjected to various mechanical stimuli and possess the capacity to 'sense' and convert these stimuli into chemical and physiological responses using a group of mechanisms termed mechanotransduction. Mechanotransduction of these stimuli enables chondro-cytes to adapt to the changes in the extracellular environment and respond appropriately to maintain optimal intracellular environment and/or to modify extracellular matrix components. Calcium signalling is a crucial factor in regulation of chondrocytic phenotype and changes in intracellular calcium ($[Ca^{2+}_i]$) have been closely linked to different mechanical signals including fluid flow (Yellowley *et al.*, 1997; Yellowley *et al.*, 1999), osmotic challenge (Urban *et al.*, 1993; Hopewell & Urban, 2003; Kerrigan & Hall, 2005; Kerrigan *et al.*, 2006), pressure (Guilak *et al.*, 1999a) and membrane deformation (Guilak *et al.*, 1999b).

During walking, the pressure on articulating cartilage oscillates between 0.2MPa and 0.3-0.5MPa and results in the deformation of cartilage and chondrocytes embedded within (Broom & Myers, 1980). Above 0.5MPa static compression causes irreversible damage to cartilage and chondrocyte metabolic activities are impaired (Burton-Wurster *et al.*, 1993; Guilak *et al.*, 1994). Pressure also induces the loss of interstitial fluid, concentration of PG's and thus an increase in extracellular osmolarity, an effect which is reversible in healthy cartilage upon removal of the load, with the tissue rehydrating until equilibrium is reached (Maroudas & Bannon, 1981; Urban, 1994). Pressure induces a set of cellular responses including integrin $\alpha5\beta1$ activation (Wright *et al.*, 1997), PLB3K-dependent calcium rise (Valhmu *et al.*, 1998) and the up-regulation of aggrecan, collagen type II, β-actin and Matrix metalloproteinase (MMP) -3 (Lee *et al.*, 2000; Millward-Sadler *et al.*, 2000).

Chondrocytes are embedded in an overall negatively charged matrix attracting cations, which in turn increase the water content of cartilage. The mobile fluid phase flows surrounding chondrocytes during joint articulation, and therefore, fluid flow has been employed *in vitro* to mimic shear-induced stress (Yellowley *et al.*, 1997). It has been observed that fluid flow induced both a G-protein-mediated Ca^{2+} release from intracellular stores and stretch-activated cation channels (SACC) activation (Yellowley *et al.*, 1997; Yellowley *et al.*, 1999). Conversely, membrane deformation, as a result of fluid flow *in vivo* or mechanical stimulation *in vitro*, has been shown to induce an intracellular store-independent $[Ca^{2+}]_i$ rise which was inhibited by pharmacological inhibitors of Sodium Calcium Exchanger (NCX) and SACC (Guilak, 1999).

NCX (also known as Solute carrier family 8 (sodium/calcium exchanger), member 3) is involved in maintaining $[Ca^{2+}]_i$ homeostasis in a wide variety of cell types with NCX3 being restricted to neurons (Thruneysen *et al.*, 2002). NCX can transport Ca^{2+} at high speed of 5,000 ions/s (Carafoli *et al.*, 2001), is regulated by $[Ca^{2+}]_i$ and is found on both the plasma membrane and intracellular organellar membranes (Gabellini, 2004). SACC, conversely, is a group of Gd^{3+}-sensitive channels that respond to mechanical 'stress' by allowing the exchange of cations.

It has been shown that freshly isolated chondrocytes, but not 2D-cultured chondrocytes, exhibited a transient increase in intracellular calcium in a gadolinium-sensitive manner in response to a hypo-osmotic challenge (Kerrigan & Hall, 2007) mediated by PLC/IP3-depandant calcium release from intracellular stores (Sanchez *et al.*, 2003), whereas only NCX was involved in hyperosmotic challenge-induce $[Ca^{2+}]_i$ rise (Sanchez & Wilkins, 2004). Moreover, treatment of 2D cultured chondrocytes with Gadolinium, a SACC inhibitor, induced the loss of a differentiated phenotype (Perkins *et al.*, 2005) potentially *via* a calcium-dependent pathway (Wright *et al.*, 1996). Therefore, investigating changes in calcium signalling pathways is an area of continued research.

1.5 Volume Regulation and 2D Expansion

In non-impacted cartilage tissue, the extracellular environment possesses an ionic concentration ranging between 355±5mOsm in the SZ and 410±30mOsm in the DZ (Urban, 1994). As previously described, joint loading induces an changes in extracellular ionic environment (Urban *et al.*, 1993; Kerrigan & Hall, 2005; Kerrigan *et al.*, 2006) and the activation of volume regulatory mechanism including Regulatory Volume Decrease (RVD) and post-RVD Regulatory Volume Increase (post-RVD RVI; Kerrigan *et al.*, 2006).

RVI and RVD are two mechanisms by which some cell types maintain constant (in dynamic equilibrium) volume and intracellular ionic strength necessary to support physiological processes and optimal metabolism during a hyperosmotic and hypo-osmotic challenges, respectively (O'Neill, 1999). These mechanisms result in an opposing water motion and gradual restoration of cell volume (Hoffmann *et al.*, 2007). RVI is mediated by several different types of membrane transporters (Figure 1.4) including sodium/potassium/chloride transporter (Trujillo *et al.*, 1999; Kerrigan *et al.*, 2006), Na^+/H^+ antiporter (Trujillo *et al.*, 1999), anion exchanger (Shrode *et al.*, 1997; Trujillo *et al.*, 1999; Yamazaki *et al.*, 2000; Tattersall *et al.*, 2003), Na^+/HCO_3^- coupled cotransporter and Na^+/K^+ pump (O'Neill, 1999).

It has been shown that deviations from range of osmolarity values found naturally *in vivo* resulted in a reduction in ECM production (Urban *et al.*, 1993; Hopewell & Urban, 2003). In OA hydrated cartilage, for example, there is a decrease in extracellular osmolarity and an increase in fluid flow (Maroudas & Venn, 1977; Mizrahi *et al.*, 1986; Bush & Hall, 2005), possibly contributing to changes in chondrocyte phenotype in OA.

Previous studies have shown variations in response to extracellular omsolarity between differentiated and 2D-cultured chondrocytes, and therefore the ability of chondrocytes to exhibit volume regulatory mechanisms appears to be closely linked to the phenotypic state. 2D-cultured chondrocytes exhibited RVI whereas freshly isolated and *in situ* chondrocytes did not (Kerrigan *et al.*, 2006), thereby confirming that 2D-cultured chondrocytes respond differently to mechanical stimuli. Nevertheless, treatment of freshly isolated chondrocytes with latrunculin B induced a bumetanide-sensitive RVI response suggesting the involvement of NKCC1 in RVI in chondrocytes. Furthermore, molecular inhibition of NKCC1 using RNA intereference (RNAi) in chondrocytic cell line C-20/A4 induced the loss of RVI mechanisms, thus confirming the role of NKCC in chondrocytes (Qusous *et al*., in press).

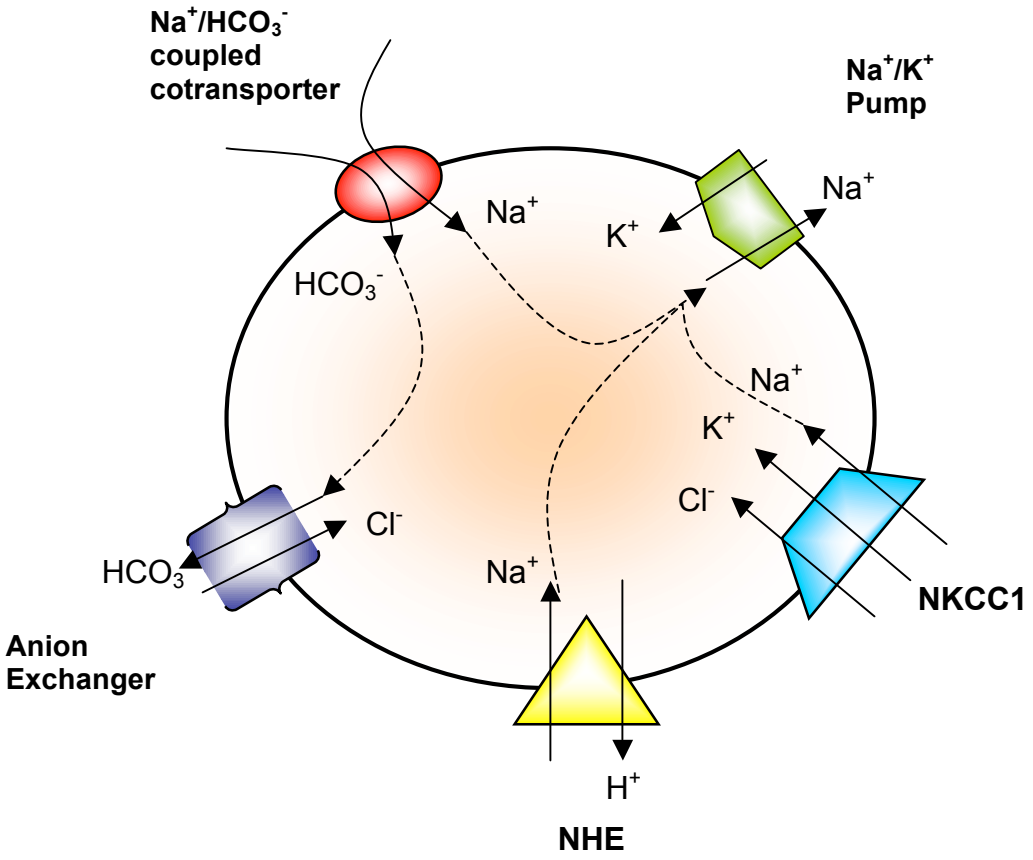

Figure 1.4: Representative Diagram of transporters involved in RVI.

NKCC1 (sky blue), Na^+/H^+ antiporter (NHE; yellow), anion exchanger (blue), Na^+/HCO_3^- coupled cotransporter (red), Na^+/K^+ pump (green). Membrane transporters pump ions into the cell cytoplasm upon cell shrinkage. This is followed by a passive water influx that restores the volume of the cell. Adapted from O'Neill, 1999.

1.6 Actin Cytoskeletal Organisation

The actin cytoskeleton is a dynamic intracellular structure, which gives mechanical support to cells and is involved in a wide range of cellular functions. Actin, reported to be the most abundant protein in eukaryotic cells with a cellular concentration of over 100μM, is a 43kDa globular protein (and thus termed G-actin) that forms a unipolymer termed F-actin. Actin polymerisation is ATP and Mg^{2+}/Ca^{2+}-dependent and is regulated by a variety of actin binding proteins including nucleation promoting proteins Arp2/3 and Profilin (Goley & Welch, 2006), depolymerising proteins ADF and Cofillin (Ono, 2007), G-actin sequestering protein Thymosin β4 (Yarmola & Bubb, 2004) and capping protein Gelsolin (Yarmola & Bubb, 2004). Other factors that influence actin organisation include hyperosmotic and hypo-osmotic conditions leading to an increase and a decrease in F-actin, respectively (Guilak *et al.*, 2002).

Several reports have demonstrated that actin organisation follows a cortical disribution with predominant localisation to the cell periphery *in situ* (Durrant *et al.*, 1999; Langelier *et al.*, 2000), in agarose 3D cultured (Idowu *et al.*, 2000; Knight *et al.*, 2001) and in high-density monolayer chondrocytes (Blain *et al.*, 2006). Conversely, in 2D cultured chondrocytes the cortical arrangement is lost and actin filaments span the whole cell (Idowu *et al.*, 2000; Loty *et al.*, 2000; Figure 1.5). Interestingly, in OA chondrocytes F-actin is less defined than in differentiated chondrocytes and localised diffusely in the cytoplasm (Fioravanti *et al.*, 2003).

The actin cytoskeleton provides chondrocytes with the mechanical integrity required to withstand compressive loads (Guilak, 1995) as seen by the reduction of chondrocyte stiffness by 90% and the increase in apparent viscosity by 80% in response to treatment with cytochalasin D (Trickey *et al.*, 2004) a fungal

metabolite that inhibits actin polymerisation (Schliwa, 1982). Furthermore, cytochalasin D treatment has been shown to reduce both the rate of matrix synthesis as well as chondrocyte anchorage to extracellular PGs, thus suggesting a role for actin in signal transduction and phenotype modulation (Nofal & Knudson, 2002). The effects of actin organisation on chondrocyte morphology and phenotype has been well documented with dedifferentiated chondrocytes re-expressing type II collagen and upregulating PGs expression in response to cytochalasin D treatment (Newman & Watt, 1988; Benz *et al.*, 2002a; Miot *et al.*, 2005b), an effect found to be independent of morphology (Brown & Benya, 1988).

As previously mentioned, freshly isolated chondrocytes do not exhibit RVI but it has been reported that chondrocytes treated with Latrunculin B, an actin capping agent, exhibited bumetanide-sensitive RVI in freshly isolated chondrocytes (Kerrigan *et al.*, 2006). Moreover, Latrunculin B treatment induced a significant increase in the number of cells expressing 'fast' RVD (Kerrigan & Hall, 2005), thereby implying that the actin cytoskeleton plays a role in the regulation of membrane transporters, possibly the NKCC, and thus the RVI mechanisms. The above findings suggest a wide role for actin in the regulation of chondrocytic phenotype and mechanotransduction.

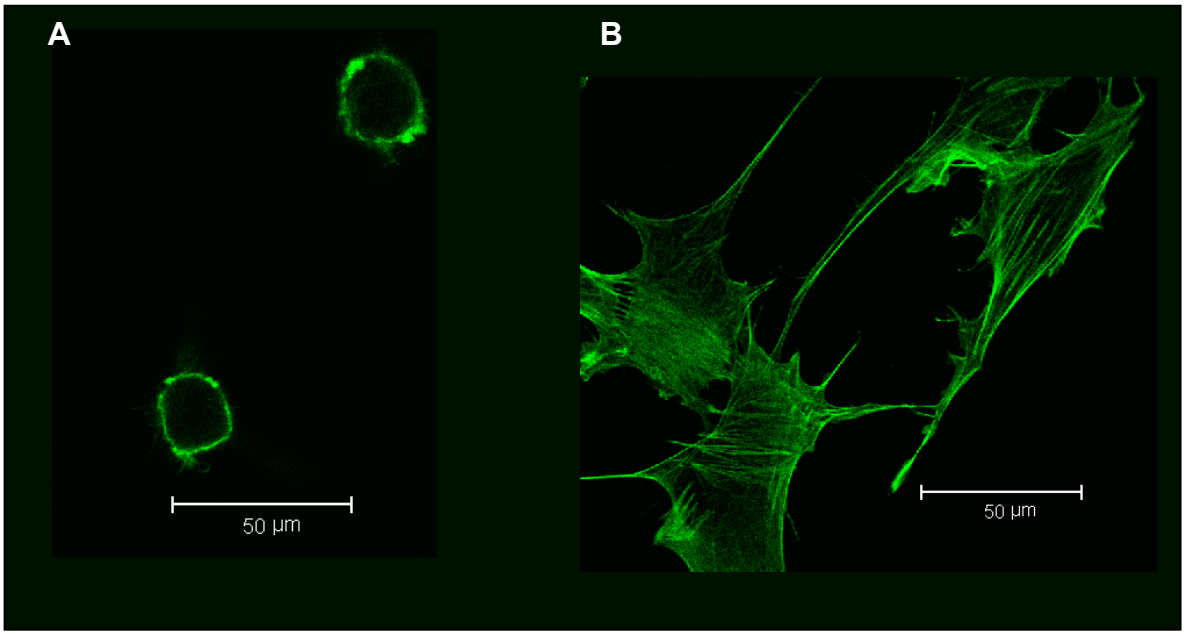

Figure 1.5: Actin organisation of freshly isolated and 2D-cultured chondrocytes

Freshly isolated and 2D-cultured chondrocytes were fixed using 3% formaldehyde, permeabilised using Triton X100 and subsequently labelled using Alexa 488-Phalloidin to label the actin cytoskeleton (Panels A and B, respectively). Freshly isolated chondrocytes (Panel A) had thick cortical actin structures whereas following 21 days in monolayer culture, 2D-cultured chondrocytes (Panel B) possessed a dense network of filamentous actin.

1.7 DEL1 and Integrin Signalling

Integrins are transmembrane homo or heterodimers composed of α and/or β chains covalently bound with a ligand affinity dependent on the combination of chains (Hemler, 1990; Hynes, 1992). Integrins are involved in a wide range of cellular functions including cellular attachment (Enomoto-Iwamoto *et al.*, 1997), maintaining shape, proliferation and actin organisation, (Hirsch *et al.*, 1997; Shakibaei *et al.*, 1997) and relaying pressure-induced mechanotransduction signals (Wright *et al.*, 1997). Changes in the expression of integrin dimers in response to 2D culture have been reported including an upregulation of α2-6 chains and $\alpha5\beta1$ (Fibronectin receptors; FnR) heterodrimers (Enomoto-Iwamoto *et al.*, 1997; Diaz-Romero *et al.*, 2005), indicating a role for Integrin signalling in the regulation of phenotype upon 2D expansion. The role of integrin signalling in differentiation and gene expression has been investigated in mammary gland epithelium (Schmidhauser *et al.*, 1992), myogenesis (Enomoto *et al.*, 1993), keratinocytes (Adams & Watt, 1991) and kidney tubule epithelium (Sorokin *et al.*, 1990).

In chondrocytes, gene mutations in integrin-mediated adhesion signalling lead to various chondroskeletal complications. α1 integrin knock-out models developed growth plate abnormalities and osteoarthritis (Zemmyo *et al.*, 2003), whereas α10 integrin knock-outs developed growth retardation, increased apoptosis and abnormal cell shape (Bengtsson *et al.*, 2005). Moreover, tissue specific knock-out of β1 integrin disorganised the growth plate and proliferative columns, reduced proliferation, caused abnormal cell shape and decreased cellular adhesion (Aszodi *et al.*, 2003).

1.7.1 Integrin Signalling

Binding of ECM ligands to integrins can induce a set of cellular responses including the expression of matrix genes (Clancy *et al.*, 1997), the degradation of the matrix by inducing the synthesis of matrix proteinases (Werb *et al.*, 1989) and organisation of the actin cytoskeleton (Turner & Burridge, 1991; Wang & Kandel, 2004). Integrins do not possess tyrosine kinase domains but are associated with a group of proteins which induce a cascade of phosphorylation. Following ligand binding and subsequent integrin activation and aggregation (Schaller *et al.*, 1994), FAK trans-autophophorylation is induced which in turn results in the activation of PI3K (Chen *et al.*, 1996) and Rho (Hotchin & Hall, 1995). PI3K activation leads to the phophorylation of Akt, whereas Rho signals induce Erk and cofilin activation which regulate the cell cycle and actin polymerisation, respectively (Renshaw *et al.*, 1996).

Akt is also involved in a number of cell signalling pathways including cell survival and motility and has been shown to regulate the expression of Basic helix-loop-helix transcription factors (Vojtek *et al.*, 2003) including Twist. There has also been evidence that the signalling strategies used by integrins include additional pathway to those employed by growth factor cell receptors. It has been found that focal contact sites do not only contain cytoskeletal-regulatory tyrosine kinases (Schaller *et al.*, 1992), but also low amounts of a number of non-enzymatic proteins that are activated by tyrosine kinases and mediate protein-protein interactions in the focal contact (Turner & Burridge, 1991).

1.7.2 Developmental Endothelial Locus 1 (DEL1)

DEL1 (also known as EGF-like repeats and discoidin I-like domains 3; Edil3) is a 52kDa matrix adhesion protein composed of two Endothelial Growth Factor-like (EGF-like) domains, the second of which containing an integrin-binding Arginine-Glycine-Aspartic acid (RGD) motif (Hidai *et al.*, 1998). Similarly to Edil1 (lactadherin; Silvestre *et al.*, 2005), DEL1 interacts with αvβ3 phosphorylating proteins in the focal contact including FAK, MAPK, Shc and Akt and providing an autocrine angiogenic pathway as evident by inhibition of productive activation of its receptor by matrix substrates (Penata *et al.*, 1998).

It has been shown that DEL1 influenced endothelial cell behaviour and played an important role in mediating angiogenesis, vessel wall remodelling and development (Aoka *et al.*, 2002; Ho *et al.*, 2004). In vascular smooth muscle cells, DEL1 is involved in adhesion, migration and proliferation through interaction with integrin αvβ3 and actin filaments re-organisation (Rezaee *et al.*, 2002). Moreover, the attachment function of DEL1 has been shown to be involved the immune system, whereby DEL1 expression by endothelial cells induced leukocyte adhesion and inflammatory recruitment (Chol *et al.*, 2008). DEL1 expression by apoptotic cells enhanced phagocytosis by immune cells by promoting attachment to phagocytic cells expressing αvβ3 integrin (Hanayama *et al.*, 2004).

DEL1 is involved in both foetal and adult differentiation via integrin signalling due to the similarity between DEL1 amnio acid sequence and the notch receptor ligands, known to inhibit terminal differentiation of a wide range of cell types (Penata *et al.*, 1998). In Xenopus embryogenesis, DEL1 is essential for dorsal development whereby DEL1 knockdown is sufficient to cause ventralisation of embryos via the attenuation of BMP-signalling (Arakanawa *et al.*, 2007). DEL1 is expressed by the keratinocytes in the dermal papilla and has been recently

shown to induce follicle development in mice skin by unknown mechanisms (Hsu *et al.*, 2008).

In chondrocytes, the expression of DEL1 has been observed in foetal tissue. An upregulation of DEL1 expression has been previously reported in high density culture but not 2D culture of foetal chondrocytes (Stokes *et al.*, 2002). The expression level and biological significance of DEL1 in adult chondrocytes, however, have not yet been investigated. Due to the established complex effect of integrin signalling on chondrocyte development and differentiation, as well as the recent observations of changes in DEL1 expression in response to 2D culture, DEL1 has become a candidate for continuing research in chondrocyte phenotypic regulation.

1.8 Aims

Due to a current gap in knowledge, I aimed to study the regulation of chondrocytic phenotype and mechanotransduction responses as a result of 2D culture. We proposed to identify the mechanism of DEL1–induced de-differentiation *via* Twist and the corresponding changes in morphology, actin organisation and mechanotransduction.

1 Quantify the changes in chondrocyte phentoype occurring in response to 2D culture including cell shape, actin organisation and expression battery.

2 Study the mechanotransduction responses of freshly isolated and 2D cultured chondrocytes in response to hyperomsmotic challenge and pharmacologically-induced $[Ca^{2+}]_i$ rise.

3 Investigate the role of DEL1 expression on chondrocyte phenotype regulation and mechanotransduction.

4 Investigate the signalling pathway of DEL1.

2 Materials and methods

2.1 Materials

2.1.1 Tissue Culture

Table 2.1: Tissue culture reagents.

Name	Company	Catalogue Number
Absolute Ethanol	VWR, Poole, UK	200-578-6
Low-melt Agarose	Invitrogen, Paisley UK	
Dulbecco's Modified Eagle Medium (DMEM)	Sigma-Aldrich, Poole, UK	D6171
DMEM Powder	Sigma-Aldrich, Poole, UK	D5523
Foetal Calf Serum	Gibco, Paisley, UK	16170-078
L-Glutamine	Sigma-Aldrich, Poole, UK	G-5763
MTT Kit	Sigma-Aldrich, Poole, UK	CGD1-1KT
Penicillin / Streptomycin Solution	Sigma-Aldrich, Poole, UK	P0781
Trypan Blue	Sigma-Aldrich, Poole, UK	T 8154
1X Trypsin-DMEM	Gibco, Paisley, UK	25300-062
Bone Morphogenetic Protein 2 (BMP2)	Heidelberg, Germany	H00000650-P01

2.1.2 Molecular Biology

Table 2.2: Reagents used in molecular biology studies.

Name	Company	Catalogue Number
Absolute Ethanol	VWR, Poole, UK	200-578-6
Agarose	Invitrogen, Paisley UK	10975-035
Custom Designed siRNA	Ambion, Cambridgeshire, UK	16100
FAM-Labelled Negative Control siRNA	Ambion, Cambridgeshire, UK	4620
HiPerfect Transfection Reagent	Qiagen, West Sussex, UK	301704
Nucleic Acid Markers 100bp ladder 200bp ladder	Invitrogen, Paisley UK	 10416-014 15628-019
ImPromII Reverse Transcription System	Promega, USA	A3800
Phenol	Sigma-Aldrich, Poole, UK	108-95-2
Phosphate Buffer Saline	Sigma-Aldrich, Poole, UK	P-4417
Primer Oligonucleotides	MWG, Ebersberg, Germany	C09041/X
Positive Control (anti-GAPD) siRNA	Ambion, Cambridgeshire, UK	AM4605
RNeasy Minikit	Qiagen, West Sussex, UK	74014
GoTaq Polymerase Master Mix	Promega, USA	M7502

2.1.3 Actin Cytoskeleton studies

Table 2.3: Reagents used to study the actin cytoskeleton.

Name	Company	Catalogue Number
Bovine Serum Albumin	Sigma-Aldrich, Poole, UK	85041C
Paraformaldehyde	Sigma-Aldrich, Poole, UK	P6148
Phosphate Buffer Saline	Sigma-Aldrich, Poole, UK	P-4417
Triton X100	VWR, Poole, UK	VW8887-4

2.1.4 Antibodies used in protein identification experiments

Table 2.4: Reagents used to study the actin cytoskeleton.

Name	Company	Catalogue Number
Rabbit anti-Akt	New England Biolabs, Hertfordshire, UK	2938
Rabbit anti-p-Akt	New England Biolabs, Hertfordshire, UK	3787
Mouse anti-DEL1 polyclonal	Stratech, Suffolk, UK	P-4417
Goat anti-Rabbit, HRP conjugated	New England Biolabs, Hertfordshire, UK	7074
Goat anti-Mouse, HRP conjugated	New England Biolabs, Hertfordshire, UK	7059
Immobilon Western Chemiluminescent HRP Substrate	Millipore, Watford, UK	WBKLS0500
Immobilin-P membrane	Millipore, Watford, UK	IPVH20200

2.1.5 Fluorophores

Table 2.5 Fluorophores used.

Name	Company	Catalogue Number
Calcein AM	Invitrogen, Paisley UK	C1430
Cy3 (conjugated to anti-DEL1 siRNA)	Ambion, Cambridgeshire, UK	AM16211
FAM-Labelled Negative Control siRNA	Ambion, Cambridgeshire, UK	4620
Fluo-4	Invitrogen, Paisley UK	A12379
Alexa 488 (conjugated to phalloidin)	Invitrogen, Paisley UK	F23917
TO-PRO3	Invitrogen, Paisley UK	T 3605

2.1.6 Pharmacological and inhibitory reagents

Table 2.6: Pharmacological agents used in calcium signalling determination.

	Target	Working concentration	Comments	references
REV5901	cysteinyl-leukotriene receptors	50μM	Inhibitor of RVD and Lipoxygenase	(Musser *et al.*, 1987; Van Inwegen *et al.*, 1987; Bush & Hall, 2001a)
U73122	PLCβ3	100μM	Highly selective	(Hou *et al.*, 2004)
Wortmannin	PI5K	1μM	Inhibits PI3K	(Liu *et al.*, 2001)
Rottlerin	PKC	100μM	Activates K+ channels	(Gschwendt *et al.*, 1994)
Neomycin	PIP2	10mM	Used at 55μM in culture as antibiotic	(James *et al.*, 2004)
Ruthenium Red	TRPV	10μM	Inhibits RyR and NCX	(Gunthorpe *et al.*, 2002)
R-Etodolac	β-catenin	500μM	-	(Behari *et al.*, 2007)
Gadolinium	SACC	100μM	-	(Sackin, 1995)
Ionomycin	mobile calcium carrier	3μM	greater selectivity for Ca^{2+} over Mg^{2+}	(Liu & Hermann, 1978)

2.2 Culture Media and Experimental Salines

The tissue culture media used was Dulbecco's Modified Eagle Medium (DMEM; Sigma) supplemented with 1% penicillin/streptomycin solution under asceptic conditions. For work on freshly isolated chondrocytes, the osmolarity of DMEM was adjusted to 380mOsm/kg H_2O (mOsm) by the addition of filter-sterilised 50mM sodium chloride (NaCl). Media used for long term culture purposes contained 1% penicillin/streptomycin solution, filter-sterilised 20mM L-Glutamine (an essential amino acid; as instructed by manufacturer), 10% Foetal Calf Serum (FCS), filter-sterilised 50µg/ml Ascorbic Acid (necessary for matrix synthesis) and 50mM NaCl (necessary to adjust the osmolarity to 380 mOsm). In experiments requiring the supplementation with Bone Morphogenetic Protein 2 (BMP2), 14-day 2D cultured chondrocytes were treated with 500ng/ml of BMP2 for 7 days to allow phenotypic switch (Minina *et al.*, 2001). For all volume regulation experiments, a bottle of powder DMEM was dissolved in double distilled water containing 15mM HEPES and the pH adjusted to 7.40±0.05. The osmolarity was measured using Vapro™ vapour pressure osmometer and adjusted using NaCl to 380±5mOsm and 700±5mOsm for Isomotic and hyperosmotic media, respectively (Kerrigan *et al.*, 2006).

As phenol red in media interferes with calcium measurement, experiments were performed using basic physiological saline (BPS) containing (in mM); HEPES (15), glucose (10), potassium chloride (KCl; 5), magnesium chloride ($MgCl_2$; 1) and calcium chloride ($CaCl_2$; 1). The pH was adjusted to 7.40 ±0.05 and the osmolarity measured using Vapro™ vapour pressure osmometer and adjusted by the addition of NaCl. When performing calcium-free experiments, calcium chloride was replaced with 2mM EGTA and when performing sodium-free experiments, the osmolarity was adjusted by the addition of choline chloride (Dascalu *et al.*, 1996).

2.3 Chondrocyte isolation and culture

Bovine metacarpal and metatarsal joints of freshly slaughtered 18-21 month old female animals were obtained from the local abattoir (with permission) and full-depth cartilage isolated into 280mOsm DMEM supplemented with 1% penicillin/streptomycin solution under aseptic conditions and chondrocytes isolated as previously described (Hall *et al.*, 1996). Cartilage explants were incubated overnight in 380mOsm DMEM (to mimic the osmolarity of cartilage and reduce the changes that may occur due to the osmolarity of the media) supplemented with 1% penicillin/streptomycin solution and 0.8mg/mL collagenase. The collagenase treatment resulted in the degradation of the ECM, thereby releasing chondrocytes into the medium.

Following incubation for 18 hours, undigested material was removed by passing the suspension through a sterile (autoclaved) tea strainer followed by a 40µm sterile cell strainer and subsequently chondrocytes washed twice by centrifugation at room temperature at 600g for 10 minutes. Finally the supernatant was discarded, the pellet resuspended in 380mOsm DMEM and chondrocyte cell suspension aliquoted onto appropriate substrate (6, 12 or 24-well plates) and used within 2-8 hours.

Chondrocytes maintained in monolayer culture were resuspended in long-term culture media (Section 2.2) and a 100µl sample was counted by mixing it with 100µl of trypan blue, loading the mixture onto a haemocytometer and observing under a light microscope. In order to optimise the culture conditions, chondrocytes were seeded and subcultured upon confluence for up to 21 days at three different culture densities; High Density (HD; $2x10^5$ cell/cm^2), Intermediate Density (MD; $1x10^5$ cell/cm^2) and Low Density (LD; $2x10^4$ cell/cm^2)

in 25 or 75cm^2 vented tissue culture flasks and incubated at 37°C in a 5% carbon dioxide humidified incubator.

Upon reaching 80% confluence, chondrocytes from one flask were lifted and split into several new flasks. Briefly, the supplemented media was removed and chondrocytes incubated in 0.05% trypsin-EDTA solution (380mOsm/kg H_2O) for 5-10 min at 37°C, thus inducing cell rounding and subsequent detachment from the substrate as observed under a light microscope. The action of trypsin was reduced by dilution in fresh culture media and cells were washed twice by centrifugation at 600g for 10 minutes. Finally chondrocytes were resuspended in fresh culture media, counted and re-seeded at the original cell density for further culture or the use in required experimentation.

Chondrocytes were counted and assayed for viability at the end of every passage using trypan blue staining and a growth curve constructed. A logarithmic growth curve of Log cell number Log(N) was plotted against time in days (t) and the regression line calculated:

$$N = N_0 \times 2^{G \times t}$$

Applying log to both sides of the equation, the doubling time was calculated from the gradients of the equation of the best fit lines:

$$\therefore \log(N) = \log(N_0) + G \times \log(2) \times t$$

The gradient of the equation of the line best fit was therefore the product of the Growth rate (G) and log(2). The time needed for the cells to double in number, doubling time, was calculated as the inverse of the growth rate (shown in Section 3.2.1). LD was deemed most suitable and thus utilised for all further culture experiments whereby chondrocytes were subcultured on days 9, 14 and 21 post seeding and termed P1, P2 and P3 chondrocytes, respectively.

The number of joints used in each experiment is denoted (N) and the number of cells, where applicable, (n).

2.4 Expression Profiling of Expanded Chondrocytes

2.4.1 RNA extraction, Reverse transcription and Polymerase Chain Reaction (PCR)

The change in expression of key differentiation genes was studied by extracting RNA from freshly isolated and 2D cultured chondrocytes at the end of each passage and on days 2, 4, 6 and 8 of 2D culture using RNeasy Mini Kit (Qiagen). Briefly, chondrocytes were treated with 0.05% Trypsin-EDTA for 5 min at 37°C causing detachment from the substrate (plastic). The suspension was diluted with culture media (DMEM; 380mOsm/kg) and chondrocytes washed twice by centrifugation at 600g. Following the final centrifugation, the pellet was lysed with RLT cell lysis buffer and 350 µl of the lysate mixed with 350µl of 70% ethanol, loaded on an RNeasy column, subjected to centrifugation at 8,000g for 30 seconds, washed by centrifugation with SW1 and twice with RPL buffer and RNA attached to the column subsequently eluted in 50µl nuclease-free water.

RNA was quantified by measuring the absorbance at 260nm using a spectrophotometer (1 absorbance unit corresponds to 40µg/ml RNA; as recommended by Qiagen) and 1µg of each sample was reverse-transcribed using ImPromII Reverse Transcription (RT) System (Promega) as per manufacturer's instructions. 0.5µg PolyT and 0.5µg random primers were mixed with 1µg of the RNA and 20u RNase inhibitor and heated to 70°C for 5 minutes to allow denaturation of the RNA secondary structures. The mixture was then quickly cooled on ice to allow the hybridisation of the primer oligonucleotides to the RNA sequences. Upon incubation on ice, 0.5mM dNTP, 4µl reaction buffer and 1µl reverse transcriptase were added to the primer-RNA solution and the reaction proceeded at 42°C overnight in the presence of 5mM $MgCl_2$ until stopped by heat inactivation at 70°C for 15 minutes.

Primers used in the study were designed for mammalian genomic sequences and thus deemed suitable for bovine material (Table 2.7). Published sequences were used (Park *et al.*, 2005) or novel sequences designed. Briefly, gene sequences of bovine and human origin were obtained from the National Center for Biotechnology Information (NCBI) website and aligned using clustalx allignment tool to obtain conserved (consensus) sequence for which primers were designed using primer3 online tools (Rozen & Skaletsky, 2000). All primers were designed such that the PCR products had a product size of >50bp suitable for visualisation on 2% agarose gels and a primer melting temperature of 58-60°C. Selected primers were tested for specifity by running an online alignment search using Basic Local Alignment Search Tool (BLAST) on the NCBI website.

Polymerase chain reaction (PCR) was used to assay the expression of key genes during chondrocyte expansion. 2µl of the reverse transcriptase reaction containing cDNA were used in the GoTaq® Green Master Mix containing 0.2µM of each primer, and PCR cycles run as recommended by manufacturer's protocol (Table 2.8). The PCR products were loaded on 2% agarose gels (suitable for the size of amplicons) made up in 1X Tris-Borate-EDTA (TBE) Buffer and the gel subsequently subjected to a constant voltage of 150V for 2 hours prior to being stained with 1% Ethidium bromide in TBE buffer, washed in distilled water and imaged using by video capture under UV excitation.

Table 2.7: Sequences of PCR primer pairs

Primers were either obtained from previous publications by others or designed using online Primer3 tool. Primers were deemed suitable for mammalian genes and checked for specificity using the online Basic Local Allignment Sequence Tool (BLAST).

	Gene	Sequence	Tm (°C)	Size of Product (bp)	Design
Positive Control	GAPD				Pimer3
	forward	AGAACGGGAAGCTTGTCATC[†]	57.3	743	
	backward	TGAGCTTGACAAAGTGGTCGT	58.3		
Matrix Proteins	DEL1				Primer3
	forward	AGTGAAAGGCACCAATGAAGAC	58.3	200	
	back	GTCCTGATTTCATACCCAGAGG	59.3		
	collagen II				(Park *et al.*, 2005)
	forward	AGCAGGTTCACATATACCGTTCTG	60.6	73	
	back	CGATCATAGTCTTGCCCCACTT	59.9		
	collagen I				(Park *et al.*, 2005)
	forward	ACATGCCGAGACTTGAGACTCA	60.3	86	
	back	GCATCCATAGTACATCCTTGGTTAGG	62.2		
Transcription Factors	SOX9				(Park *et al.,* 2005)
	forward	ACGCCGAGCTCAGCAAGA	59.3	71	
	back	CACGAACGGCCGCTTCT	58.3		
	Twist				Primer3
	forward	GGCAAGCGCGGCAAGAAG	60.9	351	
	back	CGAGAAGGCGTAGCTGAG	57.9		

[†] TT in humans, TC in cows

Table 2.8: Steps involved in Polymerase Chain Reaction (PCR) amplification.

cDNA, obtained from reverse transcription, was initially denatured by heating at 95℃ for 2 minutes, annealing at the average melting temperature (Tm) of primers (58℃) and extended at 72℃ for 2 min with a denaturation step, annealing step and extension step repeated 35 times. A final extension step at 72℃ for 5 minutes was followed by incubation at 4℃. PCR resulted in exponential amplification of DNA.

Step	Duration (minutes)	Temperature (°C)	Repetition
Initial Denaturation Step	2	94	1x
Denaturation Step	1	94	35x
Annealing Step	1	58	
Extension Step	2	72	
Final Extension Step	5	72	1x
Holding Step	∞	4	1x

2.4.2 Gel Densitometery Optimisation

Quantitative PCR was used to assay changes in expression by gel densitometery. In order to optimise the relationship between the intensity of band on an ethidium bromide-stained gel and the amount of DNA in the band, a 2% agarose gel was loaded with known amounts of 100bp DNA ladder (2ng-300ng) and imaged. Scion Image version Alpha4.0 (Scion) was used to quantify the intensity of the DNA bands (I) and background emission (I_B), the product of the difference between which and the area of the DNA band (A) was plotted against the amount of DNA in ng was plotted to demonstrate the linear relationship (ng DNA vs. $[I-I_B].A$). The relationship was shown to be linear for DNA amounts that do not exceed 120ng (suitable for PCR; Figure 2.1).

2.4.3 GAPD suitability as an internal PCR positive control

Primers for Glyceraldehyde 3-phosphate dehydrogenase (GAPD; also known as GAPDH; a housekeeping enzyme that catalyzes the sixth step of glycolysis) were included in all PCR reactions as an internal positive control. As GAPD expression levels were used as a reference to measure significant changes in the expression of other genes, the expression of GAPD was monitored during culture. No significant change ($p>0.05$) in the amount of GAPD in the PCR reaction (calculated as $[I-I_B].A$) was observed in response to 2D culture (Figure 2.2), thus demonstrating the suitability of GAPD as a positive control.

For the measurement of the expression of key genes upon culture, image were imported into Scion Image Alpha4.0 Image software and the intensity of the background, and the intensity and area of the bands corresponding to the gene of interest were measured. Moreover, the intensity and area of the band corresponding to the internal positive control was also measured. The value of $(I-I_B).A$ of every band was calculated, and that was divided over the value of $(I-I_B).A$ for the band corresponding to GAPD internal control (Figure 2.3).

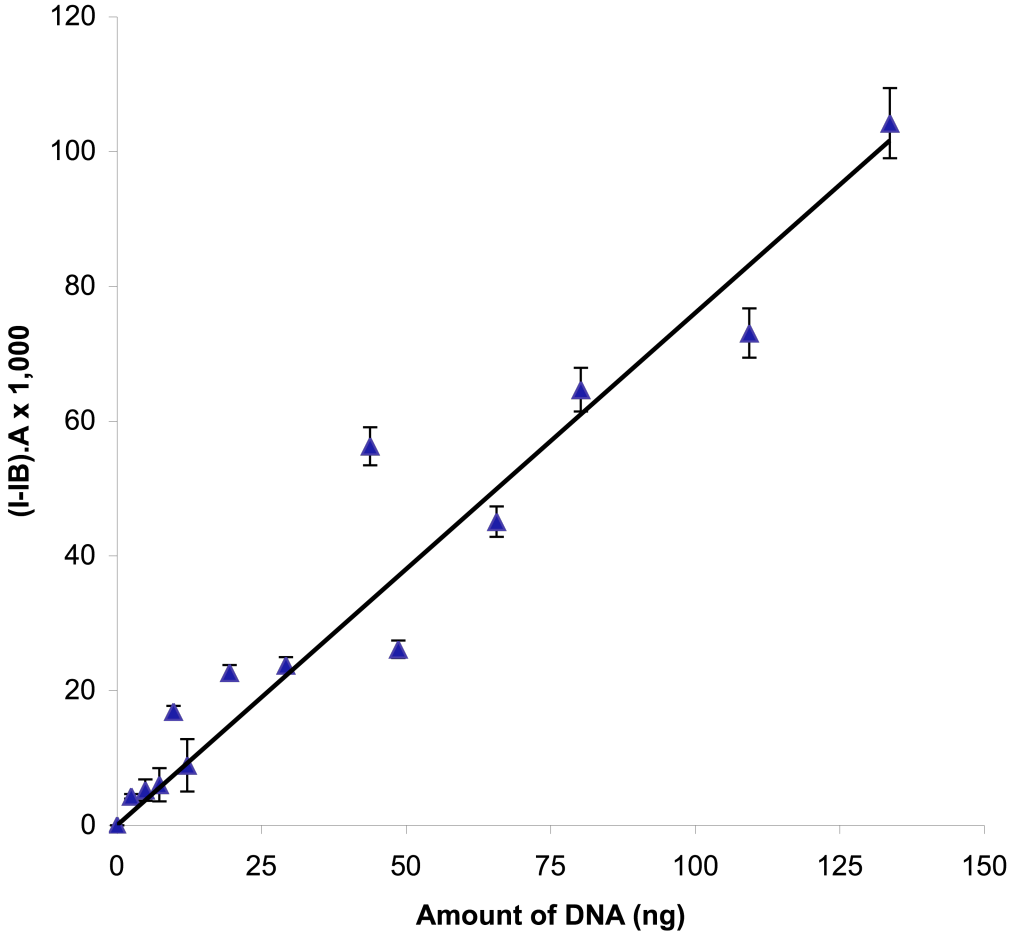

Figure 2.1: The linear relationship between the band intensity and size vs. the amount of DNA present

Known amounts of DNA (2-150ng) was run on a 2% agarose gel and the band intensity and size ($[I-I_B].A$) calculated by Scion Image Alpha4.0. The mean intensity of background was subtracted from the mean intensity of the band and subsequently multiplied by the area of the band. This product value was plotted against the amount of DNA in the band and the relationship was found to be linear for amounts of DNA <120ng. Data was pooled from 6 individual experiments. Values shown as mean ± s.e.m. R^2 = 0.936.

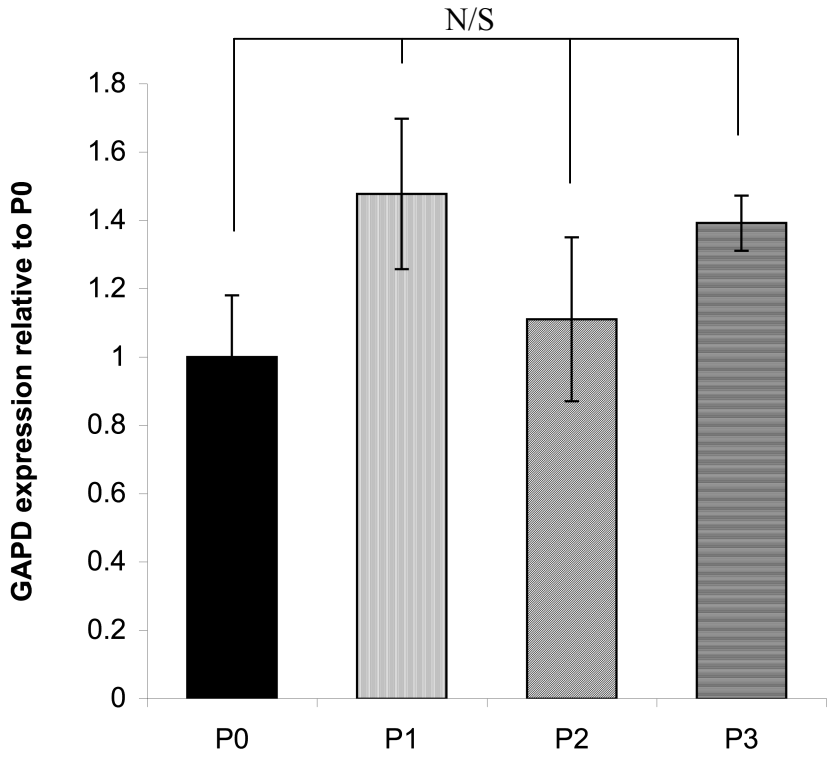

Figure 2.2: The level of expression of Glyceraldehyde 3-phosphate dehydrogenase (GAPD) during culture

The level of expression of a housekeeping gene, GAPD, was used in subsequent quantitative RT-PCR experiments as a positive control to study changes in expression of key genes during culture. RNA was isolated and reverse transcribed from freshly isolated chondrocytes (P0), after 9 days in culture (P1), after 14 days in culture (P2) and after 21 days in culture (P3) and PCR carried out using GAPD primers and the gel imaged and analysed as described. There was no significant change in GAPD expression throughout culture. Data was pooled from 7 individual experiments, N=6. Values shown as mean ± s.e.m (P>0.05).

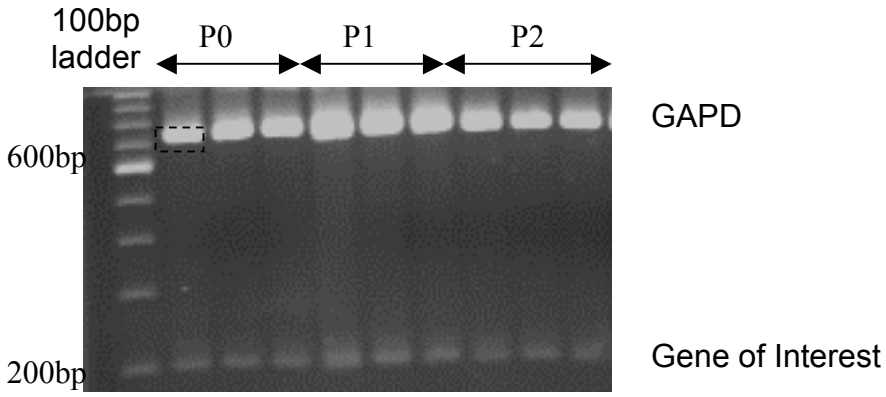

Figure 2.3: A representative image of an ethidium bromide-stained DNA gel

Products of a multiplex PCR reaction were loaded onto a 2% agarose gel and subjected to electrophoresis. Two genes were amplified in each PCR reaction, GAPD (internal positive control; with a size 743bp) and a gene of interest (200bp). Using Scion Image Alpha4.0, a region of interest was selected around each band and Scion Image Alpha4.0 used to measure the intensity and area of these bands (dashed rectangle). These data were used in the quantification of the amount of DNA present.

2.5 Confocal Microscopy

Images were acquired using a Leica SP2 TCS CLSM and Leica Software version 2.61 as previously described (Kerrigan & Hall, 2005) using grey resolution of 8 bit, pinhole radius of 1.00 Airy Unit to match to the diameter of objective used, beam splitter 488/543/633, laser speed of 400 Hz and the dipping lens HCX APO L U-V-1 63.0x 90 W.

The different fluorophores used in the experiments posessed different excitation and emission properties (Table 2.9). For the 3D reconstruction of images of chondrocytes for volume analysis, z-stack series of image slices were taken at 1μm intervals in depth whereas for localisation and actin experiments higher resolution images were acquired using Nyquist settings that were deemed suitable for deconvolution using Hygens 3.3 (SVI). Images were imported into Hygens 3.3, the image properties entered and deconvolution performed using default settings prior to reassembling the series using the Imaris version 6.3.1 (Bitplane).

Table 2.9: Fluorophores used in confocal microscopy for imaging and cell volume calculation.

Settings employed for image acquisition using Confocal Laser Scanning Microscope (CLSM) depended on the fluorophores used and the complexity of the analysis ensued. Nyquist settings were used for actin and small interfering RNA (siRNA) experiments, whereas lower resolution images were required for volume and dimensional analysis.

Dye	TO-PRO3 (1mM solution in DMSO)	FAM (conjugated to negative control siRNA)	Cy3 (conjugated to anti-DEL1 siRNA)	Alexa 488 (conjugated to phalloidin, 0.5µg/ml)	Calcein AM (1mg/ml solution in DMSO)
Settings	Nyquist Settings				Other
Maximum absorption (nm)	575nm	494nm	550nm	488nm	495nm
Maximum Emission	599nm	520nm	570nm	519nm	525nm / 512-540nm
Light Source	He/Ne 633	Kr 568	He/Ne 633	He/Ne 633	Kr 568 / 25%
Laser Strength (%)	35%	73%	73%	25%	25%
Resolution	1024x1024	1024x1024	1024x1024	1024x1024	512x512
Line averaging	4	4	4	4	1
Use	Cytoplasm and nucleus staining (working concentration 2µM)	Labelling of negative control siRNA	Labelling of oligonucleotide molecules	Labelling of phalloidin and subsequently the actin cytoskeleton	Volume marker, Measuring cell volume (working concentration 25µM)

2.6 siRNA design

RNA interference (RNAi) is a novel molecular technique that is based on a natural antiviral mechanism that involves interruption of gene expression at the messenger RNA (mRNA) translation level (Wang & Metzlaff, 2005). Short (~21nt long) double stranded (ds) sequences of small interfering RNA (siRNA) employed in this technique bind to complementary sequences on the messenger and recruit the RNA-induced silencing complex (RISC) to degrade the message (Elbashir *et al.*, 2001a; Figure 2.4). This results in a temporary knockdown of the expression which can last for up to 72 hours. Being a very specific technique when the target sequence is carefully designed, RNAi is gaining increasing interest in molecular medicine as a gene therapy technique for knocking down dominant mutated genes in hereditary diseases including retinitis pigmentosa (Kiang *et al.*, 2005) and viral sequences in infections including AIDS (Cullen, 2005). In chondrocytes, RNAi was used to study the role of various proteins including SOX9 (Wenke *et al.*, 2009), p16 (Zhou *et al.*, 2004) and NKCC1 (Qusous *et al.*, in press).

Nevertheless, RNAi, like other similar techniques of gene therapy, still faces several drawbacks. Designing a suitable vector, which protects siRNA from the action of nucleases and delivers high concentrations to particular tissues, is still a hurdle. Moreover, unlike gene knockout, RNAi has a transient effect which does not possess the potential to cure permanent or chronic diseases. This requires construction of new vectors that integrate DNA sequences encoding siRNA into the host genome (Bridge *et al.*, 2003; Lee *et al.*, 2003b; Tomar *et al.*, 2003), carrying the risk of causing insertional mutations that may lead to neoplasia. Finally, siRNA can instigate a non-specific cytokine response that involves inflammation and cell apoptosis in a mechanism similar to that triggered by a viral infection (Bridge *et al.*, 2003).

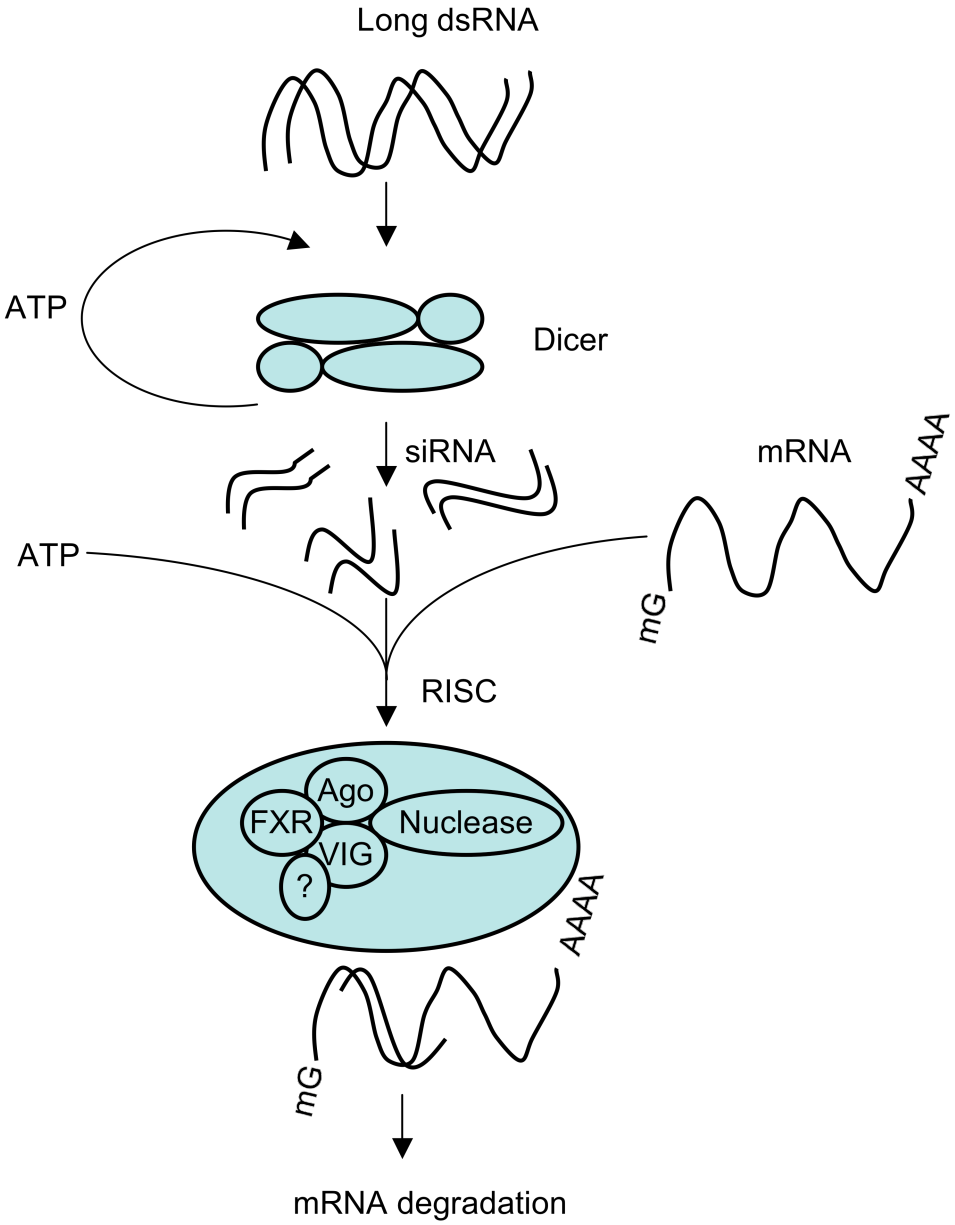

Figure 2.4: The natural anti-viral mechanism that led to the discovery of RNAi.

Viral dsRNA sequences are degraded by dsRNA-specific nuclease called "Dicer" into short (21nt) sequences termed siRNA. These short sequences form the RISC complex with at least four proteins and a nuclease in the presence of ATP. Nuclease in the RISC complex degrades complementary viral mRNA sequences. In RNAi technology, siRNA are synthesised and transfected into cells, thereby recruiting RNA-induced Silencing Complex (RISC) and inducing knockdown of complimentary mRNA sequences. Adapted from Denli & Hannon, 2003.

The biological roles of DEL1 and Twist were determined by inhibiting the expression of active proteins using siRNA technology to knock down the expression of the protein at the mRNA level. The sequence and position of specific nucleotides in the siRNA molecule are crucial factors in determining the efficacy of the knockdown for reasons that have not been fully ascertained (Elbashir *et al.*, 2001a; Elbashir *et al.*, 2001b; Reynolds *et al.*, 2004; Ui-Tei *et al.*, 2004).

The predicted sequences of the bovine DEL1 and Twist were retrieved from the National Centre for Biotechnology Information (NCBI) online database and Ambion's online siRNA Target Finder (on the website of Ambion, Cambridgeshire, UK) and were used to generate all possible siRNA sequences according to guidelines discussed by Elbashir *et al.*, 2001c. The parameters of the online tool were further refined to match the properties of effective siRNA sequences as observed by others (Elbashir *et al.*, 2001c; Reynolds *et al.*, 2004), whereby the GC content was set on a maximum of 50% and stretches of 4 or more identical nucleotides were avoided (Reynolds *et al.*, 2004). All sequences were exported into an Excel analyser workbook which analysed the sense sequence of potential siRNA molecules and rated them based on the criteria of rational siRNA design (Table 2.10) and sequences scoring below 6 were excluded (Reynolds *et al.*, 2004). The target sequences of the remaining candidates were subjected to a homology search to ensure specificity using BLAST analysis on the NCBI website. Selected siRNA sequences are shown in Table 2.11.

Anti-DEL1 and anti-Twist siRNA were purchased from Ambion (Cambridgeshire, UK) and 5'-end of the sense strand modified such that it was conjugated to Cy3 dye. Negative control 5'-carboxyfluorescein-labelled (FAM) siRNA, comprising a 'scrambled' sequence that did not resemble coding sequences, and Positive control anti-GAPD siRNA were also purchased from Ambion, (Cambridgeshire,

UK). Negative control siRNA was used in experiments to determine localisation of siRNA molecules whereas anti-GAPD positive control siRNA was used to determine transfection efficiency by inducing cell death.

Table 2.10: Criteria of the rational siRNA design.

siRNA sequences possessing the properties of rational siRNA design induce efficient knockdown. Sequences generated by Ambion online tool have appropriate GC content and no internal repeats. An Excel analyser was created to rate sense sequences according to the criteria above whereby sequences scoring below 6 were excluded (Reynolds et al., 2004).

Description	Score
Moderate to low (30%-52%) GC Content	1 point
At least 3 A/Us at positions 15-19	1 point each
A at position 19	1 point
A at position 3	1 point
U at position 10	1 point
G/C at position 19	-1 point
G at position 13	-1 point

Table 2.11: Sequences of siRNA sequences used in knockdown experiments.

The sequences of siRNA molecules were designed according to parameters previously described by others. Target sequences possessed a low GC content and no stretches of of 4 or more identical nucleotides prior to being rated according to the rational siRNA design criteria. The specificity of chosen target sequences was ensured by performing an online homology search.

Anti-DEL1	Target sequence	5'- AATCGGCTTATTTGTTTATTT
	Sense strand	5'- UCGGCUUAUUUGUUUAUUUUU
	Antisense strand	5'- AAAUAAACAAAUAAGCCGAUU
Anti-Twist	Target Sequence	5'-AAGAACACCTTTAGAAATAAA
	Sense strand	5'- GAACACCUUUAGAAAUAAAUU
	Antisense strand	5' UUUAUUUCUAAAGGUGUUCUU

2.7 siRNA and transfection

2.7.1 Optimisation of MTT viability assay

3-(4,5-Dimethylthiazol-2-yl)-2,5-diphenyltetrazolium bromide (MTT) was used as a viability assay to study anti-GAPD siRNA transfection efficiency, whereby MTT, yellow in colour, is reduced to purple formazan in the mitochondria of living (non transfected) chondrocytes.

Firstly and to confirm the linear relationship between the number of cells and the absorbance of reduced MTT, 0.1x volume of MTT solution (5mg/ml in RPMI media) was added to the culture media and chondrocytes seeded at different desnsities (0-1x10^5cells/cm^2) and incubated for three hours at 37°C. Subsequetly, media were aspirated and reduced MTT crystals dissolved in equal volume of MTT solvent, dimethyl sulfoxide (DMSO). The absorbance of the solution was measured at 570nm and the background at 690nm and the difference found to be directly proportional to the number of cells catalysing the reduction of MTT (Figure 2.5).

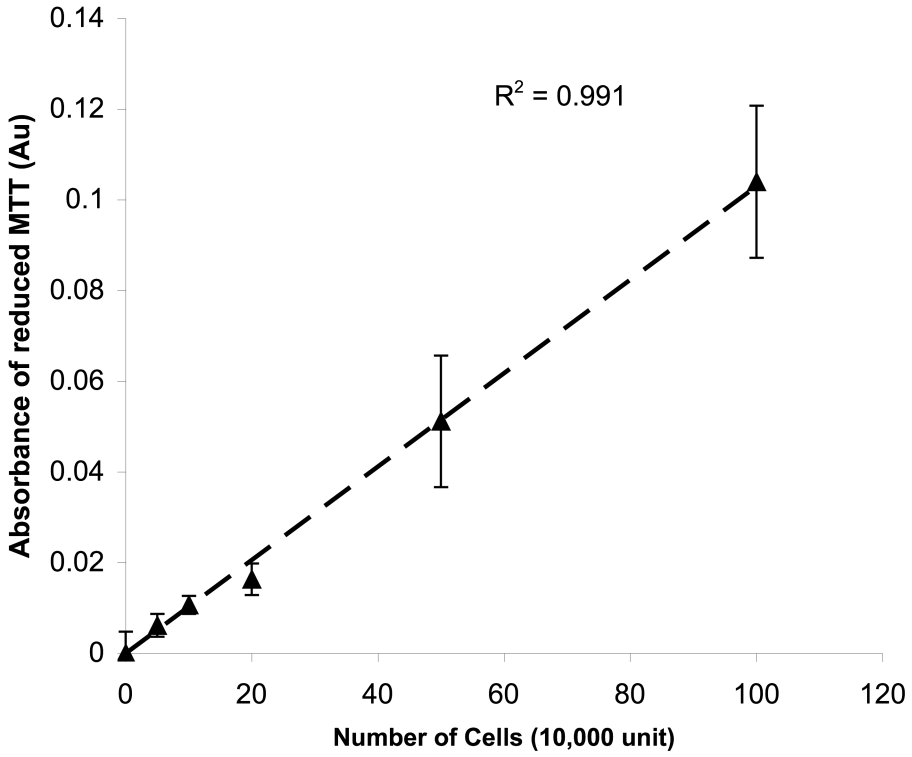

Figure 2.5: Linear relationship between the absorbance of reduced MTT crystals and the total cell number.

Chondrocytes were seeded at different desnsities into each well of a 12-well plate and incubated for three hours in the presence of 0.5mg/ml MTT solution. The media was subsequently aspirated and replaced with MTT solvent (DMSO) and the amount of MTT reduced measured by spectrophotometery at 570nm. A direct linear relationship was determined between the absorbance of reduced MTT and the number of cells. Data was pooled from three experiments. N=3. Values shown as mean ± s.e.m. R^2 value = 0.978.

2.7.2 Transfection and transfection efficiency quantification

Anti-GAPD siRNA inhibited the inability to produce ATP and inducing cellular death. The efficiency of the transfection was assayed after 48h as recommended by the manufacturer by measuring anti-GAPD siRNA-induced cell death using MTT viability test performed according to manufacturer's protocol (Sigma-Aldrich).

Freshly isolated and 2D cultured chondrocytes were assayed for transfection using HiPerfect Transfection reagent (primarily used for cell line; Qiagen) according to manufacturer's protocol by mixing different concentrations of positive control anti-GAPD siRNA (1, 5 or 10nM) with different amounts of the transfection reagent (3, 6 or 9µl/ml) in serum-free media and allowing complexes to form for 5 minutes at room temperature. Chondrocytes were seeded onto a 12-well plates at LD culture density ($2x10^4$cells/cm^2) and transfected in suspension by dropwise loading of siRNA-HiPerfect complexes.

Chondrocytes were incubated for 48 hours at 37°C in a humidified incubator prior to measurement of anti-GAPD siRNA-induced cell death using MTT assay. 0.1x volume of 5mg/ml MTT solution was added to the culture and chondrocytes incubated for 3 hours at 37°C prior to the removal of media containing excess MTT and the dissolution of formazan in DMSO and the measurement of absorbance at 570nm and 690nm.

Optimum transfection conditions were highly dependent on the phenotypic state of chondrocytes and therefore passage number. Although HiPerfect is recommended for the use with cell lines, satisfactory transfection efficiencies were obtained with freshly isolated chondrocytes optimally transfected with 10nM siRNA and 3µl/ml of HiPerfect and yielding 63.73±6.86% transfection efficiency (Figure 2.6). Upon 2D culture, however, significant differences in

transfection efficiencies were observed under similar conditions (Figure 2.7-Figure 2.8). Optimum transfection efficiencies were achieved with 10nM siRNA and 9µl/ml HiPerfect for P1 (71.38±4.24%), whereas no significant differences were observed in P2 chondrocytes with different complex combinations (1nM siRNA and 3µl/ml HiPerfect; 61.91±4.35%). Due to the high cost of the transfection reagent and the positive control siRNA, transfection efficiency experiments were performed once for every passage.

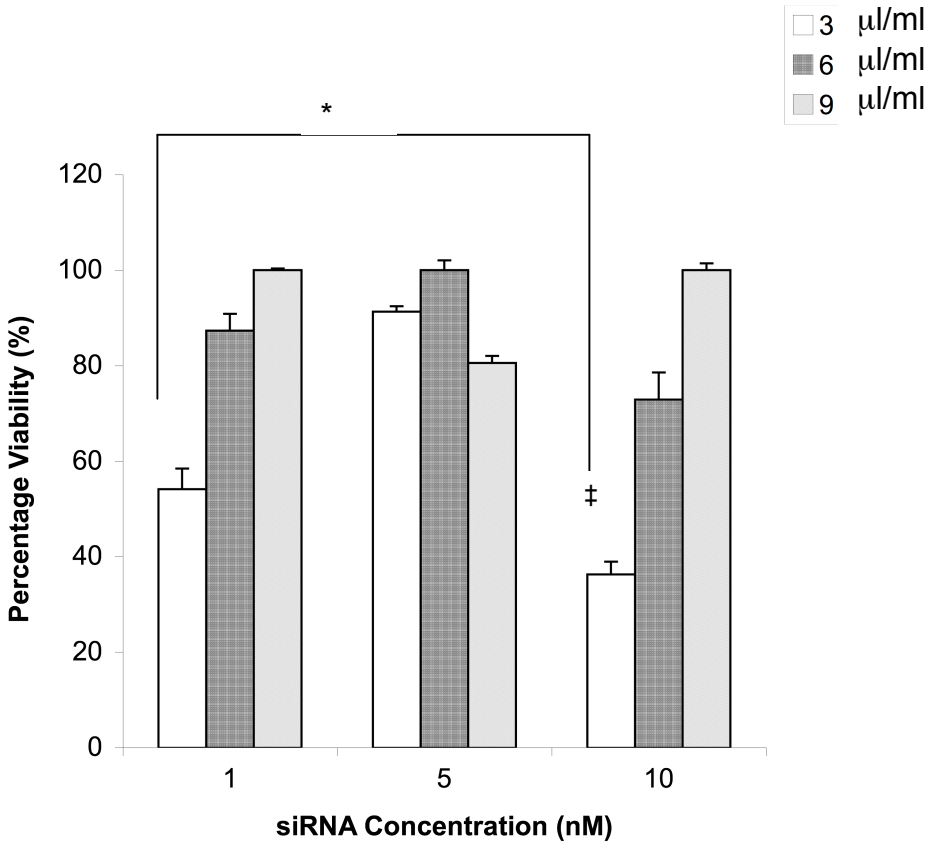

Figure 2.6: Transfection efficiency of freshly isolated chondrocytes (P0)

Chondrocytes were seeded and transfected in suspension with complexes of anti-GAPD positive control siRNA and HiPerfect transfection reagent, prepared at different concentrations. Chondrocytes were incubated for 48 hours and subsequently 0.1x volume MTT solution added and incubated for a further 3 hours. The media containing excess MTT was aspirated and replaced with MTT solvent and absorbance of reduced MTT was measured. Highest Transfection efficiency 63.7% (‡) in freshly isolated chondrocytes was obtained using 10nM siRNA and 3µl/ml HiPerfect. Experiment was performed once, N=3. Values shown as mean ± s.e.m. T-test p-values were deemed significant when p<0.05 (*) and p<0.01 (**).

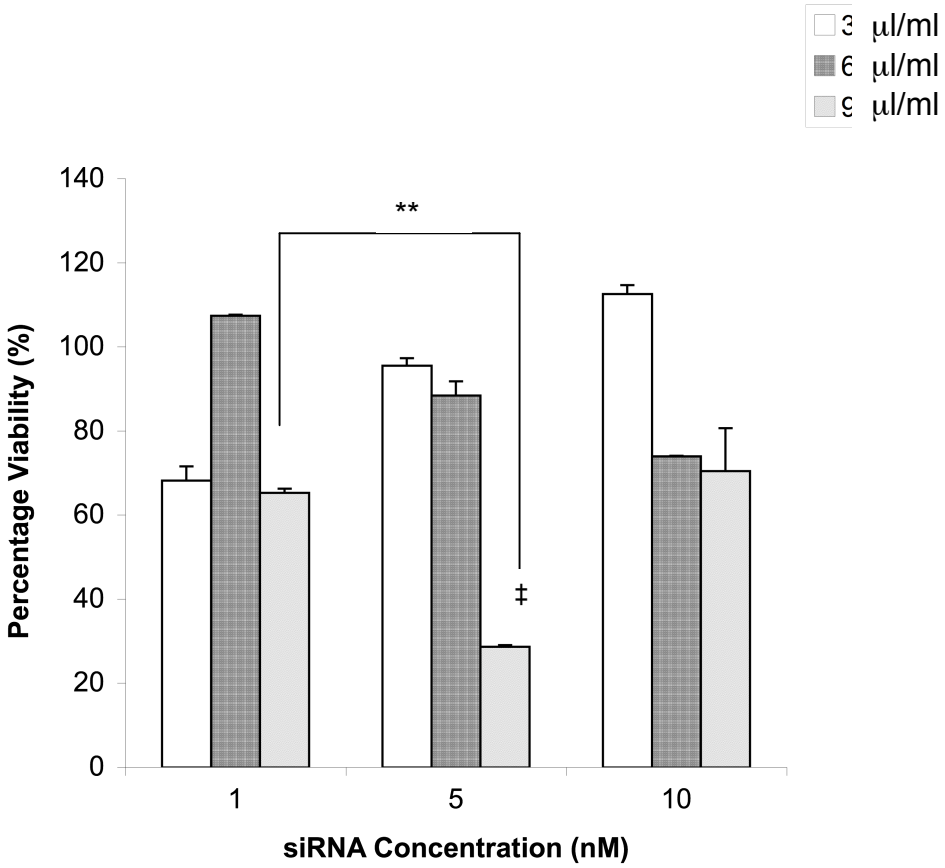

Figure 2.7: Transfection efficiency monolayer expanded chondrocytes after 9 days in culture (P1)

Chondrocytes were seeded and transfected in suspension with complexes of anti-GAPD positive control siRNA for 48 hours prior to performing a MTT viability assay. Chondrocytes were incubated with 0.5mg/ml MTT for 3 hours prior to aspiration of media and dissolution of formazan crystals in DMSO and measurement of solution absorbance. Highest Transfection efficiency of P2 chondrocytes was obtained using 5nM siRNA and 9µl/ml, transfection efficiency of 71.4% (‡). Experiment was performed once, N=3. Values shown as mean ± s.e.m. T-test p-values were deemed significant when p<0.05 (*) and p<0.01 (**).

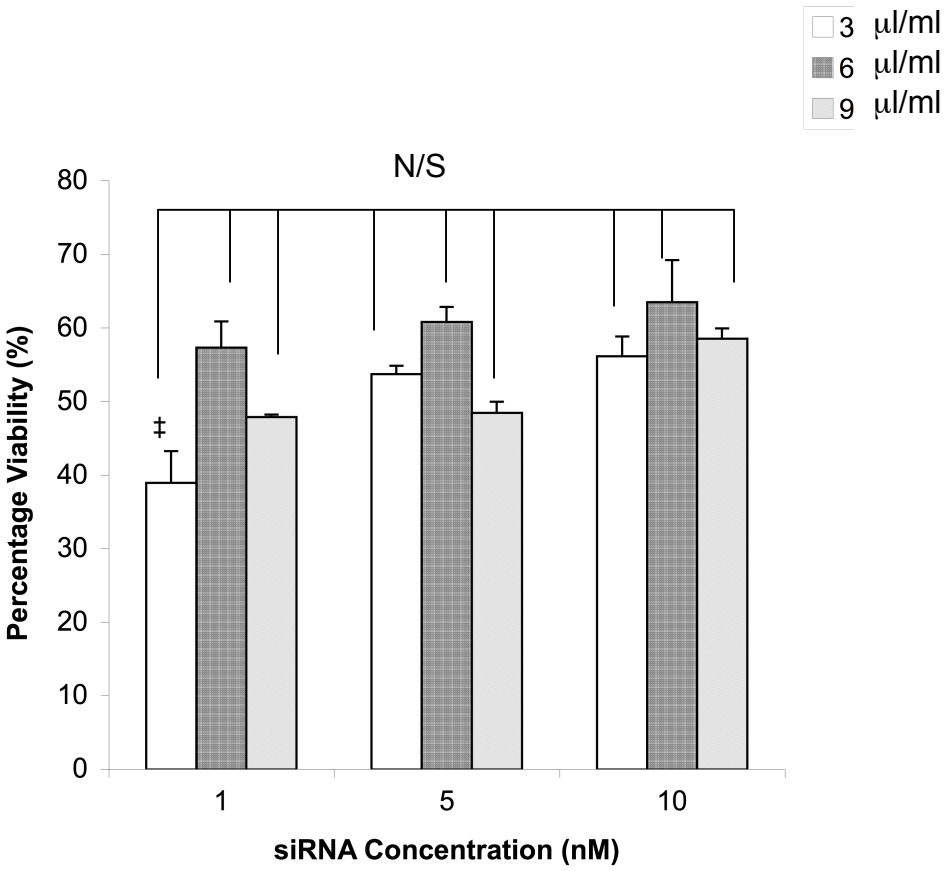

Figure 2.8: Transfection efficiency monolayer expanded chondrocytes after 14 days in culture (P2).

Chondrocytes were seeded and transfected in suspension with complexes of anti-GAPD positive control siRNA and MTT viability assay performed. Chondrocytes were incubated for 48 hours and subsequently 0.1x volume MTT solution added and incubated for a further 3 hours. The media containing excess MTT was aspirated and replaced with MTT solvent and absorbance of reduced MTT was measured. No significant differences in the transfection efficiency of P3 were observed in response to different complex combination and thus 1nM siRNA complexed with 3μl/ml HiPerfect (yielding a transfection efficiency of 61.4%) was chosen due to economic reasons (‡). Experiment was performed once, N=3. Values shown as mean ± s.e.m.

2.7.3 Uptake and localisation of siRNA

The uptake and localisation of the siRNA molecules was also confirmed by confocal microscopy using FAM-labelled negative control siRNA molecules transfected using the optimum conditions obtained from the GAPD-transfection and MTT assay. Chondrocytes were transfected in suspension and incubated for 48 hour prior to being fixed using ice-cold 3% formaldehyde for 20 minutes at 37°C, washed three times in ice-cold PBS to remove formaldehyde and then quenched for 10 minutes in ice-cold 50mM NH_4Cl. Chondrocytes were permeabilised using 0.1% Triton X100 in PBS for 5 minutes and then dipped in 100mM Glycine to stop the permeabilisation followed by washing three times in ice-cold PBS and incubation with 2μM TO-PRO3 for 45 minutes at room temperature. After the incubation period, chondrocytes were washed three times with ice-cold PBS and visualised using Confocal Laser Scaning Microscopy (CLSM). siRNA molecules were observed to be peri-nuclearly localised as described by the manufacturer (Figure 2.9).

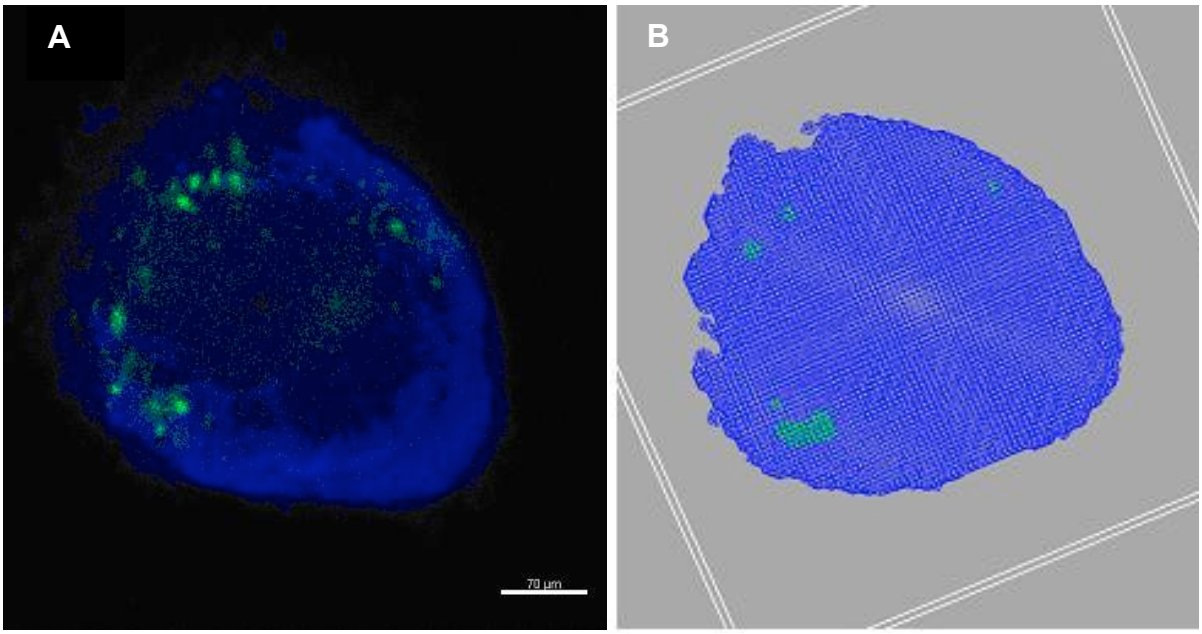

Figure 2.9: Confocal Z-stack series of images of chondrocytes after 48 hours of transfection with 10nM FAM-labelled negative control siRNA (green) and 3µl/ml of HiPerfect.

Chondrocytes were fixed using 3% formaldehyde solution, permeabilised in Triton X100 and stained with 2µM TO-PRO3 (blue). Z-stack images were acquired using confocal laser scanning microscopy (CLSM) where perinuclear localisation of the siRNA moleculesw as observed (Panel A). Z-stack series were reassembled in Imaris 6.3.1 (Bitplane) with a threshold level of 10% and 20% for TO-PRO3 and FAM, respectively, and 3D wire frame isosurface surpass applied (Panel B). Image was taken with water-immersion lens, x63.

2.8 Actin organisation

For actin labelling, chondrocytes were fixed using ice-cold 3% formaldehyde for 20 minutes at 37°C, washed three times in ice-cold PBS to remove excess formaldehyde and then quenched for 10 minutes in ice-cold 50mM NH_4Cl. Chondrocytes were subsequently permeabilised using 0.1% Triton X100 in PBS for 5 minutes and then dipped in 100mM Glycine to stop permeabilisation prior to being washed three times in ice-cold PBS and then labelled with Alexa 488-phalloidin in the dark for 45 minutes. After the incubation period, chondrocytes were washed three times with ice-cold PBS and z-stack images (series) of chondrocytes were acquired using confocal laser scanning microscopy and Nyquist settings.

Images of actin cystoskeleton were imported into Hygens 3.3 (SVI; Hilversum, The Netherlands) and deconvolved using default settings, imported into Imaris 6.3.1 (Biplane; Zurich, Switzerland) where images were created. The organisation of the actin cytoskeleton was studied using ImagePro 7.0 (Media Cybernetics; Maryland, USA) and fluorescence intensity determined using Linear Profiling across the cell diameter. The fluorescence profiling of individual chondrocytes was plotted against standardised cell diameter (%) and transcellular peaks in fluorescence corresponded to individual actin structures termed ‘striation units’ (StU), the count of which providing a representation of the number of filaments within the cellular body (Figure 2.10).

Mean of fluorescence of chondrocytes within the same passage was calculated and plotted against 10% increments in standardised cell diameter, and the first and last peaks in fluorescence (observed between 0-20% and 80-100% standardised cell diameter, respectively) were deemed cortical actin condensations. Binomial best fit curves for the mean cortical actin fluorescence

were plotted and average fluorescence across the standardised diameter of chondrocytes represented by linear regression line functions (Figure 2.11). The equations were integrated against the diameter to produce areas under the fluorescence curve used to estimate the ratio of cortical to filamentous actin as shown.

For cortical actin, the equation for best fit curve was integrated as follows.

$$y = ax^2 + bx + c$$

$$\int y = \int_{0\%}^{20\%} \frac{a}{3}x^3 + \frac{b}{2}x^2 + cx + \int_{80\%}^{100\%} \frac{a}{3}x^3 + \frac{b}{2}x^2 + cx$$

For filamentous actin, the calculation was as follows.

$$y = mx + c$$

$$\int y = \int_{20\%}^{80\%} \frac{m}{2}x^2 + cx$$

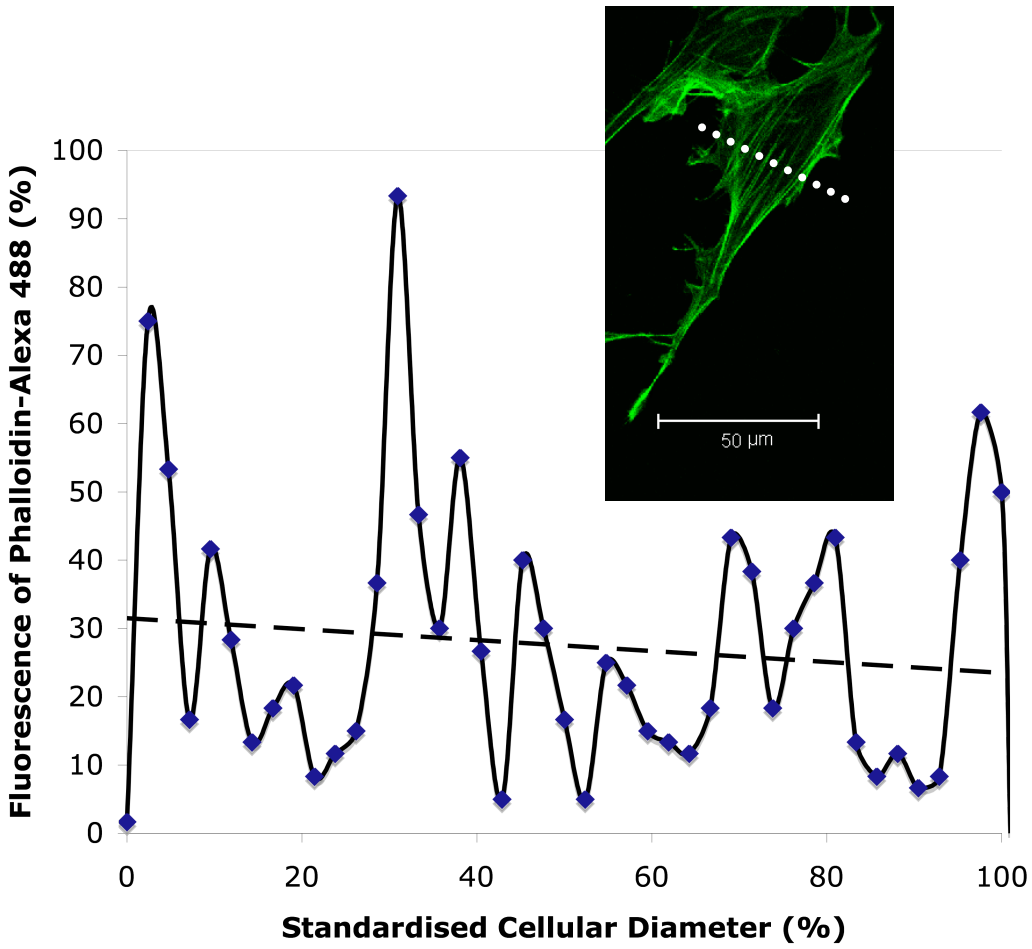

Figure 2.10 Representative diagram of fluorescence of actin-phalloidin-alexa 488 complexes across standardised cellular dimensions.

Confocal images of a P3 2D cultured chondrocyte stained for actin with phalloidin-alexa 488 was chosen at random for representative purposes (inset), deconvolved and reassembled in Image Pro as previously described. The fluorescence intensity was measured across the cell and plotted against the standardised cellular diameter (%). The first and last peaks were deamed cortical, a straight line representing background fluorescence plotted, and the number of peaks above that line counted and each deemed a striation unit.

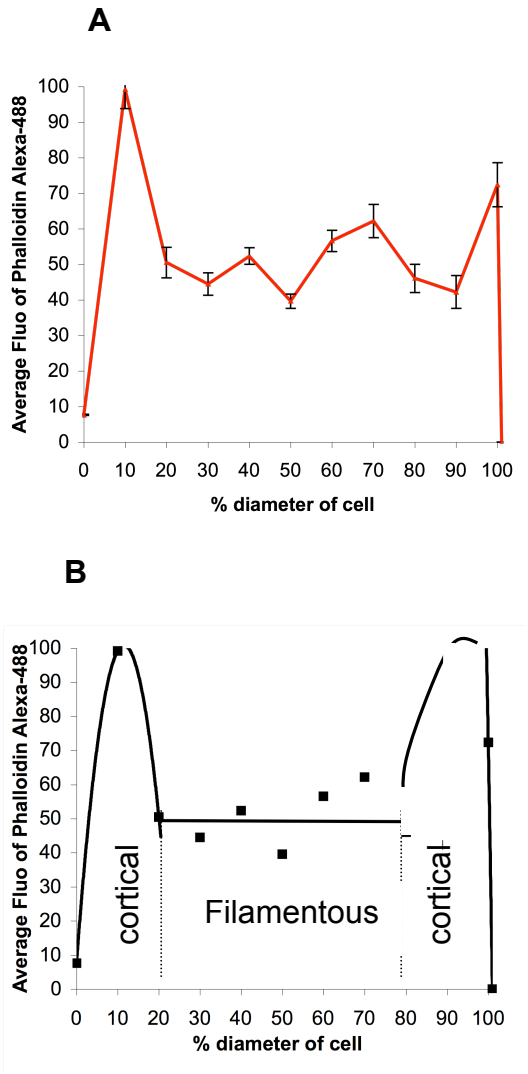

Figure 2.11: Representative mean fluorescence of phalloidin-alexa 488 across standardised cell diameter 2D cultured chondrocytes.

P3 chondrocytes chosen for illustrative purposes whereby chondrocytes were fixed and stained with phalloidin-alexa488 to detect the organisation of the actin cytoskeleton. Images were analysed using ImagePro to produce actin fluorescence against standardised cell diameter of P3 chondrocytes (Panel A). These data were used to plot a best fit binomial function representing the first and last peaks (cortical) and a best fit line for the remaining peaks (filamentous actin). The equations of the graphs were integrated to mathematically calculate the areas under the cortical and filamentous parts of the plot and consequently the ratio of cortical and filamentous actin (representation in Panel B). N=4, n=36. Data shown as mean ± s.e.m.

2.9 Volume, cellular dimensions and Sphericity of chondrocytes

2.9.1 Optimisation of Imaris Isosurface Feature using beads

In order to study changes in cellular morphology and quantify cellular dimensions in response to 2D culture, confocal microscopy was used in conjunction with the isosurface surpass feature on Imaris. The isosurface feature was used to create 3D polygon 'objects' surrounding individual cells in series of images and was initially optimised using glass beads of known volume (520μm^3) by studying the apparent volume obtained with 10% minimal threshold intervals. Voxel sizes were obtained from the series properties using Leica Lite and entered in the isosurface surpass wizard and objects closed at border.

A direct linear relationship was found between the threshold percentage and the apparent 'object' volume, and line regression performed to mathematically ascertain the percentage threshold yielding the correct volume. This value was determined at 60% threshold (Figure 2.12).

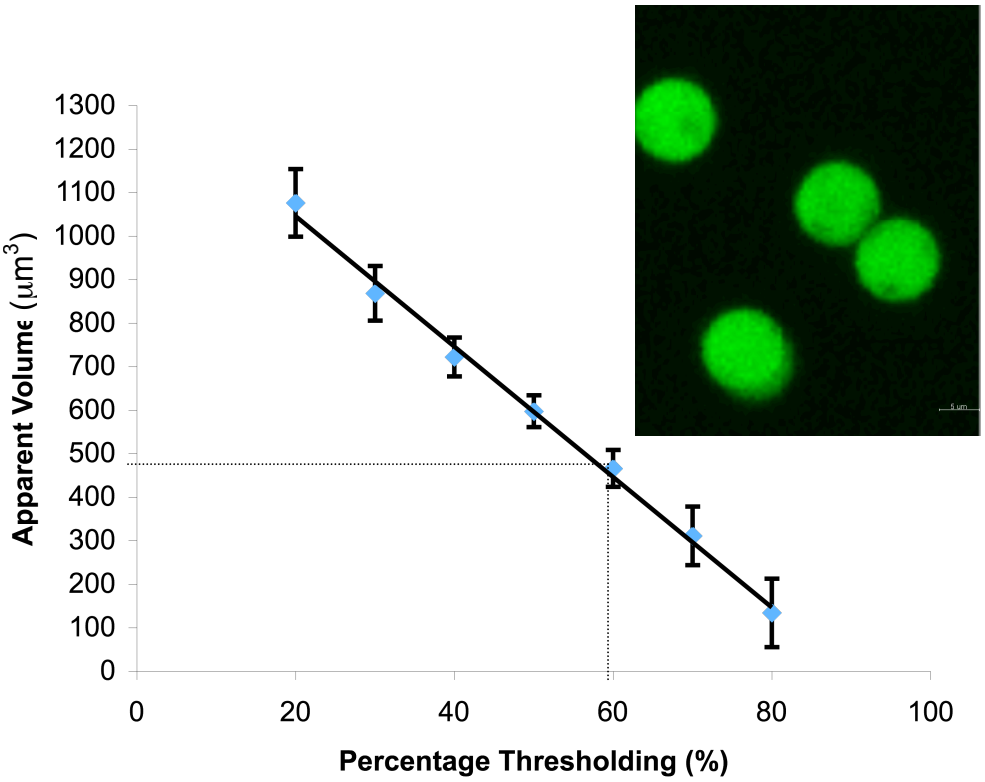

Figure 2.12: Apparent volume of beads analysed using Imaris 6.3.1 using 10-90% threshold.

Fluorcent beads of a known volume (520μm^3) were imaged using confocal laser scanning microscopy and the images imported into Imaris 6.3.1 (Bitplane) as previously described and the apparent volume acquired at 10% threshold intervals. Linear regression was used to calculate the value at which the apparent volume acquired by Imaris equalled the real volume and that was found to be at 60% threshold. Data shown as mean ± s.e.m. R^2 value = 0.952.

2.9.2 Chondrocyte Cell Dimesion and Volume Acquisition

During 2D cultures, chondrocytes undergo drastic changes in morphology from a sphere-like shape into a 'flat' fibroblast-like shape. The change in morphology of chondrocytes during culture was observed by studying the cell dimensions including depth (a), width (b), length (c), and sphericity (ψ), defined as the ratio of the surface area of a sphere with the same volume as a given chondrocyte cell to the surface area of the chondrocytes, where V is the volume of the chondrocytes and A is the surface area of the perfect sphere.

$$\Psi = \frac{\pi^{\frac{1}{3}} \times (6V)^{\frac{2}{3}}}{A}$$

Due to the change in cellular morphology upon 2D culture, a threshold of 60% was deemed unsuitable for 'flat' chondrocytes as an isosurface object merely encompassed the nucleus (Figure 2.13). The depth of the nucleus at 60% threshold was termed 'nuclear coefficient' (a_η) and was used to standardise the apparent dimensions ($b_{10\%}$ and $c_{10\%}$) and volume ($V_{10\%}$) of chondrocytes obtained at 10% threshold. The following formulae were based on the assumption that the depth of a round nucleus of a chondrocyte is approximately equal to that of the 'flat' chondrocyte.

$$\because a \approx a_\eta$$

$$\therefore V = \frac{V_{10\%}}{\left(a_{10\%} / a_\eta\right)^3}, b = \frac{b_{10\%} \times a_\eta}{a_{10\%}}, c = \frac{c_{10\%} \times a_\eta}{a_{10\%}}$$

A

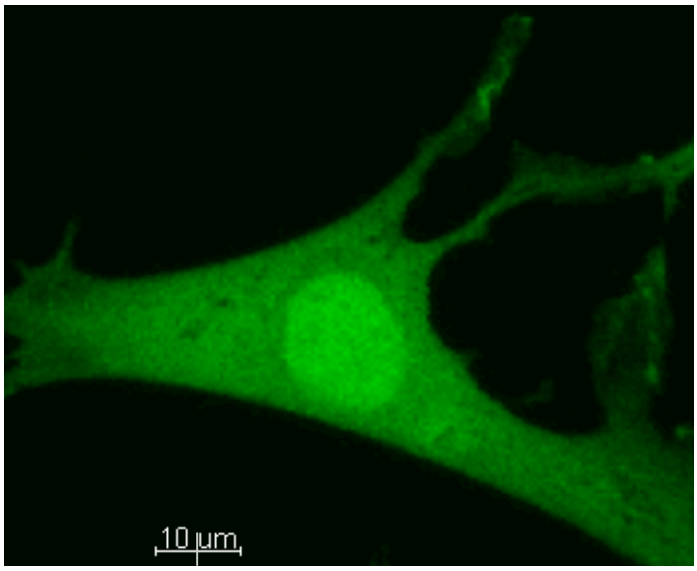

B

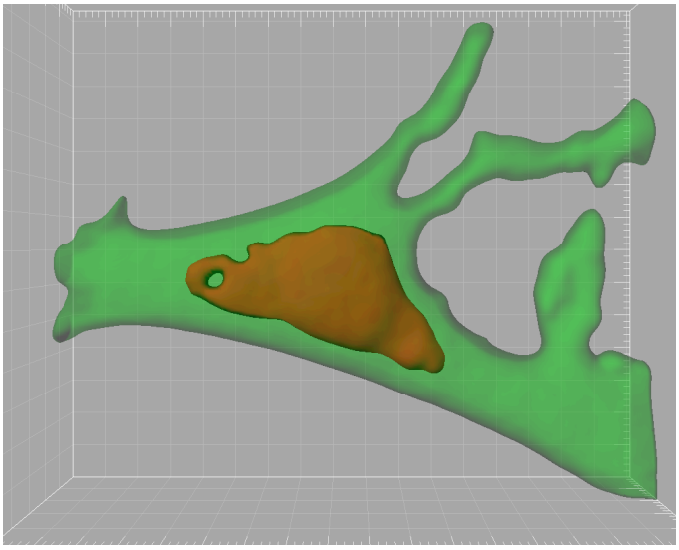

Figure 2.13: Illustrative diagram of isosurface objects created using Imaris (Bitplane) at 10% and 60% threshold.

P3 chondrocyte was chosen at random for illustrative purposes. Chondrocytes were loaded with 5µM Calcein-AM (green) and incubated for 30 min prior to image acquisition and a step size of 1µm (Panel A). The series were reassembled in Imaris 6.3.1 (Bitplane) and the isosurface function used to create 'objects' at 60% threshold (Panel B; red) and 10% threshold (Panel B; green). A threshold of 60% was deemed suitable for obtaining real volumes for round objects as optimised by using beads of known volume. A threshold of 60% in 'flat' (2D cultured chondrocytes) only yielded an object surrounding the nuclear structure, the depth of which termed nuclear coefficient and thereafter used for the standardisation of the dimensions and volume of objects created at 10% threshold.

2.9.3 RVI experiments

The capacity of chondrocytes to demonstrate RVI was studied by applying a 42% hyperosmotic challenge as previously described (Kerrigan *et al.*, 2006) and acquiring z-stack images (series) using confocal laser scanning microscopy which were subsequently reassembled in Imaris version 6.3.1 (Bitplane). Chondrocytes were seeded two hours prior to imaging and incubated in the dark with 5μM calcein AM at 37°C for 30 minutes. The medium containing excess calcein AM was aspirated and replaced with isosmotic (380mOsm) media prepared as previously described and baseline Z-stack images of chondrocytes acquired using CLSM. 1x volume of hyperosmotic media (700mOsm) was subsequently added raising the osmolarity to 540mOsm as determined by Vapro™ vapour pressure osmometer and images were acquired 1.5, 3, 5, 10 and 20 minutes post challenge. Images were reassembled in Imaris version 6.3.1 (Bitplane) and isosurface objects created at 60% and 10% threshold for freshly isolated and 2D cultured chondrocytes, respectively. Volume values were exported into Excel where changes were calculated relative to baseline values (obtained prior to hyperosmotic challenge) and plotted against time following hyperosmotic challenge.

Gradients of the lines that best fit the volume recovery points were obtained and used for the calculation of half the time required for chondrocyte to regulate 100% of initial volume in response to the challenge ($t_{½}$).

2.10 Calcium imaging

Differences in intracellular calcium ($[Ca^{2+}]_i$) signalling between freshly isolated and cultured chondrocytes were determined using a fluorescence plate reader in conjunction with the calcium indicator dye fluo-4 AM, a calcium indicator that provides a rapid and proven method of imaging intracellular calcium flux (Gandhi *et al.*, 2000). To study changes in $[Ca^{2+}]_i$, chondrocytes were seeded onto a 12-well plate at LD and allowed to adhere prior to incubation with 3μM Fluo-4 AM for 30 minutes at 37°C, and subsequently media was replaced with BPS to remove excess dye.

Firstly, the loading speed was optimised in order to reduce the effects of fluid flow (Yellowley *et al.*, 1997; Yellowley *et al.*, 1999) on calcium response. Calcium-bound fluo-4 AM was excited at 494nm and the basal fluorescence measured at 520nm bandpass prior to BPS injection at three individual speeds (420, 360 & 260 μl/s) and recording fluorescence every 14 seconds for 10 minutes (Figure 2.14). At both 420μl/s and 360μl/s, there was an immediate rise in $[Ca^{2+}]_i$ of an average of 4.52±0.34% ($p>0.05$) whereas the effects of fluid flow were diminished at 260μl/s as seen by the slight rise in calcium of 1.19±0.3%. These data concluded that 260μl/s was the injection speed deemed most suitable for further experiments (Figure 2.14)

To further optimise the protocol for Ca^{2+}-fluo-4 fluorescence measurement, Ionomycin, a calcium salt which facilitates Ca^{2+} transport across the cell membrane, was used at 3μM as a positive control (Liu & Hermann, 1978) and 2μl/ml DMSO (drug solvent) as a negative control. A DMSO solution induced a 1.34±0.6% rise in $[Ca^{2+}]_i$ which was not significantly different from the effects induced by fluid flow ($p>0.05$) whereas Ionomycin caused an influx of Ca^{2+}

raising $[Ca^{2+}]_i$ levels by 6.5±0.6%. These data confirmed that the methodology devised above is suitable for the purposes of this research (Figure 2.15).

Previous work in our group has shown that 50μM Alpha-pentyl-3-(2-quinolinylmethoxy)-benzene-methanol (REV5901) loading induced a rise in $[Ca^{2+}]_i$ (Ali *et al.*, in press) and REV5901 was therefore used as a pharmacological inducer of $[Ca^{2+}]_i$ rise. For the purposes of investigating individual channel and/or signalling molecule contribution to the calcium rise, various inhibitors were employed (Table 2.6). Sodium Calcium Exchanger (NCX) was inhibited by the use of Na^+-free physiological BPS (Sanchez & Wilkins, 2004) adjusted to 380mOsm using choline chloride (Dascalu, 1996). Stretch-activated cation channels (SACC) and transient receptor potential ion channels (TRP); were inhibited by the use of 100μM Gd^{3+}; (Kerrigan & Hall, 2008) or 10μM Ruthenium Red; (Gunthorpe *et al.*, 2002), respectively. Pharmacological inhibitors were added to culture media with fluo-4 and incubated for 30 minutes before being replaced with BPS (containing the inhibitor) and loading 1x volume 100μM REV5901 solution supplemented with the same inhibitor.

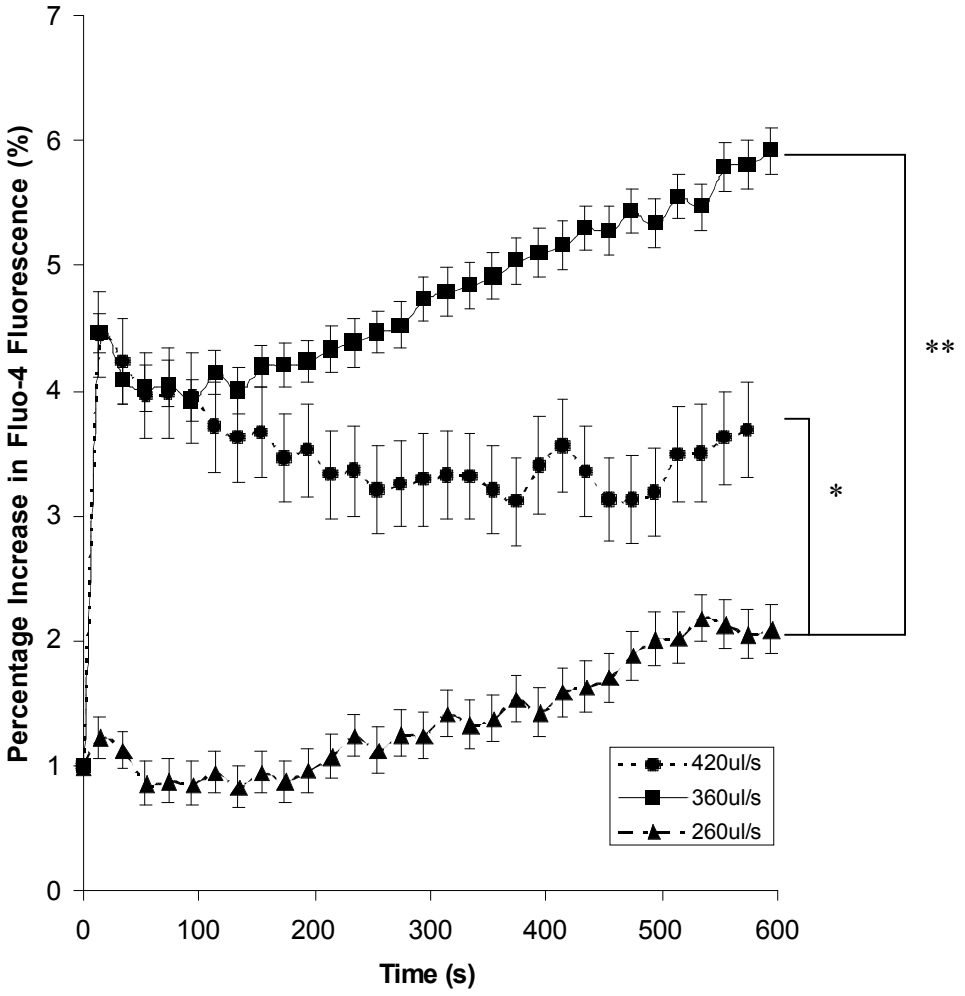

Figure 2.14: The effects of fluid flow on calcium signalling.

Freshly isolated chondrocytes were seeded at LD onto a 12 well plate and incubated in DMEM containing 3μM Fluo-4 AM for thirty minutes in the dark to allow fluorophore uptake and sufficient attachment. After the incubation period, the media containing excess dye was aspirated and replaced with 500μl calcium solution and an initial reading recorded. 500μl of the same calcium solution was injected at different speeds and the fluorescence measured every 14 seconds for 10 minutes. Experiment was performed once, N=3. Values shown as mean ± s.e.m. T-test p-values were $p<0.05$ (*) and $p<0.01$ (**).

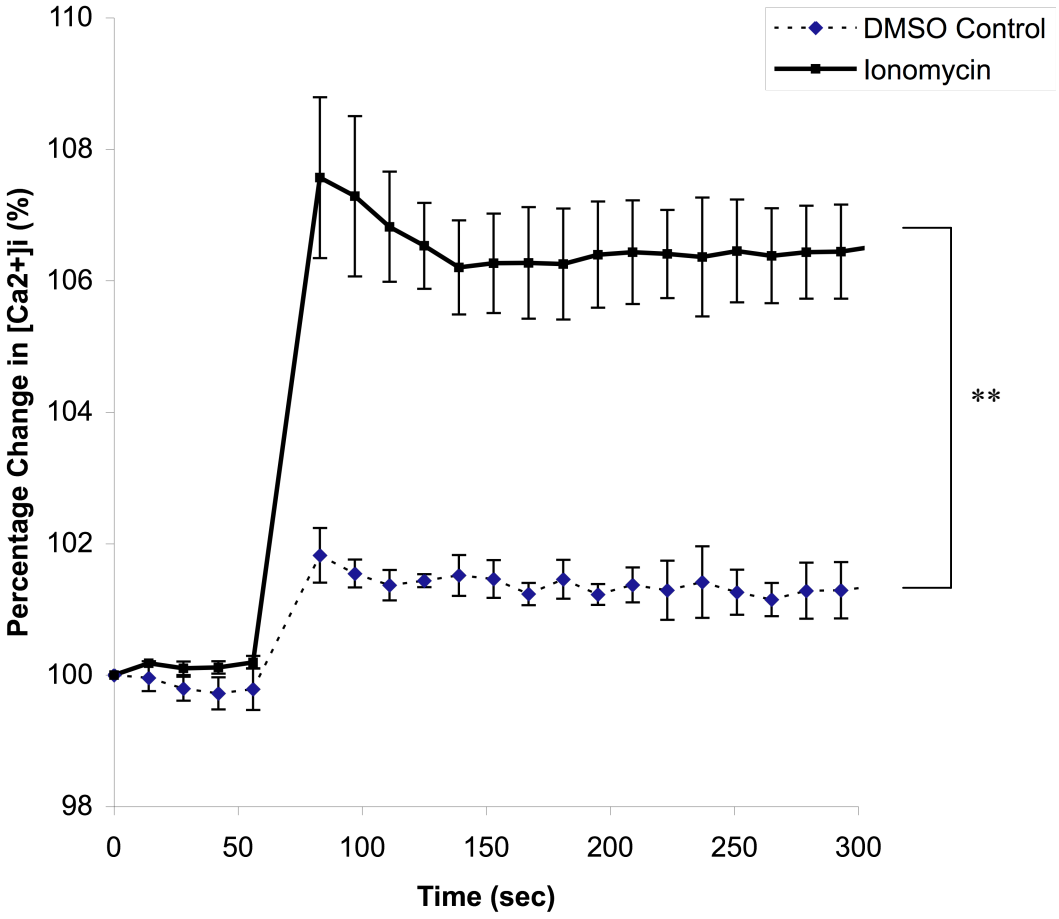

Figure 2.15: Effects of Ionomycin and negative control DMSO solution on $[Ca^{2+}]_i$ in freshly isolated chondrocytes.

The methodology devised for the calculation of changes in $[Ca^{2+}]_i$ was assayed using Ionomycin, an Ionophore used to passively raise $[Ca^{2+}]_i$. Chondrocytes were loaded with 3μM Fluo4 for 30 minutes and baseline $[Ca^{2+}]_i$ measured prior to loading of 3μM ionomycin or 2μl/ml DMSO. A DMSO solution induced a 1.34±0.6% rise in $[Ca^{2+}]_i$ (equivalent to the rise induce by fluid flow), whereas Ionomycin caused an influx of Ca^{2+} raising $[Ca^{2+}]_i$ levels by 6.5±0.6% thus indicating that the methodology is suitable for the purposes of this research. N=3, experiment repeated 6 times. Data shown as means ± s.e.m. T-test p-values were $p<0.05$ (*) and $p<0.01$ (**).

2.11 Chondrocyte Attachment Assay

The role of extracellular attachment protein, DEL1, was studied by assaying for the rate of attachment of freshly isolated and 2D cultured chondrocytes on plastic substrate. Chondrocytes were isolated (using collagenase for freshly isolated and trypsin for 2D cultured chondrocytes), washed by centrifugation, seeded at a density of $2x10^4$ cells/cm^2 (LD) and allowed to attach for 1, 2 and 4 hours in a humidified incubator at 37°C and 5% CO_2.

After the incubation period, media containing unattached chondrocytes were replaced with fresh media containing 0.5mg/ml MTT solution and chondrocytes incubated for 3 hours to allow for the reduction of MTT in the mitochondria. Excess MTT was removed and MTT solvent (DMSO) used to solubilise the reduced formazan crystals, and the absorbance measured at 570nm and 690nm (for the background) and used to quantify the number of attaching chondrocytes. The values obtained from different incubation times were used to evaluate the number of attached chondrocytes at each time point and thus calculate the rate of attachment by linear regression of number of attaching chondrocytes vs. time (hours).

2.12 Cellular protein isolation and analysis

2.12.1 Intracellular cell signal proteins

A potential cellular pathway activated by the ligand-receptor interaction between DEL1 and integrins was studied by observing the activation of protein kinase Akt by phophorylation within the pathway. Protein kinases were isolated and studied by polyacrylamide gel electrophoresis (SDS-PAGE) and western blotting using antibodies against phosphorylated and unphosphorylated forms of Akt (Silvestre *et al.*, 2005). Akt phosphorylation was studied as previously described (Sanchez-Sanchez *et al.*, 2004) by cell lysis of $3x10^5$ chondrocytes in 50µl Akt lysis buffer (20mM Tris-HCl, 120mM NaCl, 1% Trition X100, 10% glycerol, 1mM sodium pyrophosphate, 20mM sodium fluoride, 1mM sodium orthovanadate, pH=7.5 containing protease inhibitor) prior to boiling with 50µl 2x SDS-PAGE sample buffer at 95°C for 5 minutes. A sample from the extracts was diluted by a factor of 5 prior to assay using Bradford reagent due to the incompatibility of the latter with Triton in the former, protein samples were subsequently assayed and diluted to 2.5mg/ml and stored at -80°C until further use.

2.12.2 Extracellular DEL1 protein isolation

DEL1 production levels were confirmed but not quantified (due to the quality of the anti-DEL1 polyclonal antibody) in freshly isolated and 2D cultured chondrocytes using western blots and anti-DEL1 polyclonal antibody (Stratech Scientific, Suffolk). To maximise the yield of DEL1 available in the media, $2x10^4$ cells/cm^2 2D culture chondrocytes were seeded in 25cm^2 flasks, cultured for 7 days and media subsequently assayed for the production of DEL1. Conversely,

freshly isolated chondrocytes were seeded at a higher density of $3.5x10^5$ cell/cm^2, equivalent to the product of 7 (number of days of incubation for 2D cultured chondrocytes) and $5x10^4$ cell/cm^2 (the average density of 2D cultured chondrocytes within one passage period) and media isolated after 24 hour incubation. The amount of proteins produced by chondrocytes was measured by Bradford assay, the concentration calculated and samples diluted to 2.5mg/ml.

2.12.3 SDS-PAGE

Protein samples were separated in 5.7% stacking and 12.5% resolving polyacrylamide gels. Briefly, 6.7ml of acrylamide-bisacrylamide solution were dissolved in 8.0ml of water, 100µl of 20% SDS, 5ml of 4x resolving buffer (1.5M Tris-HCl, pH=8.8) and 10µl of TEMED. 150µl of freshly prepared 10% ammonium persulphate were added to the polyacrylamide solution which was allowed to set between two glass plates at room temperature under isobutanol layer to prevent oxidation. Isobutanol was removed and the gel washed twice with distilled water before overlaying the stacking gel prepared with 1.5ml of acrylamide-bisacrylamide solution, 4.4ml of water, 40µl of 20% SDS, 2ml of 4x stacking buffer (0.5M Tris-HCl, pH=6.8), 8µl of TEMED and 40µl of freshly prepared 10% ammonium persulphate.

Samples were prepared for SDS-PAGE by the addition of 1x volume of 2xSDS-PAGE loading buffer (20% glycerol, 4% SDS, 10% 2-mercaptoethanol and 0.005% bromophenol blue in stacking buffer) and the sample heated to 95°C for 5 minutes in a heating block. Wells were loaded with 100µg each, the tank filled with running buffer (25mM Tris-HCl, 0.2M glycine, 0.1% SDS, pH=8.3) and the gel subjected to 25mAmp/gel for one hour.

Protein gels were either visualised using coomassie blue staining or western immunoblotting. For the former, gels were stained in filtered staining solution (50% methanol, 10% acetic acid. 0.25% coomassie blue) with gentle shaking for 3 hours. To destain, the staining solution was decanted and sufficient destaining solution (5% acetic acid and 10% methanol) was added and replaced when necessary.

2.12.4 Western Blot

Western blot was performed in a semi-dry transfer assembly and Immobilon™-P (Millipore, Watford, UK) transfer membrane according to manufacturer's instructions. The transfer membrane was cut to the dimensions of the gel, wetted in 100% methanol for 15 seconds, placed in water for 2 minutes, and soaked in anode buffer II (25mM Tris-HCl, 10% methanol, pH=10.4) for at least 5 minutes. The gel was prepared for transfer by immersing in cathode buffer (25mM Tris base, 40mM glycine, 10% methanol, pH=9.4) and allowed to equilibrate for 15 minutes. Two sheets of filter paper were saturated in anode buffer I (0.3M Tris-HCl, 10% methanol, pH=10.4) and placed on the anode electrode plate followed by one sheet of filter paper saturated in anode buffer II, the membrane and the gel in that order. Three sheets of filter paper were wetted in cathode buffer and placed between the gel and the cathode electrode plate and the electrode leads connected and a fixed current of 100mA applied for one hour. The blotted membrane was later dried by incubation at 37°C for one hour and stored for future use at 4°C.

Western immunoblotting of Akt proteins was performed according to antibody manufacturer's instructions. Briefly, after transfer, the blot membrane was washed with Tris-buffered saline (TBS; 50mM Tris base, 0.15M NaCl, pH=7.6) for 5 minutes at room temperature, blocked in blocking buffer (5% non-fat milk, 0.1% Tween 20 in TBS) for 1 hour at room temperature and then washed three

times in TBS/T (0.1% Tween 20 in TBS) for 5 minutes each. The membrane was incubated in 10ml of TBS/T containing 10µl of the primary antibody with gentle agitation overnight at 4°C and then washed three times in TBS/T for 5 minutes each at room temperature. The blot was then incubated in 10ml of TBS/T containing 5µl goat Horseradish Peroxidase (HRP) conjugated anti-rabbit IgG at room temperature for one hour and subsequently washed 3 times with TBS/T for 5 minutes each. Upon hybrdisation, the blot was incubated in 10ml 1:1 luminol:hydrogen peroxide solution for 5 minutes, drained and exposed to x-ray film. The films were exposed to the membrane for 30 seconds prior to the former being developed and fixed in developing and fixing solutions (Kodak, Herts) for 2 minutes each. The time for exposure was adjusted if necessary.

For DEL1 western blot detection experiments, membranes were blocked in 10ml of 5% non-fat milk in 0.2% PBS/T (0.2% Tween 20 in PBS) at 4°C overnight and 10µl of anti-DEL1 polyclonal antibody (Stratech Scientific Ltd., Suffolk, UK) were added to the blocking buffer and the membrane incubated at 4°C overnight. Following incubation, the membrane was washed three times for 10 minutes each in 0.2% PBST prior to incubation in 10 ml of 5% non-fat milk in 0.1% PBST (0.1% Tween 20 in PBS) containing 2µl rabbit HRP-conjugated anti-mouse IgG at room temperature for one hour. The blot was subsequently washed 4 times with 0.2% PBST for 10 minutes each and incubated in 10ml 1:1 luminol:hydrogen peroxide solution for 5 minutes, drained and exposed to x-ray film.

Membranes were stripped for further use in the recommended buffer (100mM β-mercaptoethanol, 2% SDS, 62.5mM Tris/HCl, pH=6.7) and incubated at 50°C for 30 minutes followed by 2x wash in TBS/T for one hour each prior to drying at 37°C for 1 hour and storing at 4°C for further use.

2.12 Statistical Analysis

All statistical analysis and plotting of graphs were performed using Microsoft® Excel 2004. Equations of linear and binomial regression graphs were obtained using the 'trendline' feature and R^2 values given for every equation.

All values are shown as mean ± standard error of the mean (s.e.m) unless otherwise stated. Two-tailed homoscredastic Student's T-tests were carried out to determine whether two sets of values are different and deemed significantly different if the p value was $p<0.05$ (*) or $p<0.01$ (**).

All experiments were repeated as described in each legend. In order to reduce the effects of any genetic variation, experiments were performed with chondrocytes obtained from as many animals as possible. The number of individual joints utilised for each experiment was denoted (N) and the number of cells studied, where applicable, was denoted (n).

3 Experimental Chapter: The influence of chondrocyte expansion on phenotype, morphology and dedifferentiation.

3.1 Chapter introduction

*C*hondrocytes in adult cartilage do not undergo cell division, but upon isolation and introduction to serum-enriched media, chondrocytes are released from G0, a process termed 'expansion' (Chen *et al.*, 2003; Kino-oka *et al.*, 2005). Several methodologies for chondrocyte isolation and culture have been developed with a wide range of culture seeding densities (Table 3.1). Culture is performed using media containing 4.5g/L glucose, 10% serum, 2mM L-glutamine and 50μg/ml ascorbic acid (Reginato *et al.*, 1994) and occasionally other additional supplements including vitamin D3 (Harmand *et al.*, 1984). For purposes of expansion and subsequent re-introduction into patients, chondrocytes are cultured in monolayers or 3D matrices composed of hydrogels (Reginato *et al.*, 1994), agarose (Spirito *et al.*, 1993), collagen substrates (Ana M. Schor, 2001), pellet models (Johnstone *et al.*, 1998; Yoo *et al.*, 1998) or alginate beads (Guo *et al.*, 1989; Shakibaei & De Souza, 1997).

Changes in chondrocyte morphology, phenotype and expression in response to *in vitro* expansion have been the subject of extensive studies as previously discussed (Benya *et al.*, 1981; Benya & Shaffer, 1982a). When cultured in monolayers (in 2D) or treated with retinoic acid, the most apparent change is a switch from spherical/ellipsoid to spread/attached morphology as observed as early as the 5th day in culture (Shakibaei *et al.*, 1997), a process that could be reversed upon re-introduction of 2D cultured chondrocytes into 3D support (Benya & Shaffer, 1982b). These changes have not been quantified in the literature in dimensional terms and have been found to be independent of other changes in chondrocytic phenotype (Horton & Hassell, 1986).

It has been noted, however, that accompanying changes in actin organisation contributed to potent modulation of chondrocytic phenotype where disruption of actin filaments using cytochalasin D and dihydrocytochalasin B recaptured

chondrocyte-specific phenotype (Benya, 1988; Benya *et al.*, 1988; Loty *et al.*, 2000). A switch in actin organization from cortical localization in freshly isolated chondroctes to higly filamentous in 2D cultured chondrocytes has been widely observed (Mallein-Gerin *et al.*, 1991; Idowu *et al.*, 2000; Zwicky & Baici, 2000), but not fully quantified. Moreover, organisation of filamentous actin in response to retinoic acid treatment (Mallein-Gerin *et al.*, 1991), Gd^{3+} incubation (Perkins *et al.*, 2005) and actin depolymerising drugs have been associated with changes in morphology (Takigawa *et al.*, 1984), a switch in 'expression battery' (Brown & Benya, 1988; Newman & Watt, 1988; Loty *et al.*, 2000; Kim *et al.*, 2003) and the capacity to exhibit RVD and RVI (Kerrigan & Hall, 2005; Kerrigan *et al.*, 2006).

A decline in the expression of chondrocyte-specific type II collagen upon monolayer culture has been largely documented (Huh *et al.*, 2003; Schulze-Tanzil *et al.*, 2004; Darling & Athanasiou, 2005) and is used, often in conjunction with changes in type I collagen expression, as a phenotypic marker. Moreover, transcription factor SOX9 has been shown to play a role in chondrocyte differentiation and to be decreased in expression in response to 2D culture (Stokes *et al.*, 2002; Tallheden *et al.*, 2004). Additional genes which increased in expression upon expansion include Twist, CD44, cadherin 11 (Stokes *et al.*, 2002), insulin-like growth factor binding protein 3 (Schnabel *et al.*, 2002; Stokes *et al.*, 2002), cox-2 (Huh *et al.*, 2003), TNF-R1 (Schnabel *et al.*, 2002) and integrins $\alpha 5$, $\alpha v \beta 3$ and $\alpha 3$ (Diaz-Romero *et al.*, 2005). Other genes that are downregulated upon expansion include $\alpha 1$, LPS-R (Diaz-Romero *et al.*, 2005), aggercan, insulin-like growth factor 2, BMP6, and types IX, XI collagen (Stokes *et al.*, 2002) and type X collagen (Tallheden *et al.*, 2004).

Therefore, In order to provide a background of intensive knowledge into the changes in chondrocytic phenotype, experiments were conducted to quantitatively study changes in cell shape and actin organisation in addition to key molecular markers of chondrocyte phenotype to further our knowledge of the mechanism of loss of phenotype in 2D expansion.

Aims of Experimental Chapter

1 Optimise 2D culture methodology of chondrocytes.

2 Study changes in cell volume, shape and dimensions in response to 2D culture.

3 Quantify changes in the ‘expression battery’ upon expansion.

4 Quantify changes in the actin cytoskeletal organisation in response to 2D culture.

Table 3.1: Range of seeding densities used in the literature for in vitro expansion of chondrocytes.

Culture Seeding Density	Reference
$5x10^3$ cell/cm^2	Haisch *et al.*, 2006
$1.5x10^4$ cell/cm^2	Schnabel *et al.*, 2002; Darling & Athanasiou, 2005
$2x10^4$ cell/cm^2	Waymouth, 1974
$5x10^4$ cell/cm^2	Huh *et al.*, 2003; Diaz-Romero *et al.*, 2005
$1x10^5$ cell/cm^2	Stokes *et al.*, 2002
$2x10^5$ cell/cm^2	Johansen *et al.*, 2001; Hamilton *et al.*, 2005a; Hamilton *et al.*, 2005b
$3x10^5$ cell/cm^2	Perkins *et al.*, 2005

3.2 Results

3.2.1 Expansion and Growth Rates

Chondrocytes were isolated from bovine metacarpal and metatarsal joints into DMEM and prepared as previously described (see Materials and Methods). Briefly, cartilage explants were washed in DMEM and subsequently incubated in 0.5mg/ml collagenase in 380mOsm DMEM for 18 hours. Isolated chondrocytes were washed and seeded at different densities in culture media containing 10% FCS, 1% P/S, 50μg/ml ascorbic acid and 20mM glutamine to determine the optimal conditions for culture for all future experiments. Chondrocytes were subcultured for up to three weeks until 80% confluency was achieved, whereupon chondrocytes were trypsin-lifted, counted and re-seeded at the same density (Figure 3.1).

Chondrocytes cultured at High Density (HD) did not show an increase in cell number by the end of the first passage (day 9; Figure 3.1). This was most likely due to contact and density inhibition mechanisms inhibiting cell growth (Freshney, 2001). Conversely, chondrocytes cultured at Intermediate Density (MD) exhibited an increase of 47.50±29.44% in cell number during the first passage (9 days) and subsequently, as chondrocytes adopted a fibroblast-like morphology, ceased to increase in number. Conversely, chondrocytes cultured at $2x10^4$cells/cm^2 (Low Density; LD) demonstrated a steady increase in cell number (r^2>0.9) during the entire culture period and therefore this culture density was selected for all expansion experiments. In order to determine the maximum culture time, chondrocytes plated at LD were cultured until cellular senescence was reached upon culture to passage number 8 (60 days in culture) as observed by the inhibition of further cellular division.

After 2 days of introduction to culture, chondrocytes were collected and cell viability assayed by trypan blue and a haemocytometer. When chondrocytes were seeded at HD or MD, there was a mean viability of 90.39±4.01% or 90.06±5.46%, respectively (Figure 3.2). Converely, cell viability decreased to 71.02±8.66% in response to culture at $2x10^4$cells/cm^2 (LD).

These data suggested that despite a reduction in chondrocyte viability, LD was favourable choice for 2D cell culture and was used thereafter as part of a standard culture technique (Table 3.2).

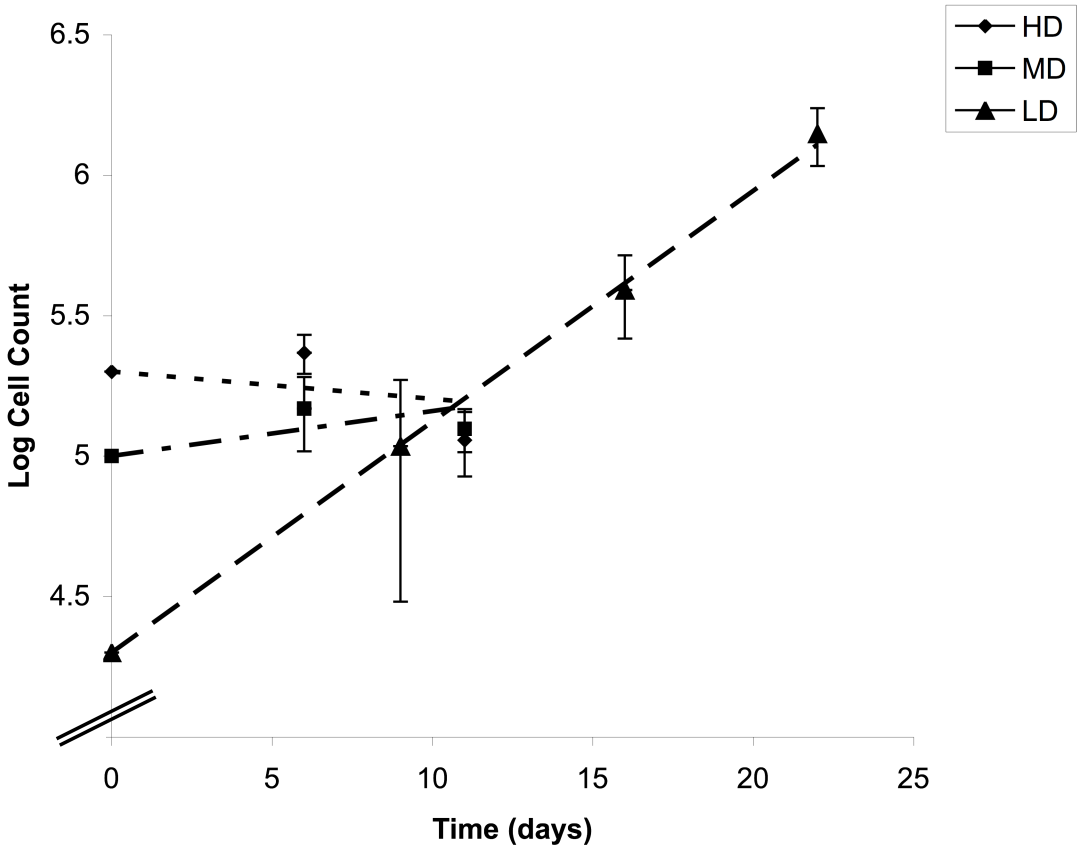

Figure 3.1: Growth curve of bovine articular chondrocyte upon in vitro culture.

Chondrocytes were isolated using 0.8mg/ml collagenase in 380mOsm DMEM overnight and seeded at different densities (High density, HD; Mean Density MD; and Low Desntity, LD) into 380mOsm media supplemented with 1% penicillin/streptomycin, 20mM L-Glutamine, 10% FCS, 50µg/ml Ascorbic Acid. Cells were subcultured upon 80% confluence, counted and re-seeded at the same density. A growth curve was plotted of log total cell number vs. time and a linear regression used to calculate growth rate and doubling time. There was a steady increase in cell number only when cultured at LD. Data were pooled from 23 individual experiments, N=12. Data shown as mean ± s.e.m. R^2 for LD = 0.998.

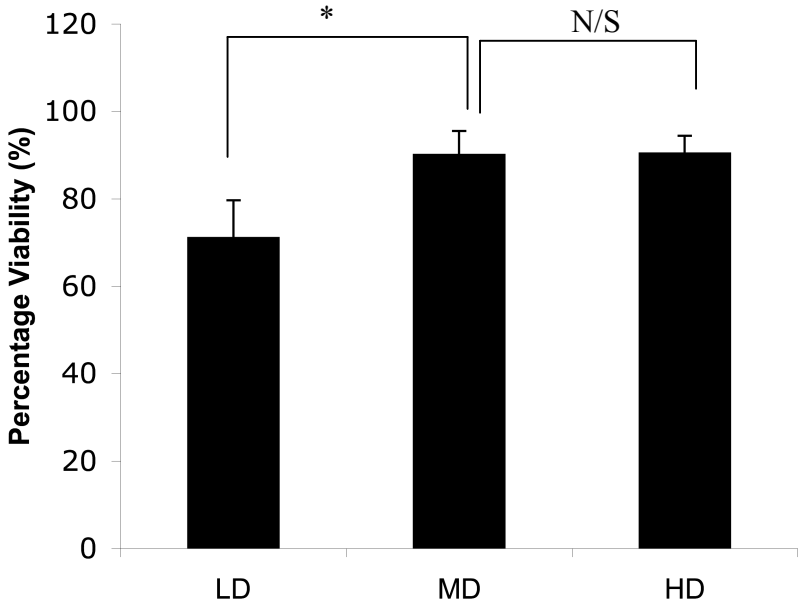

Figure 3.2: Viability assay in response to in vitro 2D culture.

The viability of chondrocytes cultured at the different densities investigated was obtained by trypan blue viability test. 2 days following the initiation of culture, chondrocytes in suspension were isolated and counted using a haemocytometer. In high density (HD) and intermediate density (MD) culture protocols, there was 90.06±5.46% and 90.39±4.01% viability, whereas low density (LD) culture yielded a reduction in cell viability to 71.02±8.66%. N=6. Data were pooled from 23 individual experiments and shown as mean ± s.e.m. T-test p-values were deemed significant when p<0.05 (*). N/S, non significant.

Table 3.2: Summary of culture properties of chondrocytes cultured at literature-based seeding densities.

It was necessary to establish the culture conditions including culture seeding density in order to ensure reproducibility of results. Three seeding densities previously used in the literature were assayed for cell growth and viability using trypan blue. Chondrocytes cultured at high density (HD) exhibited high viability upon two days in culture but did not increase significantly in number whereas at intermediate density (MD) there was a slight initial rise in cell number which was abolished upon further culture. In low density (LD) cultures, there was 71.0±4.0% viability by the second day in culture and a steady rate of cell growth with a doubling time of 3.7±0.2 days. T-test p-values were deemed significant when p<0.05 (*) and p<0.01 (**)

	Doubling time (days)	R^2 value	Viability (%)	Seeding Density (cell/cm^2)
HD	-31±1.0	0.23	90.4±8.7	2x10^5 (Johansen *et al.*, 2001; Hamilton *et al.*, 2005a; Hamilton *et al.*, 2005b)
MD	19±0.9	0.12	90.1±5.5	1x10^5 (Stokes *et al.*, 2002)
LD	3.7±0.2	0.99	71.0±4.0 (*)	2x10^4 (Waymouth, 1974)

3.2.2 Morphology, shape and volume of freshly isolated and expanded chondrocytes

Currently, the process of chondrocyte de-differentiation and the relationship between phenotype and morphology, essential data that will underpin all replacement technologies, is not fully understood, and this process was therefore investigated. For the purposes of studying the morphology and cellular dimensions of chondrocytes upon culture, freshly isolated and 2D cultured chondrocytes were incubated with 5μM calcein-AM for 30 minutes at 37°C and 3D images acquired by CLSM (Materials and Methods). Z-stacks were acquired at 1μm depth intervals and reassembled in Imaris 6.3.1 to create a 3D polygon-based isosurface 'object' for each cell (Figure 3.3). The volume, sphericity (φ), depth (a; μm), width (b; μm) and length (c; μm) of every chondrocyte were determined and exported into Microsoft Excel for statistical analysis.

Within 9 days of culture, chondrocytes lost their round morphology and acquired a 'flat' fibroblast-like structure as seen by CLSM (Figure 3.3). There was a decrease in cell depth (a) in reponse to culture from 4.08±0.11μm in freshly isolated chondrocytes to 2.24±0.19, 1.96±0.10 and 2.20±0.13 in P1, P2 and P3 chondrocytes, respectively ($p<0.05$). Conversely, a significant increase ($p<0.05$) in cell length was observed upon 9 days in culture from 6.04±0.10 to 12.51±1.82μm with no further change upon longer culture periods. No change, however was observed in cell width in response to 2D culture with an average diameter of 5.17±0.08, 5.19±0.66, 4.60±0.25 and 5.17±0.96μm in freshly isolated, P1, P2 and P3 chondrocytes, respectively ($p>0.05$).

Correspondingly, these changes were confirmed by quantitatively comparing the sphericity of the cells whereby a perfect sphere has a sphericity value φ=1, and values less than 1 indicated a deviation in any of the three principal navigation vectors (a, b and c). Freshly isolated chondrocytes exhibited a sphericity factor of 0.74±0.02 which significantly decreased ($p<0.05$) during the first passage to 0.52±0.03 with no further changes observed during the culture period (Figure 3.4; $p>0.05$).

Having determined changes in chondrocyte dimensions, it was necessary to study changes in resting cell volume. Previously acquired data assumed a high level of sphericity for volume calculation (Bush & Hall, 2001), which as it was shown to change upon culture, a new method for volume analysis for 2D cultured chondrocytes was devised. Values for cell volume of individual chondrocytes were acquired using Imaris and values for 2D cultured standardised against the nuclear coefficient as previously described (Materials and Methods). Moreover, chondrocyte cell volumes were mathematically calculated from cellular dimensions using the formula for spheroids below.

$$V = \frac{4}{3}\pi \times a \times b \times c$$

When obtained using Imaris, freshly isolated chondrocytes possessed a volume of 474.72±32.08μm^3 and a mathematically calculated volume of 522.27±34.16μm^3 with no significant differences ($p>0.05$). Upon 2D culture, however, there was a significant increase ($p<0.05$) in chondrocyte cell volume to 673.38±39.59μm^3, 724.77±39.59μm^3 and 725.20±35.55μm^3 in P1, P2 and P3 chondrocytes, respectively, as determined by Imaris. No significant differences were observed between volumes of chondrocytes cultured for different periods and no significant differences were observed between values acquired from Imaris and those mathematically calculated ($p>0.05$; Table 3.3).

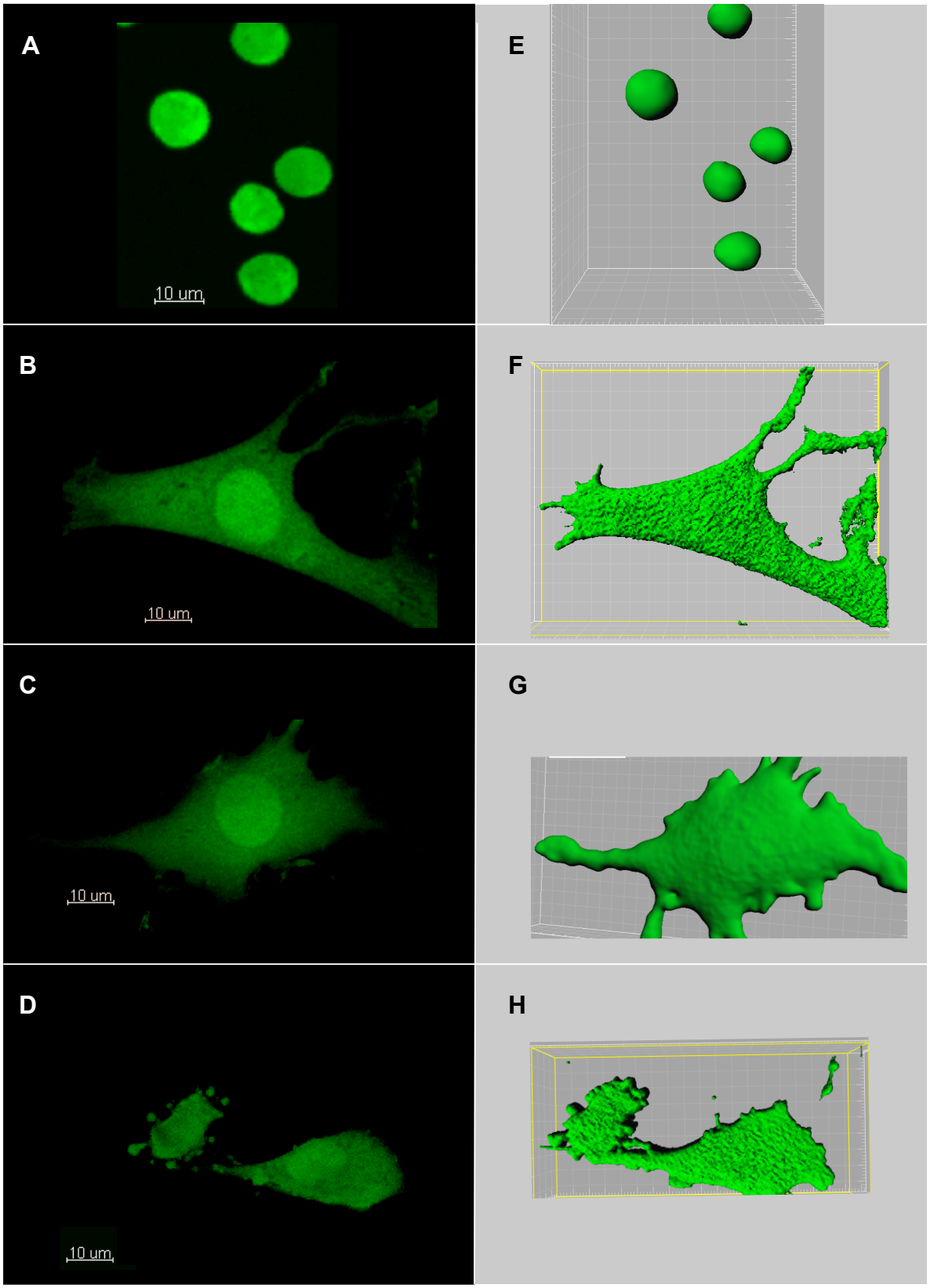
A
10 um
E
B
10 um
F
C
10 um
G
D
10 um
H

Figure 3.3: Morphology of freshly isolated and 2D cultured chondrocytes as seen under confocal microscopy.

Chondrocytes were freshly isolated (panel A) as previously described, cultured for 9, 14 or 21 days (panels B, C or D, respectively) and the loaded with 5μm calcein-AM for 30 minutes at 37°C in the dark. Chondrocytes were imaged as previously described and the series of images reassembled in Imaris as an Isosurface surpass (corresponding panels E-H) at 60% threshold for freshly isolated chondrocytes and 10% threshold for 2D cultured chondrocytes. Changes in the morphology of chondrocytes were onserved as early as 9 days post culture with a loss of a spherical cell shape. Images acquired using x63 dipping lens.

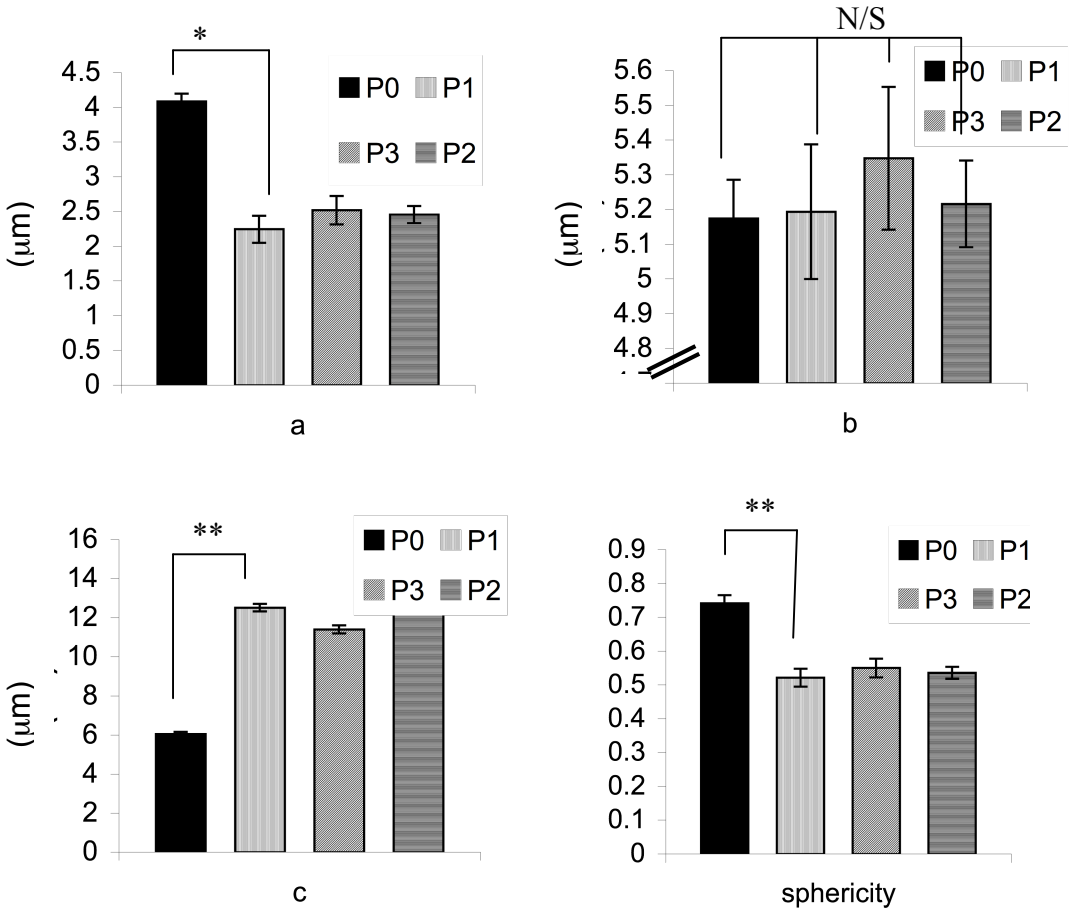

Figure 3.4: Cellular dimensions and sphericity of chondrocytes as quantified using Imaris Isosurface Surpass utility.

Series of images of chondrocytes acquired using confocal microscopy were reassembled in Imaris and isosurface 'objects' were created as described in materials and methods. Imaris was subsequently employed to determine the depth, width and length of each object (denoted a, b and c). There was a significant ~2-fold increase and decrease in chondrocyte length and depth, respectively. Moreover, there was a significant decrease in sphericity upon 9 days of culture, indicating a switch in morphology from as early as the first passage. Data pooled from 16 individual experiments. N=4, n=119. Data shown as mean ± s.e.m. T-test p-values were deemed significant when p<0.05 (*) and p<0.01 (**).

Table 3.3: Cell volume changes in freshly isolated and 2D cultured chondrocytes as acquired by Imaris and calculated mathematically.

We have devised a new protocol for the assay of cell volume in 2D cultured chondrocytes by standardising the volume of 2D cultured chondrocytes as obtained using Imaris (Bitplane) at 10% threshold against the nuclear coefficient (depth of nucleus acquired at 60% threshold). To confirm the validity of the protocol, the volumes obtained using Imaris were compared to those mathematically calculated using cellular dimensions. It was observed that there was no significant difference in the values obtained by both methods ($p>0.05$) and that both methods demonstrated an increase in chondrocyte cell volume upon 2D culture. N=4, n=119. Data shown as mean ± s.e.m. T-test p-values were deemed significant when $p<0.05$ (*) and $p<0.01$ (**); relative to P0.

	Cell Volume as acquired from Imaris (μm^3)	Cell Volume as mathematically calculated (μm^3)
Freshly Isolated (P0)	474.72 ± 32.08	522.27 ± 34.16
P1	673.38 ± 39.59 (**)	610.21 ± 35.87 (**)
P2	724.77 ± 33.03 (**)	662.80 ± 30.20 (**)
P3	725.20 ± 35.55 (**)	642.67 ± 31.51 (**)

3.2.3 Phenotype and expression profiling of cultured chondrocytes

Having determined the morphological changes which occur during culture, it was then necessary to determine changes in the key markers of the chondrocyte phenotype so these changes could be correlated. RNA was isolated from chondrocytes as previously described (Materials and Methods). Briefly, chondrocytes were treated with trypsin-EDTA to allow detachment, washed and incubated on ice in RLT lysis buffer (Qiagen, Poole) for 5 min. RNA was extracted from the lysate using RNeasy kit (Qiagen, Poole), quantified using UV spectrophotometery and reverse transcribed using ImPromII RT system (Promega, USA) as previously described. cDNA was subjected to PCR to determine the expression levels of key genes (types I and II collagens and SOX9) relative to GAPD expression levels (internal multiplexed positive control). The ratio of type II collagen to type I collagen (col2:col1) expression was determined as a marker for the state of differentiation as previously published (Benya & Shaffer, 1982b; Baici *et al.*, 1988a; Benya, 1988), whereby a high ratio is indicative of the chondrocytic phenotype.

A significant overproduction of collagen was observed as early as the first passage with relative expression level of type I collagen increasing from 1.00±0.064 to 2.70±0.63 after 9 days in culture ($p<0.01$). Expression level of type II collagen increased transiently within 9 days of culture from 0.98±0.13 to 1.58±0.15 ($p<0.05$) and subsequently returned to baseline levels after 14 days of culture with no significant differences observed ($p>0.05$). The ratio of type II collagen to type I collagen expression was therefore reduced by a factor of ~2 from as early as the first passage to 0.58±0.15 indicating an early onset switch of phenotype that was maintained for the remainder of the culture period with no futher significant change ($p>0.05$; Figure 3.5).

Expression of the chondrocytic transcription factor SOX9, a key regulator of chondrocytic phenotype was also studied upon culture to confirm the data obtained from the collagen ratio for the purpose of determining the switch in chondrocyte phenotype. A significant yet transient 1.75±0.40-fold increase in SOX9 expression ($p<0.05$) was observed within 9 days of culture. Expression levels of SOX9 expression declined upon further culture to baseline levels ($p>0.05$). This increase was associated with that of collagen indicating a potential role for SOX9 in type II collagen expression, and together the transient rise in type II collagen and SOX9 expression levels suggested that dedifferentiation occurred in a 2-step trend.

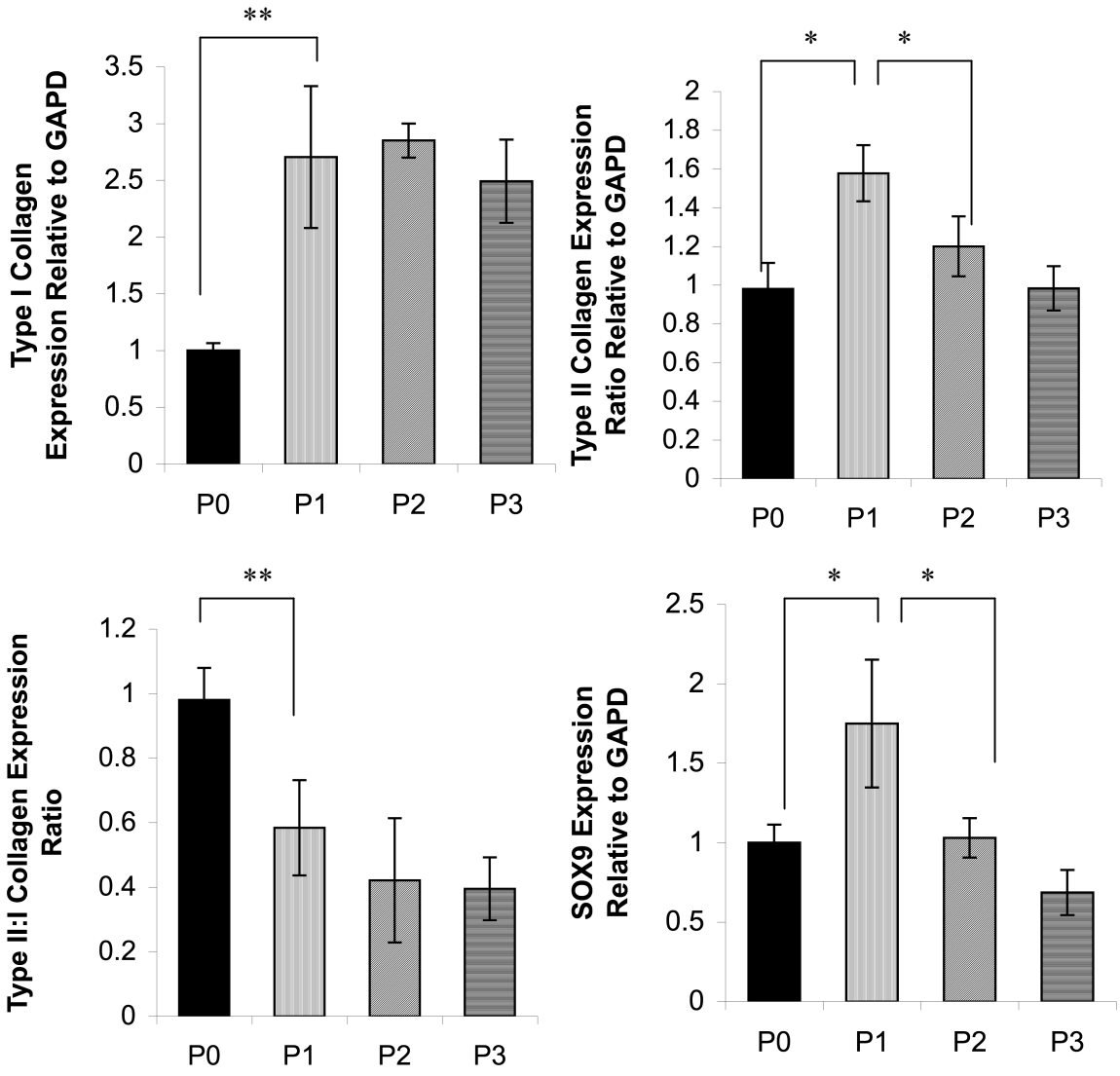

Figure 3.5 The expression profiling of chondrocytes before and throughout culture

RNA was isolated from freshly isolated and 2D-cultured chondrocytes, reverse transcribed and subjected to PCR. The amount of DNA in the PCR products was calculated from the intensity and size of the bands and calculated relative to amount of GAPD product. Changes in expression of key genes compared to amounts in freshly isolated chondrocytes (P0) and were recorded upon confluence after 9 days in culture (P1), 14 days in culture (P2) and 21 days in culture (P3). The level of expression of SOX9 declined upon culture despite the transient increase in P1. Both the expression levels of types II and I collagen increased during 2D expansion, but the ratio of type II collagen to type I collagen expression decreased significantly during the first few days of culture. Transient increase in SOX9 and type II collagen during P1 suggested that the loss of phenotype might be a multi-step process. Experiment repeated 6 times. N= 6. Values shown as mean ± s.e.m. T-test p-values were p<0.05 (*) and p<0.01 (**).

3.2.4 The regulation of actin cytoskeletal organisation upon 2D culture

The actin cytoskeleton has been shown to be a key regulator of cell morphology, cell homeostasis and has been shown to induce volume regulatory mechanisms in chondrocytes (Kerrigan & Hall, 2005; Kerrigan *et al.*, 2006). Therefore, changes in the chondrocyte actin cytoskeletal organisation were studied in response to 2D culture *in vitro*. Chondrocytes were subcultured upon 80% confluence, seeded at that density and allowed to attach overnight before being fixed in 3% formaldehyde solution. The actin cytoskeleton was labelled as previously described using phalloidin-alexa 488 and images acquired under Nyquist settings suitable for deconvolution (Kerrigan *et al.*, 2006). Images were analysed using ImagePro 7.0 (Maryland, USA) and the fluorescence intensity obtained throughout the cellular structure and plotted against the standardised cellular diameter to study the localization of the actin structures. The number of actin striation units (StU) within the cytoplasm of individual chondrocytes, shown as 'peaks' across baseline background, was obtained for further analysis of the 'branching' properties of actin filaments.

In freshly isolated chondrocytes, actin structures were mainly condensed towards the cell periphery, whereas upon 9 days of culture, actin filaments were formed throughout the cytoplasmic body as seen by confocal microscopy (Figure 3.6). There was an average of 1±1StU/cell across the cell cytoplasm of freshly isolated chondrocytes, whereas after 10 days in 2D culture, the number increased to 5±2StU/cell. There was no significant change to the number of striation units upon further culture with 6±1Stu/cell and 5±1StU/cell in P2 and P3 chondrocytes, respectively, thus confirming the loss of a differentiated, predominantly cortical actin structure within 9 days of culture (i.e. first passage; Figure 3.7).

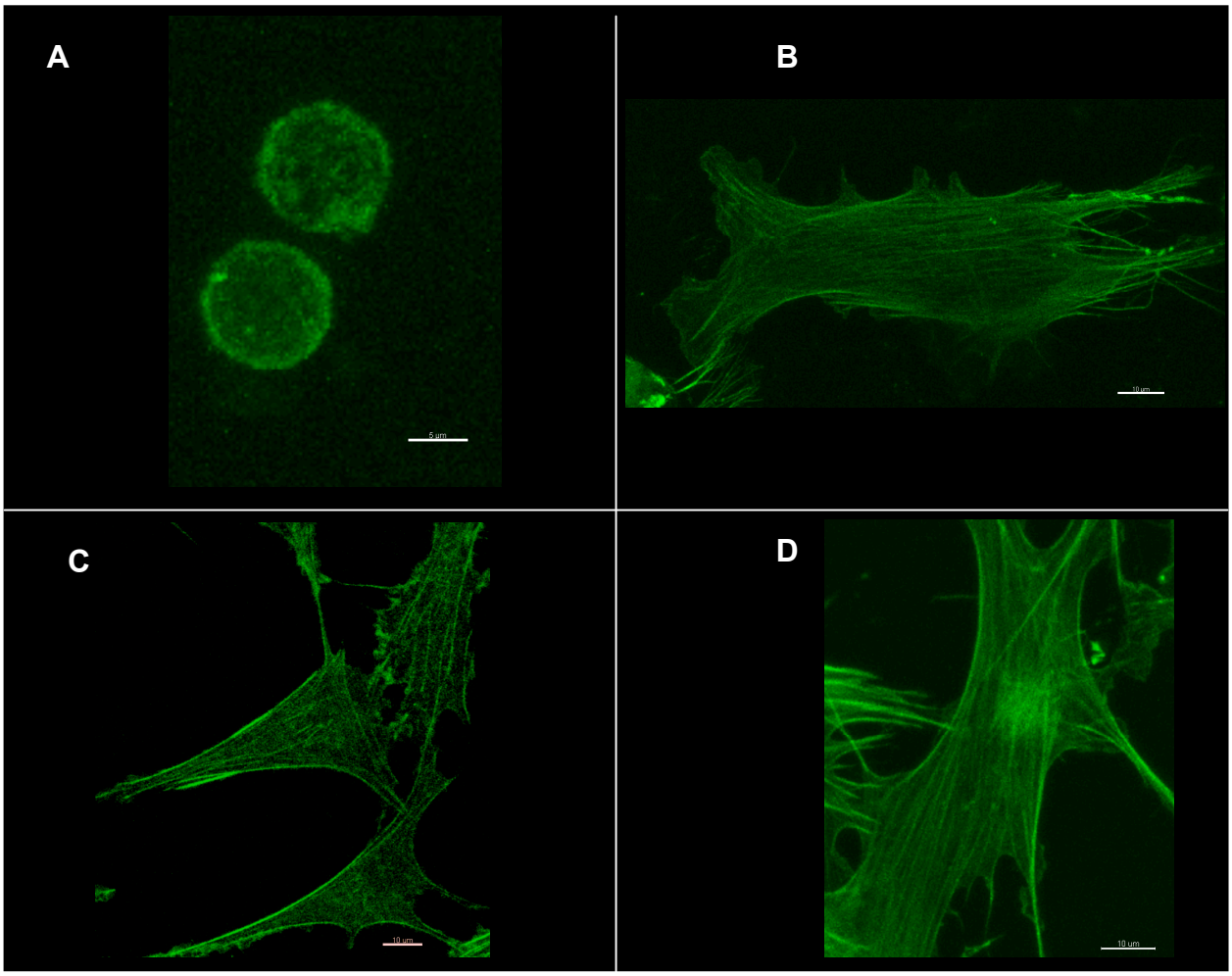

Figure 3.6: Actin organisation in freshly isolated and 2D cultured chondrocytes as seen with confocal microscopy.

Freshly isolated and 2D cultured chondrocytes were allowed to attach prior to fixing in 3% formaldehyde and staining with phalloidin-alexa 488 (green). Freshly isolated chondrocytes (panel A) acquired a round morphology with predominantly cortical actin structures, whereas upon 2D culture (panels B, C and D for P1, P2 and P3, respectively), filaments in the cell body were observed. Images acquired using 63x dipping lense.

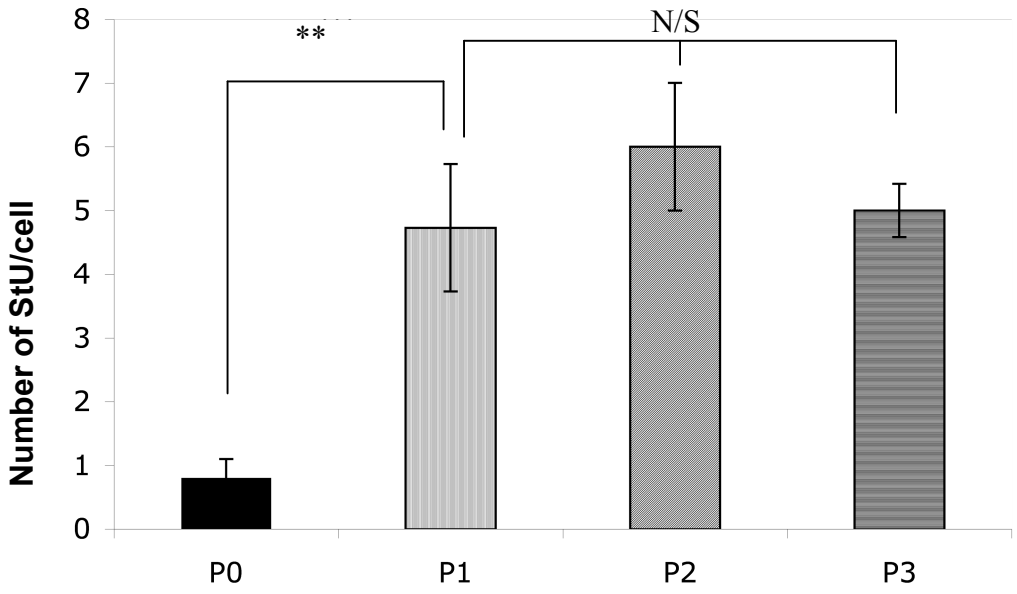

Figure 3.7: The number of actin striation units across the cell cytoplasm of freshly isolated and 2D cultured chondrocytes,

The fluorescence of actin-phalloidin-alexa 488 complexes was plotted against the standardised cell diameter and the number of peaks counted as a representative of actin striation units (StU). Freshly isolated chondrocytes possessed a mean of 1±1 StU/cell whereas upon culture there was an increase in the number of filaments reaching 5±2 StU/cell within 9 days of culture (P1). There was no significant change in the number of striation units upon further culture. Experiment repeated 3 times. N=6, n=127. Data shown as mean ± s.e.m. T-test p-values were deemed significant when p<0.01 (**). N/S, non significant.

To further investigate changes in actin organisation upon 2D culture, the values of actin-phalloidin 488 fluorescence at 10% standardised cell length intervals for all chondrocytes from one passage were obtained and the mean plotted against standard cell length as a representative of actin localisation in different passages. Distinct peaks were observed at both ends of the plot corresponding to plasma membrane-localised cortical actin structures in chondrocytes from all passage and the area under the curve representing actin fluorescence against standardised cell length was calculated by mathematical integration of the equations of the graphs (Materials and Methods).

Graphs were divided into three distinct regions corresponding to 2 cortical (binomial) and one cytoplasmic (linear) actin and the percentage of cortical and filamentous actin recorded for freshly isolated and 2D cultured chondrocytes (Figure 3.8). In freshly isolated chondrocytes 85.00±4.25% of actin structures were deemed cortical and upon 9 days in culture there was a significant decrease in the contribution of submembraneous actin structures ($p<0.05$) with only 45.00±2.25% cortical actin in P1 chondrocytes. No further significant changes in actin ratio were observed upon further culture with 47.00±2.35% and 46±2.30% cortical actin in P2 and P3 chondrocytes, respectively.

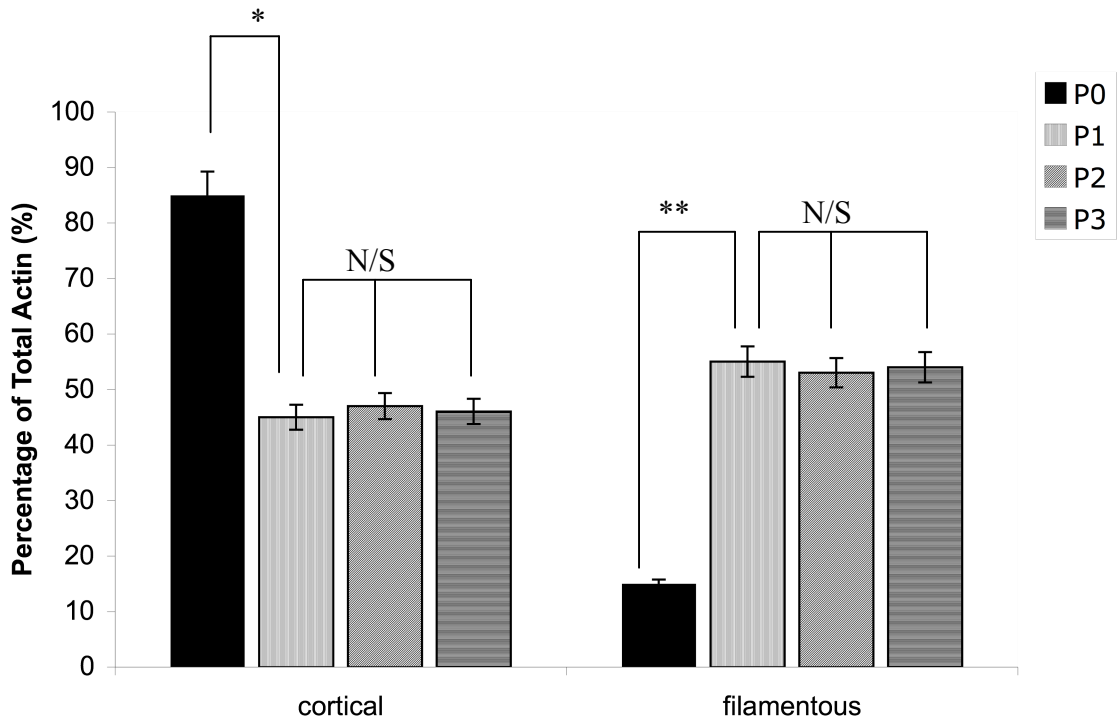

Figure 3.8: Percentage of cortical and filamentous actin structures in freshly isolated and 2D cultured chondrocytes.

Freshly isolated and 2D cultured chondrocytes were fixed and actin-phalloidin-alexa488 complexes assayed for fluorescence using confocal microscopy. The mean actin fluorescence of chondrocytes from one passage was plotted against 10% increments of standardised cell diameter and the area under the graoh integrated for two binomial curves (cortical) and an intermediate linear graph (filamentous). Actin organisation in freshly isolated chondrocytes was predominantly cortical with only 15% filamentous. The percentage of filamentous actin sharply increased upon culture rising to 45% in 9 days. Further change in actin organisation was not observed. N=6, n=119. Data shown as mean ± s.e.m. T-test p-values were p<0.05 (*) and p<0.01 (**). N/S, non significant.

3.3 Chapter Discussion

It has been well documented that *in vitro* culture of chondrocytes in 2D monolayers induces a switch in phenotype from 'differentiated' to 'fibroblast-like' dedifferentiated. These changes are evident by the loss of the round cellular shape, the acquisition of flattened irregular morphology and the decrease in type II to type I collagen expression ratio (Benya & Shaffer, 1982b; Stokes *et al.*, 2001). Therefore, the loss of the chondrocytic phenotype is a major setback to chondrocyte expansion and thus cartilage engineering. These distinct changes were studied in response to a standardised cell culture technique to further our understanding of chondrocyte phenotype and 2D culture-induced loss of differentiation.

Firstly, the culture methodology was optimised by growing freshly isolated chondrocytes at different seeding densities in serum-enriched media and studying the growth rates. At HD, chondrocytes did not undergo any cell growth possibly due to contact inhibition (Stoker, 1973) whereas chondrocytes cultured at MD increased only slightly in number prior to acquiring a 'flat' morphology which may have also promoted contact inhibition. Chondrocytes cultured at LD divided at a steady rate of 0.27 doublings/day (the equivalent of a doubling time of 3.66 days) as previously reported (Frondoza *et al.*, 1996; Lee *et al.*, 2003a). Moreover, it appeared that chondrocytes cultured at LD exhibited significantly larger cell death when compared to MD and HD cultures, which is possibly attributed to cell-to-cell interactions promoting cellular survival (Table 3.2). Similar observations have been reported upon high density culture in porcine hepatocytes whereby >90% viability initially achieved was followed by a decline with time (Chen *et al.*, 2002).

The first and most apparent effect of monolayer culture was the loss of the round morphology quantified by studying the sphericity, Ψ, of chondrocytes (defined as the ratio of the surface area of a sphere with the same volume as a given chondrocyte to the surface area of the chondrocyte). By the 9^{th} day in monolayer, a drop in sphericity was observed with no change occuring upon further culture, thereby indicating the complete loss of morphology as early as the first passage. These data were consistent with the literature, suggesting a change in morphology after the 6^{th} day in culture (Shakibaei *et al.*, 1997). This switch in morphology was further confirmed by studying accompanying changes in cellular dimensions whereby, upon culture, there was a 1.84-fold decrease in cell depth (a) and 1.97-fold increase in cell length (c) confirming that the loss of sphericity was attributed to a 'flat' morphology with irregular cellular shape (Figure 3.4).

Interestingly, in response to culture, an increase in chondrocyte cell volume was observed from 474.72±32.08μm^3 in freshly isolated chondrocytes to 673.38±39.59μm^3 following 9 days in monolayer. Whilst the former values for volume of freshly isolated chondrocytes were in accordance with those reported in the literature (Bush & Hall, 2001b), changes in cell volume of 2D cultured chondrocytes were not previously investigated due to the limitation of fluorescence technology that required the use of spherical fluorescent beads for the optimization of the methodology. A new method for obtaining volume for non-spherical 'objects' was devised using Imaris version 6.3.1 (Bitplane) and the depth of the nucleus (termed 'Nuclear Coefficient'; a_η), obtained using standard methodology for volume acquisition at 60% threshold for round objects, to standardise the dimensions and cell volume obtained at 10% threshold. Increase in cell volume may be attributed to (but not exclusively) actin reorganisation as actin reorganisation in epithelial cells has been shown to cause cellular enlargement (Boland *et al.*, 1996). Another potential reason for the increase in chondrocyte cell volume is the culture-induced release from maturational arrest otherwise observed in OA and hypertrophic chondrocytes

(Pullig *et al.*, 2000; Sandell & Aigner, 2001; Serra & Chang, 2003; Ho *et al.*, 2009).

One of the other prominent changes in chondrocytes associated with the switch in morphology was observed in the form of the reorganisation of the actin cytoskeleton where an increase in actin filaments across the cell cytoplasm has been previously observed but not quantified. Intracellular actin filaments developed in response to 2D culture with an increase from 1±1StU/cell in freshly isolated chondrocytes to 5±1StU/cell following 9 days in culture and a general increase in percentage filamentous actin from 15% to 55% (Figure 3.8).

The cause-and-effect properties of volume, morphology, actin organisation and expression battery of chondrocytes have been under intensive investigation. It has been widely documented that reversal of the actin organisation using actin-depolymerising drugs (including cytochalasin B and D) reverts the expression back to type II collagen and thus recaptures a differentiated phenotype (Brown & Benya, 1988; Mallein-Gerin *et al.*, 1991; Pirttiniemi & Kantomaa, 1998) independently of cell shape (Benya *et al.*, 1988). Furthermore, actin has been shown to influence volume regulatory mechanisms with latrunculin B (actin polymerising drug) inducing RVI in freshly isolated chondrocytes by the activation of NKCC (Kerrigan *et al.*, 2006) and it is therefore possible that the increase in chondrocyte cell volume in response to 2D culture is induced by the reorganisation of the actin cytoskeleton.

Finally, modification in the expression 'battery' of chondrocytes in response to 2D culture was documented by RT-PCR and densitometery analysis. The ratio of type II to type I collagen has long been used as a marker of chondrocyte differentiation (Benya & Shaffer, 1982b; Baici *et al.*, 1988a; Idowu *et al.*, 2000) and we have similarly reported a 0.58±0.15-fold decline in col2:col1 within the first passage (9 days of culture) which decreased insignificantly upon further culture reaching 0.39±0.1 in P3 2D cultured chondrocytes. Interestingly, the

fluctuations in the expression levels of individual collagens demonstrated more distinct changes within 2D cultured chondrocytes. The expression of the chondrocyte-specific type II collagen transiently yet significantly increased after 9 days in culture prior to returning to baseline levels observed in freshly isolated chondrocytes upon further culture. Conversely, type I collagen expression levels increased by 2.70±0.63-fold in P1 chondrocytes and remained elevated for the remainder of culture as previously reported (Stokes *et al.*, 2002), thus contributing to the decrease in col2:col1 expression ratio. These data, however, demonstrated that the loss of phenotype may occur in 2 steps when phenotype is defined according to expression levels of collagens. P1 chondrocytes upregulated the expression of both collagens prior to the ultimate suppression of type II collagen expression and this is consistent with previous findings where an increase in type II collagen expression in the first 3 passages of high-density porcine auricular chondrocyte culture was observed (Haisch *et al.*, 2006). Similar observations were reported upon culture of porcine auricular chondrocytes where a transient upregulation of type II collagen was observed up to the 12th day in culture (Haisch *et al.*, 2006).

SOX9 expression levels were also used as a marker of chondrocyte differentiation as a decline in SOX9-mediated transcription has been reported to play a role in chondrocytic phenotype (Stokes *et al.*, 2002; Tallheden *et al.*, 2004). It was, however, observed that the level of SOX9 expression increased by a factor of 1.75±0.40-fold following 9 days in culture (simultaneously to the rise in type II collagen expression) and subsequently declined upon further culture to 0.69±0.14 relative to freshly isolated chondrocytes. SOX9 has been shown to regulate the expression of type II collagen in chondrocytes (Hattori *et al.*, 2008), the increase of which was therefore attributed to an upregulation in SOX9 expression in P1 chondrocytes.

Together, these data have confirmed and quantified changes documented in response to 2D culture, and although the exact order of events observed cannot

be concluded (Figure 3.9), these differences were considered ‘markers’ of dedifferentiation necessary for future experiments. Moreover, these data suggested the existence of a distinct phenotype in P1 chondrocytes previously undefined and thereafter termed ‘mesodifferentiated[‡]’.

[‡] Greek, from mesos, *middle.*

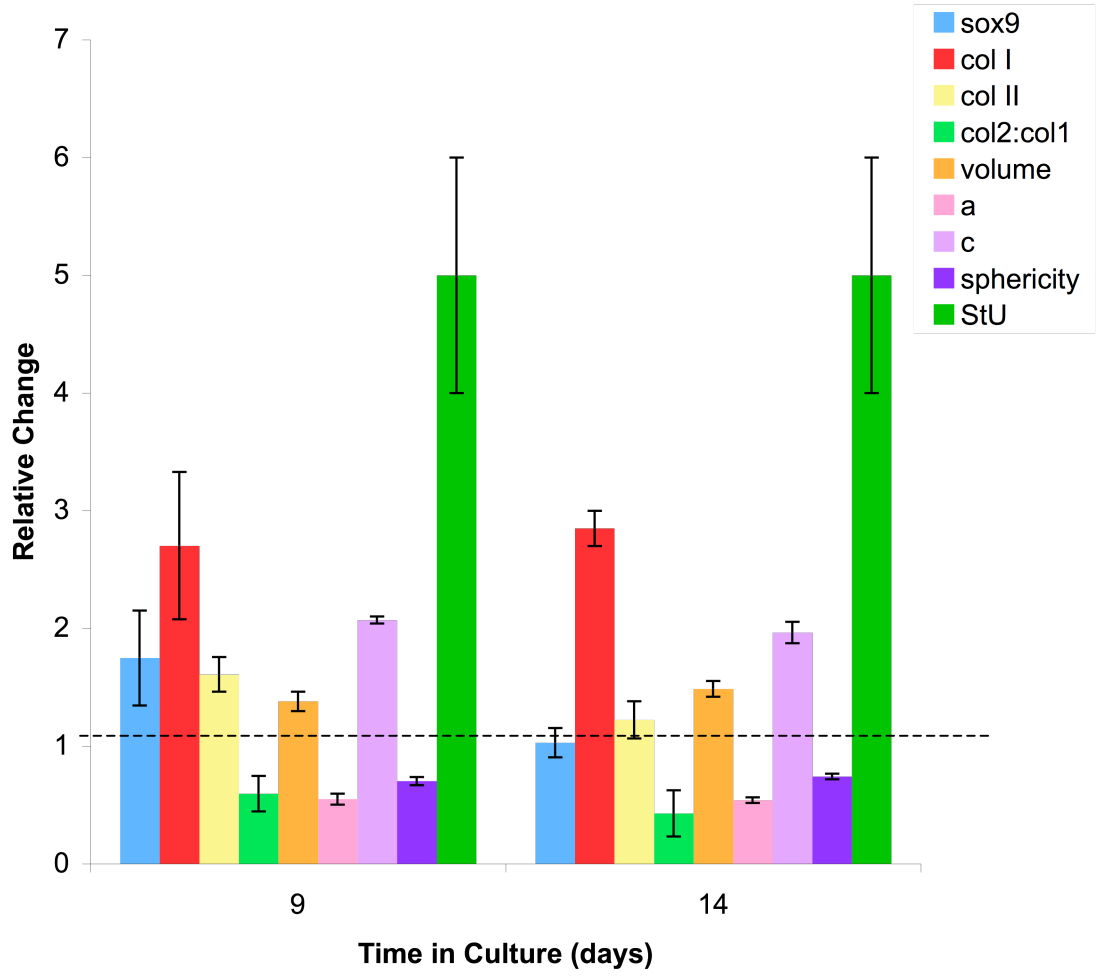

Figure 3.9: Model of the significant changes ($p<0.05$) in phenotypic markers in response to 2D culture.

The effect of 2D culture on chondrocytic phenotype was quantified and observed over a 21-day period. A new phenotype termed 'mesodifferentiated', which has not been previously described, was observed upon 9 days in culture. An increase in cell length (c; violet) and volume (orange), the decrease in cell depth (a; pink) and development of filamentous actin (StU; dark green) were observed in response to expansion. There was an increase in expression of type I collagen (red) resulting in an overall decrease in col2:col1 expression (green) which was maintained upon further culture. There was however a transient rise in SOX9 (blue) and type II collagen (yellow) in mesodifferentiated chondrocytes. Values are shown as mean ± s.e.m. All values shown were significantly different ($p<0.05$) from baseline levels observed in freshly isolated chondrocytes.

4 Experimental Chapter: The mechanotransduction properties of 2D cultured chondrocytes.

4.1 Chapter Introduction

Chondrocytes receive no direct nervous or vascular support and are nevertheless able to 'sense' and respond to external stimuli (Stockwell, 1991a) using a group of mechanisms, termed 'mechanotransduction'. External stimuli that induce a mechanotransduction response include fluid flow (Yellowley *et al.*, 1997), fluctuations in osmotic environment (Hall, 1998b), changes in pressure (Roberts *et al.*, 2001) and deformations in the cell membrane (Roberts *et al.*, 2001), all of which occur upon joint loading. Chondrocytes feed back in response to such stimuli by various mechanisms including volume regulatory mechanisms and/or Ca^{2+} signalling pathways.

4.1.1 RVI

Regulatory Volume Increase (RVI) is one of the mechanisms by which some types of cells maintain constant volume and intracellular ionic strength that supports physiological processes and optimal metabolism (O'Neill, 1999). Upon an increase in extracellular ionic concentration, passive water outflux occurs followed by cell shrinkage and activation of certain membrane transporters including the NKCC (Qusous *et al.*, in press; O'Neill, 1999). Membrane transporters involved in RVI pump ions across the plasma membrane into the cell cytoplasm resulting in water influx and gradual restoration of cell volume (O'Neill, 1999). Experiments aimed at investigating the capacity to exhibit RVI are conducted by subjecting cells to a hyperosmotic solution and recording changes in cellular volume. In chondrocytes, it has been shown that only 6% of freshly isolated and *in situ* chondrocytes exhibited RVI whereas 54% of 2D cultured chondrocytes possessed the capacity to regulate their volume in response to a hyperosmotic challenge (Kerrigan *et al.*, 2006). Therefore, the capacity of chondrocytes to exhibit RVI was further investigated in 2D

chondrocytes as a novel key mechanotransduction marker of chondrocyte dedifferentiation in response to expansion.

4.1.2 Calcium Signalling

The role of calcium within mechanotransduction is that of an intracellular secondary messenger. Transient rises in $[Ca^{2+}]_i$ have been observed in response to mechanical stimuli including, both steady (Yellowley *et al.*, 1997) and oscilliating pressure forces (Edlich *et al.*, 2001), REV5901-loading (Ali *et al.*, in press), hyperomsotic (Sanchez & Wilkins, 2004; Dascalu *et al.,*, 1996) and hypo-osmotic (Sanchez *et al.*, 2003; Pritchard *et al.,*, 2004; Kerrigan and Hall, 2008) challenges. Calcium enters the cytoplasm of chondrocytes through cell membrane calcium channels (including SACC, NCX or members of the TRPV) or via IP3-induced release from intracellular stores (Yellowley *et al.*, 1999). Moreover, previous studies have shown that an increase in $[Ca^{2+}]_i$ in response to hypo-osmotic challenge was additionally mediated by SACC and TRPV channel activation (Sanchez *et al.*, 2003). In contrast, only NCX was involved in hyperosmotic challenge-induce $[Ca^{2+}]_i$ rise (Sanchez & Wilkins, 2004) and these channels were therefore studied.

REV5901 is an antagonist of cysteinyl-leukotriene receptors (a family of G-protein coupled receptor; GPCR) in porcine epithelial cells (Van Inwegen *et al.*, 1987), an inhibitor of rat neutrophil 5-LO (Musser *et al.*, 1987) and an inhibitor of RVD in articular chondrocytes (Hall & Bush, 2001). It was also recently observed within our research group that REV5901-loading induced a sustained rise in $[Ca^{2+}]_I$, thus making REV5901 a suitable pharmacological inducer of $[Ca^{2+}]_i$ rise necessary to study $[Ca^{2+}]_i$ responses in chondrocytes. The mode of action of REV5901 has not been investigated (Ali *et al.*, in press). In response to histamine or parathyroid hormone exposure, a rise in $[Ca^{2+}]_i$ was induced by PKC activation and IP3 generation, both of which are downstream elements of GCPR (Iannotti *et al.*, 1990; Horwitz *et al.*, 1996). A known G-protein coupled

receptor-mediated pathway was thus proposed and studied in 2D cultured chondrocytes using appropriate pharmacological inhibitors.

Aims of Experimental Chapter

1 Study the cellular response to hyperosmotic challenge in freshly isolated and 2D cultured chondrocytes as a potential marker of phenotype.

2 Develop the use of REV5901 as a pharmacological inducer of calcium responses.

3 Using REV5901-induced $[Ca^{2+}]_i$ rise, investigate changes in individual channel contribution in response to 2D culture .

4 Investigate the REV5901-mediated signalling pathway responsible for inducing a rise in $[Ca^{2+}]_i$.

4.2 Results

4.2.1 Regulatory volume increase (RVI) in freshly isolated and 2D expanded chondrocytes

Previous work has shown that the capacity for chondrocytes to exhibit RVI in response to hyperosmotic challenge during culture thus providing a novel assay for the determination of phenotype and mechanotransduction (Kerrigan *et al.*, 2006). Freshly isolated and 2D-cultured chondrocytes were subjected to a hyperosmotic challenge (380-540mOsm) and z-stack images acquired at 0 (isosmotic) and subsequently at 1.5, 3, 5, 10 and 20 minutes post challenge by CLSM, as previously described (see Materials & Methods). Images were reassembled in Imaris 6.3.1 and an isosurface surpass applied and cell volume determined.

Following an increase in extracellular osmolarity, freshly isolated chondrocytes decreased in volume to 0.79±0.05 of their original volume at time 1.5 minutes and underwent further volume loss readily over the following 20 minutes, reaching 0.67±0.04 the original volume after 20mins (Figure 4.1A). Conversely, P1, P2 and P3 chondrocytes decreased in volume by 1.5 minutes to 0.87±0.03%, 0.88±0.02 and 0.86±0.03% respectively which whilst not significantly different to each other ($p>0.05$) was significantly different ($p<0.05$) from freshly isolated chondrocytes. Unlike freshly isolated chondrocytes P1-P3 chondrocytes exhibited RVI ($p<0.05$) whereby at 20mins post-osmotic challenge they had recovered 0.99±0.01, 0.99±0.03% and 0.99±0.03% of their original respectively volume, respectively (Figure 4.1B-D).

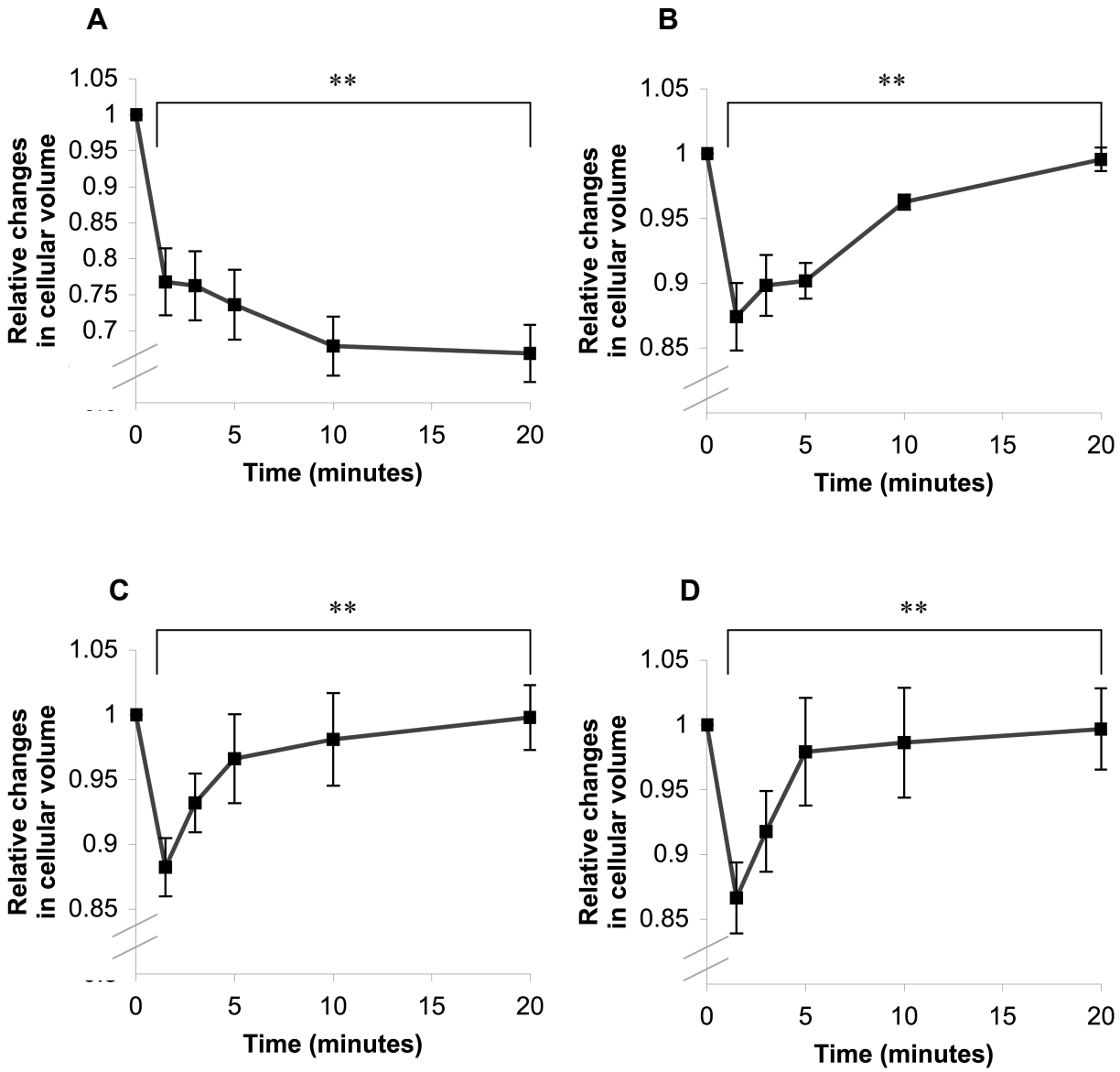

Figure 4.1: The capacity of freshly isolated and 2D expanded chondrocytes to exhibit RVI in response to hyperosmotic conditions.

Freshly isolated, P1, P2 and P3 chondrocytes (Panels A, B, C and D, respectively) were loaded with 5μM calcein-AM and imaged using CLSM before and up to 20 minutes following a 42% hyperosmotic challenge. Freshly isolated chondrocytes did not exhibit RVI whereas P1, P2 and P3 2D cultured chondrocytes reaquired 99.6%, 99.8% and 99.7% of their original volume by 20 minutes, respectively. N=4, n=119. Data shown as mean ± s.e.m. T-test p-values were p<0.01 (**).

A logarithmic rate of volume regulation was observed in P2 and P3 whereas the rate followed a linear trend in P1 chondrocytes (Figure 4.1B). Therefore, the trend of RVI in P2 and P3 was deemed 'bi-phasic' including 'robust' RVI between 1.5 and 5 minutes and 'slow' RVI between 5 and 20 minutes post challenge. P1 chondrocytes, however, solely exhibited 'slow' RVI throughout the volume recapture time (1.5->20 minutes) thus lacking 'bi-phasic' volume regulation seen in other 2D expanded cultured passages. The gradient of the lines representing 'slow' and/or 'robust' RVI were used to calculate half the time required for chondrocytes to regain 100% of their original volume (denoted $t_{½}$). Slight yet insignificant differences ($p>0.5$) in $t_{½}$ of 'slow' RVI were observed with a value of 9.6±0.6, 10.1±0.7 and 10.9±0.5 minutes in P1, P2 and P3, respectively. $t_{½}$ values for 'robust' RVI in P2 and P3 chondrocytes were 3.5±0.5 and 2.8±0.5 minutes respectively with no significant differences observed ($p>0.5$).

As previous work by others showed heterogeneity in the response to mechano-stimulation including hyperosmotic challenges (Kerrigan *et al.*, 2006), a box plot was created to study the distribution of population of chondrocytes according to percentage volume recovery within every passage. It was observed that P1 chondrocytes exhibited lower and upper quartile values of 97.10% and 102.90% volume recovery, respectively. These values were spanned over a larger range ($p<0.05$) upon further culture to 92.15 – 106.31% and 88.04 – 105.90% in P2 and P3 2D cultured chondrocytes, respectively. To further support these findings, the percentage of chondrocytes exhibiting 90-110% interquartile volume recovery was obtained for 2D cultured chondrocytes. 91.48% of P1 chondrocytes exhibited interquartile volume recovery whereas only 53.85% and 50.23% of P2 and P3 chondrocytes, respectively, showed RVI within the corresponding range values with no significant difference between P2 and P3 chondrocytes ($p>0.05$; Figure 4.2). These data indicated a distinct switch in chondrocyte mechanotransduction after 9 days in culture and yet another pattern of RVI exhibited after 14 days in culture (Table 4.1).

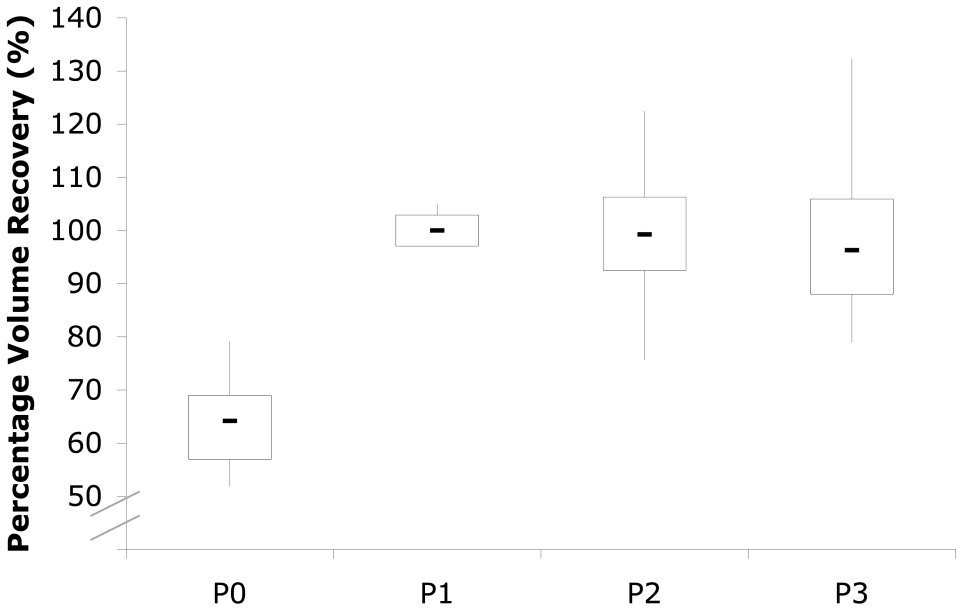

Figure 4.2: Box plot of 2D expanded chondrocytes against percentage volume recovery at time 20 minutes.

Variations in response to hyperosmotic challenge within every passage were studied by a box plot of the maximum recovery values (at t=20 minutes). P1 chondrocytes demonstrated an interpercentile volume recovery range of 97.10% – 102.9% whereas P2 and P3 chondrocytes showed a larger range of 92.51% – 106.31% and 88.04% – 105.90%, respectively. These data showed a transient increase in population homogeneity upon culture (P1 chondrocytes). N=4, n=119, experiment repeated 6 times. Data shown as median and interpercentile range ± maximum or minimum value.

Table 4.1: Volume regulatory properties of freshly isolated and 2D cultured chondrocytes.

Freshly isolated chondrocytes were characterised by their inability to volume regulate in response to hyperosmotic challenge whereas upon culture, P1 chondrocytes exhibited a homogenous 'slow' RVI response with a t½ of 9.6±0.9 min and an interpercentile range of 17.76±13.66% volume recovery. Upon further culture, however, P2 and P3 chondrocytes exhibited bi-phasic volume regulation with slow and robust RVI. P2 and P3 chondrocytes were also characterised by an increase in the heterogeneity of the response to osmotic challenge.

Cell Type	P0	P1	P2	P3
Minimal Percentage Volume (%)	79.7±4.7	87.5±2.6	83.4±2.2	81.9±2.7
Percentage Volume Recovery (%)	N/A	99.6±2.9	99.8±2.5	99.7±3.1
Robust RVI $t_{½}$ (min)	N/A	N/A	3.5±1.0	2.8±0.9
Slow RVI $t_{½}$ (min)	N/A	9.6±0.9	10.1±1.0	10.9±1.0
Interquartile range of Percentage Recovery ± average whiskers (%)	17.76±13.66	5.80±1.09	13.30±16.53	17.86±17.81
Percentage of cells Exhibiting interquartile Percentage Recovery (%)	72.72	91.48	53.85	50.23

4.2.2 Calcium mechanotransduction and Homeostasis

As mechanotransduction is linked to phenotype, changes in calcium homeostasis were investigated in response to 2D culture, whereby REV5901 was used as a pharmacological inducer of $[Ca^{2+}]_i$ rise.

4.2.2.1 The effect of REV5901 on $[Ca^{2+}]_i$ homeostasis

Preliminary work in our research group showed a significant and sustained increase in $[Ca^{2+}]_i$ in both freshly isolated and 2D expanded chondrocytes in response to 50μM REV5901 loading (Ali *et al.*, in press). In conjunction with previous work that has demonstrated the influence of REV5901 on volume regulation, these initial findings indicated an effect of REV5901 on calcium signalling and thus potentially mechanotransduction.

To determine how REV5901 affected calcium signalling, freshly isolated and 2D cultured chondrocytes were incubated with 3μM fluo-4 in BPS in the dark for 30 minutes and 37°C. Upon loading a negative control solution (DMSO carrier), freshly isolated chondrocytes exhibited 1.67±0.32% increase in $[Ca^{2+}]_i$ levels (Figure 4.3A) whereas 2D cultured chondrocytes showed 1.60±0.50%, 1.70±0.81% and 1.60±0.32% increases in P1, P2 and P3 2D cultured chondrocytes, respectively, in response to fluid flow. When perfused with a final concentration of 50μM REV5901, however, both freshly isolated and 2D cultured chondrocytes exhibited a significant and sustained rise in $[Ca^{2+}]_i$ levels. Freshly isolated chondrocytes demonstrated increased sensitivity to REV5901-loading reaching a maximum increase in $[Ca^{2+}]_i$ of 38.0±5.7% compared to P1, P2 and P3 which reached a maximum $[Ca^{2+}]_i$ increase (recorded at the end of the experiment; t=5 minutes) of 12.5±0.60%, 12.8±1.70% and 18.9±0.81%, respectively (Figure 4.3B). These data confirmed initial personal observations that suggested a role for REV5901 in the regulation of intracellular calcium homeostasis.

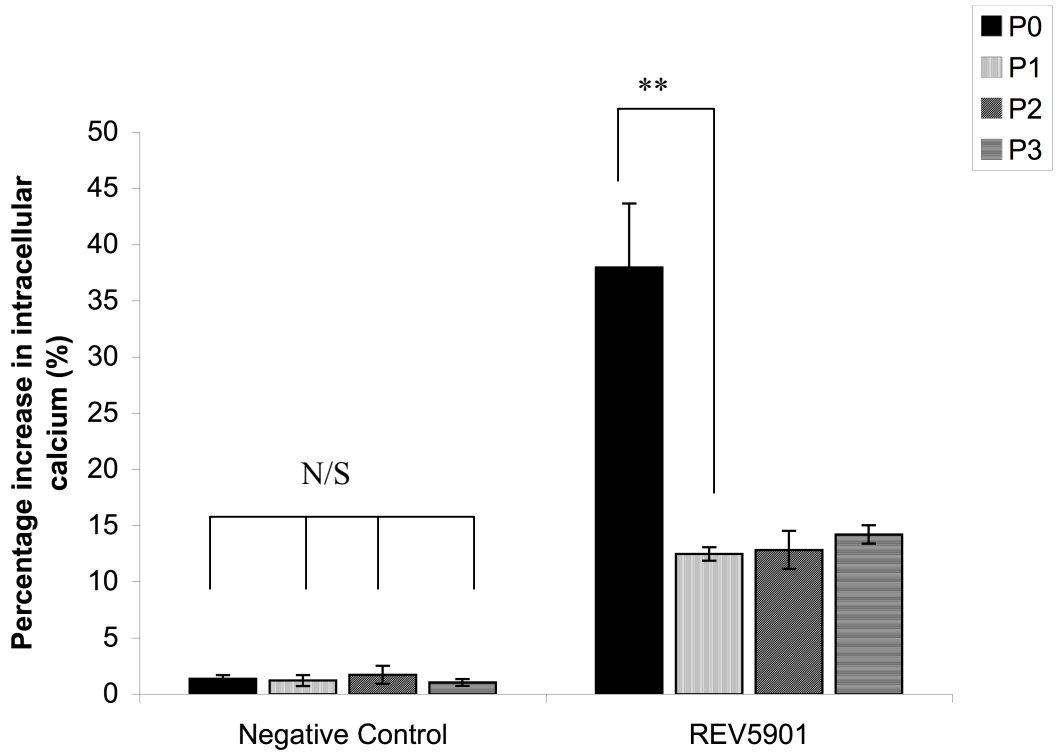

Figure 4.3: The effect of REV5901 loading on freshly isolated and 2D cultured chondrocytes.

Freshly isolated and 2D cultured chondrocytes were incubated with 3μM fluo-4 in BPS for 30 min prior to loading of 50μM REV5901 and measurement of maximal $[Ca^{2+}]_i$ change. Loading of REV5901-free BPS induced a negligible calcium rise of an average of 1.5% (Panel A). In response to REV5901 loading, however, there was a sustained rise in $[Ca^{2+}]_i$ whereby freshly isolated chondrocytes exhibited higher sensitivity to REV5901 than 2D expanded chondrocytes with a maximum increase of 37.97±1.35% and 12.47±0.61% in P0 and P1 chondrocytes, respectively, with no significant change in response to further culture. N=6, experiment repeated 4 times. Data shown as mean ± s.e.m. T-test p-values were p<0.01 (**). N/S, non significant.

4.2.2.2 Individual calcium channels contribution to calcium signalling and profiling

The ability of REV5901 to induce a rise in $[Ca^{2+}]_i$ rendered it a suitable pharmacological reagent for studying calcium channel activities and store participation in freshly isolated and 2D cultured chondrocytes to further enhance our understanding of potential changes in calcium signalling upon 2D expansion. Therefore to meet this objective, it was necessary to determine the source of the rise and the channels involved.

4.2.2.2.1 Extracellular vs. intracellular store calcium contribution to REV5901-mediated calcium rise

The contribution of the extracellular calcium influx and intracellular calcium store release in response to REV5901 loading was studied in response to 2D culture-induced loss of phenotype. 2mM EGTA solutions were used to differentiate between calcium influx and calcium release from intracellular stores by chelating extracellular calcium ions. Freshly isolated and 2D cultured chondrocytes were loaded with 3μM fluo-4 and incubated in the dark for 30 minutes prior to aspirating excess fluo-4 and loading chondrocytes in Ca^{2+}-free BPS containing 2mM EGTA. Subsequently, 50μM REV5901 in Ca^{2+}-free BPS was loaded and $[Ca^{2+}]_i$ levels measured as previously described.

In the absence of extracellular calcium, there was a decrease in REV5901-mediated $[Ca^{2+}]_i$ rise, indicating that store contributed for 27.86±3.15% $[Ca^{2+}]_i$ rise. In contrast, intracellular stores contributed for only 1.97±0.77%, 3.78±0.78% and 2.01±0.72% rise in P1, P2 and P3, respectively (Figure 4.4) with no significant changes ($p>0.05$). These data indicated a 2D culture-induced reduction in intracellular calcium store contribution to REV5901-mediated calcium rise in the absence of extracellular calcium ions.

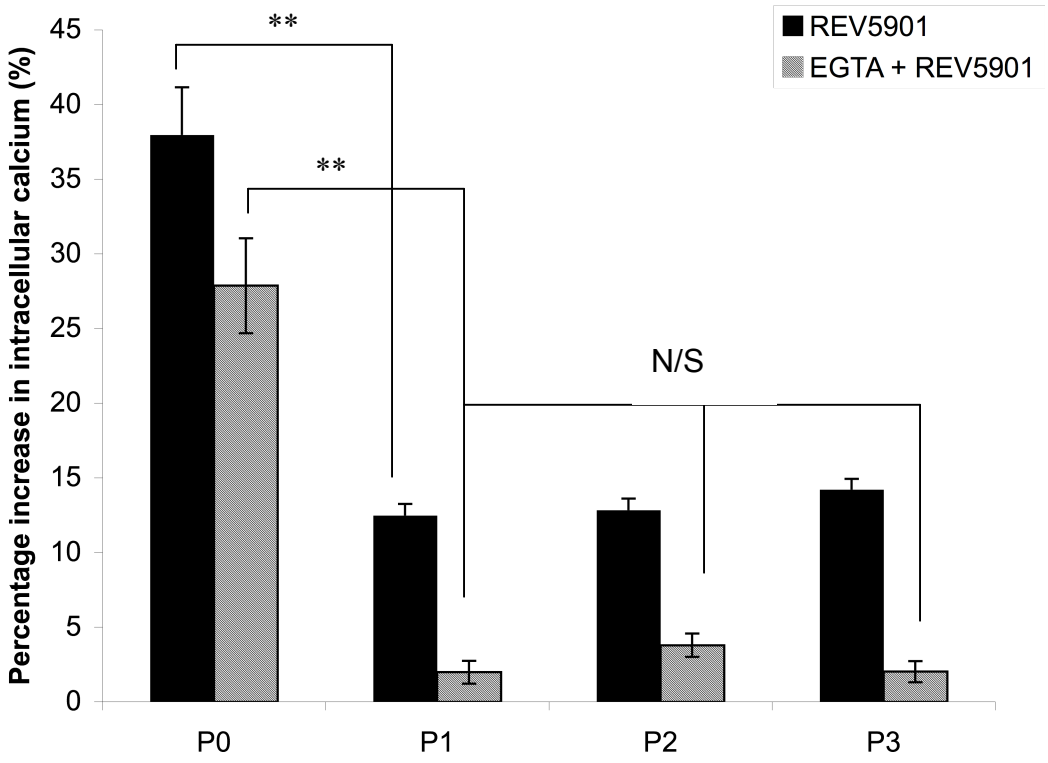

Figure 4.4: Effect of extracellular calcium removal on REV5901-induced calcium rise in freshly isolated and 2D cultured chondrocytes.

Freshly isolated and 2D cultured chondrocytes were incubated with 3μM fluo-4 in BPS for 30 minutes prior to loading of 50μM REV5901 and measurement of maximal $[Ca^{2+}]_i$ change in the presence of 2mM EGTA. In freshly isolated chondrocytes, there was a maximal $[Ca^{2+}]_i$ rise of 27.86±3.15% which dropped upon 2D culture to 1.97±0.77%, 3.78±0.78% and 2.01±0.72% in P1, P2 and P3 chondrocytes, respectively. These data induicated a reduction in store contribution to REV5901-mediared $[Ca^{2+}]_i$ rise upon 2D culture. N=6, experiment repeated 4 times. Data shown as means ± s.e.m. T-test p-values were p<0.01 (**). N/S, non significant.

4.2.2.2.2 Transmembrane channels contribution to REV5901-mediated calcium rise

As the level of REV5901-induced transmembrane Ca^{2+} influx was not affected by 2D culture, membrane channel-dependent $[Ca^{2+}]_i$ regulation was investigated as a key mechanotransduction pathway using pharmacological or chemical inhibitors to calcium influx. Individual groups of calcium channels were chosen including NCX, SACC and TRPV channels as previous work has suggested their involvement in osmotic challenge-induced $[Ca^{2+}]_i$ rise (Sanchez *et al.*, 2003; Sanchez & Wilkins, 2004). Freshly isolated and 2D cultured chondrocytes were loaded with fluo-4 and incubated in the dark for 30 minutes with or without appropriate inhibitory conditions (Table 2.6) and subsequently REV5901 loaded and $[Ca^{2+}]_I$ levels measured as previously described.

Significant differences in the sensitivity to pharmacological inhibition of calcium channels were observed between freshly isolated and cultured chondrocytes but not between 2D cultured chondrocytes from different passages, thereby indicating changes in channel physiology upon 2D culture. No significant differences ($p>0.5$) were observed in the sensitivity of freshly isolated and 2D cultured chondrocytes to ruthenium red inhibition of the TRPV channels with 46.36±6.66, 49.32±6.87%, 51.15±14.07 and 55.13±22.75% inhibition of total $[Ca^{2+}]_i$ rise in freshly isolated, P1, P2 and P3 2D cultured chondrocytes, respectively.

The sensitivity of chondrocytes to the absence of extracellular Na^+ was reduced upon culture from 84.03±9.22% inhibition of total $[Ca^{2+}]_i$ rise in freshly isolated chondrocytes to 57.86±2.76% in P1 2D cultured chondrocytes indicating a loss of dependency on NCX function upon culture with no further significant change upon subsequent culture (57.42±11.95% and 55.41±8.00% in P2 and P3 chondrocytes, respectively; $p>0.05$). Conversely, in the presence of Gd^{3+}, the inhibition of total $[Ca^{2+}]_i$ rise in chondrocytes was increased upon culture from

33.01±4.03% in freshly isolated to 57.21±1.53% in P1 2D cultured chondrocytes, respectively (Figure 4.5) and no significant change was observed in response to further culture with inhibition values of 54.22±5.24% and 50.80±1.54% in P2 and P3 2D cultured chondrocytes ($p>0.05$).

These data have demonstrated a distinct switch in the regulation of expression and/or activity calcium channels upon 2D culture of chondrocytes as observed by stimulation using REV5901. It was concluded that while freshly isolated chondrocytes depended predominantly on calcium release from intracellular stores and to a less extent on NCX channel, REV5901 induced a predominantly SACC-mediated rise in $[Ca^{2+}]_i$ in 2D cultured chondrocytes.

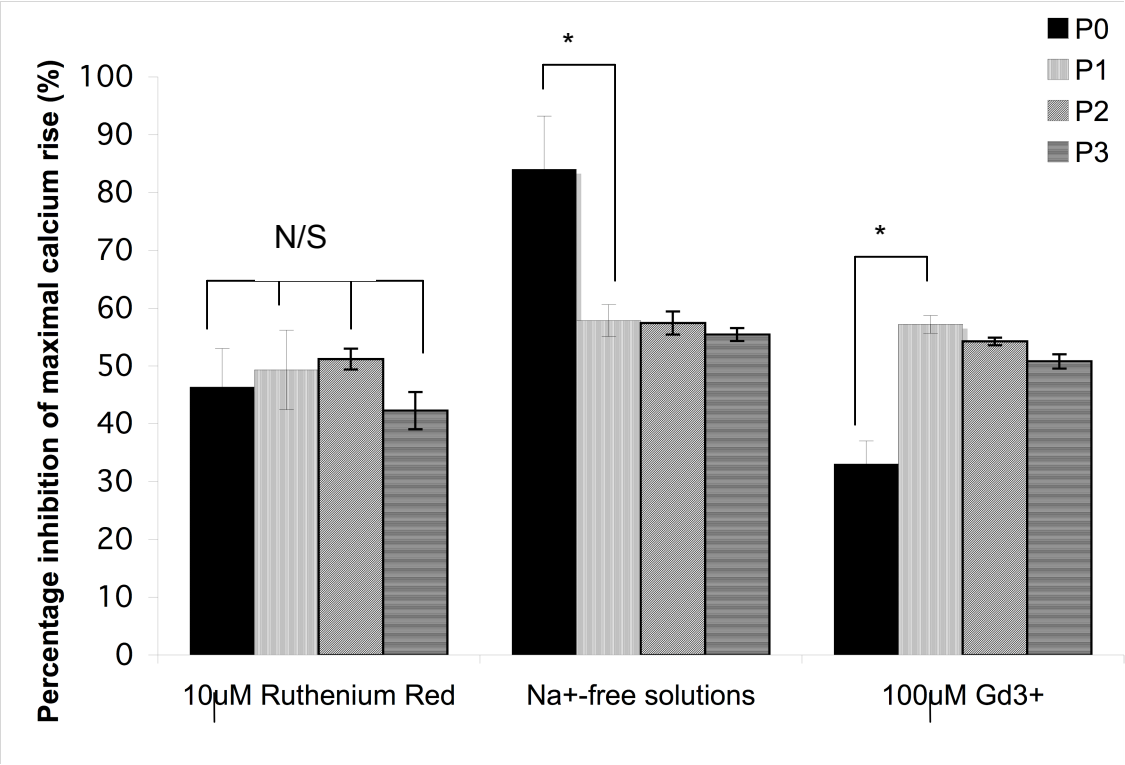

Figure 4.5: $[Ca^{2+}]_i$ rise inhibition profiling in freshly isolated and 2D cultured chondrocytes.

The dependency of freshly isolated and 2D cultured chondrocytes on individual calcium channels was investigated by loading chondrocytes with 3μM fluo-4 in appropriate inhibitory conditions prior to loading 50μM REV5901 and measurement of $[Ca^{2+}]_i$ changes. Percentage inhibition of total $[Ca^{2+}]_i$ rise in the presence of Ruthenium Red did not change upon culture, whereas inhibition of NCX and stretch-sensitive calcium channels were reduced and increased, respectively. These data indicated a change in channel expression/activity in response to 2D culture. N=6, experiment repeated 4 times. Data shown as means ± s.e.m. T-test p-values were p<0.05 (*). N/S, non significant.

4.2.2.3 The mechanism of effect of REV5901 on intracellular calcium concentration $[Ca^{2+}]_i$

REV5901 is typically used as an inhibitor of RVD mechanisms in freshly isolated chondrocytes possibly via actin re-organisation (Bush and Hall, 2001; Nadelcheva *et al.*, in press). As 2D cultured chondrocytes exhibited a reduced intracellular calcium response to REV5901, the pathway of action of REV5901 loading on $[Ca^{2+}]_i$ homeostasis was further investigated in freshly isolated chondrocytes to investigate all mechanisms which may not exist in 2D cultured counterparts. The proposed G-protein-induced pathway for REV5901-induced $[Ca^{2+}]_I$ rise using individual pharmacological agents against the individual proteins downstream of the receptor (Table 2.6). Chondrocytes were loaded with 3μM Fluo-4 in basic physiological saline (BPS) containing individual pharmacological agents for 30 minutes prior to REV5901 loading and measurement of intracellular calcium changes.

1μM Wartmannin, an inhibitor of PI5K (Liu *et al.*, 2001), did not cause inhibition of the REV5901-mediated calcium rise, indicating the lack of contribution by the PIP3/PI5K pathway to $[Ca^{2+}]_i$ levels. Neomycin sequestering of PIP2 molecules reduced the initial calcium 'burst' with maximum $[Ca^{2+}]_i$ rise of 23.79±2.21%, whereas 100μM U73122 (inhibitor PLCβ3) decreased the rate of $[Ca^{2+}]_i$ rise thus reaching a final $[Ca^{2+}]_i$ increase of 23.09±2.70%. Finally, incubation with 100μM Rottlerin reduced REV5901-induced $[Ca^{2+}]_i$ rise to 2.27±3.30% inhibition of the calcium rise demonstrating the dependency of the pathway on PKC activity (Figure 4.6).

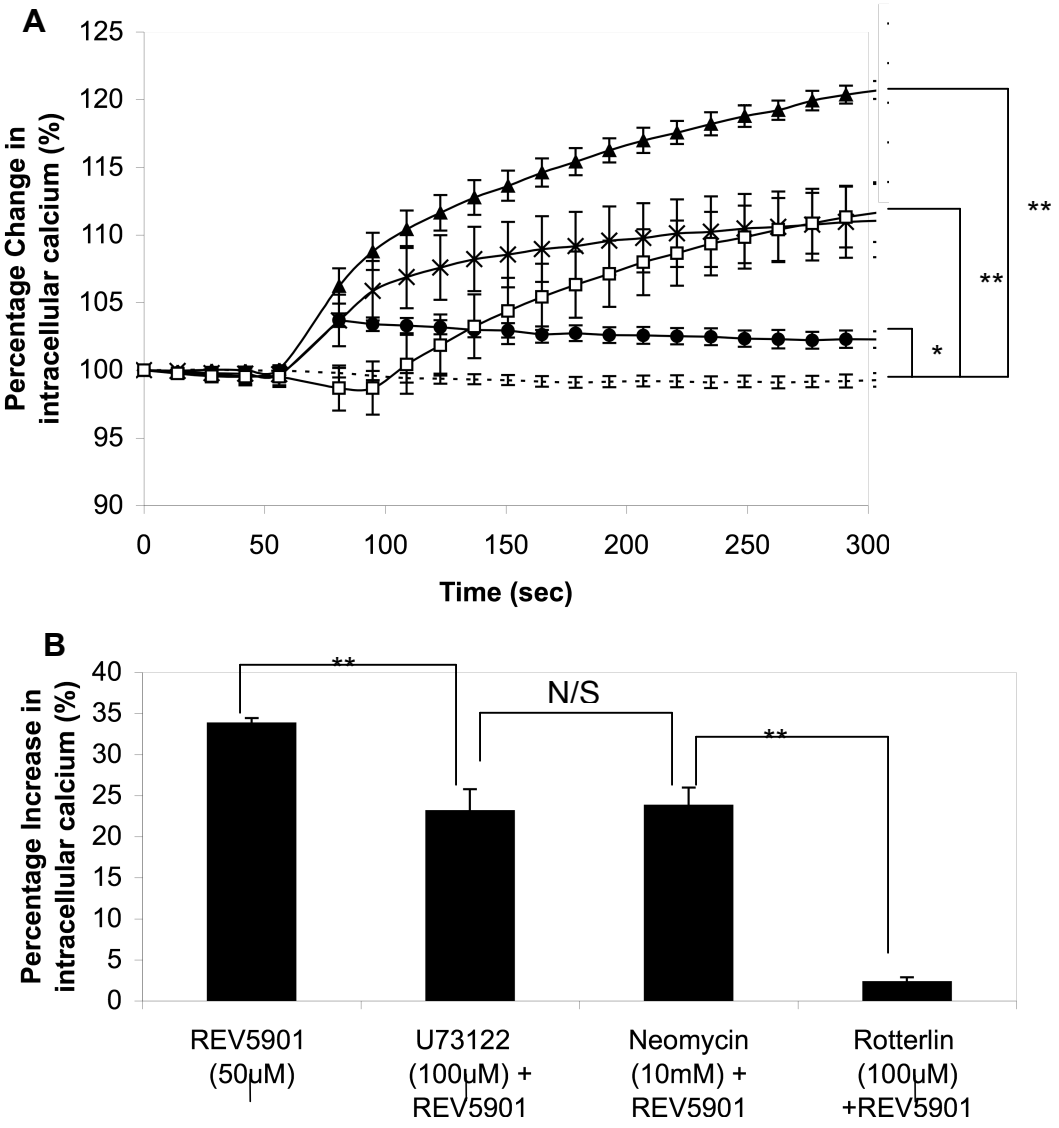

Figure 4.6: Changes in $[Ca^{2+}]_I$ in response to REV5901 loading in the presence of pharmacological inhibitors to G-protein downstream elements.

Freshly isolated chondrocytes were incubated with 3μM fluo-4 and suitable pharmacological agents required to inhibit signalling molecules downstream of G-proteins. Upon 30 minute incubation, media containing excess fluo-4 were replaced with BMP containing pharmacological agents and baseline bound $[Ca^{2+}]_i$ measured prior to loading 50μM REV5901 in BPS. Rottlerin reduced the maximal calcium rise to 2.27% compared to REV5901 control. Both U73122 and neomycin caused an overall inhibition of 45% with neomycin also causing a distinctive reduction in the original burst of $[Ca^{2+}]_i$. N=4, experiment repeated 6 times. Data shown as means ± s.e.m. T-test p-values were p<0.01 (**). N/S, non significant.

The rate of calcium increase with and without pharmacological reagents was further studied by dividing the change in percentage fluorescence over the time of measurement. REV5901 solution induced an increase in $[Ca^{2+}]_i$ at a rate of 3.81±0.42%/min which was reduced in the presence of EGTA and U73122 to 0.95±0.10%/min and 1.75±0.19%/min, respectively (Table 4.2). In the presence of Rottlerin, however, the initial rise was followed by a gradual slight decrease at 0.39±0.04%/min. Exclusively to treatment with of Neomycin, the initial calcium rise was delayed by up to 28.8 seconds post REV5901 loading increasing gradually at the same rate (3.85±0.42%/min) as a neomycin-free REV5901 solution (Table 4.2).

Table 4.2: Impact of loading of various solutions on $[Ca^{2+}]_i$ levels.

The effect of pharmacological inhibitors of signalling molecules on REV5901-induced $[Ca^{2+}]_i$ rise was investigated in freshly isolated chondrocytes to confirm the proposed G-protein-mediated pathway. EGTA inhibited the calcium rise by 57.53% whereas U73122 and neomycin induced an inhibition of 42.47%, 46.57% and 43.55%, respectively, indicating that both PLCβ3 and IP3 are necessary for intracellular calcium release from stores. Moreover, despite no effect on the rate of calcium rise in response to treatment with neomycin, there was a 28.8 second delay in the calcium rise which was not observed with the use of any other pharmacological inhibitor. While Wartmannin did not cause a significant change in the calcium response, Rottlerin abolished the REV5901-mediate $[Ca^{2+}]_i$ rise by 89.03%. N=4, experiment repeated 6 times. Data shown as means ± s.e.m. T-test p-values against REV5901 control were p<0.05 (*) and p<0.01 (**).

	Initial Rise (%, t=80.8s)	Maximum Rise (%)	Rate of Change (%/min)	Delay in Rise (s)
DMSO Control	-0.11 ±0.20	1.30 ±0.26 **	-0.14 ±0.02 **	0
3μM Ionomycin	2.20 ±0.69	6.70 ±2.70	1.19 ±0.13	0
50μM REV5901	6.23 ±1.30	33.78 ±0.66	3.81 ±0.42	0
+ 2mM EGTA	4.40 ±0.12	27.86 ±1.43 *	0.95 ±0.10 *	0
+ 100μM U73122	3.68 ±1.91	23.09 ±2.70 *	1.75 ±0.19 *	0
+ 10mM Neomycin	-1.32 ±1.66	23.78 ±2.21 *	3.90 ±0.43 *	28.8
+ 100μM Rottlerin	3.71 ±0.50	2.27 ±0.61 *	-0.39 ±0.04 **	0
+ 1μM Wartmannin	4.10 ±1.00	32.32 ±1.20	4.00 ±0.44	0

4.3 Chapter Discussion

Mechanotransduction is the term used to describe the processes by which chondrocytes 'respond' to extracellular mechanical stimuli by initiating cellular signalling pathways often involving the regulation of $[Ca^{2+}]_i$ levels. Examples of these extracellular stimuli include pressure, fluid flow and oscillations in extracellular ionic environment. Previous work has shown RVI and Gd^{3+}-sensitive calcium rise (in response to hypo-osmotic conditions) were exclusive to 2D cultured chondrocytes indicating a switch in the cellular response to external stimuli upon loss of phenotype (Kerrigan and Hall, 2008). Therefore, chondrocyte response to hyperosmotic challenge and chondrocyte calcium signalling were studied as key markers of chondrocyte phenotype.

The capacity of chondrocytes to exhibit RVI in response to a hyperosmotic challenge was studied as a key marker of differentiation. It was previously observed that freshly isolated chondrocytes did not exhibit RVI whereas upon 2D culture, RVI is activated and principally mediated by the NKCC (Kerrigan *et al.*, 2006; Qusous *et al.*, in press). Furthermore, volume regulatory mechanisms have been previously classified into 'slow' and 'robust' (Kerrigan & Hall, 2008) but passage-dependency was not investigated. We have shown that P1 chondrocytes exhibited linear volume recovery deemed 'slow' RVI over the course of the experiment recovering at a t½ of 9.60±0.9 minutes. Conversely, P2 and P3 chondrocytes exhibited logarithmic volume recovery deemed 'biphasic' with robust RVI at a rate of t½ of 3.5±1.0 and 2.8±0.39 minutes, respectively, followed by slow RVI at a rate of t½ of 10.1±1.0 and 10.9±1.0 (Table 4.1).

These data confirm previous work by others who suggested that cultured chondrocytes undergo a switch in mechanotransduction responses (Kerrigan *et*

al., 2006; Kerrigan & Hall, 2008), and our earlier observations that an intermediate dedifferentiated phenotype (termed 'mesodifferentiated') existed in P1 chondrocytes prior to final dedifferentiation upon further culture. The difference in RVI response in P1 could be mediated by the NKCC as previous work has shown that bumentanide-sensitive RVI can be induced in freshly isolated chondrocytes by actin depolymerisation (Kerrigan *et al.*, 2006). No change in NKCC expression was reported in response to 2D culture (Stokes *et al.*, 2002) and it is therefore conceivable that a change in NKCC activity, possibly regulated by actin organisation, rather than expression, is accountable for the lack of robust RVI in P1 chondrocytes.

Furthermore, chondrocytes have been found not to exhibit RVI *in situ* in response to hyperosmotic conditions, and therefore cell shrinkage provided chondrocytes with protective mechanism from joint articulation (Parker *et al.*, in press). It is therefore possible that differentiated chondrocytes do not exhibit RVI to maximise these benefits of cellular shrinkage which may lose significance upon loss of the differentiated state. This might furthermore explain the existence of a small population of chondrocytes possessing a volume of $2500\mu m^3$ in degenerate cartilage tissue (Bush & Hall, 2005) where loss of phenotype occurs.

The variation within chondrocyte populations of the same passage number was observed using box plot analysis, which indicated a more homogenous response in P1 chondrocytes when compared to freshly isolated chondrocytes, P2 or P3 chondrocytes (Figure 4.2). Chondrocytes *in situ* possess a wide range of cell volume (Bush and Hall, 2001) and are exposed to different extents of mechanical stimuli (Urban, 1994). Our results showed that freshly isolated chondrocytes appear to constitute a heterogeneous population as observed by the response to hyperosmotic conditions. The loss of heterogeneity upon introduction to culture may be attributed to what appears to be a relatively selective culture technique and thus a more homogenous response in

mesodifferentiated chondrocytes. Upon further culture, chondrocytes appear to dedifferentiate into another heterogeneous population capable of a wide range of response to a hyperosmotic challenge.

Intracellular calcium is a key regulator of various intracellular functions including mechanotransduction, and changes in $[Ca^{2+}]_i$ levels have been observed in response to various other mechanical stimuli. Previous work has shown that incubation with REV5901 induced an immediate and sustained elevation in $[Ca^{2+}]_i$ (Ali *et al.*, in press), thereby suggesting a potential mechanism by which REV5901 inhibits other cellular functions including RVD and 5-Lipoxygenase activity. The ability of REV5901 to induce a rise in $[Ca^{2+}]_i$ rendered it a suitable pharmacological candidate for modulation of $[Ca^{2+}]_i$ levels for further studies aimed at using calcium homeostasis mechanisms as a marker of phenotype.

Changes in $[Ca^{2+}]_i$ signalling in response to expansion were studied using REV5901 as an inducer of $[Ca^{2+}]_i$ rise and it was observed that there was a decrease in REV5901-induced intracellular store-mediated calcium release in response to 2D culture. Previous work has shown that mechanical pressure enhanced the sensitivity of IP3R channel (Zhang *et al.*, 2006) possibly due to chondroprotective calcium mechanisms (Amin *et al.*, 2008). Therefore, it is suggested that, like the loss of mechanical stimuli, the loss of phenotype may decrease sensitivity of intracellular calcium stores to REV5901 in 2D cultured chondrocytes. Conversely, an increase in store operation, via various stimuli including IP3 receptor upregulation, has been seen in response to culture of both myocytes and smooth muscle cells (Dreja *et al., 2001;* Berra-Romani *et al.*, 2008).

No change in extracellular calcium influx was observed in REV5901 treated 2D chondrocytes despite changes in individual channel contribution to calcium influx as determined by using calcium channel inhibitors (Figure 4.4). Incubation with 75μM ruthenium red prior to REV5901 loading induced a 46.36±2.53% inhibition

in $[Ca^{2+}]_i$ rise which did undergo any significant change upon culture, suggesting no change in the role of TRPV channels in calcium homeostasis upon 2D culture. Nevertheless, Previous work has shown that TRPV1 is upregulated in response to expansion (van Rossum & Patterson, 2009) and that TRPV4 regulated SOX9 expression and thus played a role in chondrocyte differentiation (Muramatsu *et al.*, 2007). Our work was limited by the non-specific inhibitory effects of ruthenium red on all members of TRPV channels as well as others including NCX (Gunthorpe *et al.*, 2002).

Changes in the capacity of NCX and SACC to regulate REV5901-mediated rise in $[Ca^{2+}]_i$ in response to culture were more prominent. The use of sodium-free BPS induced a 84.03±3.50% inhibition, whereas upon culture there was a reduction in calcium inhibition to 55.413±1.13%. Conversely, the sensitivity of REV5901-induced $[Ca^{2+}]_i$ rise to Gd^{3+} inhibition increased upon 2D culture from 33.02±1.53% to 50.80±1.22% confirming previous reports that SACC is involved in chondrocyte dedifferentiation (Perkins *et al.*, 2005; Kerrigan & Hall, 2008).

The REV5901-induced signalling pathway was investigated in freshly isolated chondrocytes using pharmacological inhibitors of selected intracellular proteins / molecules involved in known Ca^{2+} regulatory signals. GCPR have been shown to induce the activation of G-proteins including $G\alpha$ and Gq, both of which are capable of inducing a $[Ca^{2+}]_i$ rise via IP3 production in various cell types including leukocytes and epithelial cells (Verghese *et al.*, 1986; Muallem & Wilkie, 1999; Liu & Wu, 2004). The necessity of IP3 in REV5901 calcium modulation was confirmed by prior incubation with 10mM neomycin (James *et al.*, 2004) where it was observed that despite the lack of change in the rate of $[Ca^{2+}]_i$ rise, neomycin induced a ~30 second delay in the calcium response to REV5901 and thus a decrease in final $[Ca^{2+}]_i$ rise. Nevertheless, the reason for a steady rise in $[Ca^{2+}]_i$ was possibly the over-production of IP3 during the 30 second delay to compensate for the sequestering of PIP2 molecules by neomycin.

Incubation with, wartmannin, an inhibitor of PI5K at 100nM (Liu *et al.*, 2001), prior to REV5901-loading did not have a significant effect on $[Ca^{2+}]_i$ rise, thereby indicating that REV5901-induced $[Ca^{2+}]_i$ rise was not PI5K-dependent and therefore not mediated by Gq-PI5K pathway. The significance of Gα-PLCβ3 pathway in REV5901-induced $[Ca^{2+}]_i$ was investigated using U73122, a pharmacological inhibitor of PLCβ3 at 100μM (Hou *et al.*, 2004) and a 2.18-fold reduction in the rate of $[Ca^{2+}]_i$ rise was obtained, thus confirming that REV5901 acts on G-protein α signal via PLCβ3 (Figure 4.7). Similarly, the role of IP3 in $[Ca^{2+}]_i$ has been previously seen in chondrocytes in response to a hypo-osmotic challenge (Sanchez *et al.,* 2003*).*

The signalling pathway was further investigated by the inhibition of PKC using 100μM Rottlerin (Gschwendt *et al.*, 1994) which reduced the $[Ca^{2+}]_i$ rise to 2.27±0.61%. The inhibitory effect of Rottlerin may, however, be grossly overestimated as recent reports have demonstrated an inhibitory effect of Rottlerin on other kinase and non-kinase proteins *in vitro* (Davies *et al.*, 2000) including potassium channels (Zakharov *et al.*, 2005). Nevertheless, It was, therefore, concluded that REV5901 induced (but not exclusively) the activation of GCPR which in turn stimulated diacylglycerol (DAG) release by PLCβ3 and the activation of PKC, thus augmenting the signal and promoting the accumulation of IP3 molecules required for $[Ca^{2+}]_i$ release from intracellular stores by IP3 receptors (IP3R; Figure 4.7).

Most noticeable variations in the effects of pharmacological inhibitors were difference in the magnitude of inhibition between U73122, neomycin and Rottlerin. Both U73122 and neomycin reduced the $[Ca^{2+}]_i$ rise to ~23.00%, a non-significantly different value to that obtained in the presence of 2mM EGTA in PBS, thus suggesting that IP3 was not necessary for calcium influx across the plasma membrane. The use of Rottlerin, however, demonstrated an augmented inhibitory effect on $[Ca^{2+}]_i$ rise, thus indicating that PKC is involved in the store-

independent direct activation of calcium channels. Potential channel targets of PKC activation may include TRPV1 as recent reports have shown that the phospohorylation of TRPV1 requires PKC, protein kinase A and protein phosphatase 2B in embryonic kidney cell line (van Rossum & Patterson, 2009). The expression of TRPV1 has been confirmed in both freshly isolated and 2D cultured chondrocytes (Gavenis *et al.*, 2009).

In conclusion, these data have quantified changes in mechanotransduction responses to expansion. In contrast to freshly isolated chondrocytes, 2D cultured chondrocytes exhibited RVI with a distinct response trend in P1 chondrocytes confirming the existence of a different phenotype in the first 9 days of culture. REV5901-induced rise in $[Ca^{2+}]_i$ was investigated and a reduction in store-sensitivity observed upon culture. Moreover, the role of NCX, SACC and possibly TRPV1 has been suggested in chondrocyte homeostasis with changes in individual contributions reported in response to 2D culture. Finally, these data have documented changes in mechanotransduction upon 2D culture, thereby indicating that these responses may be used as phenotypic markers of a differentiated chondrocyte phenotype to ensure optimal performance of expanded chondrocytes in artificial cartilage.

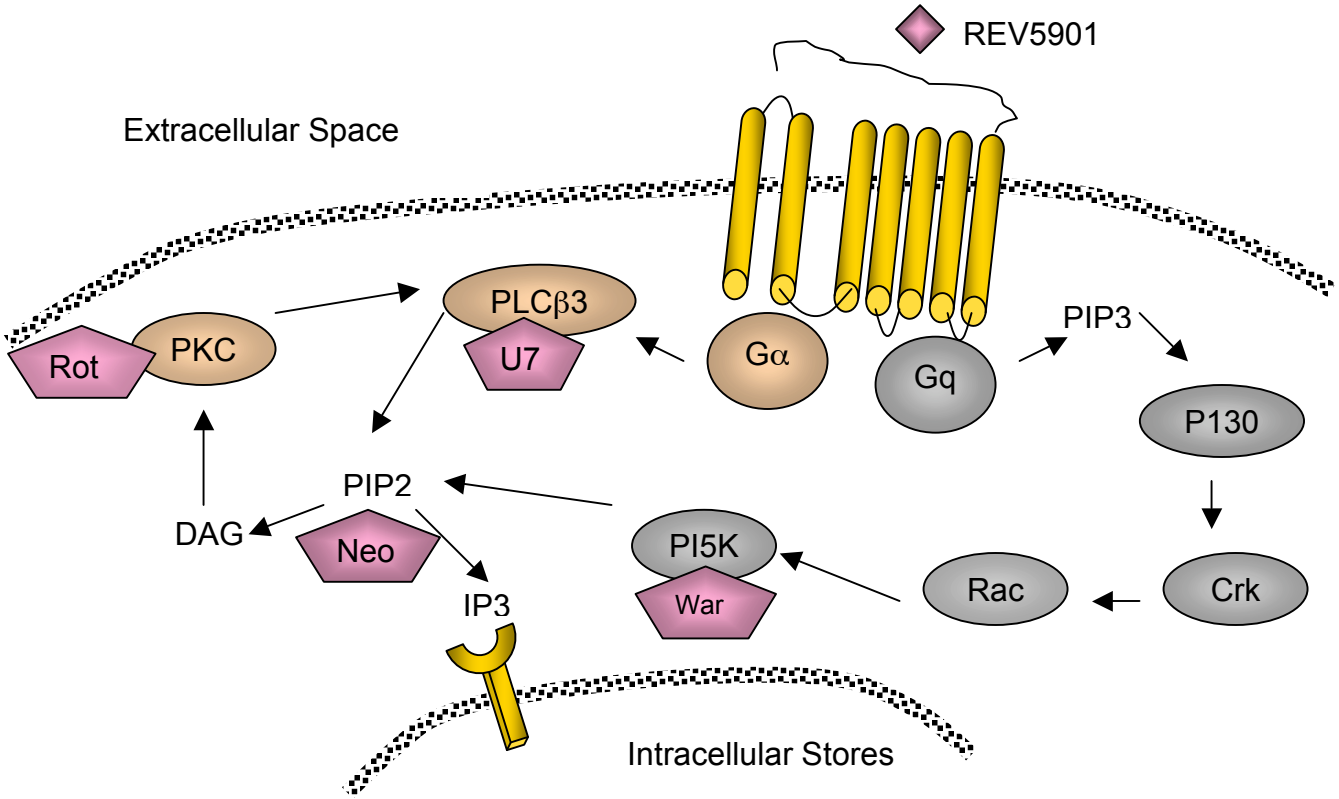

Figure 4.7: Representative diagram of currently known intracellular calcium signalling pathways.

REV5901 has been shown to be an antagonist to cysteinyl leukotrine receptor, a member of G-protein coupled receptors superfamily. Two potential pathways of action for G-proteins on $[Ca^{2+}]_i$ were proposed and investigated; the PLCβ3 and PI5K pathways. We have confirmed that PLCβ3 pathway is not involved in REV5901-mediated calcium rise as inhibition of PI5K using Wartmannin (War) did not inhibit the calcium rise (pathway shaded in grey). Conversely, the use of U73122 (U7), Rottlerin (Rot) or Neomycin (Neo) negatively influenced the maximum change in $[Ca^{2+}]_i$ recorded, suggesting that $[Ca^{2+}]_i$ manipulating properties of REV5901 acted via the PLCβ3 pathway.

5 Experimental Chapter: The role of DEL1 in 2D chondrocytes expansion

5.1 Chapter introduction

Integrin signalling has been the subject of intensive studies over the last 2 decades since the term was first used to describe cell surface receptors which mediate cellular adhesion and interaction with the extracellular matrix (Tamkun *et al.*, 1986; Ruoslahti & Pierschbacher, 1987). Integrins are transmembrane dimers composed of α and/or β chains non-covalently bound together with ligand specificity determined by the combination of the chains (Hemler, 1990; Hynes, 1992). In chondrocytes of healthy cartilage, several integrins have been found to be expressed with especially elevated levels of $\alpha1\beta1$, $\alpha5\beta1$ (fibronectin recpetor; FnR) and $\alpha v\beta5$ in addition to $\alpha3\beta1$ and $\alpha v\beta3$ (Woods *et al.*, 1994). Conversely, chondrocytes from OA cartilage expressed elevated levels of $\alpha2$, $\alpha4$ and $\beta2$ chains (Ostergaard *et al.*, 1998) with a reduction in $\beta1$ chains inversely related to the progression of OA (Lapadula *et al.*, 1997, 1998). Upon isolation, chondrocytes have been shown to possess elevated levels of $\alpha2$, $\alpha5$, $\alpha6$, αv and $\beta1$ chains (Durr *et al.*, 1993) whereas upon monolayer culture there was a decrease in $\alpha1$ and an increase in $\alpha2$-6 chains and $\alpha5\beta1$ heterodimers (Enomoto-Iwamoto *et al.*, 1997; Diaz-Romero *et al.*, 2005). These findings indicate a role for integrins in the maintenance of chondrocyte homeostasis in different conditions and thus the regulation of chondrocytic phenotype.

Integrin signalling induces a set of cellular functions including differentiation, morphology switch, actin organtisation, growth and survival as well as cellular attachment, the initial and most anticipated function (Aszodi *et al.*, 2003; Zemmyo *et al.*, 2003; Bengtsson *et al.*, 2005). $\alpha2\beta1$ chains were identified as essential for chondrocyte attachment on type II collagen-coated plates whereas $\alpha5\beta1$ chains were required for attachment on fibronectin-coated plates (Enomoto-Iwamoto *et al.*, 1997) or on a monolayer of fibroblasts (Ramachandrula *et al.*, 1992). It was observed that $\alpha2$, $\alpha3$ and $\beta1$ chains are

involved in mediating a signal that promotes collagen X production with the β1 being additionally involved in actin polymerisation and survival (Hirsch *et al.*, 1997), maintanance of spherical morphology (Shakibaei *et al.*, 1997), and enhancing TGF-induced differentiated phenotype (Scully *et al.*, 2001). Conversely, α5β1 heterodimer has been shown to induce collagenase and stromelysin production in synovial fibroblasts (Werb *et al.*, 1989), coordinate cartilage differentiation in mouse embryos (Garciadiego-Cazares *et al.*, 2004), mediate a switch to fibroblast-like morphology (Ramachandrula *et al.*, 1992) and proliferation in articular chondrocytes (Enomoto-Iwamoto *et al.*, 1997).

DEL1 is a 52-kDa extracellular matrix integrin ligand composed of two carbohydrate-binding discoidin domains and two EGF-like Ca^{2+}-binding repeats, the second of which contains an RGD motif (Hidai *et al.*, 1998). DEL1 is expressed by endothelial cells during embryological vascular development and has been shown to be expressed in angiogenic neoplastic tissue (Aoka *et al.*, 2002), ischemic tissue (Ho *et al.*, 2004) and human foetal chondrocytes (Stokes *et al.*, 2002). Similarly to another member of the EGF-like repeats and discoidin I-like proteins (Lactadherin; EDIL1), DEL1 activity requires the interaction with integrin αvβ3 (Penta *et al.*, 1999; Silvestre *et al.*, 2005) and upon DEL1 ligation, integrins undergo aggregation and induce phophorylation of downstream signalling proteins (Penta *et al.*, 1999).

The expression level of DEL1 in adult chondrocytes and biological significance of DEL1/integrin interaction has not been previously investigated. As expansion for tissue engineering purposes requires a 3D matrix that would provide the correct integrin signals (van der Kraan *et al.*, 2002), we have studied the role of DEL1 in bovine articular chondrocyte 2D expansion in this experimental chapter.

Aims of Experimental Chapter

1 Study the level of DEL1 expression in response to 2D culture.

2 Successfully perform DEL1 knockdown using the designed siRNA molecules

3 Study the role of DEL1 in attachment.

4 Investigate the effect of DEL1 knockdown on phenotypic markers including:
   i. Expression battery of chondrocytes
   ii. RVI response
   iii. REV5901-mediated rise in $[Ca^{2+}]_i$

5.2 Results

5.2.1 The expression level of DEL1 in response to 2D culture of chondrocytes

As previously mentioned, the loss of DEL1 upregulation in 2D cultured foetal chondrocytes suggested a potentially important role in the regulation of the chondrocytic phenotype (Stokes *et al.*, 2002), and therefore the next part of the project was to determine the bio-significance of DEL1 in 2D cultured chondrocytes. Freshly isolated and 2D cultured chondrocytes were collected by centrifugation and RNA isolated and reverse transcribed as previously described. The level of DEL1 transcription was subsequently studied by PCR and densitometery DNA electrophoresis (Materials and Methods).

There was a 2.48±0.34-fold increase in the level of DEL1 expression upon 9 days of culture ($p<0.05$) and subsequently declined in culture reaching 0.68±0.04 and 0.86±0.08 of baseline levels in P2 and P3 chondrocytes, respectively (Figure 5.1), with no significant changes observed ($p>0.05$). The increase in DEL1 expression in P1 chondrocytes was simultaneous to the 1.75-fold increase in SOX9 expression and the switch in type II:I collagen expression ratio as previously discussed (Section 3.2.3). These data, therefore, suggested a potential role for DEL1 in phenotype loss and an association between the expression of DEL1 and SOX9.

To further elucidate the time of the rise in DEL1 expression in the first passage, RNA was isolated from 2D cultured chondrocytes after 2, 4 and 6 days in culture and RT-PCR analysis performed as previously described. The level of DEL1 expression increased upon 2 days in culture reaching 12.19±1.67-fold increase

compared to freshly isolated chondrocytes and declined to 10.44±1.43, 6.02±0.82 and 2.48±0.34-fold increase after 4, 6 and 9 days, respectively (Figure 5.2A).

Changes in the ratio of type II:I collagen expression were observed to be of later onset than those in DEL1 expression, whereby no significant change in collagen expression ratio was observed by the 2nd day in culture with a value of 1.12±0.15 as standardised against freshly isolated chondrocytes. The switch in collagen ratio expression, however, only occurred by the 4th day in culture (Figure 5.2B) with a decrease to 0.67±0.11 in the expression ratio, which further declined to 0.30±0.10 and 0.39±0.10 upon 6 and 9 days in culture, respectively. These data suggested a switch in collagen phenotype of chondrocytes following a 12.19±0.15-fold increase in DEL1 expression at the commencement of culture.

The expression and secretion of DEL1 proteins was confirmed by western blot but not quantified due to the poor quality of anti-DEL1 polyclonal preparation. Media from chondrocytes were collected as previously described (Materials and Methods) and subjected to 12.5% polyacrylamide SDS-PAGE and gels blotted on membrane and probed for DEL1 expression. DEL1 proteins were detected in freshly isolated and 2D cultured chondrocytes (Figure 5.3) confirming the expression of DEL1 in adult bovine chondrocytes.

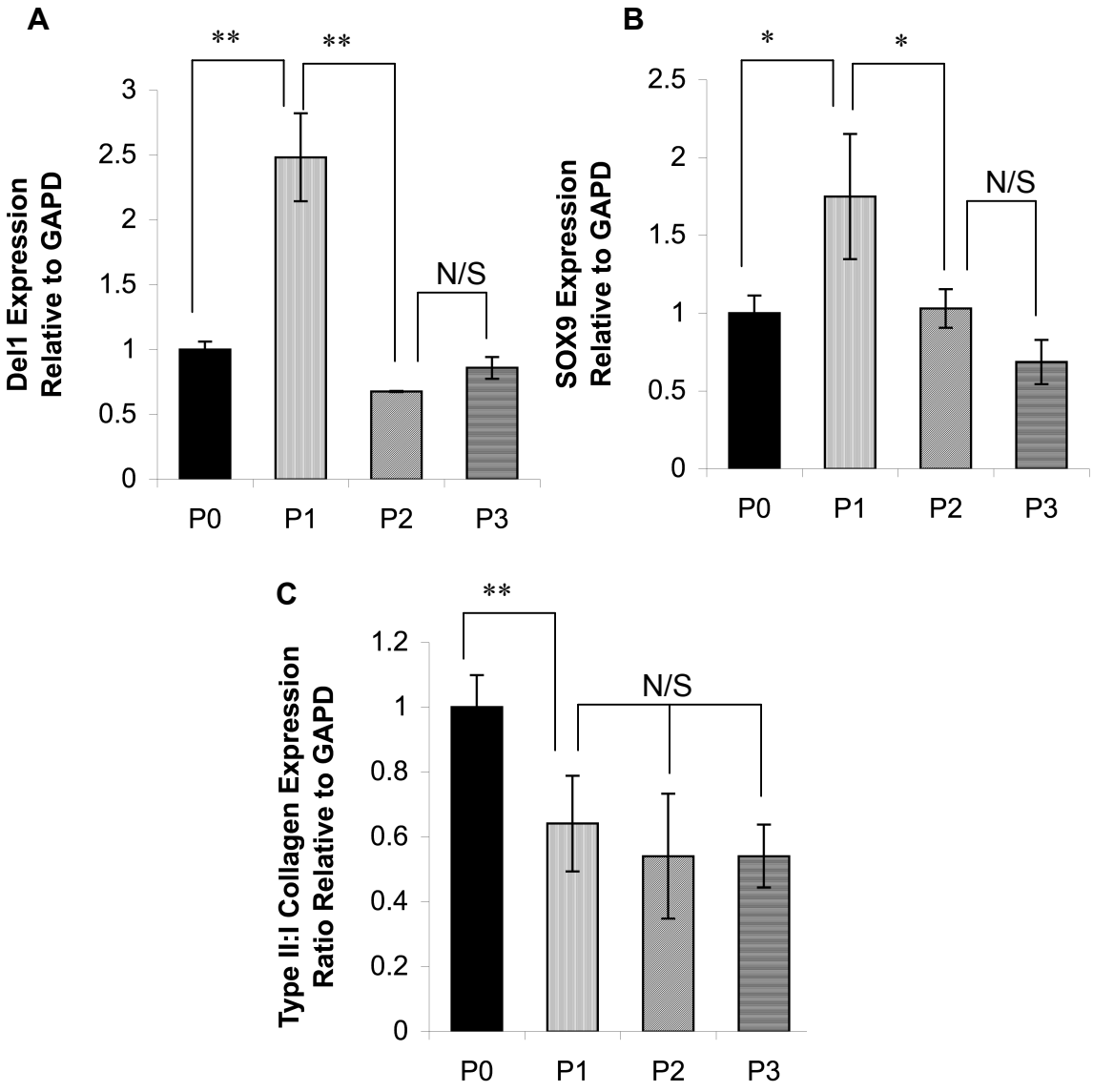

Figure 5.1: Changes in the expression of DEL1 in chondrocytes upon 2D culture.

RNA was isolated from freshly isolated and 2D-cultured chondrocytes for 9 (P1) days, 14 (P2) and 21 (P3) days, reverse transcribed and subjected to PCR. The amount of DNA in the PCR products was calculated from the intensity and size of the bands and calculated relative to amount of GAPD product. The level of expression of SOX9 declined upon culture despite the transient increase in P1 (panel B) whereas the ratio of type II:I collagen expression decreased significantly upon culture. DEL1 expression levels were associated with those of SOX9 with a transient ~2.5-fold-increase in P1 chondrocytes ($p<0.05$) with a decrease to baseline levels upon further culture. N=7, experiment repeated 6 times Values shown as mean ± s.e.m. T-test p-values were $p<0.05$ (*) and $p<0.01$ (**). N/S, non significant.

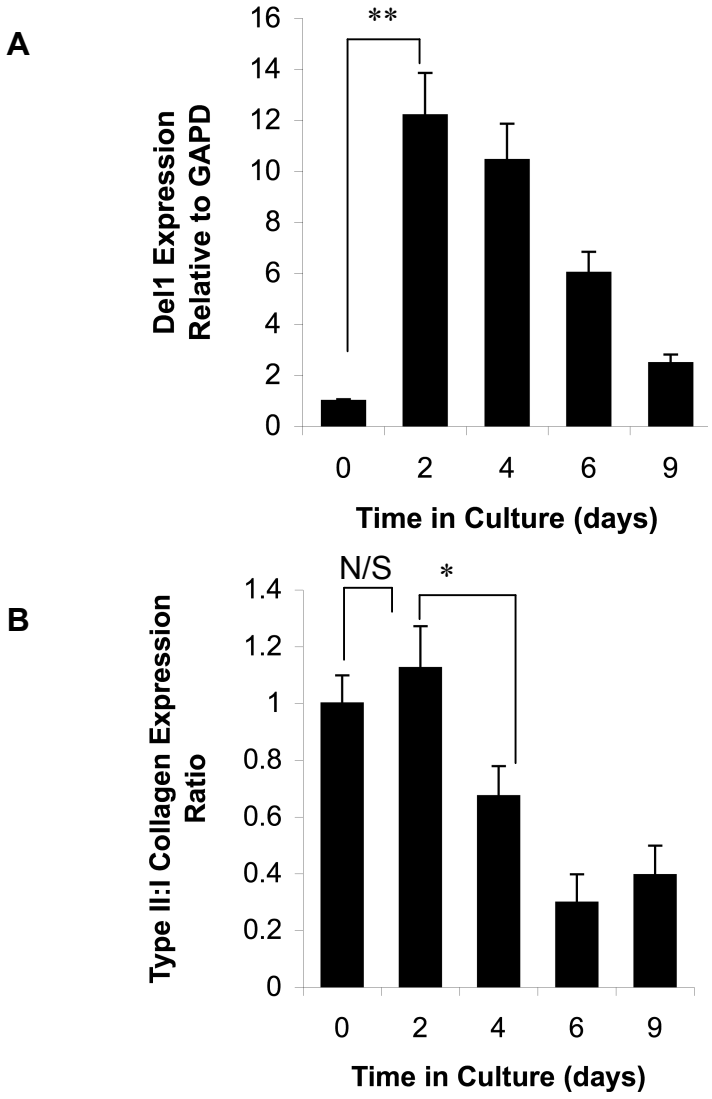

Figure 5.2: Changes in DEL1 and collagen expression ratio within the first 9 days of 2D culture.

RNA was isolated from freshly isolated and 2D-cultured chondrocytes after 2, 4 6 and 9 (P1) days in culture. RNA was reverse transcribed and subjected to PCR. Changes in expression DEL1 and col2:col1 expression were quantified relative to expression levels in freshly isolated chondrocytes (P0). A more extensive study to assay changes within the first 9 days of culture showed a 12.19±1.67-fold rise in DEL1 expression from as early as 2 days (Panel A) in culture and a significant decrease in type II:I collagen ratio observed by 4th day in culture (Panel B). N=7, experiment repeated 6 times. Values shown as mean ± s.e.m. T-test p-values were p<0.05 (*) and p<0.01 (**). N/S, non significant.

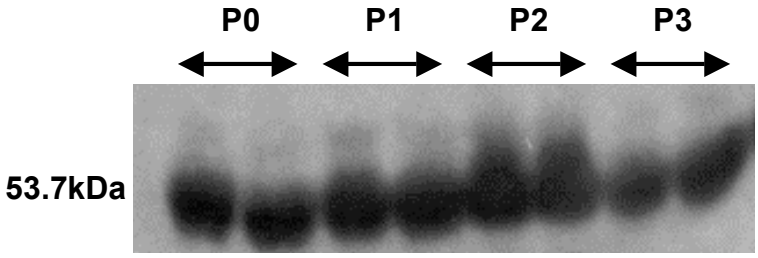

Figure 5.3: Western blot image of chondrocyte supernatant assayed for DEL1 protein.

Media supernatants from freshly isolated (P0) and 2D cultured chondrocytes (P1, P2 and P3) were isolated and assayed by bradford reagent prior to being resolved on 12.5% polyacrylamide SDS-PAGE. Western blot was performed and the membranes probed using anti-DEL1 polyclonal antibodies. DEL1 proteins were detected in both freshly isolated and 2D cultured chondrocytes but images were not quantifiable due to the poor quality of the antibodies. N=4, experiment repeated 2 times.

5.2.2 DEL1 knockdown using RNAi technology

To investigate the role of DEL1 on chondrocytic phenotype, RNAi technology was employed by transfecting freshly isolated chondrocytes with anti-DEL1 siRNA molecules prior culture-stimulated DEL1 rise. Firstly, to study the efficacy and duration of the siRNA molecules designed, freshly isolated chondrocytes were transfected in suspension with 10nM and 3μl/ml HiPerfect transfection reagent, as previously described, and incubated in serum-free 380mOsm media at 37°C in a humidified 5% CO_2 incubator. RNA was extracted after 2, 4, 6 and 9 days and RT-PCR performed to assay the levels of DEL1 expression.

Anti-DEL1 siRNA molecules achieved successful knockdown with the level of DEL1 expression reduced to 0.24±0.01-fold (relative to freshly isolated chondrocytes) after 2 days of transfection and the knockdown state was maintained for at least another 4 days reaching 0.24±0.01% and 0.39±0.02% with no significant differences ($p>0.05$) by the 4^{th} and 6^{th} days post-transfection. After 9 days of transfection, however, DEL1 expression resumed reaching 1.51±0.08 baseline levels ($p<0.05$; Figure 5.4). These data confirmed the transience of siRNA-mediated knockdown observed to last for a mere 6 days post-transfection and demonstrated the efficacy of anti-DEL1 siRNA sequences designed. The effect of anti-DEL1 siRNA molecules on the growth curve of chondrocytes was assayed by trypan blue assay after 2, 4, and 6 days of culture and no significant difference was observed in the growth curve of anti-DEL1 siRNA transfected, mock transfected, or non transfected chondrocytes (doubling times of 4.02, 3.66 and 3.73 days, respectively; $p>0.05$; Table 5.1).

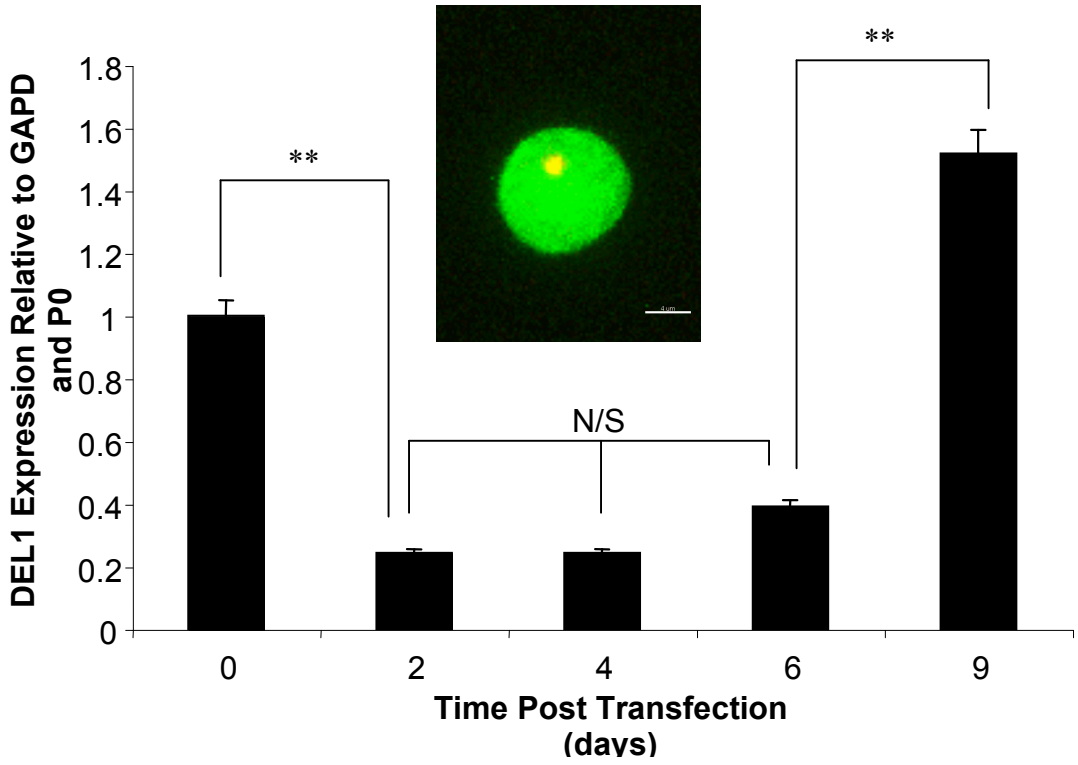

Figure 5.4: The transience inhibition effect of anti-DEL1 siRNA transfection on DEL1 mRNA levels.

Freshly isolated chondrocytes were transfected in suspension using 10nM anti-DEL1 Cy3-tagged siRNA (inset red; appears yellow due to overlay) freshly prepared with 3μl/ml HiPerfect Reagent and incubated in culture media for 6 hours prior to being imaged using confocal microscopy where siRNA molecules were observed around the nucleus of the Calcein-AM-labelled chondrocyte (green). DEL1(-) chondrocytes were cultured for 2, 4, 6 and 9 days, RNA isolated and RT-PCR performed to assay changes in DEL1 expression in response to transfection. Upon 2 days of trasfection, DEL1 expression was significantly reduced to 0.24±0.01 of baseline levels and remained diminished for another 4 days. DEL1 expression levels were restored upon 9 days in culture with 1.52±0.08% relative to freshly isolated chondrocytes. Values shown as mean ± s.e.m. N=4, experiment repeated 3 times. T-test p-values were p<0.01 (**). N/S, non significant.

Table 5.1: Growth rate properties of P1 and DEL1(-)/P1 chondrocytes.

The effect of siRNA transfection on the growth rate of chondrocytes was assayed by transfection of freshly isolated chondrocytes in suspension prior to introduction to culture and performing cell count every 2 days in culture using trypan blue and a haemocytometer. The rates of cell division and doubling times were obtained from a linear regression of Log(cell number) vs time in culture and no significant change in the growth rate was observed upon transfection or DEL1 knockdown. N=4, experiment repeated 6 times. Data shown as means ± s.e.m.

	Doubling time (days)	R^2 value	Viability (%)
P1	3.7±0.2	0.99	71.0±4.0
DEL1(-)/P1	4.0±0.3	0.99	65.2±5.5
Mock-tranfected P1	3.7±0.1	0.91	68.5±4.0

5.2.3 The role of DEL1 knockdown on chondrocytic phenotype, morphology and mechanotransduction

Having determined a change in DEL1 expression following culture, the effect of DEL1 expression on phenotypic properties was studied by long-term knockdown of DEL1 using RNAi. Freshly isolated chondrocytes were transfected with anti-DEL1 siRNA in suspension prior to commencing culture in serum-enriched media for 9 days (chondrocytes termed DEL1(-)/P1). Due to the transiency of the knockdown, chondrocytes were repeat-transfected after 6 days in culture to maintain the inhibition of DEL1 translation. Control chondrocytes employed in these experiments were P1 chondrocytes mock-transfected using negative control (scrambled) siRNA (Ambion).

5.2.3.1 The role of DEL1 on chondrocyte attachment

The role of DEL1, defined as a matrix adhesion protein, on cellular attachment in chondrocytes was investigated during 2D culture. Briefly, freshly isolated and 2D cultured chondrocytes (isolated by trypsinisation) were washed and seeded at LD as previously described. Chondrocytes were subsequently incubated for 1, 2 or 4 hours at 37°C in a humidified CO_2 incubator prior to removal of the media containing unattached cell suspension and the addition of fresh media containing 0.5mg/ml MTT and incubation for 3 hours at 37°C.The number of attached chondrocytes was ascertained by measuring the absorbance of reduced MTT as previously described (Materials and Methods).

After one hour in 380mOsm media, 78.20±2.29% of freshly isolated chondrocytes seeded were attached whereas after 9 days in culture, 55.00±2.74% of P1 chondrocytes underwent attachment in one hour of seeding. When cultured for longer periods, however, chondrocytes recovered their original quick-onset attachment properties with 87.5±3.35% and 91.2±3.35%

attachment after 1 hour of seeding in P2 and P3 2D cultured chondrocytes, respectively. The lack of initial attachment response (after 1 hour of seeding) in P1 2D cultured chondrocytes was associated with an over-expression of DEL1 in 2D culture. Following incubation for 4 hour, attachment reached 105.40±2.19, 98.33±7.16, 120.33±2.13 and 116.48±2.12 in P0, P1, P2 and P3 chondrocytes respectively, with no significant difference observed ($p>0.05$; Figure 5.5).

The rate of attachment was additionally studied by linear regression of percentage attachment over time. Freshly isolated, P2 and P3 chondrocytes exhibited a rate of attachment of 10.13%/hour, whereas P1 chondrocytes possessed a significantly higher rate of 15.07%/hour ($p<0.05$), suggesting that despite a late onset attachment in P1 chondrocytes, a higher rate of attachment was exhibited in the presence of elevated levels of DEL1 expression. These data suggested a potential role for DEL1 in the regulation of P1-exculsive attachment profile characterised by an increased rate yet slow onset attachment.

5.2.3.1.1 The effect of DEL1 knockdown on the rate of attachment of chondrocytes

Therefore, the necessity for DEL1 in attachment of chondrocytes was assayed upon continuous knockdown of P1 chondrocytes for 9 days prior to isolation by trypsinisation, seeding and performing MTT attachment assay as previously described. Initial attachment (upon 1 hour in culture) was significantly reduced from 55.0±2.74% in control P1 chondrocytes to 8.12±3.33% ($p<0.05$) and percentage attachment after 4 hours in culture from 98.33±7.16% to 24.59±1.83% ($p<0.05$; Figure 5.6). These data have shown a decreased rate of attachment in the absence of DEL1 expression from 15.07%/hour in control chondrocytes to 5.12%/hour ($p<0.05$). It was thus concluded that an increase in release of DEL1 in P1, if time-dependent and therefore of late onset, is necessary for the attachment of chondrocytes for at least 9 days upon culture, thus contributing to higher attachment rates in P1 chondrocytes (Table 5.2).

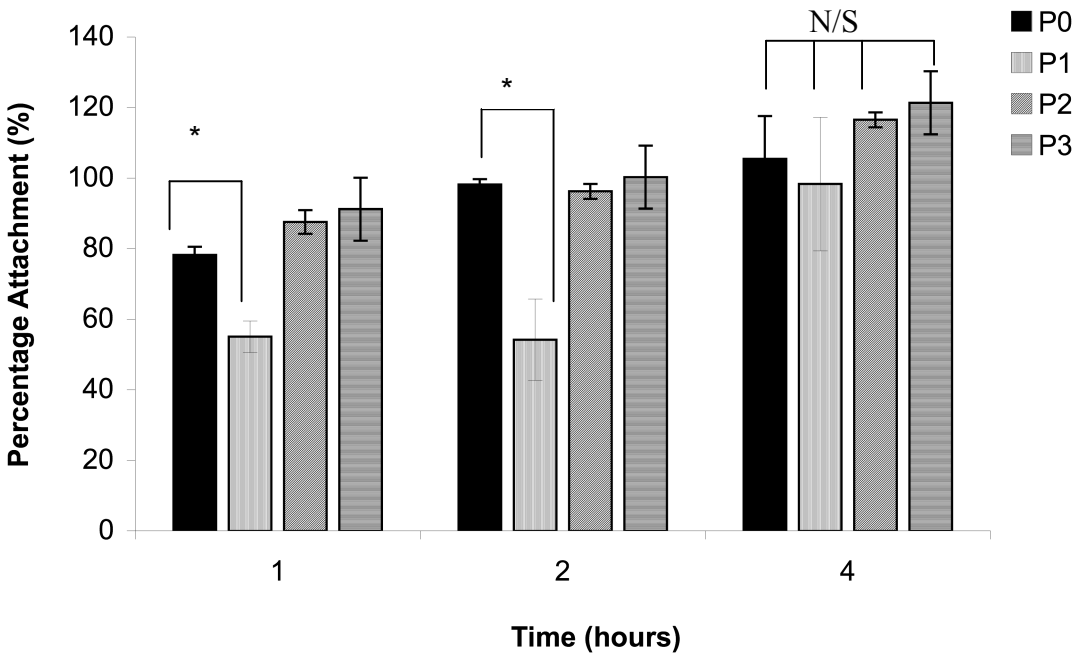

Figure 5.5: Percentage attachment of freshly isolated and 2D cultured chondrocytes.

Chondrocytes were isolated and cultured for 9, 14 and 21 days prior to isolation and seeding at culture density and incubation at 37°C in a humidified incubator. Following incubation for 1, 2 and 4 hours, media containing unattached chondrocytes were aspirated and replaced with culture media containing 0.5mg/ml MTT to assay for cell viability as previously described. Freshly isolated (P0), P2 and P3 chondrocytes exhibited an early onset attachment with 78.20±2.29%, 91.16±3.35% and 87.52±3.35% attachment within an hour of seeding, respectively, whereas only 55.00±12.74% of P1 chondrocytes attached under identical conditions ($p<0.05$). Following 4 hours of seeding, chondrocytes reached high levels of attachment with no significant differences observed in response to 2D culture ($p>0.05$) with 105.40±12.19%, 98.32±12.12%, 110±17.07% and 105.93±17.07 attachment in freshly isolated, P1, P2 and P3 chondrocytes. Values shown as mean ± s.e.m. N=4, experiment repeated 3 times. T-test p-values were $p<0.05$ (*). N/S, non significant.

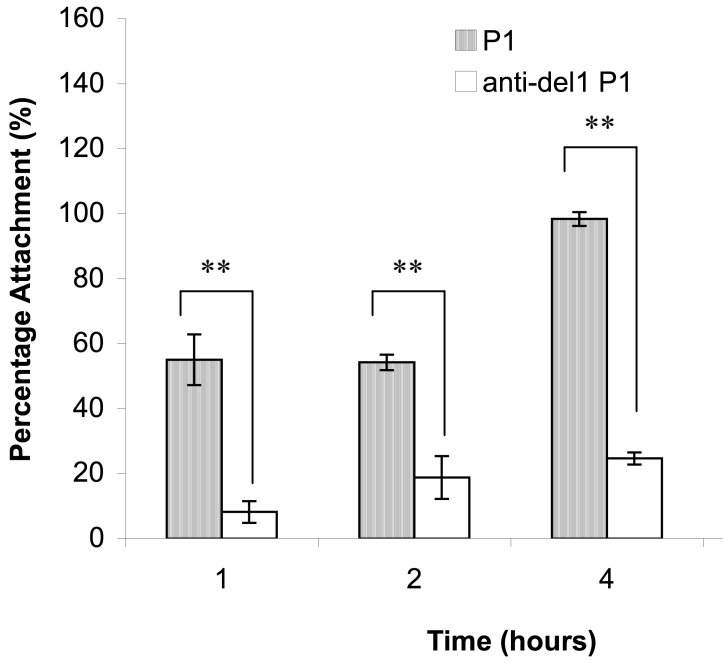

Figure 5.6: Percentage attachment of chondrocytes against time in control and Del(-)/P1 chondrocytes.

To confirm the necessity for DEL1 in cellular attachment in P1 chondrocytes, freshly isolated chondrocytes were transfected with anti-DEL1 siRNA and cultured as previously described. Upon reaching P1, chondrocytes were collected by trypsin treatment and centrifugation, seeded at the culture density and incubated at 37°C prior to removal of the supernatant containing unattached cell suspsension at 1, 2 and 4 hours post-seeding. The number of attached chondrocytes was measured using 0.5mg/ml MTT as previously described. Upon DEL1 knockdown there was a decrease in initial attachment from 55.00±2.74% in P1 mock transfected chondrocytes to 8.12±3.33% and in final attachment from 98.33±7.16 to 24.59±1.83 at 4 hours post seeding. N=4, experiment repeated 3 times. Data shown as means ± s.e.m. T-test p-values were p<0.01 (**).

Table 5.2: Summary of attachment properties of freshly isolated and 2D cultured chondrocytes.

Freshly isolated (P0) and P2 and P3 chondrocytes exhibited quick onset attachment properties with 80.60% of chondrocytes attaching within 1 hour of seeding, whereas only 55.00±2.74% of P1 chondrocytes attached within the same time. After 4 hours in culture, however, P1 chondrocytes reached a similar plateau of cellular attachment to the one observed in P0, P2 and P3 chondrocytes, thus demonstrating a higher rate of attachment. Upon DEL1 knockdown, however, there was a significant reduction in both intital attachment and attachment rate. N=10, experiment repeated 6 times. Data shown as means ± s.e.m. T-test p-values (against freshly isolated chondrocytes) were p<0.05 (*) and p<0.01 (**).

	Rate (Δ %/h)	Initial Percentage attachment	Onset	Time for 100% attachment (hour)	Efficiency
P0	10.13	80.60±2.29%	Fast	1.92	Low
P1	15.07 *	55.00±2.74% **	Slow	4.45 *	High
P2	10.13	80.60±3.35%	Fast	1.92	Low
P3	10.13	80.60±3.22%	Fast	1.92	Low
DEL1(-)/P1	5.1 **	8.10±3.33 % **	Slow	18.51**	Low

5.2.3.2 Chondrocyte Morphology

To study the effect of DEL1 knockdown on chondrocyte morphology, DEL1(-)/P1 chondrocytes were cultured under conditions of longterm DEL1 knockdown, loaded with 5μM calcein-AM to stain the cellular body and subsequently imaged using CLSM with 1μm depth steps. Images were loaded in Imaris 6.3.1, isosurface surpace 'objects' created around the cellular structures and cell dimensions obtained as previously described.

No significant differences were observed in cell depth (a) of P1 chondrocytes upon knockdown with values of 2.24±0.19μm and 2.04±0.36μm in control P1 chondrocytes and DEL1(-)/P1 counterparts, respectively ($p>0.05$). Furthermore cell width (b) of P1 chondrocytes was determined at 5.19±0.66μm and 5.52±0.50μm upon knockdown with no significant changes observed ($p>0.05$). Finally, chondrocyte length (c) decreased upon knockdown from 12.51±1.82μm in mock transfected 2D cultured P1 chondrocytes to 11.12±1.00μm in DEL1(-)/P1 chondrocytes with no significant differences observed ($p>0.05$; Figure 5.7).

There was no significant change ($p>0.05$) in the sphericity upon knockdown with sphericity values determined at 0.52±0.03 and 0.50±0.03 in control P1 and DEL1(-)/P1 chondrocytes, indicating that the knockdown of DEL1 was not sufficient to restore chondrocytic 'round' morphology. There was, however, a significant decrease in cell volume in response to DEL1 knockdown from 673.38±39.59 in mock transfected P1 chondrocytes to 440.02±46.74μm3 in DEL1(-)/P1 chondrocytes, rendering the latter of the two groups more similar to freshly isolated chondrocytes in size ($p<0.05$; Figure 5.7). These data indicated that DEL1 contributed to an increase in cell length upon culture and played a role in cell volume expansion upon 2D culture.

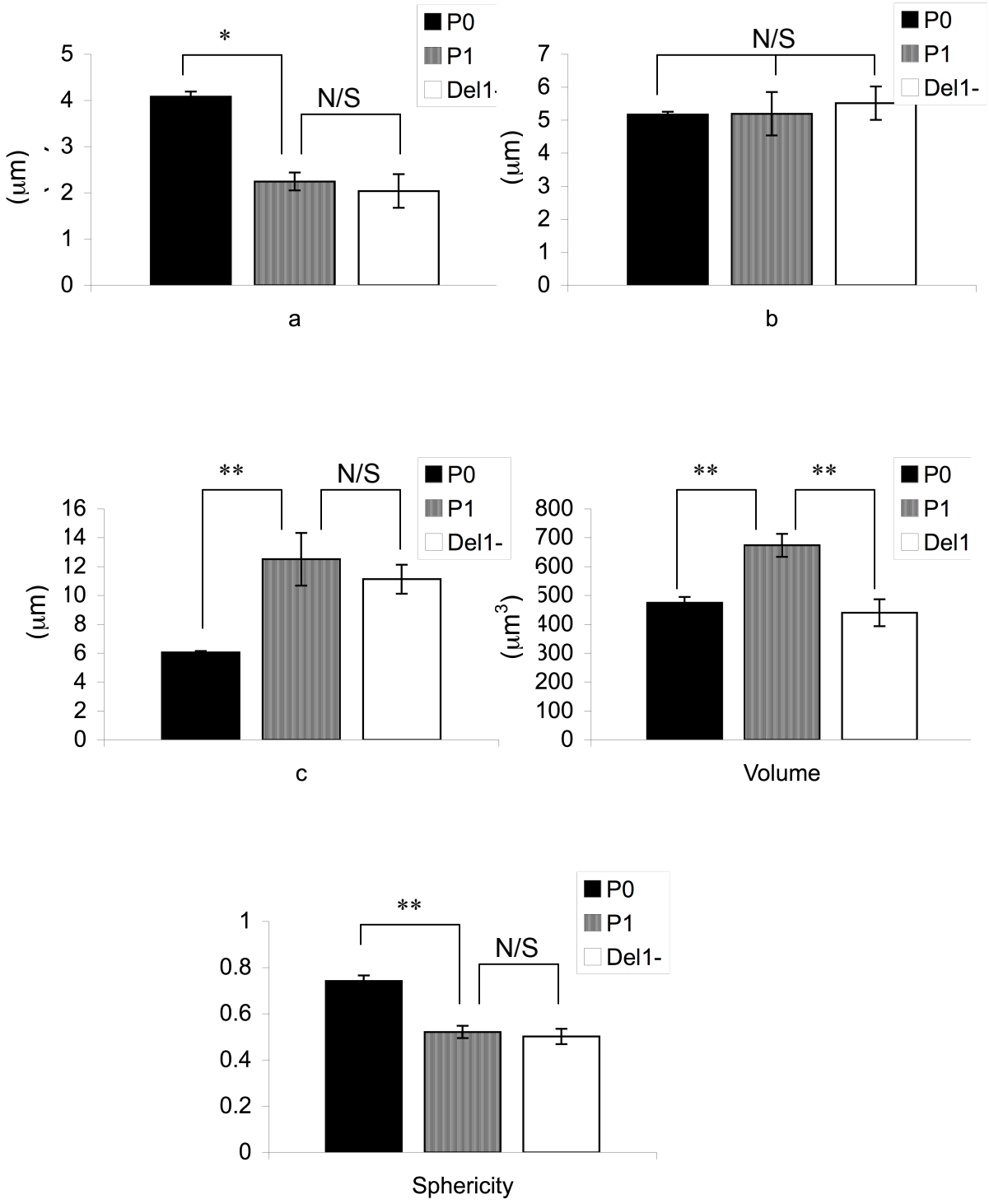
P0
P1
Del1-
*
N/S
(µm)
a
N/S
(µm)
b
**
N/S
(µm)
c
**
**
(µm3)
Volume
**
N/S
Sphericity

Figure 5.7: Changes in chondrocyte morphology and cellular dimension in response to long-term DEL1 knockdown.

Series of images of chondrocytes acquired using confocal microscopy were reassembled in Imaris and isosurface 'objects' created as described (Materials and Methods). Imaris was subsequently employed to determine the depth, width and length of each object (denoted a, b and c). No significant changes were observed in the depth and width between control mock transfected and DEL1(-) chondrocytes but there was, however, a significant decrease in cell length in response to DEL1 knockdown ($p<0.05$). There was no significant change in the sphericity factor but a decrease in cell volume upon DEL1 knock down from 673.38±39.59 to 440.02±46.74μm^3 was observed, values previously observed in freshly isolated chondrocytes. Data pooled from 16 individual experiments. N=4, n=85. Data shown as mean ± s.e.m. T-test p-values were $p<0.05$ (*) and $p<0.01$ (**). N/S, non significant.

5.2.3.3 Chondrocyte expression battery

RNA was extracted from DEL1(-)/P1 chondrocytes upon confluence and subjected to RT-PCR to assay the expression of key genes in chondrocyte phenotype including types I and II collagens and SOX9. The level of expression of key genes was calculated using gel densitometery and was expressed relatively to the level of expression in freshly isolated chondrocytes.

No significant changes were observed in the expression of type II collagen ($p>0.05$) between control chondrocytes and DEL1(-)/P1 with expression levels determined at 1.57±0.43 and 1.18±0.27 relative to freshly isolated chondrocytes. The level of type I collagen expression, however, was significantly reduced ($p<0.05$) from 2.71±0.63 to 1.08±0.34-fold in control and DEL1(-)/P1, respectively, with no significant differences between DEL1(-)/P1 and freshly isolated chondrocytes ($p>0.05$). Therefore, the ratio of type II to I collagen in DEL1(-)/P1 chondrocytes was determined at 1.14±0.15 and was not significantly different from that obtained for freshly isolated chondrocytes ($p>0.05$) but significantly elevated compared to the expression ratio in P1 chondrocytes (0.58±0.15; $p<0.05$). These data indicated that DEL1 knockdown maintained the collagen-dependent phenotype state of chondrocytes (Figure 5.8).

There was however no change in the level of SOX9 expression in response to DEL1 knockdown with expression levels of 1.75±0.40 and 1.81±0.36-fold baseline in control P1 and DEL1(-)/P1 chondrocytes, respectively.

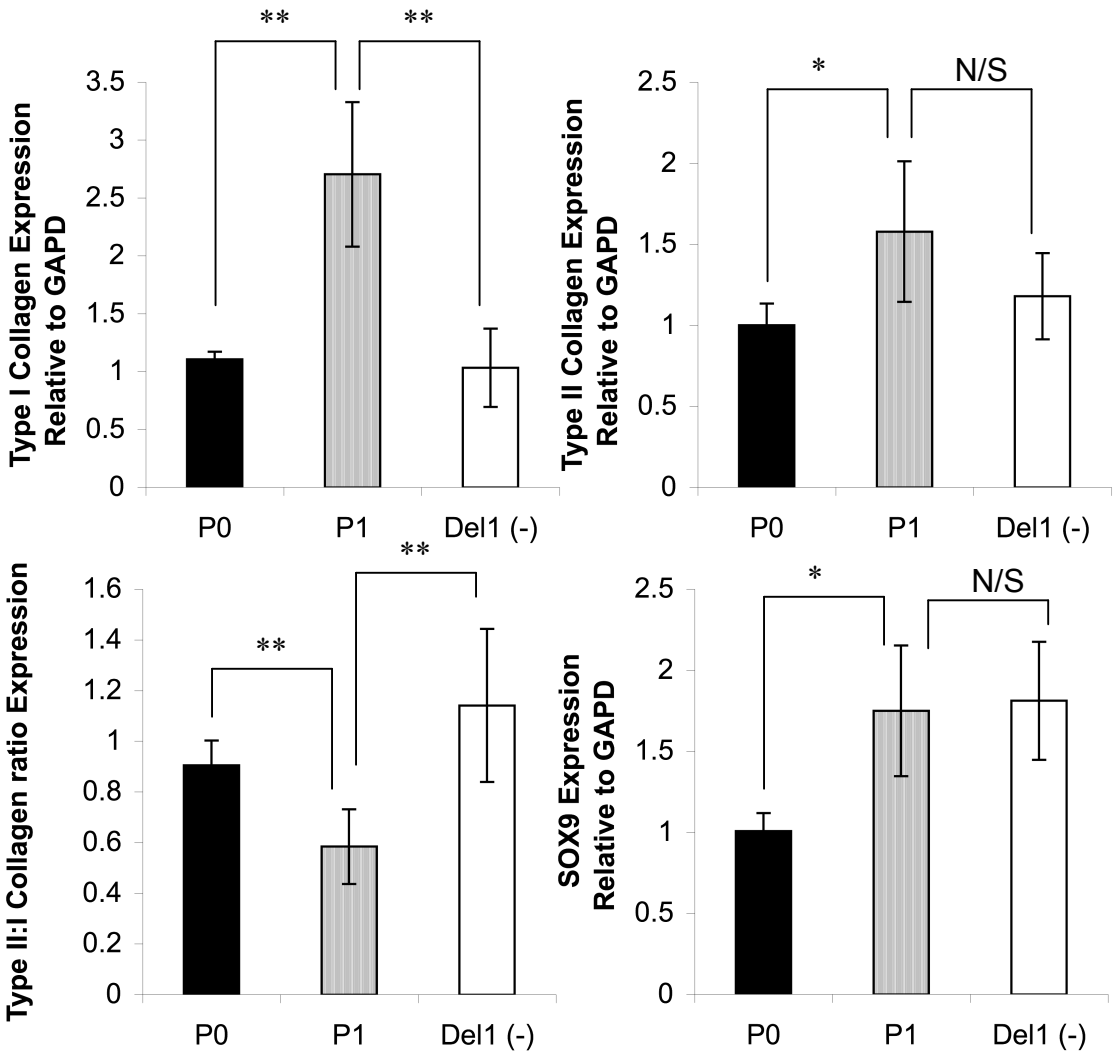

Figure 5.8: Changes in chondrocyte expression battery in response to DEL1 knockdown.

RNA was isolated from freshly isolated, P1 2D-cultured and DEL1(-)/P1 chondrocytes, reverse transcribed and subjected to PCR. The amount of DNA in the PCR products was calculated from the intensity and size of the bands and calculated relative to freshly isolated chondrocytes. No change in the level of expression of SOX9 and type II collagen upon DEL1 knockdown was observed, whereas a significant (2.62-fold) decrease in type I collagen expression was recorded in response to DEL1 knockdown. Therefore, the ratio of type II to I collagen expression increased significantly in response to DEL1 knockdown reaching 1.14 relative to freshly isolated chondrocytes. N=4, experiment repeated 4 times Values shown as mean ± s.e.m. T-test p-values were $p<0.05$ (*) and $p<0.01$ (**). N/S, non significant.

5.2.3.4 The effect of DEL1 on actin organisation

DEL1(-)/P1 and P1 chondrocytes were allowed to attach overnight prior to being fixed in 3% formaldehyde and stained for actin cytoskeleton using phalloidin-alexa 488. Images were acquired using CLSM under Nyquest settings, deconvolved, reassembled in Imaris (Bitplane) and then fluorescence of actin-phalloidin-alexa 488 complexes assayed using Image Pro version 7.0 (Maryland, USA). The number of striation units (as the number of peaks in fluorescence across the cell body) in each chondrocyte was recorded, and the mean fluorescence plotted against 10% intervals of a standardised cell diameter. The areas under the graphs were mathematically calculated by the integration of the equations of the graphs, as previously described (Materials and Methods).

DEL1 knockdown induced a significant increase in the mean number of striation units in P1 chondrocytes to 7±1StU/cell compared to 5±1StU/cell in control mock-transfected chondrocytes ($p<0.05$), and therefore the percentage of filamentous actin, correspondingly, increased from 45.0±2.3% in control chondrocytes to 48.0±2.4% in DEL1(-)/P1. The increase in filamentous actin percentage, however, was deemed insignificant ($p>0.05$) suggesting that DEL1 is involved in the intensification of the cortical localisation of actin.

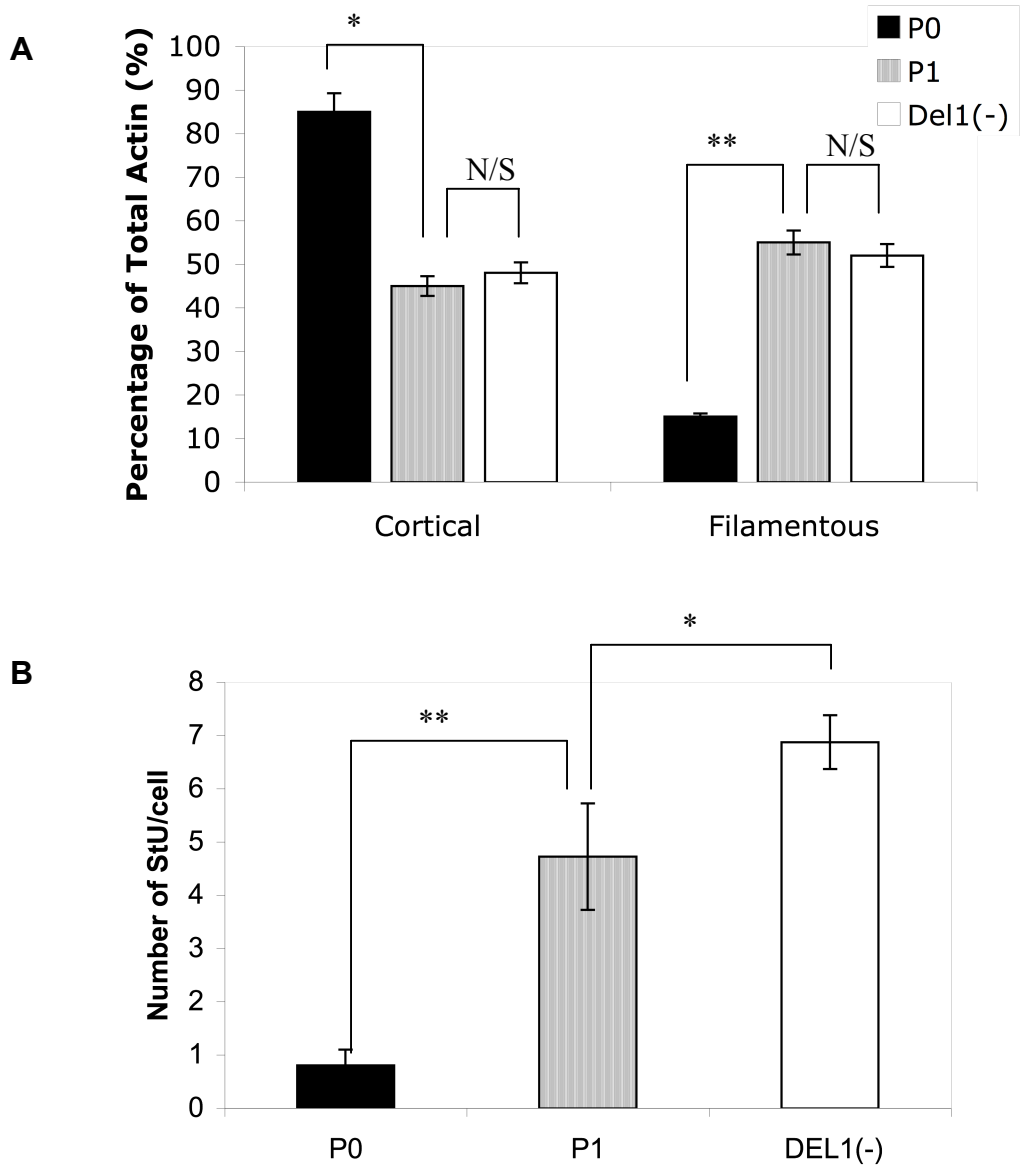

Figure 5.9: Actin organisation upon DEL1 knockdown

Mock transfected P1 and DEL1(-)/P1 chondrocytes were fixed. stained with actin-phalloidin-alexa488 and assayed for fluorescence by linear profiling. There was a significant increase in the number of striation units (StU) in response to DEL1 knockdown ($p<0.05$) from 5±1 to 7±1StU./cell (Panel B) and change in the percentage of cortical and filamentous actin (Panel A). N=6, n=102. Data shown as means ± s.e.m. T-test p-values were $p<0.05$ (*) and $p<0.01$ (**). N/S, non significant.

5.2.3.5 The role of DEL1 in volume regulatory mechanisms

The effect of the expression of DEL1 in P1 chondrocytes on the internal ionic homeostasis was studied by subjecting DEL1(-)/P1 chondrocytes to a hyperosmotic challenge and recording changes in volume. Chondrocytes were loaded with 5μM Calcein-AM and incubated for 30 minutes prior to acquiring Z-stack images at 1μm step size using CLSM. Chondrocytes were subjected to 42% osmotic challenge and images acquired at 1.5, 3, 5,10 and 20 minutes post challenge. Images were subsequently reassembled in Imaris 6.3.1 (Bitplane) and volume obtained as previously described.

Upon introduction to hyperosmotic conditions, DEL1(-)/P1 chondrocytes reduced in volume to 0.85±0.02-fold the original volume (compared to 0.88±0.03% in control cells; $p>0.05$) and underwent further gradual volume loss settling at 0.77±0.04 at time 20 minutes. Control chondrocytes, however, exhibited 'slow' RVI recapturing 0.99±0.01-fold of the orignal volume by 20 minutes. These data show similarity in the response of freshly isolated and DEL1(-)/P1 chondrocytes to hyperosmotic conditions, indicating that DEL1 plays a role in the loss of chondrocyte-specific response to ionic environment upon culture.

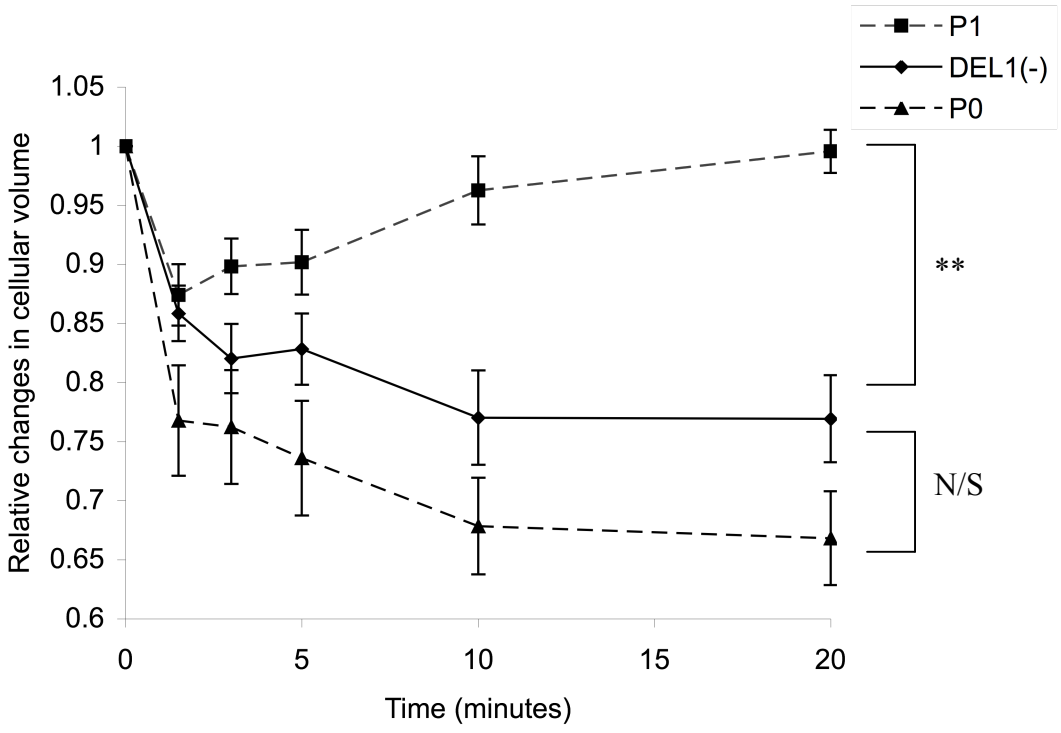

Figure 5.10: RVI in DEL1(-)/P1 chondrocytes in response to hyperosmotic challenge.

P0, mock transfected P1 and DEL1(-)/P1 chondrocytes were loaded with 5μM calein-AM and imaged using CLSM to obtain baseline cell volume and record changes for up to 20 minutes in response to a 42% hyperosmotic challenge. P1 chondrocytes reaquired 99.6±1.91% of their original volume by 20 minutes whereas DEL1(-)/P1 chondrocytes did not exhibit RVI with a final volume of 76.93±3.68% of original volume. N=3, n=43. Data shown as means ± s.e.m. T-test p-values were p<0.01 (**). N/S, non significant.

5.2.3.6 The effect of DEL1 knockdown on calcium channel phenotyping in response to REV5901

As changes in the contribution of intracellular stores and calcium membrane channels to REV5901-induced $[Ca^{2+}]_i$ rise have been observed in response to 2D culture, the role of DEL1 in $[Ca^{2+}]_i$ homeostasis was investigated. Freshly isolated, P1 and DEL1(-)/P1 chondrocytes were loaded with 3μM fluo-4 prior to perfusion in 50μM REV5901 and measurement of calcium changes in the presence of various inhibiting conditions (2mM EGTA to chelate extracellular calcium ions; Na^+-free solution, NCX inhibition; Gd^{3+}, inhibitor of SACC). The effect of REV5901 on DEL1(-)/P1 chondrocyte was not significantly different from that observed in P1 chondrocytes with maximal rise in $[Ca^{2+}]_i$ of 11.6±0.6% and 12.5±0.4% and no significant differences ($p>0.05$). Moreover the rise in $[Ca^{2+}]_i$ in the presence of 2mM EGTA was not significantly different between DEL1(-)/P1 and control mock transfected chondrocytes with 3.69±1.04% and 1.97±0.77%, respectively (Figure 5.12).

Changes in the sensitivity to individual channel-inhibiting conditions were however more prominent. There was an increase in NCX inhibition in Na^+-free conditions in Del(-)/P1 chondrocytes compared to control cells from 57.9±1.2% to 67.6±4.3% inhibition ($p<0.05$), rendering DEL1(-)/P1 more similar to freshly isolated chondrocytes with 84.0±3.4% inhibition ($p>0.05$; Figure 5.12).

The sensitivity of Del(-)/P1 chondrocytes to Gd^{3+} inhibition of SACC, however, did not increase upon DEL1 knockdown unlike control P1 chondrocytes. Freshly isolated chondrocytes exhibited 33.0±9.2% inhibition to REV5901 loading in the presence of Gd^{3+} which increased upon culture reaching 57.2±5.4% in P1 chondrocytes. In response to long-term DEL1 knockdown, sensitivity of chondrocytes to SACC inhibition using Gd^{3+} showed a similar trend to freshly isolated chondrocytes with a percentage inhibition of 24.9±6.0% ($p<0.05$; Figure 5.12). These data indicated that the transient increase in DEL1 expression is required for the increase in activity and/or expression of SACC.

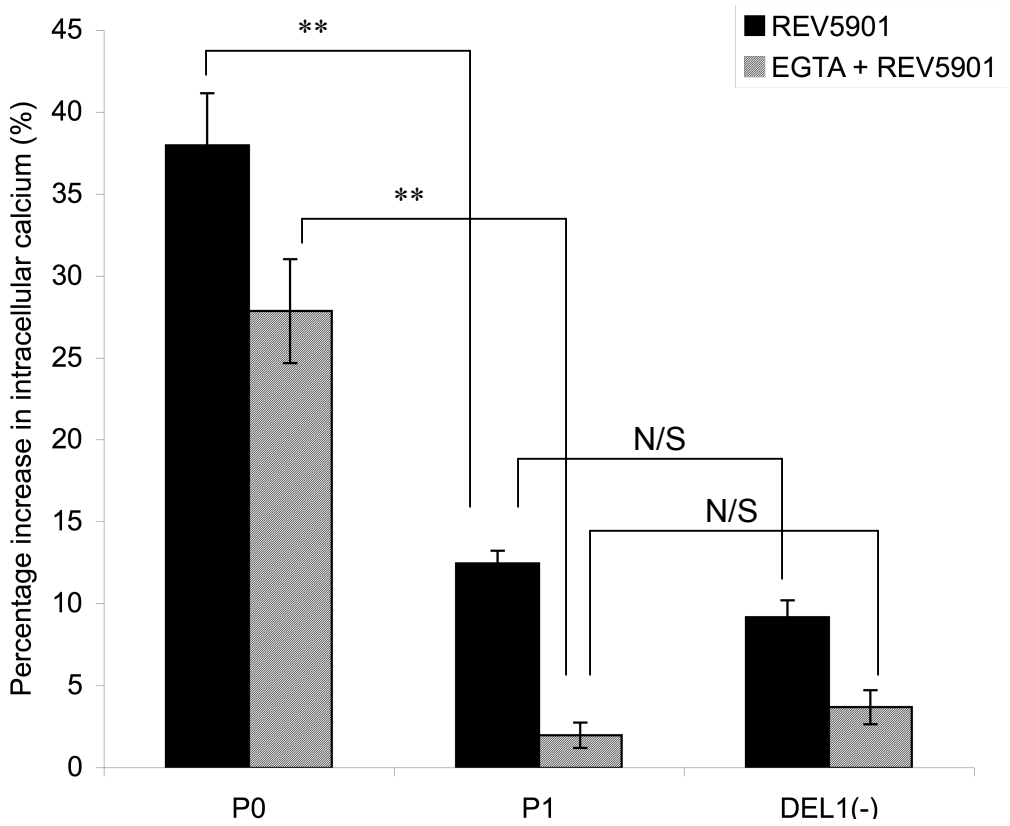

Figure 5.11: Contribution of store-mediated calcium release to REV5901-induced calcium rise.

Freshly isolated, P1 and DEL1(-)/P1 chondrocytes were incubated with 3μM fluo-4 in BPS for 30 min prior to loading of 50μM REV5901 and measurement of maximal [Ca2+]i change with or without the presence of 2mM EGTA. The source of calcium rise in freshly isolated chondrocytes was predominantly mediated by intracellular store-release which significantly decreased upon culture. No change, however, was observed in the store-mediated $[Ca^{2+}]_i$ rise in response to DEL1 knockdown. N=6, experiment repeated 4 times. Data shown as means ± s.e.m. T-test p-values were p<0.01 (**). N/S, non significant.

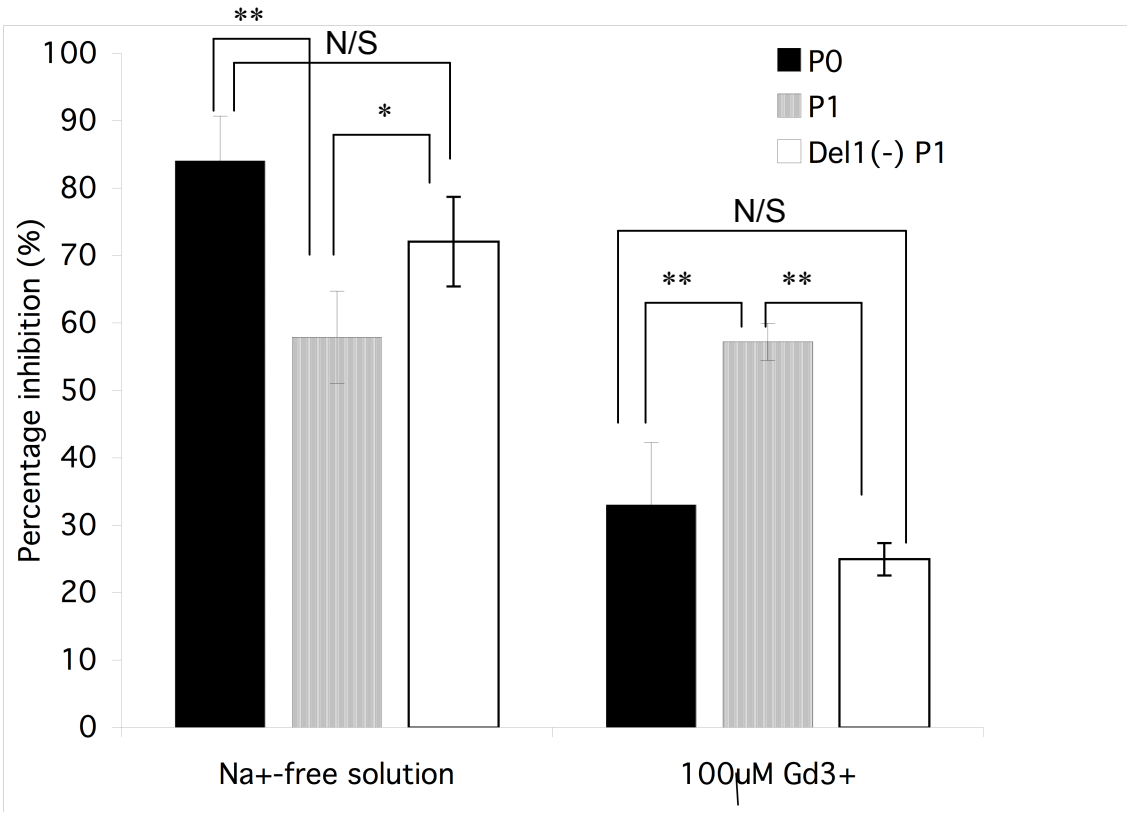

Figure 5.12: The sensitivity of DEL1(-) chondrocytes to calcium channel inhibitors.

Freshly isolated, P1 and DEL1(-)/P1 chondrocytes were loaded with 3µM fluo-4 and appropriate calcium channel inhibitory conditions and baseline calcium-fluo-4 fluorescence measured. REV5901 was loaded in a final concentration of 50µM and fluorescence measured and differences in the effect of pharmacological inhibitors on the REV5901-mediated $[Ca^{2+}]_i$ rise recorded. There was an increase in NCX inhibition using Na^+-free solution between control P1 chondrocytes and DEL1(-)/P1 chondrocytes and a significant decrease in the inhibition of stretch-activated calcium channels in chondrocytes upon DEL1 knockdown from 57.02±0.19% to 24.94±0.43%, thereby rendering DEL1(-)/P1 chondrocytes more similar to freshly isolated chondrocytes. N=4, data was pooled from 10 individual experiments. Data shown as means ± s.e.m. T-test p-values were p<0.05 (*) and p<0.01 (**). N/S, non significant.

5.3 Chapter Discussion

DEL1 is an extracellular integrin ligand shown to have influence on attachment, differentiation and migration in other tissues including angiogenic neoplastic tissue (Aoka *et al.*, 2002) and ischemic tissue (Ho *et al.*, 2004). Despite reports in the literature indicating a role for integrin in the expression of type II collagen and members of SOX family (Lee and Kim *et al.,* 2009*)*, the expression of DEL1 has only been previously shown in foetal chondrocytes (Stokes *et al.*, 2002).

We have confirmed the expression of DEL1 in adult bovine chondrocytes and shown a transient rise in DEL1 expression in P1 chondrocytes similarly to previously reported levels observed in hydrogel cultured foetal chondrocytes (Stokes *et al.*, 2002) where phenotype is thought to be preserved for up to 180 days (Reginato *et al.*, 1994). The rise in DEL1 expression has been found to occur simultaneously with a transient rise in SOX9 and collagen II expression and the decline in col2:col1. Therefore to further our knowledge of the cause-and-effect status of DEL1 rise, the expression of DEL1 and collagens was investigated at days 2, 4 , 6 and 9 of P1.

It was observed that the rise in DEL1 expression occurred as early as the 2^{nd} day in culture with ~12-fold increase in expression followed by the decline in col2:col1 expression on the 4^{th} day in culture (Figure 5.2). These data indicated a potential role for DEL1 in chondrocyte phenotype and confirmed earlier observations of mesodifferentiated phenotype. The role of DEL1 expression in chondrocyte phenotype was therefore further investigated using RNAi technology.

The efficacy of the anti-DEL1 siRNA sequences designed was studied and knockdown confirmed to last for up to 6 days. In response to longterm DEL1

knockdown, there was a reduction in type I collagen expression and therefore an increase in col2:col1 to levels seen in freshly isolated chondrocytes (Figure 5.8). These data confirmed that the loss of phenotype appeared to require transient increase in DEL1 expression which may affect the expression of SOX9 and/or Twist (key regulators of collagen expression and chondrocytic phenotype).

The role of DEL1 as an attachment protein was studied during 2D culture and it was observed that although DEL1 was present at higher concentrations in P1 chondrocytes, the initial attachment was significantly reduced compared to that observed in freshly isolated and 2D cultured chondrocytes. This was possibly due to the time required for DEL1 protein accumulation post trypsinisation. It was noted, however, that attachment levels similar to those in P0, P2 and P3 chondrocytes were obtained 4 hours post seeding, thus indicating an elevated rate of attachment in P1 chondrocytes. Moreover, in response to knockdown, there was a sharp decrease in both initial attachment and rate of attachment suggesting that DEL1 is necessary for attachment in P1 mesodifferentiated chondrocytes (Table 5.2).

The effect of DEL1 on the chondrocyte differentiated phenotype was studied by longterm knockdown of DEL1. Upon DEL1 knockdown, a significant decrease in both types collagen I and II expression was observed with an overall increase in col2:col1 expression to values previously observed in freshly isolated chondrocytes (Figure 5.8). Therefore and despite having no effect on the expression levels of SOX9, DEL1 knockdown appeared to conserve a differentiated phenotype (as defined by col2:col1 expression) for at least 9 days in 2D culture.

Cellular dimensions and actin organisation were studied in response to DEL1 knockdown whereby an increase in the number of striation units was seen from 5±2 in control mock transfected P1 chondrocytes to 7±1 in DEL1(-)/P1 chondrocytes. The DEL1-mediated decrease in the number of striation units

could be caused by the recruitment of actin regulatory proteins and the creation of subcortical focal contacts (Schaller *et al.*, 1992), thereby reducing the availability of monomeric G-actin molecules for the formation of actin filaments. A reduction in chondrocyte length (c) and a significant decrease in cell volume were additionally observed in DEL1(-)/P1 chondrocytes and could be possibly attributed to the accompanying changes in actin cytoskeletal organisation and thus volume regulatory mechanisms. Conversely, a significant increase in both stress fibres and actin localisation within the focal contact has been previously observed in response to DEL1 ligation in vascular smooth muscle cells (Razaee *et al.,* 2002*).*

Finally the effect of DEL1 knockdown on mechanotransduction processes previously studied (RVI and REV5901-induced $[Ca^{2+}]_i$ rise) was investigated as a final confirmation of the effect of DEL1 on chondrocytic phenotype. In response to DEL1 knockdown followed by a hyperosmotic challenge, DEL1(-)/P1 chondrocytes did not exhibit RVI unlike their control mock-transfected counterparts (Figure 5.10), rendering the former with a similar response to a hyperosmotic challenge to that observed in freshly isolated chondrocytes. Work by others has shown that the depolymerisation of actin using LB induced NKCC-mediated RVI in freshly isolated chondrocytes (Kerrigan *et al.*, 2006), and it appears that the increase in filamentous actin polymerisation in response to DEL1 knockdown inhibited RVI mechanisms observed in control P1 chondrocytes (slow RVI). Consequently, it could be argued the abolishment of a RVI response upon knockdown may possibly be due to the previously discussed changes in actin organisation, a key regulator of RVI.

The role of DEL1 in calcium homeostasis was investigated using REV5901 as pharmacological inducer of $[Ca^{2+}]_i$ rise and there was no change in the magnitude of $[Ca^{2+}]_i$ rise, the contribution of intracellular stores in response to DEL1 knockdown. There was however, an increase and decrease in the NCX and SACC contribution, respectively, to REV5901-induced $[Ca^{2+}]_i$ rise to levels

observed in freshly isolated chondrocytes. Gd^{3+}-sensitive SACC has been implicated in the loss of phenotype in rat chondrosarcoma cell line (Perkins *et al.*, 2005) and shown to play a role in $[Ca^{2+}]_i$ homeostasis of 2D cultured chondrocytes (Kerrigan and Hall, 2008). Our observations of a reduced SACC contribution upon DEL1 knockdown suggested that the loss of differentiated phenotype may be mediated, but not exclusively, by an alteration in activity of SACC, which may indeed be directly manipulated by co-localisation with integrins as previously reported (Shakibaei and Mobasheri, 2003).

In conclusion, DEL1 has been shown to induce a decrease in col2:col1, increase the rate of attachment, increase cell volume, increase cell length, increase activity of SACC and induce slow RVI in response to hyperosmotic conditions. Taken together these data confirmed the role of DEL1 in initiating the loss of phenotype upon expansion by inducing a mesodifferentiated phenotype characterised by the upregulation of DEL1 (Table 5.3) and proposed a DEL1 signalling pathway mediating the loss of phenotype (possibly via SOX9 and Twist; investigated in the following chapter).

Table 5.3: Summary of changes observed upon DEL1 knockdown and possible mode of action.

Changes in key markers of differentiation were observed in response to DEL1 knockdown. It was concluded that DEL1 mediated the loss of the differentiated state of col2:col1 expression accompanied by the increase in cell volume to values previously recorded in 2D cultured chondrocyte chondrocytes. DEL1 was sufficient to induce an increase in SACC activity, a decrease in NCX regulation and the activation of slow RVI mechanisms. DEL1 was, furthermore, associated with an increased condensation of cortical actin possibly via the creation of focal contacts.

	Effect of DEL1	Type of Effect	Possible Reason
Col2:Col1 expression	YES	Decrease	DEL1 mediate signal via TWIST
Cell length (c)	YES	Increase	Increase in adhesion surface
Actin organisation	YES	Decrease in StU	Condensation of actin molecules at focal contacts
RVI	YES	Activation	Reorganisation of actin cytoskeleton
Volume	YES	Increase	Activation of RVI by actin organisation
Rate of Attachment	YES	Increase	Superiority of DEL1/Integrin attachment mechanisms
Onset of attachment	YES	Decrease	Time requirement for DEL1 production
Store activity	NO	-	-
SACC activity	YES	Increase	Increase in activity and/or expression
NCX	YES	Decrease	Decrease in activity and/or expression

6 Experimental Chapter: The molecular signalling pathway of DEL1 in chondrocytes.

6.1 Chapter Introduction

Integrin signalling pathway was investigated when it was first observed that integrin-ligand interaction induces integrin aggregation and the initiation of the signal (Schaller *et al.*, 1994). Following integrin activation, FAK trans-autophosphorylation occurs which in turn induces the activation of PI3K (Chen *et al.*, 1996) and Rho (Hotchin & Hall, 1995) thereby activating Akt and Erk, respectively (Renshaw *et al.*, 1996). Erk and Akt signals initiate a switch in expression battery and promote survival and cell proliferation. Furthermore, Rho activates actin polymerisation proteins including cofilin, via PIP2 and possibly $[Ca^{2+}]_i$ regulation (Chong *et al.*, 1994; Hartwig *et al.*, 1995; Gilmore & Burridge, 1996).

The cellular signalling pathway of DEL1 binding was investigated by stable transfection of osteosarcoma cells with recombinant DEL1 sequence using a viral vector (Penta *et al.*, 1999). It was concluded that DEL1 attachment was associated with clustering of integrins, recruitment of actin-binding proteins including Talin and Vinculin and the activation of FAK. *In ovo*, DEL1 possessed highly angiogenic properties which were inhibited upon using anti-αvβ3 antibodies (Penta *et al.*, 1999). Moreover, DEL1 has been shown to induce angiogenesis and a switch in gene expression through interaction with αvβ3 heterodimers upon transfer to ischemic muscular tissue (Zhong *et al.*, 2003; Ho *et al.*, 2004). Finally, it has been confirmed that a close relative of DEL1, Edil1, promotes neovascularisation *in vivo* via αvβ3-dependent Akt phophorylation (Silvestre *et al.*, 2005).

SOX9 is a transcription factor that plays a role in chondrocyte differentiation by binding to the promoters and activating the transcription of chondrocyte-specific genes including type II collagen and aggrecan (de Crombrugghe *et al.*, 2000;

Uusitalo *et al.*, 2001), and our previous work has shown an association between DEL1 and SOX9 levels of expression (Section 5.2.1). Therefore, the effect of SOX9 on the transcription levels of DEL1 was studied using BMP2-induced rise in SOX9 levels in 2D cultured chondrocytes.

BMP2 is a member of the TGF-β protein superfamily and is involved in the development of bone and cartilage. It is expressed in the perichondrium/ periosteum (Zou *et al.*, 1997; Pathi *et al.*, 1999) and signals back to initiate key cellular functions including proliferation (Venezian *et al.*, 1998), hypertrophic differentiation (De Luca *et al.*, 2001; Li *et al.*, 2006) and extracellular matrix accumulation (Cheng *et al.*, 2007). It was recently reported that BMP2 induced chondrocyte-specific genes (including SOX9, type II collagen and aggrecan) in synovium-derived progenitor cells (Park *et al.*, 2005), an effect which could be inhibited by the expression of Twist (Reinhold *et al.*, 2006).

Twist is a member of basic helix loop helix (bHLH) transcription factors found to be expressed in mesoderm-derived adult tissue including cartilage, and it was recently observed to be overexpressed in 2D cultured chondrocytes (Stokes *et al.*, 2002). Twist has the capacity to form complexes with various transcription factors thus performing various functions which include cell survival (Maestro *et al.*, 1999; Dupont *et al.*, 2001; Valsesia-Wittmann *et al.*, 2004), cell death (Sosic *et al.*, 2003; Ota *et al.*, 2004), differentiation (Chen & Behringer, 1995; Spicer *et al.*, 1996; Ishii *et al.*, 2003; Bialek *et al.*, 2004) and most recently chondrocyte maturation and dedifferentiation (Dong *et al.*, 2007).

It has been hypothesised that Twist inhibited chondrocyte-specific phenotype by direct interaction with the p65 subunit of NFκB transcription complex (Sosic *et al.*, 2003) and/or p300, a close associate of SOX9 and enhancer of type II collagen production (Hamamori *et al.*, 1999; Tsuda *et al.*, 2003). Reinhold *et al.* reported that Twist expression was mediated by the canonical Wnt signalling pathway involving β-catenin and GSK3-mediated β-catenin ubiquitination

complex (Giles *et al.*, 2003) as observed by the overexpression of Twist in the presence of Wnt3a or a pharmacological GSK3 inhibitor.

In this chapter, Akt, a biological GSK3 inhibitor, was studied as a potential downstream element of DEL1, and key regulator of β-catenin levels (pharmacologically inhibited using 500μM R-Etodolac; Behari *et al.*, 2007) and thus Twist expression. Furthermore, the effect of Twist knockdown using siRNA was also investigated as a key indicator of the role of Twist in chondrocyte phenotype manipulation.

Aims of Experimental Chapter

1 Determine the SOX9 regulatory effects on DEL1 expression using BMP2.

2 Determine the activation of Akt in response to elevated DEL1 expression.

3 Investigate the role of β-catenin in mediating DEL1-Twist signal.

4 Investigate the expression level of Twist in response to 2D culture.

5 Investigate the role of DEL1 on Twist expression.

6 Establish Twist knockdown using the designed Twist siRNA.

7 Study the effect of Twist knockdown on gene expression.

6.2 Results

6.2.1 The role of DEL1 on Akt activation signalling

6.2.1.1 Akt activity throughout 2D culture in bovine articular chondrocytes

Being an indirect β-catenin activator and an integrin-mediated signalling downstream element, Akt activation was studied upon 2D culture using western blot and phosphorylation-sensitive antibodies. Freshly isolated and 2D cultured P1, P2 and P3 chondrocytes were collected, proteins extracted as previously described and subjected to SDS-PAGE. Membranes were probed with phosphorylation-sensitive anti-Akt antibodies and visualised using x-ray film before being stripped in stripping buffer for 30 minutes at 50°C and re-probed with anti-p-Akt antibodies to study Akt activity as the ratio of p-Akt:Akt.

No significant changes in the levels of Akt production were observed upon culture ($p>0.05$) compared to freshly isolated chondrorocytes with 1.07±0.07, 1.03±0.08 and 0.94±0.07 in P1, P2 and P3 chondrocytes respectively. Conversely, the levels of phosphorylated Akt detected transiently increased by 1.35±0.23 during the first passage ($p<0.05$) and declined to baseline levels upon further culture reaching 0.97±0.05 and 0.93±0.07 in P2 and P3 chondrocytes, respectively. Therefore, the relative activity of Akt transiently increased by 22.4±7.18% during the first passage prior to returning to levels observed in freshly isolated chondrocytes with 0.92±0.01 in P2 chondrocytes (Figure 6.1).

These data indicated that the increase in DEL1 expression previously observed was simultaneous with changes observed in Akt activity in response to 2D culture, thereby suggesting a role for DEL1 on Akt activation.

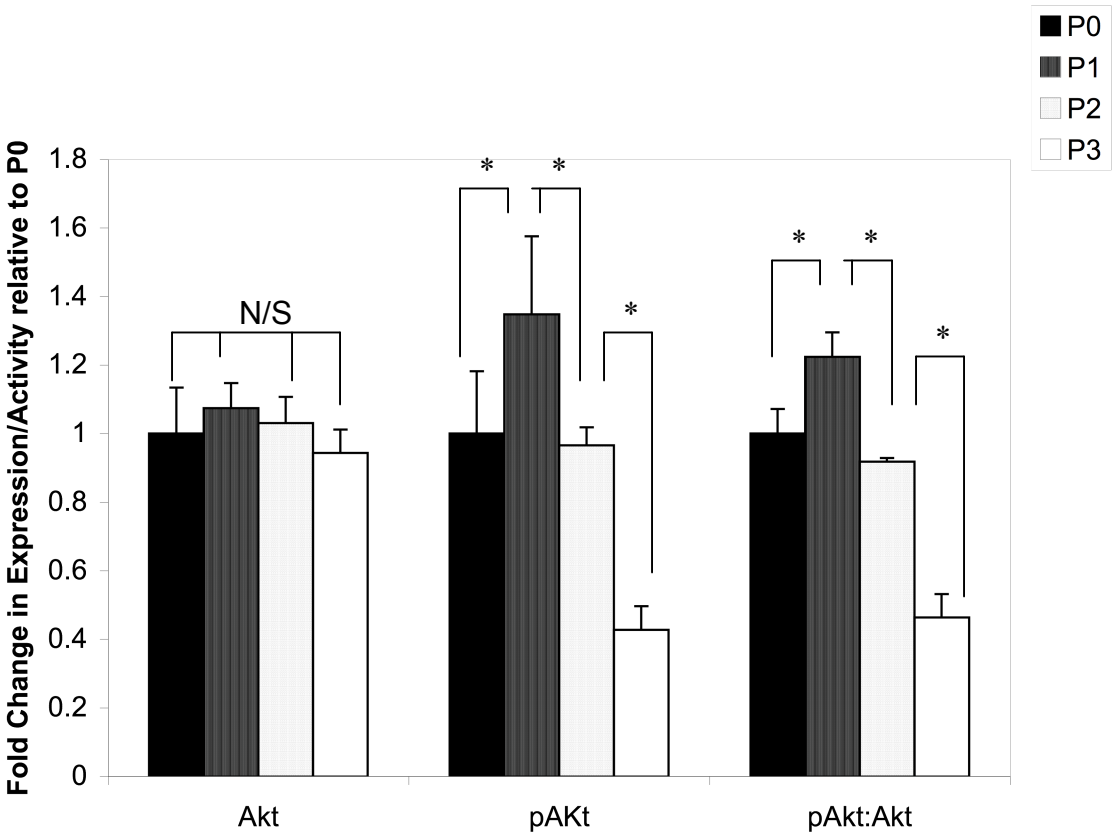

Figure 6.1: Changes in Akt phosphorylation and activity upon 2D culture.

Changes in Akt phosphorylation in response to 2D culture were investigated to establish baseline activity of Akt in chondrocytes. Freshly isolated and 2D cultured chondrocytes were isolated by trypsinisation and centrifugation prior to protein extraction in Akt lysis buffer and performing SDS-PAGE and western blot. Membranes were probed for Akt using phosphorylation sensitive antibodies. No change was observed in the protein content of Akt upon 2D culture, whereas there was an increase in Akt phosphorylation (and thus activity) in P1 chondrocytes by 22.35±7.18%. Akt activity returned to baseline levels upon further culture with no significant difference observed. N=4, experiment repeated 3 times. Data shown as means ± s.e.m. T-test p-values were p<0.05 (*). N/S, non significant.

6.2.1.2 Akt activity in response to DEL1 knockdown

To further investigate the effect of DEL1 on Akt activation, RNAi technology was used to diminish DEL1 expression and study the effect on Akt phosphorylation. Freshly isolated chondrocytes were seeded and transfected with 10nM anti-DEL1 siRNA and 3µl/ml HiPerfect transfection reagent and chondrocytes cultured for up to 9 days under longterm knockdown conditions as previously described. Proteins were extracted from DEL1(-)/P1 and mock transfected P1 chondrocytes as previously described and the proteins assayed by western blot for Akt and p-Akt proteins.

No significant change was observed ($p>0.05$) in Akt protein expression in response to knockdown but there was a 47.39±1.87% reduction in p-Akt levels upon knockdown leading to an overall 37.94±3.58 % decrease in Akt activation in DEL1(-)/P1 chondrocytes compared to mock transfected P1 chondrocytes (Figure 6.2). These data confirmed that Akt activation was regulated by DEL1/integrin interaction and that the rise in Akt activity after 9 days in culture was induced by DEL1-dependent signalling pathway.

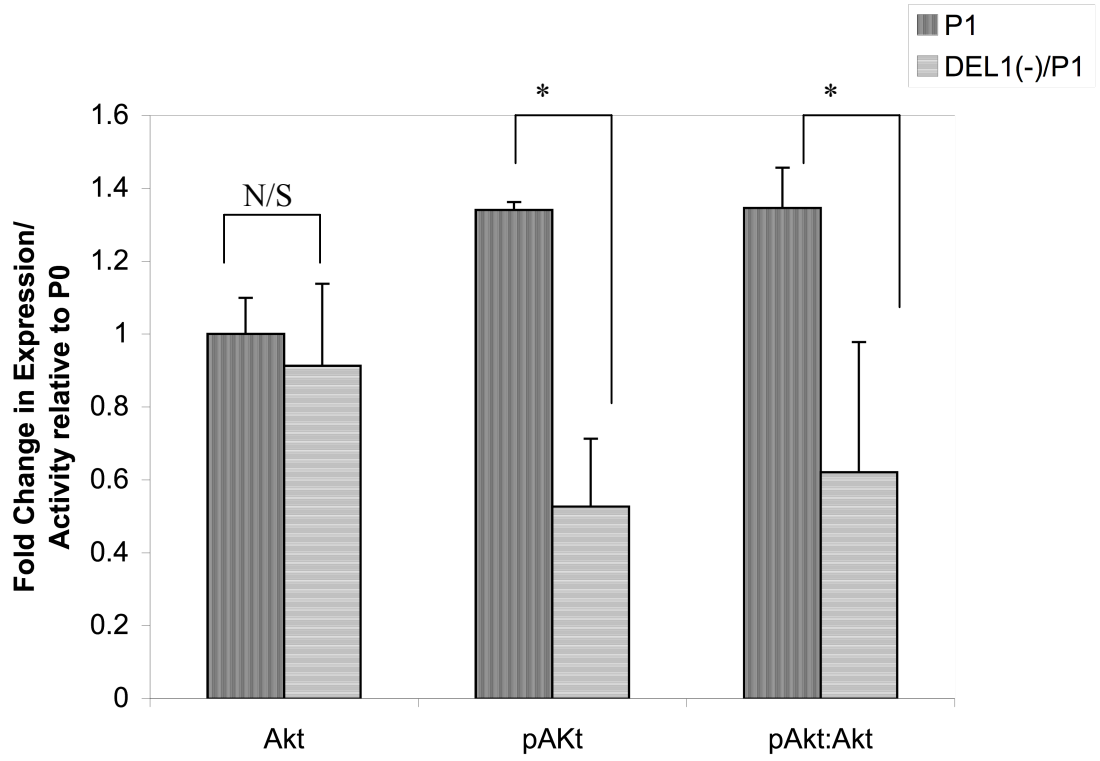

Figure 6.2: The effect of DEL1 knockdown on the phosphorylation and activity of Akt.

To confirm the association between the upregulation of DEL1 and the activation of Akt, the phosphorylation of Akt in response to DEL1 knockdown was assayed by western blot. Briefly, freshly isolated chondrocytes were transfected in suspension with 1nM anti-DEL1 siRNA and 9μl/ml HiPerfect transfection reagent and cultured for 9 days under long term knockdown conditions. There was no change in the protein level of Akt whereas there was a significant 72.5% decrease of in the phosphorylation of Akt and thus Akt activity, suggesting that DEL1 expression is necessary for Akt activation as observed in P1 chondrocytes. N=4, experiment repeated 6 times. Data shown as means ± s.e.m. T-test p-values were p<0.05 (*). N/S, non significant.

6.2.2 The expression and role of Twist in 2D expansion of chondrocytes

6.2.2.1 Changes in Twist expression upon 2D chondrocyte culture

Being a potential downstream element of DEL1 and a key regulator of chondrocytic phenotype, Twist expression was assayed before and upon culture as a first indicator of its biological relevance. Freshly isolated and 2D cultured chondrocytes were collected and RNA extracted and subjected to RT-PCR to assay Twist expression. PCR products were separated using 2% agarose gel electrophoresis and band intensity assayed by ethidium bromide densitometery as previously described (see Materials and Methods).

There was a significant increase ($p<0.05$) in the level of Twist relative expression from 1.08±0.08 to 3.00±0.54 after 9 days in culture and this elevation in Twist expression was maintained for the remainder of culture period studied with no further significant changes ($p>0.05$) with 3.33±0.54 and 3.32±0.53 in P2 and P3 2D cultured chondrocytes, respectively. These data confirmed reported findings that suggest a role for Twist expression in the loss of differentiated chondrocytic phenotype upon 2D culture.

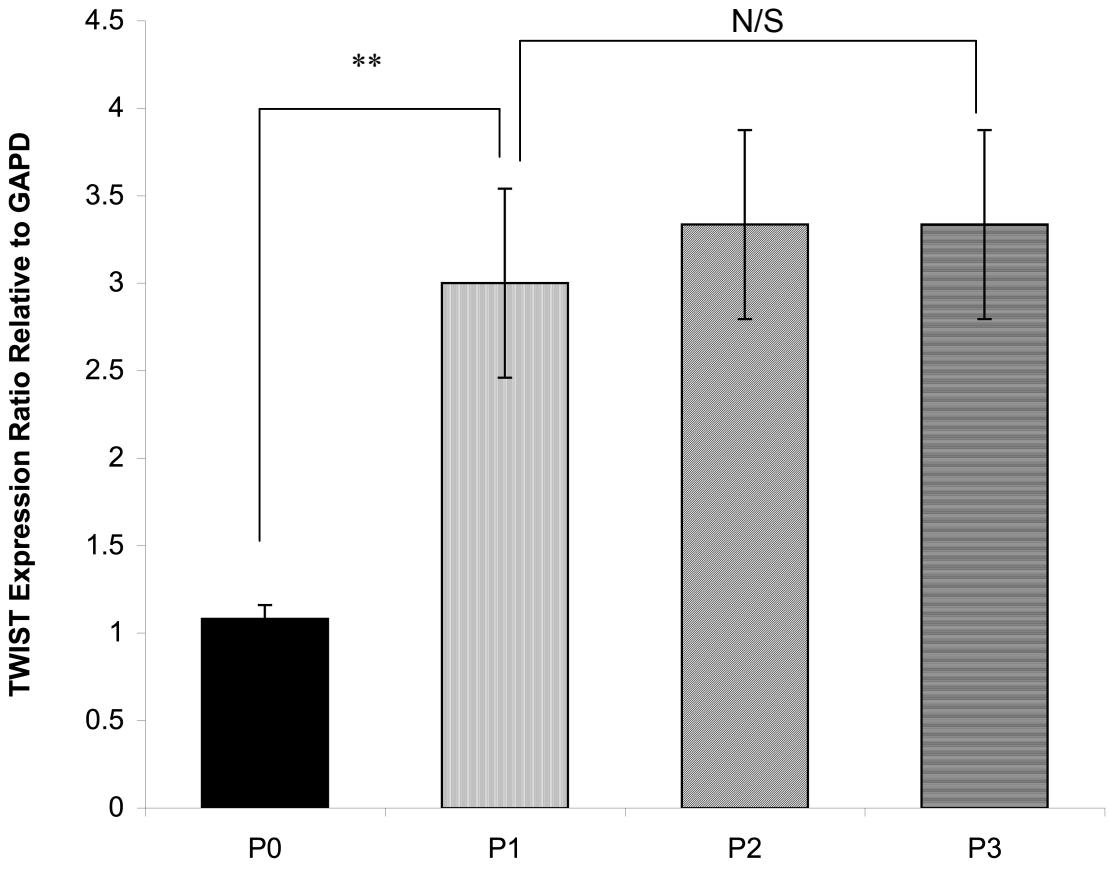

Figure 6.3: The level of Twist expression in freshly isolated and 2D cultured chondrocytes.

Freshly isolated and 2D cultured chondrocytes were isolated and RNA extracted using RNeasy minikit, reverse transcribed and PCR performed using Twist primers. There was a ~3-fold increase in Twist expression upon culture and these elevated levels of expression were maintained for the remainder of the culture period with no further significant differences observed. These data indicated a role for Twist in the loss of a chondrocytic differentiated phenotype. N=3, experiment repeated 3 times. Data shown as means ± s.e.m. T-test p-values were p<0.01 (**). N/S, non significant.

6.2.3 The dependency of Twist expression on DEL1 level in 2D culture of chondrocytes

Data shown above indicated a change in Twist regulation occurring simultaneously with the transient rise in DEL1 expression. Therefore, the effect of DEL1 expression on Twist levels in 2D culture was further investigated by abolishing the former and studying changes in the latter. Anti-DEL1 siRNA was employed to inhibit the translation of DEL1 mRNA and consequent changes in Twist expression were recorded using RT-PCR. Briefly, freshly isolated chondrocytes were isolated transfected in suspension with 10nM anti-DEL1 siRNA molecules complexed with 3μl/ml HiPerfect transfection reagent and incubated in culture media. Media was replaced after 6 days and chondrocytes repeat-transfected every 6 days with anti-DEL1 siRNA prior to RNA isolation.

Upon 9 days in culture, P1 2D cultured chondrocytes exhibited 3.00±0.54-fold increase in Twist expression compared to freshly isolated chondrocytes as previously shown. This increase in Twist expression, however, was abolished in the absence of a transient increase in DEL1 expression upon knockdown with anti-DEL1 siRNA molecules with only 0.97±0.50 ($p<0.05$) which was not deemed significantly different from values obtained for freshly isolated chondrocytes ($p<0.05$). These data indicated a role for DEL1 in the regulation of Twist expression.

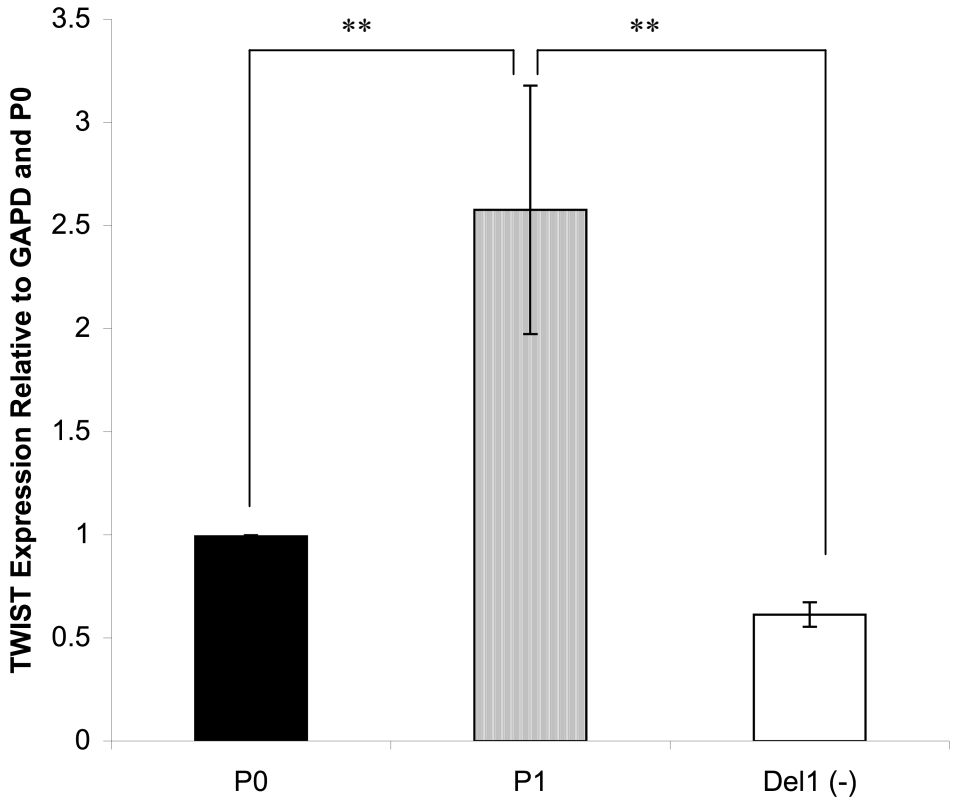

Figure 6.4: The effect of DEL1 knockdown on the expression of Twist in P1 chondrocytes.

The effect of DEL1 upregulation in P1 chondrocytes on the expression of Twist was studied by DEL1 knockdown prior to culture, and observing Twist expression using RT-PCR. Following 9 days in culture, mock-transfected P1 chondrocytes demonstrated a significant 3.00±0.54-fold increase in Twist expression which was abolished in the absence of DEL1. These data indicated a role for DEL1 in the upregulation of Twist expression in mesodifferentiated chondrocytes. N=4, experiment repeated 6 times. Data shown as means ± s.e.m. T-test p-values were p<0.01 (**).

6.2.3.1 The role of the β-catenin-dependent DEL1/Akt signal on Twist expression

To further study the signal between DEL1/integrin interaction and Twist expression, a pharmacological inhibitor of β-catenin, R-Etodolac, was used to confirm the necessity for β-catenin for the expression of Twist suggested by others (Reinhold *et al.*, 2006). Freshly isolated chondrocytes were seeded in culture media with or without the presence of 500μM R-Etodolac and cultured as previously described. Upon confluence, RNA was extracted from P1 chondrocytes using RNeasy minikit and subjected to RT-PCR to study the changes in Twist expression.

As previously observed, there was an increase ($p>0.05$) in Twist expression by the end of the first passage to 3.00±0.54 which was significantly reduced ($p<0.05$) to 1.70±0.61% in the presence of R-Etodolac ($p<0.05$). Despite Twist expression levels not returning to baseline levels upon R-Etodolac treatment ($p<0.05$), these data indicated that the upregulation of Twist was significantly reduced by inhibition of intracellular β-catenin levels, which were in turn potentially regulated by Akt activity and DEL1 expression levels.

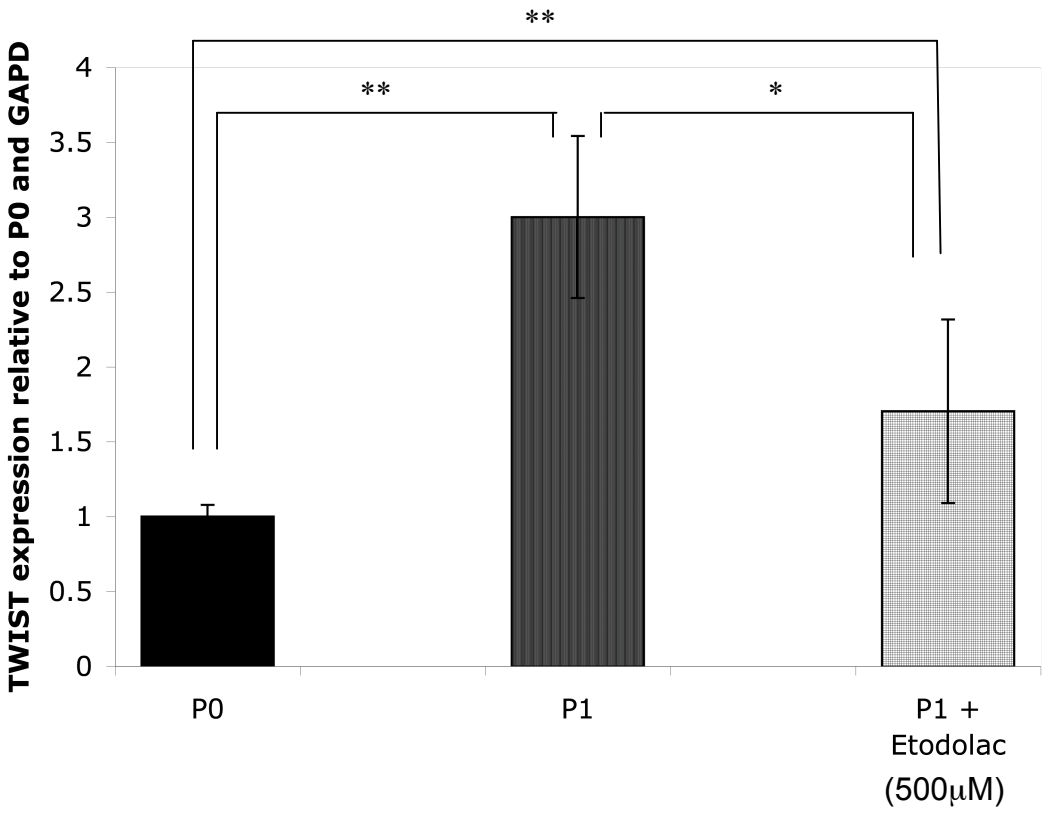

Figure 6.5: The effect of pharmacological inhibition of β-catenin on Twist expression.

The necessity of β-catenin for DEL1-mediated upregulation of Twist via Akt was studied using a pharmacological inhibitor of β-catenin (R-Etodolac) in the culture technique. Freshly isolated chondrocytes were seeded in the presence of 500μM R-Etodolac and cultured for 9 days prior to RNA isolation using RNeasy minikit as previously described. In response to culture in R-Etodolac, there was a significant decrease in Twist expression from 3.00±0.50 in control P1 chondrocytes to 1.79±0.61 (relative to values obtained in freshly isolated chondrocytes). These data indicated that β-catenin was necessary for the expression of Twist in mesodifferentiated chondrocytes. N=4, experiment repeated 6 times. Data shown as means ± s.e.m. T-test p-values were p<0.05 (*) and p<0.01 (**).

6.2.4 The feedback effect of Twist and SOX9 on DEL1 expression

As Twist has been shown to inhibit BMP2-induced SOX9 activity and as we have shown that DEL1 induced the expression of Twist, it was now necessary to investigate the effect of Twist and SOX9 on the expression of DEL1. This was investigated using BMP2 (inducer of SOX9 expression) and anti-Twist siRNA to investigate a potential feedback autocrine signalling loop. For the following experiments, P3 chondrocytes were selected due to expression profile characterised by the reduced DEL1 and SOX9 expression and elevated Twist expression levels.

6.2.4.1 The role of BMP2 dependent SOX9 expression on DEL1 levels

Expression level of SOX9 is tightly regulated by BMP2 and therefore the effect of SOX9 on DEL1 expression was investigated by biochemical induction of SOX9 expression using BMP2 supplementation. Upon reaching confluence, P2 chondrocytes were subcultured at optimum seeding density and incubated in culture media containing 500ng/ml BMP2 and cultured for 7 days as previously described (Minina *et al.*, 2001). Upon reaching P3, chondrocytes were isolated by trypsinisation and gentle centrifugation and RNA isolated using RNeasy Minikit (Materials and Methods). RT-PCR was performed to study the expression levels of SOX9 and DEL1 in response to BMP2 treatment relative to the expression levels in freshly isolated chondrocytes.

P3 chondrocytes expressed baseline levels of SOX9 expression (0.69±0.14–fold relative to freshly isolated chondrocytes) with no significant differences observed ($p>0.05$), whereas upon culture in 500ng/ml BMP2 for 7 days, there was an increase in SOX9 expression reaching 1.40±0.40% of baseline levels. The

BMP2-mediated SOX9 rise was not significantly different ($p>0.05$) from naturally occurring rise in SOX9 previously observed in P1 chondrocytes (Figure 6.6).

It was observed that in the presence of SOX9 upregulation in response to BMP2 treatment, there was an overexpression of DEL1 on RNA level relative to baseline expression in freshly isolated chondrocytes ($p<0.05$). In the presence of 500ng/ml BMP2 and thus higher levels of SOX9 expression, there was a ~3-fold increase in DEL1 expression levels reaching 3.01±0.67 relative baseline levels, a rise deemed not significantly different ($p>0.05$) from the rise in DEL1 expression observed in P1 chondrocytes (Figure 6.6). These data confirmed that BMP2 is a key regulator of SOX9 expression levels, which in turn appeared to be regulate the expression of DEL1. These data support the theory that SOX9 and DEL1 upregulation in P1 chondrocytes is part of a regulatory pathway involved in chondrocyte differentiation. No further rise in Twist expression in BMP2-treated P3 chondrocytes was observed, thereby indicating no regulatory role for SOX9 on the expression of Twist in dedifferentiated chondrocytes ($p>0.05$).

There was, however, no change in the expression of types I and II collagens and thus no change in col2:col1 expression in response to BMP2 treatment. Control P3 chondrocytes and BMP2-treated exhibited relative expression of 2.49±0.37 and 1.43±0.51 of type I collagen and 0.98±0.34 and 0.78±0.52 of type II collagen, respectively. These data indicated that while BMP2 treatment induced a mesodifferentiated-like phenotype in dedifferentiated chondrocytes as characterised by SOX9, DEL1 and col2:col1 expression, it was not sufficient to recapture the differentiated phenotype in P3 chondrocytes following expansion (Figure 6.7).

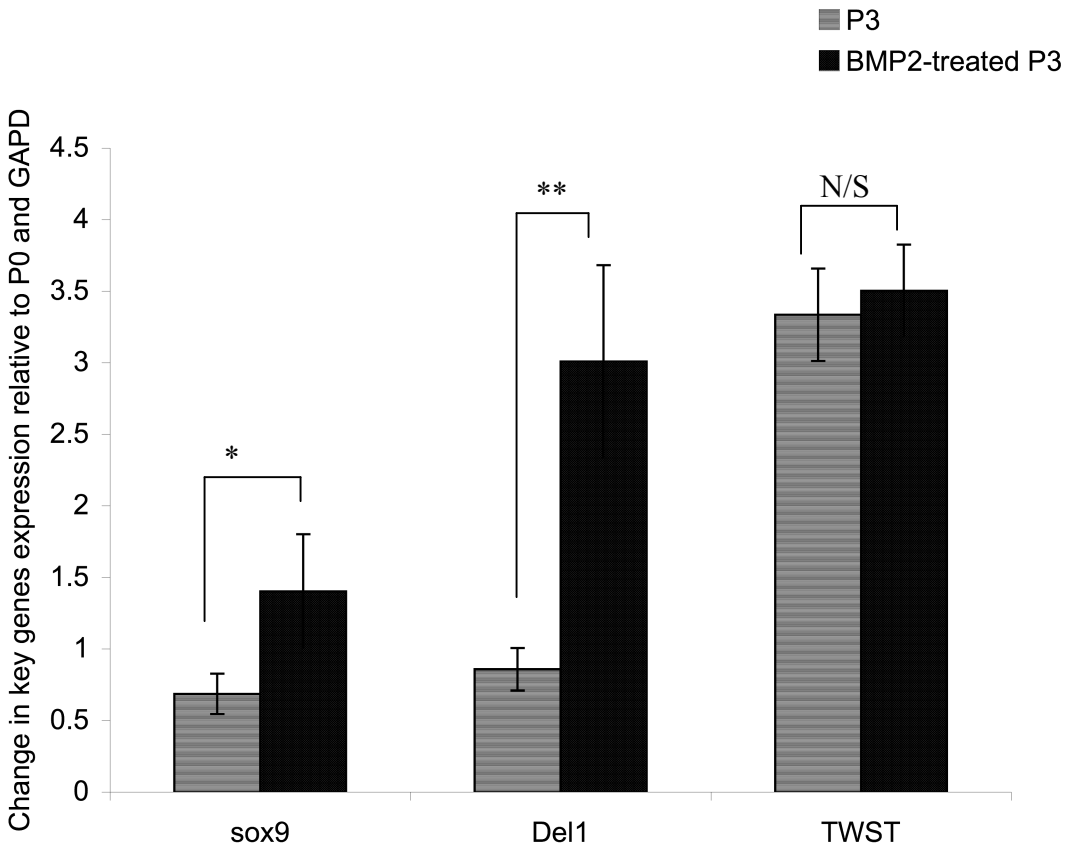

Figure 6.6: The effect of BMP2 treatment on the expression of SOX9, Twist and DEL1.

The effect of SOX9 level on the regulation of expression of DEL1 and Twist was investigated by biochemical induction of SOX9 expression using BMP2. Upon confluence, P2 chondrocytes were subcultured in the presence 500ng/ml BMP2 for 7 days and RNA subsequently isolated and RT-PCR performed. In response to BMP2 treatment, P3 chondrocytes exhibited a rise in SOX9 and DEL1 expression to 1.40±0.40 and 3.00±0.67, respectively, thereby inducing mesodifferentiated-like phenotype in P3 chondrocytes. No change, however, was observed in Twist expression. These data indicated that a BMP2-induced rise in SOX9 was sufficient to upregulate the expression of DEL1. N=4, experiment repeated 6 times. Data shown as means ± s.e.m. T-test p-values were p<0.05 (*) and p<0.01 (**). N/S, non significant.

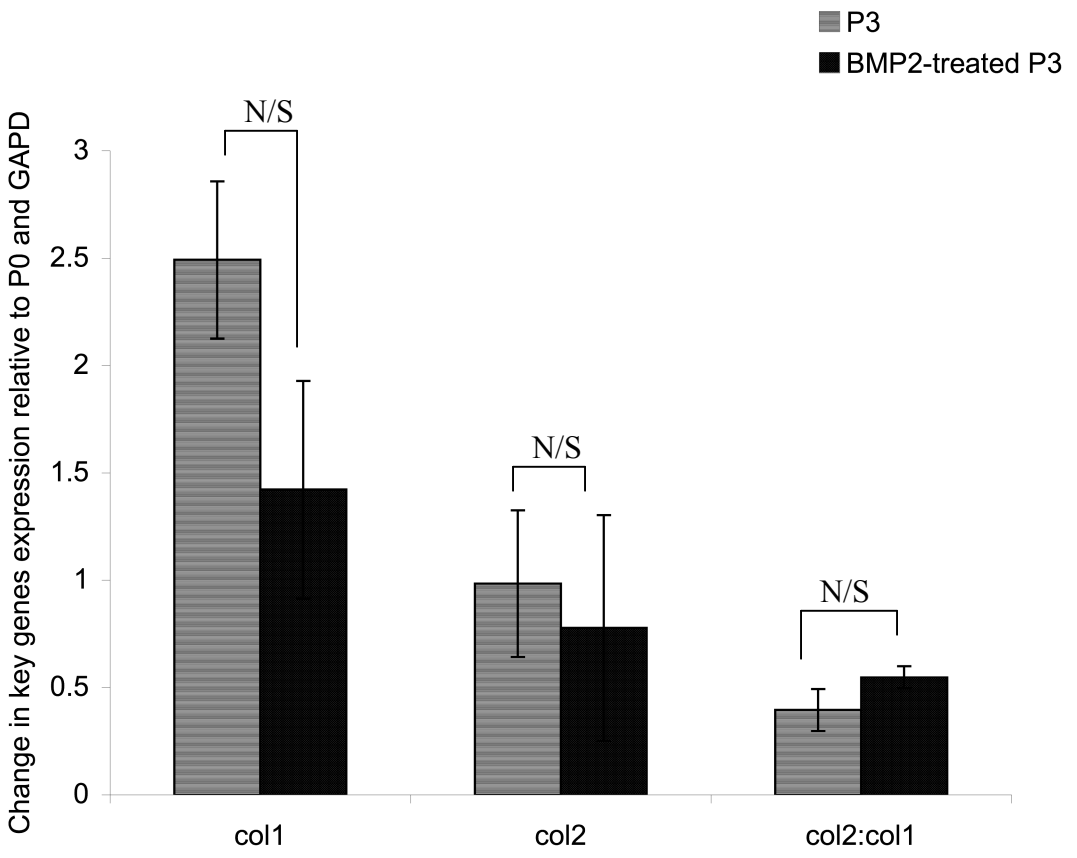

Figure 6.7: Changes in the expression of collagen molecules in response to BMP2 treatment in P3 chondrocytes.

The capacity of BMP2 treatment to recapture a differentiated phenotype as defined by the regulation of collagen expression was studied in P3 chondrocytes by culture in 500ng/ml BMP2 followed by RNA isolation and RT-PCR. There was a slight yet insignificant decrease in the expression of types I and II collagens in response to BMP2 treatment and thus no significant change in col2:col1 expression. These data suggested that despite a rise in SOX9 expression following BMP2 treatment, there was no recapture of a differentiated phenotype. N=3, experiment repeated 3 times. Data shown as means ± s.e.m. T-test p-values were p>0.05 (N/S, non significant).

6.2.4.2 Twist knockdown using RNAi

To further assay the direct effect of Twist on chondrocytic phenotype, RNAi technology was employed to knockdown Twist expression and record changes in DEL1 expression. Anti-Twist siRNA were designed as previously described (Materials and Methods) and the efficacy of the knockdown of the selected sequences studied in P3 2D cultured chondrocytes where Twist overexpression was observed and deemed stable.

Confluent P2 2D cultured chondrocytes were isolated by trypsin treatment and centrifugation prior to transfection in suspension using anti-Twist siRNA complexes freshly prepared with 1nM siRNA complexed with 3µl/ml HiPerfect transfection reagent (See Materials and Methods). Chondrocytes were seeded at standard seeding density, RNA isolated every 2 days in culture until reaching P3, and the levels of Twist expression studied by RT-PCR relative to GAPD and freshly isolated chondrocytes.

Upon 2 days of transfection, there was a decrease in Twist expression to 0.73±0.04-fold relative to control expression levels ($p<0.05$), indicating successful knockdown using the sequences designed. These values of expression were maintained for a further 2 days with no significant differences observed ($p>0.05$), whereas following 6 days of transfection, the levels of Twist expression increased reaching 2.50±0.13% of baseline P3 Twist expression (Figure 6.8). These data confirmed the transience of RNAi knockdown and were necessary to determine the frequency of repeat-transfection required to establish long-term Twist knockdown.

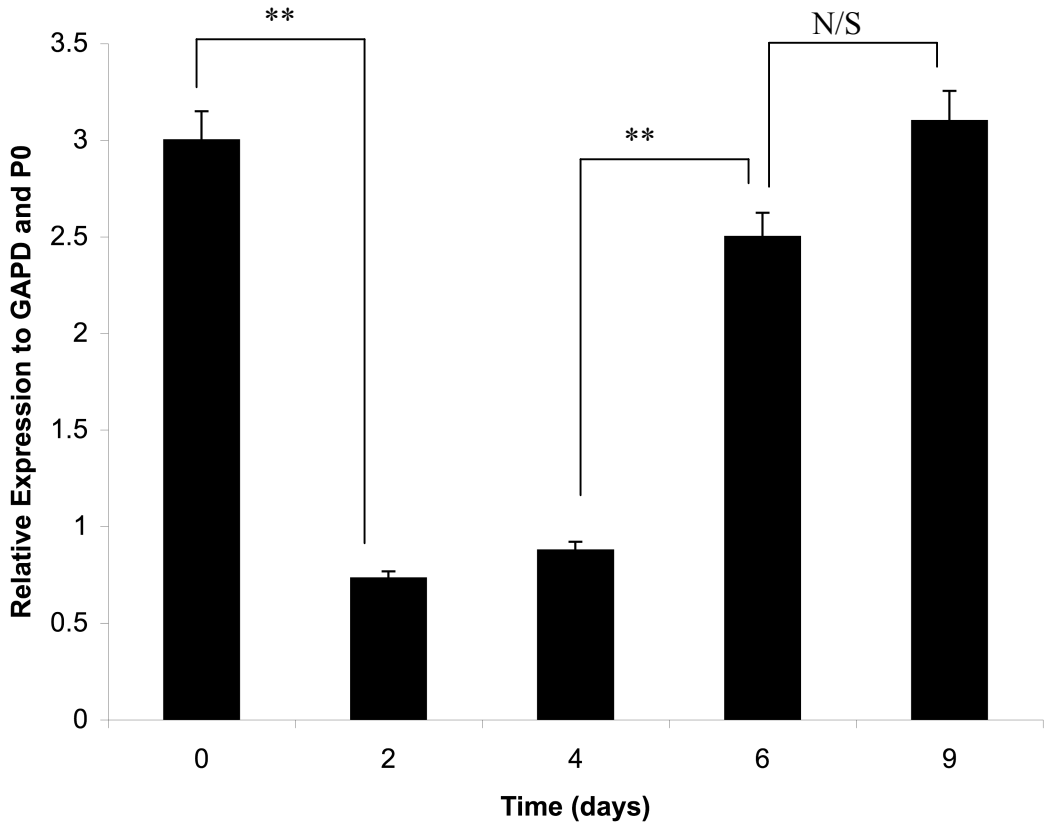

Figure 6.8: Twist expression upon knockdown using anti-Twist siRNA.

The efficacy of the anti-Twist siRNA molecules designed was studied to determine their capacity to induce a knockdown in Twist expression. Briefly, P2 chondrocytes were transfected in suspension using 1nM siRNA complexed with 3μl/ml HiPerfect transfection reagent and seeded for culture. Following 2, 4, 6 and 9 days in culture, chondrocytes were isolated by trypsin treatment and centrifugation, RNA extracted and RT-PCR performed to study the expression of Twist upon transfection. Successful knockdown was obtained as early as 2 days with level of expression decreasing to 0.73±0.04 relative to P0, with no significant differences recorded for a further 2 days. 6 days post transfection, however, there was an increase in Twist expression to 2.50±0.25, deemed not significantly different from baseline P3 expression levels. These data confirmed the efficacy and transience of knockdown using anti-Twist siRNA molecules designed. Repeat-transfection was therefore required every 4 days to maintain longterm Twist knockdown. N=3, experiment repeated 3 times. Data shown as means ± s.e.m. T-test p-values were p<0.05 (*) and p<0.01 (**). N/S, non significant.

6.2.4.3 The effect of Twist knockdown on chondrocyte phenotype as characterised by collagen expression

The effect of Twist expression on chondrocyte phenotype regulation was investigated using anti-Twist siRNA. Briefly, P2 chondrocytes were tryspinised upon confluence and transfected in suspension with 1nM anti-Twist siRNA and 3μl/ml HiPerfect transfection reagent and repeat transfected every 4 days to maintain long term Twist knockdown. Upon confluence, RNA extracted from control P3 and Twist-knockdown P3 chondrocytes and subjected to RT-PCR to assay the expression of key genes including types I and II collagen. The level of expression was calculated using gel densitometry and was expressed relative to the level of expression in freshly isolated chondrocytes.

Twist knockdown did not have a significant effect on the regulation of types II and I collagen expression (Figure 6.9). There was a slight yet insignificant increase in the expression of type I collagen in response to Twist knockdown from 2.22±0.35 in P3 cultured chondrocytes to 3.26±0.34 in Twist knockdown P3 chondrocytes (relative to freshly isolated chondrocytes; $p>0.05$). Similarly, collagen II expression increased from 1.50±0.09 in control mock-transfected P3 chondrocytes to 1.82±0.12 upon Twist knockdown with no significant differences observed ($p>0.05$).

There was therefore no significant change in the type II to type I collagen expression ratio upon Twist knockdown with a slight decrease from 0.71±0.16 in mock-transfected P3 chondrocytes to 0.56±0.02 in Twist knockdown P3 chondrocytes relative to levels determined in freshly isolated chondrocytes ($p>0.05$). These details indicate that Twist knockdown is not sufficient to induce a restoration of chondrocyte differentiated phenotype.

Interestingly, a ~2-fold increase in DEL1 expression was observed upon Twist knockdown with expression values of 1.88±0.37 relative to freshly isolated

chondrocytes ($p<0.05$; Figure 6.10). Furthermore, Twist knockdown had no significant effect on SOX9 expression with 0.69 ± 0.14 of baseline expression observed in mock transfected and Twist knockdown P3 chondrocytes. These data showed that Twist knockdown induced DEL1 expression possibly via activation rather than upregulation of SOX9.

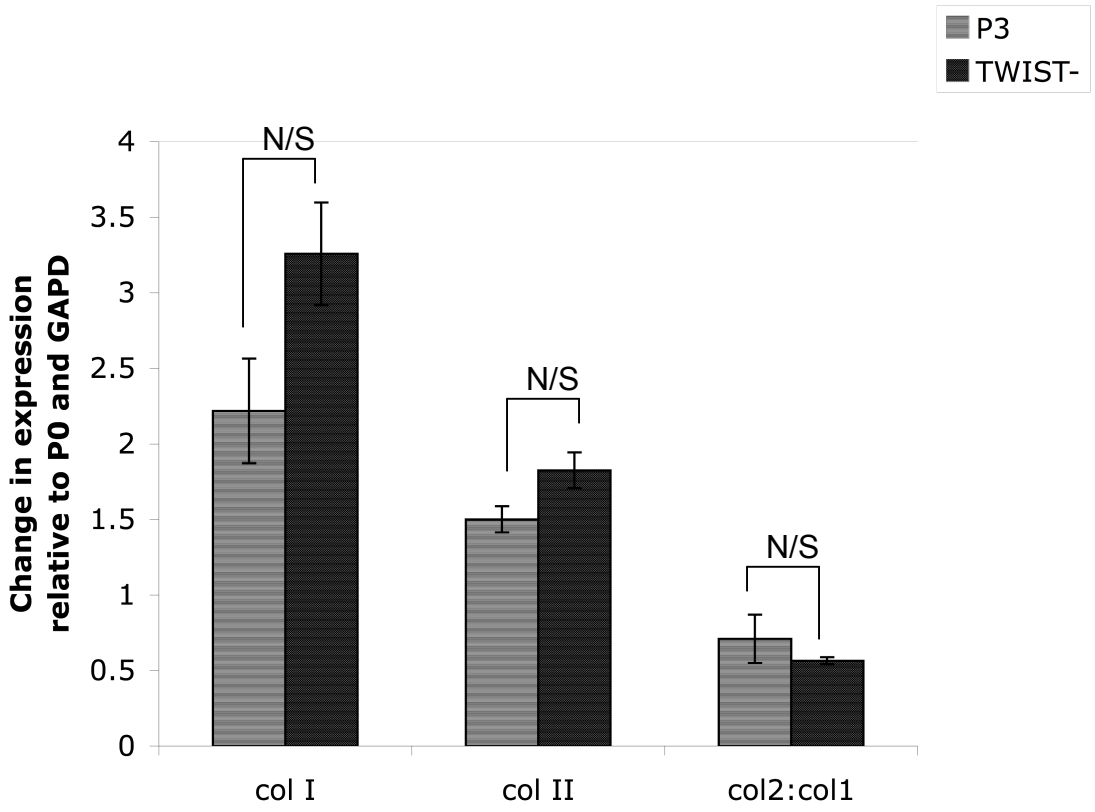

Figure 6.9: Changes in Expression of collagens in P3 chondrocytes in response to Twist knockdown using anti-Twist siRNA.

The effect of Twist on the loss of differentiated phenotype was investigated by Twist knockdown in P3 chondrocytes. Briefly, P2 chondrocytes were transfected with 1nM siRNA and 3μl/ml HiPerfect transfection reagent, cultured as previously described and repeat transfected following 4 days of seeding to ensure long-term knockdown. Upon confluence, RNA was isolated, reverse transcribed and PCR performed to study the expression of key collagen genes. No significant change in the expression of collagens was observed in response to Twist knockdown indicating that while Twist may play a role in loss of differentiated phenotype, Twist knockdown is not sufficient to cause a recapture of phenotype. N=3, experiment repeated 3 times. Data shown as means ± s.e.m. T test values were p>0.05 (N/S, non significant).

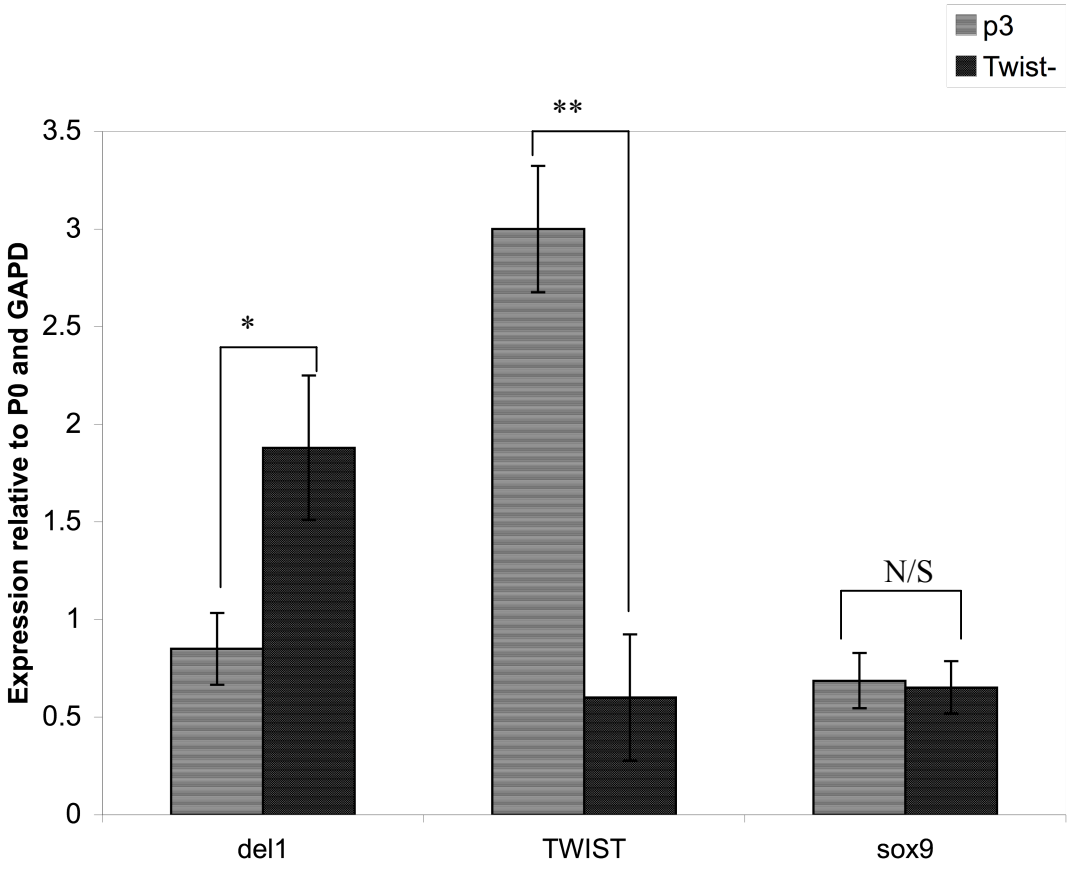

Figure 6.10: The effect of Twist knockdown on the expression of DEL1 and SOX9.

Having determined the role of DEL1 on Twist expression, the effect of the latter on the regulation on SOX9 and DEL1 as a last step in a potential feedback autocrine loop was investigated using anti-Twist knockdown. P2 chondrocytes were transfected in suspension upon confluency using 1nM anti-Twist siRNA and 3μl/ml HiPerfect and Twist knockdown maintained for the remainder of culture by repeat-transfection. 7 days post seeding, P3 chondrocytes were isolated and RNA extracted, reverse transcribed and subjected to PCR. Upon Twist knockdown there was an increase in DEL1 expression from 0.85±0.18 in control mock transfected P3 chondrocytes to 1.88±0.37 in Twist(-) P3 chondrocytes. There was, however, no change in SOX9 expression indicating that Twist inhibited DEL1 expression by interfering with SOX9 activity rather than expression. N=3, experiment repeated 3 times. Data shown as means ± s.e.m. T-test p-values were p<0.05 (*) and p<0.01 (**). N/S, non significant.

6.3 Chapter Discussion

Having confirmed the role of DEL1 in chondrocyte phenotype regulation, it was necessary to investigate the proposed DEL1-integrin signalling pathway. Despite inducing the expression of chondrocyte-specific genes in mesenchymal and synovium-derived progenior cells (Park *et al.,* 2005; Reinhold *et al.*, 2005), BMP signalling plays a key role in mouse chondrocytes maturation (Li *et al.*, 2006). Conversely, Twist has been shown to interfere with BMP2-induced gene and cause the downregulation of aggrecan and type II collagen, thereby promoting dedifferentiation (Reinhold et al., 2006).

The biosignificance of the simultaneous increase in DEL1 and SOX9 expression in mesodifferentiated chondrocytes was investigated by biological stimulation of SOX9 expression in P3 chondrocytes by supplementation with 500ng/ml BMP-2 (Minina *et al.*, 2001) for 7 days in culture as previously described (Park *et al.*, 2005). An increase in SOX9 expression was obtained and was accompanied with a 3-fold rise in DEL1 expression with both rises deemed similar to those observed naturally in P1 chondrocytes. These observations confirmed our hypothesis that DEL1 expression is mediated by SOX9 (Figure 6.6). Incubation with BMP2 was, nevertheless, not sufficient to recapture a differentiated phenotype but maintained a mesodifferentiated phenotype as defined by the expression of collagens (col2:col1 expression).

Previous work has shown that members of Edil family of extracellular proteins act by the activation of Akt signalling protein (Silvestre *et al.*, 2005) and our data confirmed a rise in Akt activity in P1 chondrocytes where DEL1 expression levels were elevated. To further investigate the effect of DEL1 on Akt activity, the latter was studied in response to DEL1 knockdown where it was shown that

knockdown reduced the activity of Akt by 46.12% (Figure 6.2). These data indicated the necessity of DEL1 for an overactivation of Akt in P1 chondrocytes.

To investigate the potential signal initiated by DEL1, the expression levels of Twist, a potential downstream element of the DEL1 signal, were assayed in response to culture. A significant and sustained rise in Twist expression was observed as early as 9 days post culture (P1 chondrocytes). Upon DEL1 knockdown, Twist expression was abolished (Figure 6.4) suggesting that the rise in Twist expression is mediated by DEL1-intgerin signalling pathway.

It has been shown by others that Twist-induced dedifferentiation is tightly regulated by β-catenin levels (Reinhold *et al.*, 2006), which are in turn indirectly positively influenced by Akt activity (Giles *et al.*, 2003). Previous work has shown that the accumilation of β-catenin caused dedifferentiation in rabbit articular chondrocytes as characterised by a decrease in col2:col1 expression (Hwang *et al.*, 2005). The role of β-catenin signal on Twist expression was therefore investigated using R-Etodolac, a pharmacological inhibitor of β-catenin at 500μM (Behari *et al.*, 2007), to knock down the levels of β-catenin. Similarly to DEL1 knockdown, the reduction in β-catenin levels inhibited the expression of Twist at the end of P1 (Figure 6.5) confirming the dependency of Twist expression on β-catenin levels mediated by DEL1-induced Akt activation.

To further study the role of Twist on chondrocyte phenotype, siRNA sequences designed to inhibit Twist expression were used and our data confirmed that the sequences selected induced Twist knockdown with 75.92% reduction in expression in P3 chondrocytes and possessed an effect lasting for up to 4 days post transfection. RNA isolated from Twist(-)/P3 chondrocytes did not show a recapture of phenotype as determined by the lack of change in the expression of SOX9 or col2:col1 despite an increase in type II collagen expression as reported elsewhere (Reinhold *et al.*, 2006). Additionally, there was an increase in DEL1 expression in response to Twist knockdown, thus indicating that Twist did not

inhibit the expression of SOX9 but inhibited SOX9 activity which included the transcription of type II collagen and DEL1. These data, however, showed that Twist knockdown (similarly to BMP2 treatment) was not sufficient to induce the recapture of the differentiated phenotype.

In summary, we have investigated the proposed pathway involving DEL1-induced dedifferentiation. These results concluded that DEL1 expression is mediated by SOX9 transcription and showed that DEL1 secretion induces an autocrine signal, most possibly upon interaction with $\alpha v\beta 3$ as previously reported (Hidai *et al.*, 1998). Upon DEL1 upregulation, an increase in Akt activation was observed possibly inducing a rise in the level of β-catenin, which was necessary for the expression of Twist as previously recorded (Reinhold *et al.*, 2006). In endothelial cells, DEL1-mediated autocrine pathway (Penata *et al.*, 1999) and integrin-Akt-β-catenin signals (Joshi *et al.*, 2007) have been previously observed in endothelial cells. We have confirmed that Twist inhibited SOX9 activity and thus created a negative feedback loop knocking down DEL1 and type II collagen and initiating terminal dedifferentiation (Figure 6.11).

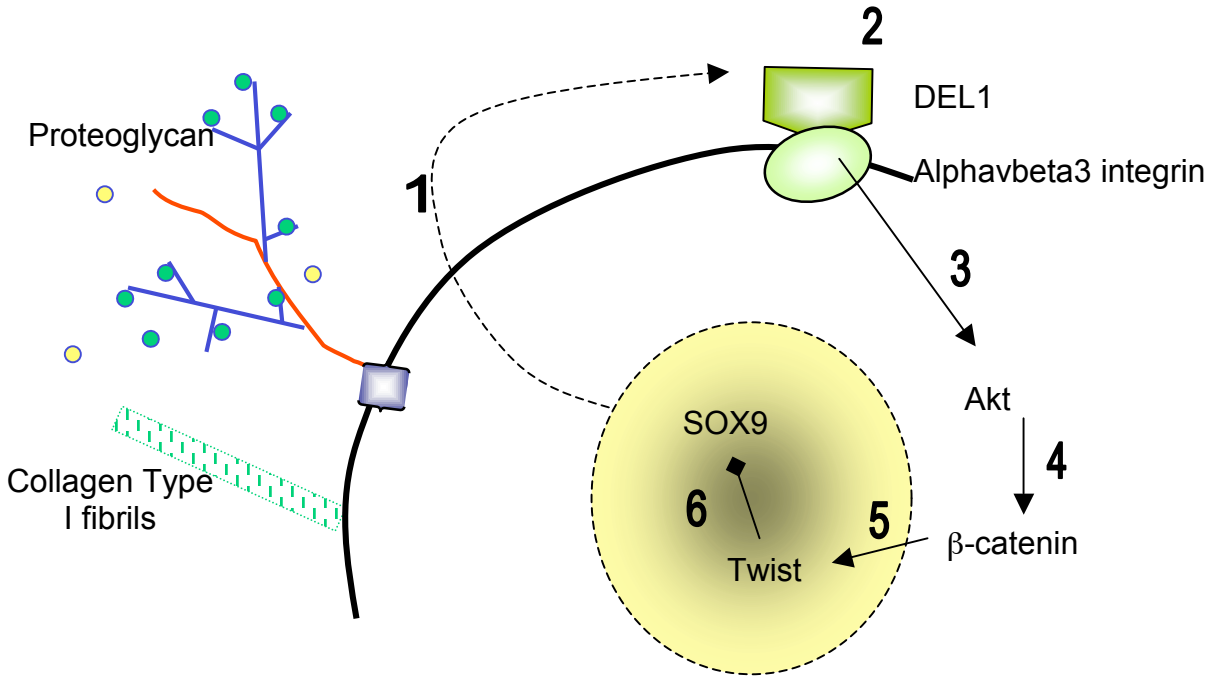

Figure 6.11: The proposed pathway of action of DEL1.

SOX9 induced the expression of DEL1 (1) which subsequently bound to integrins (2) and in turn activating other key signalling proteins including Akt (3). Akt is indirectly involved in the regulation of intracellular levels of β-catenin (4), a key inducer of the expression of transcription factors including Twist (5). Twist was found to be responsible for the suppression of SOX9 activity (6) and therefore downregulation of DEL1 expression and initiation of dedifferentiation.

7 Discussion, Conclusion and Future Work

7.1 Quantification of changes in phenotypic markers in response to 2D culture

Expansion and *in vitro* tissue engineering are novel promising techniques for treatment of OA, are challenged by the ultimate loss of chondrocytic phenotype in response to chondrocyte monolayer culture. We have aimed to further our knowledge of the phenotypic changes occurring upon chondrocyte expansion, with quantification when possible, of key differentiation markers including cell shape and actin organisation, expression battery and mechanotransduction.

Prior to studying the effects of 2D culture, it was necessary to establish a standard culture methodology to eliminate errors incurred by variation in length of time in culture. Several culture densities in the literature were studied and cell viability assayed (HD, MD and LD; Johansen *et al.*, 2001; Hamilton *et al.*, 2005a; Hamilton *et al.*, 2005b Stokes *et al.*, 2002 Waymouth, 1974). Despite obtaining higher levels of cell death in LD when compared to other culture densities, there was a steady increase in cell number upon LD 2D culture, and time points for subculture were determined at 9, 14 and 21 days post culture (termed P1, P2 and P3, respectively). Therefore, LD culture density was selected for cell culture methodology performed (Table 3.2).

Some of the first and most obvious changes in phenotype include a switch in cell morphology from ‘round’ to a ‘flat’ fibroblast-like shape. These changes were further confirmed by studying the dimensions and sphericity factors of individual chondrocytes at different culture intervals using CLSM. It was confirmed that a loss of sphericity occurred as early as the 9^{th} day in culture (P1) and was due to an increase in cell length (c) and a reduction in cell depth (a). These changes were also accompanied with an increase in chondrocyte cell volume which was

additionally confirmed by mathematical calculation from values obtained for cellular dimensions (Table 3.3).

Furthermore, changes in the actin cytoskeleton were observed in response to culture with a visually assessable increase in trans-cellular actin organisation in the form of actin filaments. We devised a new method for the analysis of the localisation and number of actin 'striation units' enabling us to quantify these changes. There was a marked increase in the percentage of filamentous actin seen as early as the first passage (Figure 3.8), and these changes were confirmed by the increase of trans-cellular actin filaments (Figure 3.7). Similarly to alterations in cell volume, sphericity and dimensions, no further reorganisation of the actin cytoskeleton was observed in response to further culture.

On a molecular level, the loss of chondrocyte phenotype in response to 2D culture was confirmed by studying changes in expression of key genes and a switch from chondrocyte-specific type II collagen to type I (represented as col2:col1). Firstly, the expression of DEL1 in bovine articular chondrocytes was confirmed using RT-PCR and western blot and upon 9 days in culture, there was an increase in DEL1 expression, only previously observed in hydrogel-cultured foetal chondrocytes (Stokes *et al.*, 2002). Moreover upon 9 days in culture, there was a rise in type II collagen, type I collagen, differentiation transcription factor SOX9, dedifferentiation transcription factor Twist and a decrease in col2:col1 expression, thereby indicating the loss of differentiated phenotype (Figure 3.9, Figure 6.3). While changes in col2:col1 expression have been widely reported in response to 2D culture (Benya & Shaffer, 1982b; Stokes *et al.*, 2001), an increase in type II collagen was not previously observed. Upon further culture, however, there was no change in col2:col1 ratio, type I collagen or Twist but a decline in the expression level of type II collagen, SOX9 and DEL1 was recorded.

The effect of cellular expansion on mechanotransduction was also used as a key marker of chondrocytic phenotype as previous work has shown that RVI and Gd^{3+}-sensitive rise in $[Ca^{2+}]_i$ (in response to hypo-osmotic conditions) were solely exhibited by 2D cultured chondrocytes (Kerrigan & Hall, 2008). We were able to confirm that whereas freshly isolated chondrocytes did not exhibit RVI, P1 2D cultured chondrocytes recovered cell volume in a linear fashion with a t½ of 9.60 minutes post challenge. Conversely, P2 and P3 chondrocytes exhibited a logarithmic and thus 'biphasic' volume recovery pattern with robust RVI at t½ = 3.45 minutes and slow RVI similar to that observed in P1 chondrocytes (Table 4.1). Actin organisation has been shown to regulate the capacity of chondrocytes to exhibit RVI, whereby treatment with LB (an actin deploymerising toxin) induced bumentanide-sensitive RVI in freshly isolated chondrocytes (Kerrigan *et al.*, 2006). Therefore, the activation of RVI mechanisms upon culture, possibly via actin reorganisation and thus NKCC activation, may contribute to the increase in cell volume discussed previously.

To investigate changes in mechanotransduction responses upon expansion, the calcium responses of freshly isolated and 2D cultured chondrocytes were studied using REV5901 as a pharmacological stimulus of $[Ca^{2+}]_i$ rise. It was observed that freshly isolated chondrocytes were more sensitive to REV5901 loading compared to 2D cultured chondrocytes (Figure 4.4) and the decrease in sensitivity was confirmed to be due to a reduction in intracellular calcium store release upon 2D culture. It was previously reported that mechanical pressure not only induced a rise in $[Ca^{2+}]_i$ (Guilak *et al.*, 1999a), but also increased the activity of IP3R channels on intracellular stores in 2D cultured chondrocytes (Zhang *et al.*, 2006), thus suggesting a reduction in store sensitivity upon culture. Moreover, research has indicated that a rise in REV5901 provided chondrocytes with protective mechanisms from the effects of pressure, possibly via $[Ca^{2+}]_i$ rise (Amin *et al*., 2008, Parker *et al.*, in press). Taken together, these data suggest that an increase in store sensitivity plays a crucial role in differentiatied load-bearing chondrocyte which may be lost upon 2D culture.

As the contribution of transmembrane extracellular calcium influx in response to REV5901 was not altered upon expansion, the participation of membrane channels was assayed by incubation with channel inhibitors prior to REV5901 loading. Upon 2D culture, there was a decrease in inhibition of $[Ca^{2+}]_i$ rise in the absence of extracellular sodium and an increase in inhibition in the presence of Gd^{3+} indicating a decrease in NCX activity and an increase in SACC activity (Figure 4.5). Previous work has reported a decrease in NCX expression in chondrocytes taken from OA tissue (Trujillo *et al.*, 1999) suggesting that the loss of apparent NCX contribution is possibly due to a similar down-regulation of NCX upon 2D culture. Conversely, previous work has shown that inhibition of SACC using Gd^{3+} inhibited hypo-osmotic challenge-induced $[Ca^{2+}]_i$ rise in 2D cultured but not freshly isolated chondrocytes (Kerrigan & Hall, 2008) and induced a loss of phenotype in rat chondrosarcoma cell line (Perkins *et al.*, 2005) confirming our results that SACC activity is phenotype-dependent and/or phenotype-regulatory.

These data demonstrated the existence of a third phenotype, termed mesodifferentiated, previously unrecorded as defined by the RVI response in P1 chondrocytes and the expression battery (

Table 7.1).

7.2 The role of DEL1 in the regulation of chondrocyte phenotype

As it has been shown that the expression of DEL1 was associated with the upregulation of SOX9, the potential role of SOX9 on DEL1 expression was investigated by biochemical induction of SOX9 using BMP2 (Minina *et al.*, 2001). There was an increase in SOX9 expression in response to BMP2 treatment and that was associated with a rise in DEL1 expression, thus confirming that SOX9 is necessary for DEL1 expression. Moreover, there was an increase in type II collagen expression confirming that observed changes are in response to SOX9 upregulation.

To further our understanding of the cause and effect relationship of DEL1 in chondrocyte 2D culture, the expression level of DEL1 and col2:col1 was further investigated within the first week of culture. There was a ~10-fold increase in DEL1 expression 2 days following 2D culture and the expression declined upon further culture, whereas the decline in col2:col1 expression was initiated following 4 days in culture (Figure 5.2). These data proposed a role for DEL1 in the regulation of chondrocyte phenotype which was further investigated using anti-DEL1 siRNA molecules to induce DEL1 knockdown in P1 chondrocytes.

Upon DEL1 knockdown, there was no increase in type I collagen expression in response to 2D culture and thus no decline in col2:col1 ratio indicating the preservation of a differentiated phenotype. Furthermore, DEL1 knockdown and pharmacological inhibition of β-catenin induced the knockdown of Twist expression suggesting that the expression of Twist is mediated by an integrin signal involving DEL1 and relayed by β-catenin (Figure 6.2, Figure 6.5). It has been therefore confirmed that β-catenin levels regulated the expression of Twist in chondrocytes as previously investigated by others (Reinhold *et al.*, 2006).

The effect of DEL1 on mechanotransduction responses was investigated upon knockdown in P1 chondrocytes to confirm observations of phenotype preservation in response to DEL1 knockdown. It has been shown that DEL1-knockdown P1 chondrocytes did not exhibit slow RVI as observed in control

mock transfected P1 chondrocytes and this was possibly due to changes in actin organisation in response to DEL1 knockdown. Furthermore, the effect of DEL1 on calcium channel activation was seen in the decrease in SACC contribution in response to knockdown, rendering DEL1(-)/P1 similar to freshly isolated chondrocytes in the regulation of calcium homeostasis (Table 5.3).

Due to the apparent effect of DEL1 on various phenotypic markers, the role of DEL1 in initiating an integrin-mediated signal was investigated with Twist as the final target. Being a downstream element of various integrin-ligand interactions including EDIL3 ligand (Silvestre *et al.*, 2005), Akt activity was studied in culture and in response to DEL1 knockdown. It was observed that upregulation of DEL1 expression in P1 mesodifferentiated chondrocytes was associated with an increase in Akt activity, which was abolished in response to DEL1 knockdown (Figure 6.1, Figure 6.2).

Finally, Twist has been shown to inhibit BMP2-induced differentiation and thus SOX9 function (Reinhold *et al.*, 2006) and these findings were confirmed using anti-Twist siRNA to inhibit the expression of Twist in P3 chondrocytes and assay the expression of key genes. While Twist knockdown did not induce a significant switch in col2:col1 expression, a sharp increase in the expression of DEL1 and type II collagen, two product genes of SOX9 transcription, was observed. No change, however, was observed in the level of SOX9 expression suggesting that Twist inhibited SOX9 activity rather than expression. These findings thus completed an autocrine feedback loop whereby DEL1-induced Akt activation, β-catenin accumulation and consequently Twist expression which in turn inhibited SOX9 expression and finalised the dedifferentiation process (Figure 6.11).

7.3 Summary and concluding remarks

In summary, we have reported the existence of a new (possibly homogenous) chondrocyte population upon 9 days in culture with a phenotype previously undefined (

Table 7.1). Mesodifferentiated chondrocytes are characterised by an elevation of SOX9 and DEL1 expression, and a decrease in col2:col1 expression, suggesting that dedifferentiation occurs in a multi-step process. Elevated levels of DEL1 expression have been shown to induce a switch in phenotype via Akt & β-catenin activation and Twist (an antagonist of SOX9) upregulation.

DEL1 knockdown induced an inhibition of a group of mesodifferentiated mechanotransduction markers including slow RVI and elevated SACC activity without significant effect on culture properties. Therefore these data suggested that longterm DEL1 knockdown may be used in expansion to maintain chondrocytic differentiated phenotype.

Chondrocyte expansion and matrix-induced autologous chondrocyte implantation (MACI) are currently under research in an attempt to offer a 'cure' for osteoarthritis, but due to difficulties in clinical testing, there has been relatively slow progress in the innovation of commercial technologies. The technique involves 2D culture of mature chondrocytes or mesenchymal stem cells (MSC) from a patient prior to introduction into a 3D scaffold, and is currently limited in potential due to several hurdles.

Firstly, neither 2D cultured adult chondrocytes nor MSCs exhibit suitable phenotypes. Whilst adult chondrocytes lose their differentiated phenotype upon culture, MSC's have shown inclination to differentiation into fibrocartilage or scar tissue rather than hyaline cartilage for reasons yet to be elucidated. One of the

sets of markers used to screen and monitor cultures of 2D cultured chondrocytes is the SOX transcription factors (Polak *et al.*, 2008). The use of serum-free media for the culture of chondrocytes has been suggested to limit dedifferentiation, and despite retention of elevated levels of SOX9 and a reduction in cellular hypertrophy, the expression of type I collagen was not halted (Ho *et al.*, 2009). We have shown that a longterm DEL1 knockdown is sufficient to maintain the upregulation of SOX9, type II collagen and thus the differentiated state, whilst inhibiting collagen type I. Moreover, DEL1(-) chondrocytes have demonstrated a decrease in hypertrophy and can be cultured effectively in standardised economical serum-enriched systems.

Due to the conservation of phenotype, DEL1(-) 2D cultured chondrocytes retained the expression of type II collagen, thus offering the advantage of the capacity to produce and maintain a potentially cartilage-like matrix upon introduction into 3D scaffold. This eliminates the need for synthetic matrices required for cell entrapment and strength. Finally and unlike conventionally selected cultures, DEL1(-) chondrocytes have additionally differentiated-like mechanotransduction responses including the lack of RVI and SACC activity.

Future work to support these observations includes transfection using a viral vector containing an inducible promotor for the transfer of siRNA gene prior to culture in the presence of an inducer. Adenoassociated virus is a relatively safe choice with no risk of infections or insertional mutations, and upon integration, offers a constitutive siRNA expression. Upon successful knockdown and sufficient expansion, chondrocytes would be introduced to 3D scaffold for further investigation of phenotype, mechanotransduction and matrix metabolism.

Several steps would be taken to improve current methodologies including the use of more selective inhibitors (or possibly the use of RNAi) for the investigation of individual membrane channel contribution to both RVI and $[Ca^{2+}]_i$ rise. Additionally, the filament tracer add-on in Imaris 6.3.1 allows for the

creation of filamentous structures and calculates the number of branch points, thereby providing more sophisticated data with improved accuracy for the estimation of actin reorganisation (Figure 7.1).

Table 7.1: Summary of the properties of differentiated, mesodifferentiated and dedifferentiated chondrocytes as defined using key markers of phenotype.

Marker	Differentiated	Mesodifferentiated	Dedifferentiated
DEL1	Low	High	Low
sox9	Intermediate	High	Low
col I	Low	High	High
col II	Intermediate	High	Low
col2:col1	High	Low	Low
Twist	Low	High	High
Volume	Low	High	High
a	High	Low	Low
c	Low	High	High
φ	High	Low	Low
StU	Low	High	High
Intracellular store release	High	Low	Low
NCX	High	Low	Low
SACC	Low	High	High
attachment rate	Low	High	Low
Akt activity	Low	High	Low
RVI	None	Slow	Biphasic

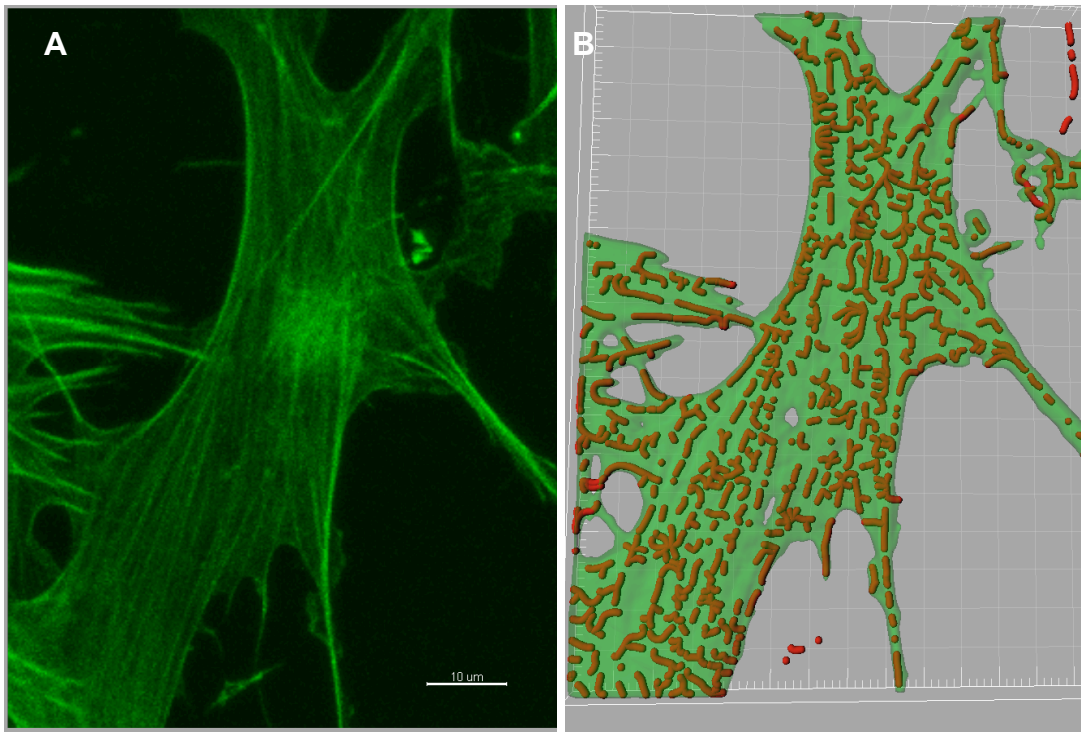

Figure 7.1: New Analysis tool for the study of filamentous actin organisation.

Confocal images of a P3 2D cultured chondrocyte stained for actin with phalloidin-alexa 488 was chosen at random for representative purposes, deconvolved and reassembled in Imaris 6.31 (PanelA; Bitplane). The filament tracer add-on was used with default settings to produce filamentous structures (Panel B; red) and an isosurface object was added for the same channel (green) for illustration. Imaris filament tracer can be used to record various parameters including the number of branch points, number of filaments and length of filaments, and can therefore be used for future actin analysis.

8 References and bibliography

Adams JC & Watt FM. (1991). Expression of beta 1, beta 3, beta 4, and beta 5 integrins by human epidermal keratinocytes and non-differentiating keratinocytes. *The Journal of cell biology* **115,** 829-841.

Aigner T, Dietz U, Stoss H & von der Mark K. (1995). Differential expression of collagen types I, II, III, and X in human osteophytes. *Lab Invest* **73,** 236-243.

Aigner T & McKenna L. (2002). Molecular pathology and pathobiology of osteoarthritic cartilage. *Cell Mol Life Sci* **59,** 5-18.

Alvarez J, Balbin M, Fernandez M & Lopez JM. (2001). Collagen metabolism is markedly altered in the hypertrophic cartilage of growth plates from rats with growth impairment secondary to chronic renal failure. *J Bone Miner Res* **16,** 511-524.

Ali N, Getting S & Kerrigan MJP. (2008). The effect of hypotonicity on chondrocyte volume regulation and intracellular calcium signalling. Proceedings of the British Pharmacological Society. Vol 6, Issue 2.

Ana M. Schor IE, Seth L. Schor. (2001). *Chemotaxis and Chemokinesis in 3D Macromolecular Matrices: Relevance to Angiogenesis*, vol. 46. Springer.

Anderson JJ & Felson DT. (1988). Factors associated with osteoarthritis of the knee in the first national Health and Nutrition Examination Survey (HANES I). Evidence for an association with overweight, race, and physical demands of work. *Am J Epidemiol* **128,** 179-189.

Aoka Y, Johnson FL, Penta K, Hirata Ki K, Hidai C, Schatzman R, Varner JA & Quertermous T. (2002). The embryonic angiogenic factor DEL1 accelerates tumor growth by enhancing vascular formation. *Microvascular research* **64,** 148-161.

Arakawa A, Matsuo-Takasaki M, Takai A, Inomata H, Matsumura M, Ikeya M, Takahashi K, Miyachi Y, Sasai N & Sasai Y. (2007). The secreted EGF-Discoidin factor xDEL1 is essential fr dorsal development of Xenopus embryo. *Dev Biol*, **306**, 160-9.

Archer CW & Francis-West P. (2003). The chondrocyte. *Int J Biochem Cell Biol* **35,** 401-404.

Aszodi A, Hunziker EB, Brakebusch C & Fassler R. (2003). Beta1 integrins regulate chondrocyte rotation, G1 progression, and cytokinesis. *Genes Dev* **17,** 2465-2479.

Baici A, Lang A, Horler D & Knopfel M. (1988a). Cathepsin B as a marker of the dedifferentiated chondrocyte phenotype. *Ann Rheum Dis* **47,** 684-691.

Baici A, Lang A, Horler D & M. K. (1988b). Cathepsin B as a marker of the dedifferentiated chondrocyte phenotype. *Ann Rheum Dis* **47,** 684-691.

Ballock RT, Heydemann A, Wakefield LM, Flanders KC, Roberts AB & Sporn MB. (1993). TGF-beta 1 prevents hypertrophy of epiphyseal chondrocytes: regulation of gene expression for cartilage matrix proteins and metalloproteases. *Developmental biology* **158,** 414-429.

Ballock RT & O'Keefe RJ. (2003). The biology of the growth plate. *J Bone Joint Surg Am* **85-A,** 715-726.

Beekman B, Verzijl N, Bank RA, von der Mark K & TeKoppele JM. (1997). Synthesis of collagen by bovine chondrocytes cultured in alginate; Posttranslational modifications and cell-matrix interaction. *Exp Cell Res* **237,** 135-141.

Behari J, Zeng G, Otruba W, Thompson MD, Muller P, Micsenyi A, Sekhon SS, Leoni L & Monga SP. (2007). R-R-Etodolac decreases beta-catenin levels along with survival and proliferation of hepatoma cells. *J Hepatol* **46,** 849-857.

Bengtsson T, Aszodi A, Nicolae C, Hunziker EB, Lundgren-Akerlund E & Fassler R. (2005). Loss of alpha10beta1 integrin expression leads to moderate dysfunction of growth plate chondrocytes. *J Cell Sci* **118,** 929-936.

Benya PD. (1988). Modulation and reexpression of the chondrocyte phenotype; mediation by cell shape and microfilament modification. *Pathol Immunopathol Res* **7,** 51-54.

Benya PD, Brown PD & Padilla SR. (1988). Microfilament modification by dihydrocytochalasin B causes retinoic acid-modulated chondrocytes to reexpress the differentiated collagen phenotype without a change in shape. *J Cell Biol* **106,** 161-170.

Benya PD & Shaffer JD. (1982a). Dedifferentiated Chondrocytes Reexpress the Differentiated Collagen Phenotype When Cultured in Agarose Gels. *Cell* **30,** 215-224.

Benya PD & Shaffer JD. (1982b). Dedifferentiated chondrocytes reexpress the differentiated collagen phenotype when cultured in agarose gels. *Cell* **30,** 215-224.

Benya PD, Shaffer JD & Nimni ME. (1981). Flexibility of the Chondrocyte Collagen Phenotype. *Semin Arthritis Rheum* **11,** 44-45.

Benz K, Breit S, Lukoschek M, Mau H & Richter W. (2002a). Molecular analysis of expansion, differentiation, and growth factor treatment of human chondrocytes identifies differentiation markers and growth-related genes. *Biochem Biophys Res Commun* **293,** 284-292.

Benz K, Breit S, Lukoschek M, Mau H & Richter W. (2002b). Molecular analysis of expansion, differentiation, and growth factor treatment of human chondrocytes identifies differentiation markers and growth-related genes. *Biochem Biophys Res Commun* **293,** 284-292.

Berra-Romani R, Mazzocco-Spezzia A, Pulina MV & Golovina VA. (2008). Ca2+ handling is altered when arterial myocytes progress from a contractile to a proliferative phenotype in culture. *Am J Physiol Cell Physiol*, **295**, C779-90.

Bialek P, Kern B, Yang X, Schrock M, Sosic D, Hong N, Wu H, Yu K, Ornitz DM, Olson EN, Justice MJ & Karsenty G. (2004). A twist code determines the onset of osteoblast differentiation. *Dev Cell* **6,** 423-435.

Blain EJ, Gilbert SJ, Hayes AJ & Duance VC. (2006). Disassembly of the vimentin cytoskeleton disrupts articular cartilage chondrocyte homeostasis. *Matrix Biol* **25,** 398-408.

Bohme K, Winterhalter KH & Bruckner P. (1995). Terminal differentiation of chondrocytes in culture is a spontaneous process and is arrested by transforming growth factor-beta 2 and basic fibroblast growth factor in synergy. *Exp Cell Res* **216,** 191-198.

Boland S, Boisview-Ulrich E, Houcine O, Baeza-Squiban A, Pouchelet M, Schoevaert D & Marano F. (1996). TGF beta 1 promotes actin cytoskeleton reorganisation and migratory phenotype in epithelial tracheal cells in primary culture. *J Cell Sci*., **109**, 2207-19.

Bridge AJ, Pebernard S, Ducraux A, Nicoulaz AL & Iggo R. (2003). Induction of an interferon response by RNAi vectors in mammalian cells. *Nat Genet* **34,** 263-264.

Broom ND & Myers DB. (1980). A study of the structural response of wet hyaline cartilage to various loading situations. *Connect Tissue Res* **7,** 227-237.

Brown PD & Benya PD. (1988). Alterations in chondrocyte cytoskeletal architecture during phenotypic modulation by retinoic acid and dihydrocytochalasin B-induced reexpression. *J Cell Biol* **106,** 171-179.

Buckwalter JA & Mankin HJ. (1998). Articular cartilage: tissue design and chondrocyte-matrix interactions. *Instr Course Lect* **47,** 477-486.

Buckwalter JA, Mower D, Ungar R, Schaeffer J & Ginsberg B. (1986). Morphometric analysis of chondrocyte hypertrophy. *J Bone Joint Surg Am* **68,** 243-255.

Bulstrode CB, J; Carr, A.; Marsh, L.; Fairbank, J.; Wilson-MacDonald, J.; Bowden, G. (2002). *Oxford Textbook of Orthopaedics and Trauma*. Oxford University Press.

Burton-Wurster N, Vernier-Singer M, Farquhar T & Lust G. (1993). Effect of compressive loading and unloading on the synthesis of total protein, proteoglycan, and fibronectin by canine cartilage explants. *J Orthop Res* **11,** 717-729.

Buschmann MD, Hunziker EB, Kim YJ & Grodzinsky AJ. (1996). Altered aggrecan synthesis correlates with cell and nucleus structure in statically compressed cartilage. *J Cell Sci* **109 (Pt 2),** 499-508.

Bush PG & Hall AC. (2001a). Regulatory volume decrease (RVD) by isolated and in situ bovine articular chondrocytes. *J Cell Physiol* **187,** 304-314.

Bush PG & Hall AC. (2001b). The osmotic sensitivity of isolated and in situ bovine articular chondrocytes. *J Orthop Res* **19,** 768-778.

Bush PG & Hall AC. (2003). The volume and morphology of chondrocytes within non-degenerate and degenerate human articular cartilage. *Osteoarthritis Cartilage* **11,** 242-251.

Bush PG & Hall AC. (2005). Passive osmotic properties of in situ human articular chondrocytes within non-degenerate and degenerate cartilage. *J Cell Physiol* **204,** 309-319.

Byers PD, Maroudase A, Oztop F, Stockwell RA & Venn MF. (1977). Histological and biochemical studies on cartilage from osteoarthrotic femoral heads with special reference to surface characteristics. *Connect Tissue Res* **5,** 41-49.

Chen G, Sato T, Ushida T, Hirochika R & Tateishi T. (2003). Redifferentiation of dedifferentiated bovine chondrocytes when cultured in vitro in a PLGA-collagen hybrid mesh. *FEBS Lett* **542,** 95-99.

Chen Q, Lin TH, Der CJ & Juliano RL. (1996). Integrin-mediated activation of MEK and mitogen-activated protein kinase is independent of Ras [corrected]. *J Biol Chem* **271,** 18122-18127.

Chen Z, Ding Y & Zhang H. (2002). Morphology, viability and functions of suckling pig hepatocytes cultured in serum-free medium at high density. *Dig Surg*, **19**, 184-91.

Chen ZF & Behringer RR. (1995). twist is required in head mesenchyme for cranial neural tube morphogenesis. *Genes Dev* **9,** 686-699.

Cheng C, Conte E, Pleshko-Camacho N & Hidaka C. (2007). Differences in matrix accumulation and hypertrophy in superficial and deep zone chondrocytes are controlled by bone morphogenetic protein. *Matrix Biol* **26,** 541-553.

Chong LD, Traynor-Kaplan A, Bokoch GM & Schwartz MA. (1994). The small GTP-binding protein Rho regulates a phosphatidylinositol 4-phosphate 5-kinase in mammalian cells. *Cell* **79,** 507-513.

Clancy RM, Rediske J, Tang X, Nijher N, Frenkel S, Philips M & Abramson SB. (1997). Outside-in signaling in the chondrocyte. Nitric oxide disrupts fibronectin-induced assembly of a subplasmalemmal actin/rho A/focal adhesion kinase signaling complex. *The Journal of clinical investigation* **100,** 1789-1796.

Cullen BR. (2005). Does RNA interference have a future as a treatment for HIV-1 induced disease? *AIDS Rev* **7,** 22-25.

Darling EM & Athanasiou KA. (2005). Rapid phenotypic changes in passaged articular chondrocyte subpopulations. *J Orthop Res* **23,** 425-432.

Dascalu A, Korenstein R, Oron Y & Nevo Z. (1996). A hyperosmotic stimulus regulates intracellular pH, calcium, and S-100 protein levels in avian chondrocytes. *Biochem Biophys Res Commun* **227,** 368-373.

de Crombrugghe B, Lefebvre V, Behringer RR, Bi W, Murakami S & Huang W. (2000). Transcriptional mechanisms of chondrocyte differentiation. *Matrix Biol* **19,** 389-394.

De Luca F, Barnes KM, Uyeda JA, De-Levi S, Abad V, Palese T, Mericq V & Baron J. (2001). Regulation of growth plate chondrogenesis by bone morphogenetic protein-2. *Endocrinology* **142,** 430-436.

Dedhar S & Gray V. (1990). Isolation of a novel integrin receptor mediating Arg-Gly-Asp-directed cell adhesion to fibronectin and type I collagen from human neuroblastoma cells. Association of a novel beta 1-related subunit with alpha v. *J Cell Biol* **110,** 2185-2193.

DeLise AM, Fischer L & Tuan RS. (2000). Cellular interactions and signaling in cartilage development. *Osteoarthritis Cartilage* **8,** 309-334.

Denli AM & Hannon GJ. (2003). RNAi: an ever-growing puzzle. *Trends Biochem Sci* **28,** 196-201.

Diaz-Romero J, Gaillard JP, Grogan SP, Nesic D, Trub T & Mainil-Varlet P. (2005). Immunophenotypic analysis of human articular chondrocytes: changes in surface markers associated with cell expansion in monolayer culture. *J Cell Physiol* **202,** 731-742.

Dong YF, Soung do Y, Chang Y, Enomoto-Iwamoto M, Paris M, O'Keefe RJ, Schwarz EM & Drissi H. (2007). Transforming growth factor-beta and Wnt

signals regulate chondrocyte differentiation through Twist1 in a stage-specific manner. *Mol Endocrinol* **21,** 2805-2820.

Dreja K, Nordstrom I & Hellstrand P. (2001). Rat arterial smooth muscle devoid of ryanodine recepto function: effect on cellular ca(2+) handling. *Br J Pharmacol*, **132**, 1957-66.

Drissi H, Zuscik M, Rosier R & O'Keefe R. (2005). Transcriptional regulation of chondrocyte maturation: potential involvement of transcription factors in OA pathogenesis. *Molecular aspects of medicine* **26,** 169-179.

Dupont J, Fernandez AM, Glackin CA, Helman L & LeRoith D. (2001). Insulin-like growth factor 1 (IGF-1)-induced twist expression is involved in the anti-apoptotic effects of the IGF-1 receptor. *J Biol Chem* **276,** 26699-26707.

Durr J, Goodman S, Potocnik A, von der Mark H & von der Mark K. (1993). Localization of beta 1-integrins in human cartilage and their role in chondrocyte adhesion to collagen and fibronectin. *Exp Cell Res* **207,** 235-244.

Durrant LA, Archer CW, Benjamin M & Ralphs JR. (1999). Organisation of the chondrocyte cytoskeleton and its response to changing mechanical conditions in organ culture. *J Anat* **194 (Pt 3),** 343-353.

Edlich M, Yellowley CE, Jacobs CR & Donahue HJ. (2001). Oscillating fluid flow regulates cytosolic calcium concentration in bovine articular chondrocytes. *J Biomech* **34,** 59-65.

Elbashir SM, Harborth J, Lendeckel W, Yalcin A, Weber K & Tuschl T. (2001a). Duplexes of 21-nucleotide RNAs mediate RNA interference in cultured mammalian cells. *Nature* **411,** 494-498.

Elbashir SM, Lendeckel W & Tuschl T. (2001b). RNA interference is mediated by 21- and 22-nucleotide RNAs. *Genes & development* **15,** 188-200.

Elbashir SM, Martinez J, Patkaniowska A, Lendeckel W & Tuschl T. (2001c). Functional anatomy of siRNAs for mediating efficient RNAi in Drosophila melanogaster embryo lysate. *Embo J* **20,** 6877-6888.

Enomoto MI, Boettiger D & Menko AS. (1993). Alpha 5 integrin is a critical component of adhesion plaques in myogenesis. *Developmental biology* **155,** 180-197.

Enomoto-Iwamoto M, Iwamoto M, Nakashima K, Mukudai Y, Boettiger D, Pacifici M, Kurisu K & Suzuki F. (1997). Involvement of alpha5beta1 integrin in matrix interactions and proliferation of chondrocytes. *J Bone Miner Res* **12,** 1124-1132.

Eyre DR, Wu JJ, Fernandes RJ, Pietka TA & Weis MA. (2002). Recent developments in cartilage research: matrix biology of the collagen II/IX/XI heterofibril network. *Biochem Soc Trans* **30,** 893-899.

Fernandes JC, Martel-Pelletier J & Pelletier JP. (2002). The role of cytokines in osteoarthritis pathophysiology. *Biorheology* **39,** 237-246.

Fioravanti A, Nerucci F, Annefeld M, Collodel G & Marcolongo R. (2003). Morphological and cytoskeletal aspects of cultivated normal and osteoarthritic human articular chondrocytes after cyclical pressure: a pilot study. *Clin Exp Rheumatol* **21,** 739-746.

Freshney RI. (2001). *Culture of Animal Cells - A manual of Basic Technique*. Wiley-Liss, New York.

Frondoza C, Sohrabi A & Hungerford D. (1996). Human chondrocytes proliferate and produce matrix components in microcarrier suspension culture. *Biomaterials* **17,** 879-888.

Gandhi CS, Loots E & Isacoff EY. (2000). Reconstructing voltage sensor-pore interaction from a fluorescence scan of a voltage-gated K+ channel. *Neuron* **27,** 585-595.

Garciadiego-Cazares D, Rosales C, Katoh M & Chimal-Monroy J. (2004). Coordination of chondrocyte differentiation and joint formation by alpha5beta1 integrin in the developing appendicular skeleton. *Development* **131,** 4735-4742.

Gavenis K, Schumacher C, Schneider U, Eisfeld J, Mollenhauer J & Schmidt-Rohlfing B. (2009). Expression of ion channels of the TRP family in articular chondrocytes from osteoarthritic patients: changes between native and in vitro propagated chondrocytes. *Mol Cell Biochem* **321,** 135-143.

Gebhard PM, Gehrsitz A, Bau B, Soder S, Eger W & Aigner T. (2003). Quantification of expression levels of cellular differentiation markers does not support a general shift in the cellular phenotype of osteoarthritic chondrocytes. *J Orthop Res* **21,** 96-101.

Giannoni P, Pagano A, Maggi E, Arbico R, Randazzo N, Grandizio M, Cancedda R & Dozin B. (2005). Autologous chondrocyte implantation (ACI) for aged

patients: development of the proper cell expansion conditions for possible therapeutic applications. *Osteoarthritis Cartilage* **13,** 589-600.

Giles RH, van Es JH & Clevers H. (2003). Caught up in a Wnt storm: Wnt signaling in cancer. *Biochim Biophys Acta* **1653,** 1-24.

Gilmore AP & Burridge K. (1996). Molecular mechanisms for focal adhesion assembly through regulation of protein-protein interactions. *Structure* **4,** 647-651.

Goley ED & Welch MD. (2006). The ARP2/3 complex: an actin nucleator comes of age. *Nat Rev Mol Cell Biol* **7,** 713-726.

Gray H. (2000). *Anatomy of the Human Body*. BARTLEBY.COM, New York.

Grimsrud CD, Romano PR, D'Souza M, Puzas JE, Schwarz EM, Reynolds PR, Roiser RN & O'Keefe RJ. (2001). BMP signaling stimulates chondrocyte maturation and the expression of Indian hedgehog. *J Orthop Res* **19,** 18-25.

Gschwendt M, Muller HJ, Kielbassa K, Zang R, Kittstein W, Rincke G & Marks F. (1994). Rottlerin, a novel protein kinase inhibitor. *Biochem Biophys Res Commun* **199,** 93-98.

Guilak F. (1995). Compression-induced changes in the shape and volume of the chondrocyte nucleus. *J Biomech* **28,** 1529-1541.

Guilak F, Erickson GR & Ting-Beall HP. (2002). The effects of osmotic stress on the viscoelastic and physical properties of articular chondrocytes. *Biophys J* **82,** 720-727.

Guilak F, Jones WR, Ting-Beall HP & Lee GM. (1999a). The deformation behavior and mechanical properties of chondrocytes in articular cartilage. *Osteoarthritis Cartilage* **7,** 59-70.

Guilak F, Meyer BC, Ratcliffe A & Mow VC. (1994). The effects of matrix compression on proteoglycan metabolism in articular cartilage explants. *Osteoarthritis Cartilage* **2,** 91-101.

Guilak F, Zell RA, Erickson GR, Grande DA, Rubin CT, McLeod KJ & Donahue HJ. (1999b). Mechanically induced calcium waves in articular chondrocytes are inhibited by gadolinium and amiloride. *J Orthop Res* **17,** 421-429.

Gunthorpe MJ, Benham CD, Randall A & Davis JB. (2002). The diversity in the vanilloid (TRPV) receptor family of ion channels. *Trends Pharmacol Sci* **23,** 183-191.

Guo JF, Jourdian GW & MacCallum DK. (1989). Culture and growth characteristics of chondrocytes encapsulated in alginate beads. *Connect Tissue Res* **19,** 277-297.

Haag J, Gebhard PM & Aigner T. (2008). SOX gene expression in human osteoarthritic cartilage. *Pathobiology* **75,** 195-199.

Haisch A, Marzahn U, Mobasheri A, Schulze-Tanzil G & Shakibaei M. (2006). Development and phenotypic characterization of a high density in vitro model of auricular chondrocytes with applications in reconstructive plastic surgery. *Histol Histopathol* **21,** 467-476.

Hall AC. (1998a). *Physiology of Cartilage*. W. B. Saunders.

Hall AC, ed. (1998b). *Physiology of Cartilage*. W.B. Saunders, London.

Hall AC & Bush PG. (2001). The role of a swelling-activated taurine transport pathway in the regulation of articular chondrocyte volume. *Pflugers Arch* **442,** 771-781.

Hall AC, Starks I, Shoults CL & Rashidbigi S. (1996). Pathways for K+ transport across the bovine articular chondrocyte membrane and their sensitivity to cell volume. *The American journal of physiology* **270,** C1300-1310.

Hall BK & Miyake T. (1992). The membranous skeleton: the role of cell condensations in vertebrate skeletogenesis. *Anat Embryol (Berl)* **186,** 107-124.

Hamamori Y, Sartorelli V, Ogryzko V, Puri PL, Wu HY, Wang JY, Nakatani Y & Kedes L. (1999). Regulation of histone acetyltransferases p300 and PCAF by the bHLH protein twist and adenoviral oncoprotein E1A. *Cell* **96,** 405-413.

Hamilton DW, Riehle MO, Monaghan W & Curtis AS. (2005a). Articular chondrocyte passage number: influence on adhesion, migration, cytoskeletal organisation and phenotype in response to nano- and micro-metric topography. *Cell biology international* **29,** 408-421.

Hamilton DW, Riehle MO, Rappuoli R, Monaghan W, Barbucci R & Curtis AS. (2005b). The response of primary articular chondrocytes to micrometric surface topography and sulphated hyaluronic acid-based matrices. *Cell biology international* **29,** 605-615.

Hanayama R, Tanaka M, Miwa K & Nagata S. (2004). Expression of developmental endothelial locus-1 in a subset of macrophages for engulfment of apoptotic cells. *J immunol*, **172**, 3876-82.

Harmand MF, Thomasset M, Rouais F & Ducassou D. (1984). In vitro stimulation of articular chondrocyte differentiated function by 1,25-dihydroxycholecalciferol or 24R,25-dihydroxycholecalciferol. *J Cell Physiol* **119,** 359-365.

Hartwig JH, Bokoch GM, Carpenter CL, Janmey PA, Taylor LA, Toker A & Stossel TP. (1995). Thrombin receptor ligation and activated Rac uncap actin filament barbed ends through phosphoinositide synthesis in permeabilized human platelets. *Cell* **82,** 643-653.

Hattori T, Coustry F, Stephens S, Eberspaecher H, Takigawa M, Yasuda H & de Crombrugghe B. (2008). Transcriptional regulation of chondrogenesis by coactivator Tip60 via chromatin association with Sox9 and Sox5. *Nucleic Acids Res* **36,** 3011-3024.

Hauselmann HJ, Fernandes RJ, Mok SS, Schmid TM, Block JA, Aydelotte MB, Kuettner KE & Thonar EJ. (1994). Phenotypic stability of bovine articular chondrocytes after long-term culture in alginate beads. *J Cell Sci* **107 (Pt 1),** 17-27.

Hauselmann HJ, Masuda K, Hunziker EB, Neidhart M, Mok SS, Michel BA & Thonar EJ. (1996). Adult human chondrocytes cultured in alginate form a matrix similar to native human articular cartilage. *Am J Physiol* **271,** C742-752.

Hayes AJ, Benjamin M & Ralphs JR. (2001). Extracellular matrix in development of the intervertebral disc. *Matrix Biol* **20,** 107-121.

Hemler ME. (1990). VLA proteins in the integrin family: structures, functions, and their role on leukocytes. *Annu Rev Immunol* **8,** 365-400.

Heyland J, Wiegandt K, Goepfert C, Nagel-Heyer S, Illinich E, Schmacher U & Portner R. (2006). Redifferentiation of chondrocytes and cartilage formation under intermittent hydrostatic pressure. *Biotechnol Lett*, **28**, 1641-8.

Hidai C, Zupancic T, Penta K, Mikhail A, Kawana M, Quertermous EE, Aoka Y, Fukagawa M, Matsui Y, Platika D, Auerbach R, Hogan BL, Snodgrass R & Quertermous T. (1998). Cloning and characterization of developmental endothelial locus-1: an embryonic endothelial cell protein that binds the alphavbeta3 integrin receptor. *Genes Dev* **12,** 21-33.

Hirsch MS, Lunsford LE, Trinkaus-Randall V & Svoboda KK. (1997). Chondrocyte survival and differentiation in situ are integrin mediated. *Dev Dyn* **210,** 249-263.

Ho HK, Jang JJ, Kaji S, Spektor G, Fong A, Yang P, Hu BS, Schatzman R, Quertermous T & Cooke JP. (2004). Developmental endothelial locus-1 (Del-1), a novel angiogenic protein: its role in ischemia. *Circulation* **109,** 1314-1319.

Ho STB, Yang Z, Hui HPJ, Oh KESO, Choo BHA & Lee EH. (2009). A serum free approach towards the conservation of chondrogenic phenotype during *in vitro* cell expansion. *Growth Factors* **27**, 321-333.

Hodge WA, Fijan, R. S., Carlson, K. L., Burgess, R. G., Harris W. H. and Mann, R.W. (1986). Contact Pressures in the human hip joint measured in vivo. *Proc Natl Acad Sci U S A* **83,** 2879-2883.

Hoffmann EK, Schettino T & Marshall WS. (2007). The role of volume-sensitive ion transport systems in regulation of epithelial transport. *Comparative biochemistry and physiology* **148,** 29-43.

Holmes MW, Bayliss MT & Muir H. (1988). Hyaluronic acid in human articular cartilage. Age-related changes in content and size. *The Biochemical journal* **250,** 435-441.

Hopewell B & Urban JP. (2003). Adaptation of articular chondrocytes to changes in osmolality. *Biorheology* **40,** 73-77.

Horton W & Hassell JR. (1986). Independence of cell shape and loss of cartilage matrix production during retinoic acid treatment of cultured chondrocytes. *Dev Biol* **115,** 392-397.

Horton WE, Jr., Balakir R, Precht P & Liang CT. (1991). 1,25-Dihydroxyvitamin D3 down-regulates aggrecan proteoglycan expression in immortalized rat chondrocytes through a post-transcriptional mechanism. *J Biol Chem* **266,** 24804-24808.

Horwitz ER, Higgins TM & Harvey BJ. (1996). Histamine-induced cytosolic calcium increase in porcine articular chondrocytes. *Biochim Biophys Acta* **1313,** 95-100.

Hotchin NA & Hall A. (1995). The assembly of integrin adhesion complexes requires both extracellular matrix and intracellular rho/rac GTPases. *J Cell Biol* **131,** 1857-1865.

Hou C, Kirchner T, Singer M, Matheis M, Argentieri D & Cavender D. (2004). In vivo activity of a phospholipase C inhibitor, 1-(6-((17beta-3-methoxyestra-

1,3,5(10)-trien-17-yl)amino)hexyl)-1H-pyrrole -2,5-dione (U73122), in acute and chronic inflammatory reactions. *J Pharmacol Exp Ther* **309,** 697-704.

Hsu GP, Mathy JA, Wang Z, Xia W, Sakamoto G, Kundu R, Longaker MT, Quertermous T & Yang GP. (2008). Increased rate of hair regrowth in mice with constitutive overexpression of DEL1. *J Surg Res*, **146**, 73-80.

Hughes SaM, I., ed. (1997). *Sciences Basic to Orthopaedics*. Saunders, Oxford.

Huh YH, Kim SH, Kim SJ & Chun JS. (2003). Differentiation status-dependent regulation of cyclooxygenase-2 expression and prostaglandin E2 production by epidermal growth factor via mitogen-activated protein kinase in articular chondrocytes. *J Biol Chem* **278,** 9691-9697.

Hwang SG, Yu SS, Lee SW & Chun JS. (2005). Wnt-3a regulates chondrocyte differentiation via c-Jun/AP-1 pathway. *FEBS Lett*, **21**, 4837-42.

Hynes RO. (1992). Integrins: versatility, modulation, and signaling in cell adhesion. *Cell* **69,** 11-25.

Iannotti JP, Brighton CT, Iannotti V & Ohishi T. (1990). Mechanism of action of parathyroid hormone-induced proteoglycan synthesis in the growth plate chondrocyte. *J Orthop Res* **8,** 136-145.

Idowu BD, Knight MM, Bader DL & Lee DA. (2000). Confocal analysis of cytoskeletal organisation within isolated chondrocyte sub-populations cultured in agarose. *Histochem J* **32,** 165-174.

Ikebe T, Hirata M & Koga T. (1988). Effects of human recombinant tumor necrosis factor-alpha and interleukin 1 on the synthesis of

glycosaminoglycan and DNA in cultured rat costal chondrocytes. *J Immunol* **140,** 827-831.

Ishii M, Merrill AE, Chan YS, Gitelman I, Rice DP, Sucov HM & Maxson RE, Jr. (2003). Msx2 and Twist cooperatively control the development of the neural crest-derived skeletogenic mesenchyme of the murine skull vault. *Development* **130,** 6131-6142.

James DJ, Salaun C, Brandie FM, Connell JM & Chamberlain LH. (2004). Neomycin prevents the wortmannin inhibition of insulin-stimulated Glut4 translocation and glucose transport in 3T3-L1 adipocytes. *J Biol Chem* **279,** 20567-20570.

Johansen JS, Olee T, Price PA, Hashimoto S, Ochs RL & Lotz M. (2001). Regulation of YKL-40 production by human articular chondrocytes. *Arthritis Rheum* **44,** 826-837.

Johnstone B, Hering TM, Caplan AI, Goldberg VM & Yoo JU. (1998). In vitro chondrogenesis of bone marrow-derived mesenchymal progenitor cells. *Exp Cell Res* **238,** 265-272.

Joshi MB, Ivanov D, Philippova M, Erne P & Resink TJ. (2007). Integrin-linked kinase is an essential mediator for T-cadherin-dependent signalling via Akt and GSK3beta in endothelial cells. *FASEB J*, **12**, 3083-95.

Kawanishi M, Oura A, Furukawa K, Fukubayashi T, Nakamura K, Tateishi T & Ushida T. (2007). Redifferetiation of dedifferentiated bovine articular chondrocytes enhanced by cyclic hydrostatic pressure under a gas-controlled system. *Tissue Eng.*, **13**, 957-64.

Kerrigan MJ & Hall AC. (2005). Stimulation of regulatory volume decrease (RVD) by isolated bovine articular chondrocytes following F-actin disruption using latrunculin B. *Biorheology* **42,** 283-293.

Kerrigan MJ & Hall AC. (2007). Control of chondrocyte regulatory volume decrease (RVD) by [Ca(2+)](i) and cell shape. *Osteoarthritis Cartilage*.

Kerrigan MJ & Hall AC. (2008). Control of chondrocyte regulatory volume decrease (RVD) by [Ca2+]i and cell shape. *Osteoarthritis Cartilage* **16,** 312-322.

Kerrigan MJ, Hook CS, Qusous A & Hall AC. (2006). Regulatory volume increase (RVI) by in situ and isolated bovine articular chondrocytes. *J Cell Physiol* **209,** 481-492.

Kiang AS, Palfi A, Ader M, Kenna PF, Millington-Ward S, Clark G, Kennan A, O'Reilly M, Tam LC, Aherne A, McNally N, Humphries P & Farrar GJ. (2005). Toward a Gene Therapy for Dominant Disease: Validation of an RNA Interference-Based Mutation-Independent Approach. *Mol Ther*.

Kim SJ, Hwang SG, Kim IC & Chun JS. (2003). Actin cytoskeletal architecture regulates nitric oxide-induced apoptosis, dedifferentiation, and cyclooxygenase-2 expression in articular chondrocytes via mitogen-activated protein kinase and protein kinase C pathways. *J Biol Chem* **278,** 42448-42456.

Kino-oka M, Maeda Y, Ota Y, Yashiki S, Sugawara K & Taya M. (2005). Process design of chondrocyte cultures with monolayer growth for cell expansion and subsequent three-dimensional growth for production of cultured cartilage. *J Biosci Bioeng* **100,** 67-76.

Knight MM, Idowu BD, Lee DA & Bader DL. (2001). Temporal changes in cytoskeletal organisation within isolated chondrocytes quantified using a novel image analysis technique. *Med Biol Eng Comput* **39,** 397-404.

Koumakis E, Wipff J, Avouac J, Kahan A & Allanore Y. (2009). Severe Refractory Rheumatoid Arthritis Successfully Treated with Combination Rituximab and Anti-Tumor Necrosis Factor-{alpha}-Blocking Agents. *J Rheumatol* **36,** 2125-2126.

Langelier E, Suetterlin R, Hoemann CD, Aebi U & Buschmann MD. (2000). The chondrocyte cytoskeleton in mature articular cartilage: structure and distribution of actin, tubulin, and vimentin filaments. *J Histochem Cytochem* **48,** 1307-1320.

Lapadula G, Iannone F, Zuccaro C, Grattagliano V, Covelli M, Patella V, Lo Bianco G & Pipitone V. (1997). Integrin expression on chondrocytes: correlations with the degree of cartilage damage in human osteoarthritis. *Clin Exp Rheumatol* **15,** 247-254.

Lapadula G, Iannone F, Zuccaro C, Grattagliano V, Covelli M, Patella V, Lo Bianco G & Pipitone V. (1998). Chondrocyte phenotyping in human osteoarthritis. *Clin Rheumatol* **17,** 99-104.

Lee DA, Reisler T & Bader DL. (2003a). Expansion of chondrocytes for tissue engineering in alginate beads enhances chondrocytic phenotype compared to conventional monolayer techniques. *Acta Orthop Scand* **74,** 6-15.

Lee HS, Millward-Sadler SJ, Wright MO, Nuki G & Salter DM. (2000). Integrin and mechanosensitive ion channel-dependent tyrosine phosphorylation of

focal adhesion proteins and beta-catenin in human articular chondrocytes after mechanical stimulation. *J Bone Miner Res* **15,** 1501-1509.

Lee MT, Coburn GA, McClure MO & Cullen BR. (2003b). Inhibition of human immunodeficiency virus type 1 replication in primary macrophages by using Tat- or CCR5-specific small interfering RNAs expressed from a lentivirus vector. *J Virol* **77,** 11964-11972.

LeGrand A, Fermor B, Fink C, Pisetsky DS, Weinberg JB, Vail TP & Guilak F. (2001). Interleukin-1, tumor necrosis factor alpha, and interleukin-17 synergistically up-regulate nitric oxide and prostaglandin E2 production in explants of human osteoarthritic knee menisci. *Arthritis Rheum* **44,** 2078-2083.

Lin Z, Willers C, Xu J & Zheng MH. (2006). The chondrocyte: biology and clinical application. *Tissue Eng* **12,** 1971-1984.

Liu B & Wu D. (2004). Analysis of G protein-mediated activation of phospholipase C in cultured cells. *Methods Mol Biol* **237,** 99-102.

Liu C & Hermann TE. (1978). Characterization of ionomycin as a calcium ionophore. *J Biol Chem* **253,** 5892-5894.

Liu CJ. (2009). The role of ADAMTS-7 and ADAMTS-12 in the pathogenesis of arthritis. *Nat Clin Pract Rheumatol* **5,** 38-45.

Liu Y, Wang W, Cao Y, Shang Q & Zhong W. (1998). [Culture of chondrocytes seeded onto chitin scaffoldings coating with different materials: experimental study]. *Zhonghua Wai Ke Za Zhi* **36,** 495-496.

Liu Y, Wang Y, Yamakuchi M, Masuda S, Tokioka T, Yamaoka S, Maruyama I & Kitajima I. (2001). Phosphoinositide-3 kinase-PKB/Akt pathway activation is involved in fibroblast Rat-1 transformation by human T-cell leukemia virus type I tax. *Oncogene* **20,** 2514-2526.

Loty S, Sautier JM & Forest N. (2000). Phenotypic modulation of nasal septal chondrocytes by cytoskeleton modification. *Biorheology* **37,** 117-125.

Lui VC, Ng LJ, Nicholls J, Tam PP & Cheah KS. (1995). Tissue-specific and differential expression of alternatively spliced alpha 1(II) collagen mRNAs in early human embryos. *Dev Dyn* **203,** 198-211.

Luo G, D'Souza R, Hogue D & Karsenty G. (1995). The matrix Gla protein gene is a marker of the chondrogenesis cell lineage during mouse development. *J Bone Miner Res* **10,** 325-334.

Maestro R, Dei Tos AP, Hamamori Y, Krasnokutsky S, Sartorelli V, Kedes L, Doglioni C, Beach DH & Hannon GJ. (1999). Twist is a potential oncogene that inhibits apoptosis. *Genes Dev* **13,** 2207-2217.

Mallein-Gerin F, Garrone R & van der Rest M. (1991). Proteoglycan and collagen synthesis are correlated with actin organization in dedifferentiating chondrocytes. *Eur J Cell Biol* **56,** 364-373.

Maroudas A & Bannon C. (1981). Measurement of swelling pressure in cartilage and comparison with the osmotic pressure of constituent proteoglycans. *Biorheology* **18,** 619-632.

Maroudas A & Venn M. (1977). Chemical composition and swelling of normal and osteoarthrotic femoral head cartilage. II. Swelling. *Ann Rheum Dis* **36,** 399-406.

Martin I, Jakob M, Schafer D, Dick W, Spagnoli G & Heberer M. (2001). Quantitative analysis of gene expression in human articular cartilage from normal and osteoarthritic joints. *Osteoarthritis Cartilage* **9,** 112-118.

Matyas JR, Adams ME, Huang D & Sandell LJ. (1995). Discoordinate gene expression of aggrecan and type II collagen in experimental osteoarthritis. *Arthritis and rheumatism* **38,** 420-425.

Melrose J, Smith SM, Smith MM & Little CB. (2008). The use of Histochoice for histological examination of articular and growth plate cartilages, intervertebral disc and meniscus. *Biotech Histochem* **83,** 47-53.

Mertens M & Singh JA. (2009). Anakinra for rheumatoid arthritis: a systematic review. *J Rheumatol* **36,** 1118-1125.

Millward-Sadler SJ, Wright MO, Lee H, Caldwell H, Nuki G & Salter DM. (2000). Altered electrophysiological responses to mechanical stimulation and abnormal signalling through alpha5beta1 integrin in chondrocytes from osteoarthritic cartilage. *Osteoarthritis Cartilage* **8,** 272-278.

Minina E, Wenzel HM, Kreschel C, Karp S, Gaffield W, McMahon AP & Vortkamp A. (2001). BMP and Ihh/PTHrP signaling interact to coordinate chondrocyte proliferation and differentiation. *Development* **128,** 4523-4534.

Miot S, Woodfield T, Daniels AU, Suetterlin R, Peterschmitt I, Heberer M, van Blitterswijk CA, Riesle J & Martin I. (2005a). Effects of scaffold composition and architecture on human nasal chondrocyte redifferentiation and cartilaginous matrix deposition. *Biomaterials* **26,** 2479-2489.

Miot S, Woodfield T, Daniels AU, Suetterlin R, Peterschmitt I, Heberer M, van Blitterswijk CA, Riesle J & Martin I. (2005b). Effects of scaffold composition and architecture on human nasal chondrocyte redifferentiation and cartilaginous matrix deposition. *Biomaterials* **26,** 2479-2489.

Mizrahi J, Maroudas A, Lanir Y, Ziv I & Webber TJ. (1986). The "instantaneous" deformation of cartilage: effects of collagen fiber orientation and osmotic stress. *Biorheology* **23,** 311-330.

Mototani H, Mabuchi A, Saito S, Fujioka M, Iida A, Takatori Y, Kotani A, Kubo T, Nakamura K, Sekine A, Murakami Y, Tsunoda T, Notoya K, Nakamura Y & Ikegawa S. (2005). A functional single nucleotide polymorphism in the core promoter region of CALM1 is associated with hip osteoarthritis in Japanese. *Hum Mol Genet* **14,** 1009-1017.

Muallem S & Wilkie TM. (1999). G protein-dependent Ca2+ signaling complexes in polarized cells. *Cell Calcium* **26,** 173-180.

Muramatsu S, Wakabayashi M, Ohno T, Amano K, Ooishi R, Sugahara T, Shiojiri S, Tashiro K, Suzuki Y, Nishimura R, Kuhara S, Sugano S, Yoneda T & Matsuda A. (2007). Functional gene screening system identified TRPV4 as a regulator of chondrogenic differentiation. *J Biol Chem* **282,** 32158-32167.

Musser JH, Chakraborty UR, Sciortino S, Gordon RJ, Khandwala A, Neiss ES, Pruss TP, Van Inwegen R, Weinryb I & Coutts SM. (1987). Substituted arylmethyl phenyl ethers. 1. A novel series of 5-lipoxygenase inhibitors and leukotriene antagonists. *J Med Chem* **30,** 96-104.

Nakou M, Katsikas G, Sidiropoulos P, Bertsias G, Papadimitraki E, Raptopoulou A, Koutala H, Papadaki HA, Kritikos H & Boumpas DT. (2009). Rituximab therapy reduces activated B cells both in the peripheral blood and bone marrow of patients with rheumatoid arthritis: depletion of memory B cells correlates with clinical response. *Arthritis Res Ther* **11,** R131.

Nalin AM, Greenlee TK, Jr. & Sandell LJ. (1995). Collagen gene expression during development of avian synovial joints: transient expression of types II and XI collagen genes in the joint capsule. *Dev Dyn* **203,** 352-362.

Nedelcheva Y, Getting SJ & Kerrigan MJP. (2008). The role of the aactin skeleton in chondrocyte protection following single impact. Proceedings of the British Pharmacological Society. Vol 6, Issue 4.

Nehrer S, Breinan HA, Ramappa A, Shortkroff S, Young G, Minas T, Sledge CB, Yannas IV & Spector M. (1997). Canine chondrocytes seeded in type I and type II collagen implants investigated in vitro. *J Biomed Mater Res*, **38**, 95-104.

Newman P & Watt FM. (1988). Influence of cytochalasin D-induced changes in cell shape on proteoglycan synthesis by cultured articular chondrocytes. *Exp Cell Res* **178,** 199-210.

Ng LJ, Wheatley S, Muscat GE, Conway-Campbell J, Bowles J, Wright E, Bell DM, Tam PP, Cheah KS & Koopman P. (1997). SOX9 binds DNA, activates transcription, and coexpresses with type II collagen during chondrogenesis in the mouse. *Dev Biol* **183,** 108-121.

Nofal GA & Knudson CB. (2002). Latrunculin and cytochalasin decrease chondrocyte matrix retention. *J Histochem Cytochem* **50,** 1313-1324.

Nusse R. (2005). Wnt signaling in disease and in development. *Cell Res* **15,** 28-32.

O'Neill WC. (1999). Physiological significance of volume-regulatory transporters. *The American journal of physiology* **276,** C995-C1011.

Ono S. (2007). Mechanism of depolymerization and severing of actin filaments and its significance in cytoskeletal dynamics. *Int Rev Cytol* **258,** 1-82.

Ostergaard K, Salter DM, Petersen J, Bendtzen K, Hvolris J & Andersen CB. (1998). Expression of alpha and beta subunits of the integrin superfamily in articular cartilage from macroscopically normal and osteoarthritic human femoral heads. *Ann Rheum Dis* **57,** 303-308.

Ota MS, Loebel DA, O'Rourke MP, Wong N, Tsoi B & Tam PP. (2004). Twist is required for patterning the cranial nerves and maintaining the viability of mesodermal cells. *Dev Dyn* **230,** 216-228.

Park Y, Sugimoto M, Watrin A, Chiquet M & Hunziker EB. (2005). BMP-2 induces the expression of chondrocyte-specific genes in bovine synovium-derived progenitor cells cultured in three-dimensional alginate hydrogel. *Osteoarthritis Cartilage* **13,** 527-536.

Parker E, Getting SJ, Hucklebridge F, Vleck VE & Kerrigan MJP. (2008). The effects of REV5901 on chondrocyte viability following mechanical trauma. Proceedings of the British Pharmacological Society. Vol 7, Issue 4.

Pathi S, Rutenberg JB, Johnson RL & Vortkamp A. (1999). Interaction of Ihh and BMP/Noggin signaling during cartilage differentiation. *Dev Biol* **209,** 239-253.

Peach CA, Carr AJ & Loughlin J. (2005). Recent advances in the genetic investigation of osteoarthritis. *Trends in molecular medicine* **11,** 186-191.

Penta K, Varner JA, Liaw L, Hidai C, Schatzman R & Quertermous T. (1999). DEL1 induces integrin signaling and angiogenesis by ligation of alphaVbeta3. *J Biol Chem* **274,** 11101-11109.

Perkins GL, Derfoul A, Ast A & Hall DJ. (2005). An inhibitor of the stretch-activated cation receptor exerts a potent effect on chondrocyte phenotype. *Differentiation* **73,** 199-211.

Pirttiniemi P & Kantomaa T. (1998). Effect of cytochalasin D on articular cartilage cell phenotype and shape in long-term organ culture. *Eur J Orthod* **20,** 491-499.

Polak JM, Mantalaris S & Harding SE. (2008). Advances in Tissue Engineering: Cartilage. London: Imperial College Press.

Pollard TD & Borisy GG. (2003). Cellular motility driven by assembly and disassembly of actin filaments. *Cell* **112,** 453-465.

Pritchard S & Guilak F. (2004). The role of F-actin in hypo-osmotically induced cell volume change and calcium signaling in anulus fibrosus cells. *Ann Biomed Eng* **32,** 103-111.

Pullig O, Weseloh G, Ronneberger D, Kakonen S & Swoboda B. (2000). Chondrocyte differentiation in human osteoarthritis: expression of osteocalcin in normal and osteoarthritic cartilage and bone. *Calcif Tissue Int* **67,** 230-240.

Qusous A, Hook C, Nedelcheva Y & Kerrigan MJP. (2010). siRNA mediated

inhibition of Regulatory Volume Increase (RVI) in the chondrocyte cell line C20/A4. In press.

Rajpurohit R, Koch CJ, Tao Z, Teixeira CM & Shapiro IM. (1996). Adaptation of chondrocytes to low oxygen tension: relationship between hypoxia and cellular metabolism. *J Cell Physiol* **168,** 424-432.

Ramachandrula A, Tiku K & Tiku ML. (1992). Tripeptide RGD-dependent adhesion of articular chondrocytes to synovial fibroblasts. *J Cell Sci* **101 (Pt 4),** 859-871.

Reginato AM, Iozzo RV & Jimenez SA. (1994). Formation of nodular structures resembling mature articular cartilage in long-term primary cultures of human fetal epiphyseal chondrocytes on a hydrogel substrate. *Arthritis Rheum* **37,** 1338-1349.

Reinhold MI, Kapadia RM, Liao Z & Naski MC. (2006). The Wnt-inducible transcription factor Twist1 inhibits chondrogenesis. *J Biol Chem* **281,** 1381-1388.

Renshaw MW, Toksoz D & Schwartz MA. (1996). Involvement of the small GTPase rho in integrin-mediated activation of mitogen-activated protein kinase. *J Biol Chem* **271,** 21691-21694.

Reynolds A, Leake D, Boese Q, Scaringe S, Marshall WS & Khvorova A. (2004). Rational siRNA design for RNA interference. *Nat Biotechnol* **22,** 326-330.

Rezaee M, Penta K & Quertermous T. (2002). DEL1 mediates VSMC adhesion, migration, and proliferation through interaction with integrin alpha(v)beta(3). *Am J Physiol Heart Circ Physiol* **282,** H1924-1932.

Roberts S. (1985). Collagen of the calcified layer of human articular cartilage. *Experientia* **41,** 1138-1139.

Roberts SR, Knight MM, Lee DA & Bader DL. (2001). Mechanical compression influences intracellular Ca2+ signaling in chondrocytes seeded in agarose constructs. *J Appl Physiol* **90,** 1385-1391.

Roos EM, Roos HP, Lohmander LS, Ekdahl C & Beynnon BD. (1998). Knee Injury and Osteoarthritis Outcome Score (KOOS)--development of a self-administered outcome measure. *J Orthop Sports Phys Ther* **28,** 88-96.

Rozen S & Skaletsky H. (2000). Primer3 on the WWW for general users and for biologist programmers. *Methods in molecular biology (Clifton, NJ* **132,** 365-386.

Ruoslahti E & Pierschbacher MD. (1987). New perspectives in cell adhesion: RGD and integrins. *Science* **238,** 491-497.

Ryan MC & Sandell LJ. (1990). Differential expression of a cysteine-rich domain in the amino-terminal propeptide of type II (cartilage) procollagen by alternative splicing of mRNA. *J Biol Chem* **265,** 10334-10339.

Sackin H. (1995). Stretch-activated ion channels. *Kidney Int* **48,** 1134-1147.

Sailor LZ, Hewick RM & Morris EA. (1996). Recombinant human bone morphogenetic protein-2 maintains the articular chondrocyte phenotype in long-term culture. *J Orthop Res* **14,** 937-945.

Sanchez JC, Danks TA & Wilkins RJ. (2003). Mechanisms involved in the increase in intracellular calcium following hypotonic shock in bovine articular chondrocytes. *Gen Physiol Biophys* **22,** 487-500.

Sanchez JC & Wilkins RJ. (2004). Changes in intracellular calcium concentration in response to hypertonicity in bovine articular chondrocytes. *Comp Biochem Physiol A Mol Integr Physiol* **137,** 173-182.

Sandell LJ & Aigner T. (2001). Articular cartilage and changes in arthritis. An introduction: cell biology of osteoarthritis. *Arthritis Res* **3,** 107-113.

Sandell LJ, Morris N, Robbins JR & Goldring MB. (1991). Alternatively spliced type II procollagen mRNAs define distinct populations of cells during vertebral development: differential expression of the amino-propeptide. *J Cell Biol* **114,** 1307-1319.

Schaller MD, Borgman CA, Cobb BS, Vines RR, Reynolds AB & Parsons JT. (1992). pp125FAK a structurally distinctive protein-tyrosine kinase associated with focal adhesions. *Proceedings of the National Academy of Sciences of the United States of America* **89,** 5192-5196.

Schaller MD, Hildebrand JD, Shannon JD, Fox JW, Vines RR & Parsons JT. (1994). Autophosphorylation of the focal adhesion kinase, pp125FAK, directs SH2-dependent binding of pp60src. *Mol Cell Biol* **14,** 1680-1688.

Schliwa M. (1982). Action of cytochalasin D on cytoskeletal networks. *J Cell Biol* **92,** 79-91.

Schmid TM, Bonen DK, Luchene L & Linsenmayer TF. (1991). Late events in chondrocyte differentiation: hypertrophy, type X collagen synthesis and matrix calcification. *In vivo (Athens, Greece)* **5,** 533-540.

Schmidhauser C, Casperson GF, Myers CA, Sanzo KT, Bolten S & Bissell MJ. (1992). A novel transcriptional enhancer is involved in the prolactin- and extracellular matrix-dependent regulation of beta-casein gene expression. *Molecular biology of the cell* **3,** 699-709.

Schnabel M, Marlovits S, Eckhoff G, Fichtel I, Gotzen L, Vecsei V & Schlegel J. (2002). Dedifferentiation-associated changes in morphology and gene expression in primary human articular chondrocytes in cell culture. *Osteoarthritis Cartilage* **10,** 62-70.

Schulze-Tanzil G, Mobasheri A, de Souza P, John T & Shakibaei M. (2004). Loss of chondrogenic potential in dedifferentiated chondrocytes correlates with deficient Shc-Erk interaction and apoptosis. *Osteoarthritis Cartilage* **12,** 448-458.

Scully SP, Lee JW, Ghert PMA & Qi W. (2001). The role of the extracellular matrix in articular chondrocyte regulation. *Clin Orthop Relat Res***,** S72-89.

Serra R & Chang C. (2003). TGF-beta signaling in human skeletal and patterning disorders. *Birth Defects Res C Embryo Today* **69,** 333-351.

Serra R, Karaplis A & Sohn P. (1999). Parathyroid hormone-related peptide (PTHrP)-dependent and -independent effects of transforming growth factor beta (TGF-beta) on endochondral bone formation. *The Journal of cell biology* **145,** 783-794.

Sgaglione NA. (2005). Biologic approaches to articular cartilage surgery: Future trends. *Orthop Clin North Am* **36,** 485-+.

Shakibaei M & De Souza P. (1997). Differentiation of mesenchymal limb bud cells to chondrocytes in alginate beads. *Cell Biol Int* **21,** 75-86.

Shakibaei M, De Souza P & Merker HJ. (1997). Integrin expression and collagen type II implicated in maintenance of chondrocyte shape in monolayer culture: an immunomorphological study. *Cell Biol Int* **21,** 115-125.

Shrode LD, Klein JD, Douglas PB, O'Neill WC & Putnam RW. (1997). Shrinkage-induced activation of Na+/H+ exchange: role of cell density and myosin light chain phosphorylation. *The American journal of physiology* **272,** C1968-1979.

Silvestre JS, Thery C, Hamard G, Boddaert J, Aguilar B, Delcayre A, Houbron C, Tamarat R, Blanc-Brude O, Heeneman S, Clergue M, Duriez M, Merval R, Levy B, Tedgui A, Amigorena S & Mallat Z. (2005). Lactadherin promotes VEGF-dependent neovascularization. *Nat Med* **11,** 499-506.

Sock E, Pagon RA, Keymolen K, Lissens W, Wegner M & Scherer G. (2003). Loss of DNA-dependent dimerization of the transcription factor SOX9 as a cause for campomelic dysplasia. *Hum Mol Genet* **12,** 1439-1447.

Soder S, Hambach L, Lissner R, Kirchner T & Aigner T. (2002). Ultrastructural localization of type VI collagen in normal adult and osteoarthritic human articular cartilage. *Osteoarthritis Cartilage* **10,** 464-470.

Song HR, Lee KS, Li QW, Koo SK & Jung SC. (2003). Identification of cartilage oligomeric matrix protein (COMP) gene mutations in patients with pseudoachondroplasia and multiple epiphyseal dysplasia. *J Hum Genet* **48,** 222-225.

Sorokin L, Sonnenberg A, Aumailley M, Timpl R & Ekblom P. (1990). Recognition of the laminin E8 cell-binding site by an integrin possessing the alpha 6 subunit is essential for epithelial polarization in developing kidney tubules. *The Journal of cell biology* **111,** 1265-1273.

Sosic D, Richardson JA, Yu K, Ornitz DM & Olson EN. (2003). Twist regulates cytokine gene expression through a negative feedback loop that represses NF-kappaB activity. *Cell* **112,** 169-180.

Spicer DB, Rhee J, Cheung WL & Lassar AB. (1996). Inhibition of myogenic bHLH and MEF2 transcription factors by the bHLH protein Twist. *Science* **272,** 1476-1480.

Spirito S, Goldberg RL & Di Pasquale G. (1993). A comparison of chondrocyte proteoglycan metabolism in monolayer and agarose cultures. *Agents Actions* **39 Spec No,** C160-162.

Stevens A & Lowe JS. (2000). *Pathology*. Elsevier Health Sciences.

Stockwell RA. (1971a). The interrelationship of cell density and cartilage thickness in mammalian articular cartilage. *J Anat* **109,** 411-421.

Stockwell RA. (1971b). The interrelationship of cell density and cartilage thickness in mammalian articular cartilage. *J Anat* **109,** 411-421.

Stockwell RA. (1971c). The ultrastructure of cartilage canals and the surrounding cartilage in the sheep fetus. *J Anat* **109,** 397-410.

Stockwell RA. (1978). Chondrocytes. *J Clin Pathol Suppl (R Coll Pathol)* **12,** 7-13.

Stockwell RA. (1979). *The Biology of Catrilage Cells*. Cambridge Univeristy Press, Cambridge.

Stockwell RA. (1991a). Cartilage Failure in Osteoarthritis: Relevance of Normal Structure and Function. A Review. *Clinical Anatomy* **4,** 161-191.

Stockwell RA. (1991b). Morphometry of cytoplasmic components of mammalian articular chondrocytes and corneal keratocytes: species and zonal variations of mitochondria in relation to nutrition. *J Anat* **175,** 251-261.

Stoker MG. (1973). Role of diffusion boundary layer in contact inhibition of growth. *Nature* **246,** 200-203.

Stokes DG, Liu G, Coimbra IB, Piera-Velazquez S, Crowl RM & Jimenez SA. (2002). Assessment of the gene expression profile of differentiated and dedifferentiated human fetal chondrocytes by microarray analysis. *Arthritis Rheum* **46,** 404-419.

Stokes DG, Liu G, Dharmavaram R, Hawkins D, Piera-Velazquez S & Jimenez SA. (2001). Regulation of type-II collagen gene expression during human chondrocyte de-differentiation and recovery of chondrocyte-specific phenotype in culture involves Sry-type high-mobility-group box (SOX) transcription factors. *The Biochemical journal* **360,** 461-470.

Sung LY, Chiu HY, Chen YL, Chuang CK & Hu YC. (2009). Baculovirus-mediated growth factor expression in dedifferentiated chondrocytes accelerates redifferentiation: effects of combinational transduction. *Tissue Eng*, **15**, 1353-62.

Takigawa M, Takano T, Shirai E & Suzuki F. (1984). Cytoskeleton and differentiation: effects of cytochalasin B and colchicine on expression of

the differentiated phenotype of rabbit costal chondrocytes in culture. *Cell Differ* **14,** 197-204.

Tallheden T, Karlsson C, Brunner A, Van Der Lee J, Hagg R, Tommasini R & Lindahl A. (2004). Gene expression during redifferentiation of human articular chondrocytes. *Osteoarthritis Cartilage* **12,** 525-535.

Tallheden T, van der Lee J, Brantsing C, Mansson JE, Sjogren-Jansson E & Lindahl A. (2005). Human serum for culture of articular chondrocytes. *Cell Transplant* **14,** 469-479.

Tamkun JW, DeSimone DW, Fonda D, Patel RS, Buck C, Horwitz AF & Hynes RO. (1986). Structure of integrin, a glycoprotein involved in the transmembrane linkage between fibronectin and actin. *Cell* **46,** 271-282.

Tan K, Duquette M, Joachimiak A & Lawler J. (2009). The crystal structure of the signature domain of cartilage oligomeric matrix protein: implications for collagen, glycosaminoglycan and integrin binding. *Faseb J* **23,** 2490-2501.

Tattersall A, Meredith D, Furla P, Shen MR, Ellory C & Wilkins R. (2003). Molecular and functional identification of the Na(+)/H(+) exchange isoforms NHE1 and NHE3 in isolated bovine articular chondrocytes. *Cell Physiol Biochem* **13,** 215-222.

Tetlow LC, Adlam DJ & Woolley DE. (2001). Matrix metalloproteinase and proinflammatory cytokine production by chondrocytes of human osteoarthritic cartilage: associations with degenerative changes. *Arthritis Rheum* **44,** 585-594.

Tomar RS, Matta H & Chaudhary PM. (2003). Use of adeno-associated viral vector for delivery of small interfering RNA. *Oncogene* **22,** 5712-5715.

Trickey WR, Vail TP & Guilak F. (2004). The role of the cytoskeleton in the viscoelastic properties of human articular chondrocytes. *J Orthop Res* **22,** 131-139.

Trujillo E, Alvarez de la Rosa D, Mobasheri A, Gonzalez T, Canessa CM & Martin-Vasallo P. (1999). Sodium transport systems in human chondrocytes. II. Expression of NCX, Na+/K+/2Cl- cotransporter and Na+/H+ exchangers in healthy and arthritic chondrocytes. *Histology and histopathology* **14,** 1023-1031.

Tsiakalos AP, Avgoustidis NK & Moutsopoulos HM. (2008). Rituximab therapy in Greek patients with rheumatoid arthritis. *Biologics* **2,** 911-916.

Tsuda M, Takahashi S, Takahashi Y & Asahara H. (2003). Transcriptional co-activators CREB-binding protein and p300 regulate chondrocyte-specific gene expression via association with Sox9. *J Biol Chem* **278,** 27224-27229.

Tufan AC, Satiroglu-Tufan NL, Jackson GC, Semerci CN, Solak S & Yagci B. (2007). Serum or plasma cartilage oligomeric matrix protein concentration as a diagnostic marker in pseudoachondroplasia: differential diagnosis of a family. *Eur J Hum Genet* **15,** 1023-1028.

Turner CE & Burridge K. (1991). Transmembrane molecular assemblies in cell-extracellular matrix interactions. *Current opinion in cell biology* **3,** 849-853.

Tyler JA & Benton HP. (1988). Synthesis of type II collagen is decreased in cartilage cultured with interleukin 1 while the rate of intracellular degradation remains unchanged. *Coll Relat Res* **8,** 393-405.

Ui-Tei K, Naito Y, Takahashi F, Haraguchi T, Ohki-Hamazaki H, Juni A, Ueda R & Saigo K. (2004). Guidelines for the selection of highly effective siRNA sequences for mammalian and chick RNA interference. *Nucleic acids research* **32,** 936-948.

Urban JP. (1994). The chondrocyte: a cell under pressure. *British journal of rheumatology* **33,** 901-908.

Urban JP, Hall AC & Gehl KA. (1993). Regulation of matrix synthesis rates by the ionic and osmotic environment of articular chondrocytes. *J Cell Physiol* **154,** 262-270.

Uusitalo H, Hiltunen A, Ahonen M, Gao TJ, Lefebvre V, Harley V, Kahari VM & Vuorio E. (2001). Accelerated up-regulation of L-Sox5, Sox6, and Sox9 by BMP-2 gene transfer during murine fracture healing. *J Bone Miner Res* **16,** 1837-1845.

Valhmu WB, Stazzone EJ, Bachrach NM, Saed-Nejad F, Fischer SG, Mow VC & Ratcliffe A. (1998). Load-controlled compression of articular cartilage induces a transient stimulation of aggrecan gene expression. *Arch Biochem Biophys* **353,** 29-36.

Valsesia-Wittmann S, Magdeleine M, Dupasquier S, Garin E, Jallas AC, Combaret V, Krause A, Leissner P & Puisieux A. (2004). Oncogenic cooperation between H-Twist and N-Myc overrides failsafe programs in cancer cells. *Cancer Cell* **6,** 625-630.

van der Kraan PM, Buma P, van Kuppevelt T & van den Berg WB. (2002). Interaction of chondrocytes, extracellular matrix and growth factors: relevance for articular cartilage tissue engineering. *Osteoarthritis Cartilage* **10,** 631-637.

Van Inwegen RG, Khandwala A, Gordon R, Sonnino P, Coutts S & Jolly S. (1987). REV 5901: an orally effective peptidoleukotriene antagonist, detailed biochemical/pharmacological profile. *J Pharmacol Exp Ther* **241,** 117-124.

Van Der Windt A, Jahr H, Farrell E, Verhaar J, Weinans H & van Osch G. (2009). Calcineurin inhibitors promote chondrocgenic marker expressive of dedifferentiated human adult chondrocytes via stimulation of TGF-ss1 production. Tissue Eng, ahead of print.

van Rossum DB & Patterson RL. (2009). PKC and PLA2: probing the complexities of the calcium network. *Cell Calcium* **45,** 535-545.

Venezian R, Shenker BJ, Datar S & Leboy PS. (1998). Modulation of chondrocyte proliferation by ascorbic acid and BMP-2. *J Cell Physiol* **174,** 331-341.

Verghese MW, Smith CD & Snyderman R. (1986). Role of guanine nucleotide regulatory protein in polyphosphoinositide degradation and activation of phagocytic leukocytes by chemoattractants. *J Cell Biochem* **32,** 59-69.

Vojtek AB, Taylor J, DeRuiter SL, Yu JY, Figueroa C, Kwok RP & Turner DL. (2003). Akt regulates basic helix-loop-helix transcription factor-coactivator complex formation and activity during neuronal differentiation. *Molecular and cellular biology* **23,** 4417-4427.

Wang H & Kandel RA. (2004). Chondrocytes attach to hyaline or calcified cartilage and bone. *Osteoarthritis Cartilage* **12,** 56-64.

Wang MB & Metzlaff M. (2005). RNA silencing and antiviral defense in plants. *Curr Opin Plant Biol* **8,** 216-222.

Waymouth C. (1974). "Feeding the baby"--designing the culture milieu to enhance cell stability. *Journal of the National Cancer Institute* **53,** 1443-1448.

Wenke AK, Grassel S, Moser M & Bosserhoff AK. (2009). The cartilage-specific transcription factor Sox9 regulates AP-2epsilon expression in chondrocytes. *Febs J* **276,** 2494-2504.

Werb Z, Tremble PM, Behrendtsen O, Crowley E & Damsky CH. (1989). Signal transduction through the fibronectin receptor induces collagenase and stromelysin gene expression. *The Journal of cell biology* **109,** 877-889.

Wilkins RJ, Browning JA & Ellory JC. (2000). Surviving in a matrix: membrane transport in articular chondrocytes. *The Journal of membrane biology* **177,** 95-108.

Williams GR, Robson H & Shalet SM. (1998). Thyroid hormone actions on cartilage and bone: interactions with other hormones at the epiphyseal plate and effects on linear growth. *The Journal of endocrinology* **157,** 391-403.

Woods VL, Jr., Schreck PJ, Gesink DS, Pacheco HO, Amiel D, Akeson WH & Lotz M. (1994). Integrin expression by human articular chondrocytes. *Arthritis Rheum* **37,** 537-544.

Wright M, Jobanputra P, Bavington C, Salter DM & Nuki G. (1996). Effects of intermittent pressure-induced strain on the electrophysiology of cultured human chondrocytes: evidence for the presence of stretch-activated membrane ion channels. *Clin Sci (Lond)* **90,** 61-71.

Wright MO, Nishida K, Bavington C, Godolphin JL, Dunne E, Walmsley S, Jobanputra P, Nuki G & Salter DM. (1997). Hyperpolarisation of cultured human chondrocytes following cyclical pressure-induced strain: evidence of a role for alpha 5 beta 1 integrin as a chondrocyte mechanoreceptor. *J Orthop Res* **15,** 742-747.

Yamazaki N, Browning JA & Wilkins RJ. (2000). Modulation of Na(+) x H(+) exchange by osmotic shock in isolated bovinearticular chondrocytes. *Acta physiologica Scandinavica* **169,** 221-228.

Yarmola EG & Bubb MR. (2004). Effects of profilin and thymosin beta4 on the critical concentration of actin demonstrated in vitro and in cell extracts with a novel direct assay. *J Biol Chem* **279,** 33519-33527.

Yaron I, Meyer FA, Dayer JM, Bleiberg I & Yaron M. (1989). Some recombinant human cytokines stimulate glycosaminoglycan synthesis in human synovial fibroblast cultures and inhibit it in human articular cartilage cultures. *Arthritis Rheum* **32,** 173-180.

Yellowley CE, Jacobs CR & Donahue HJ. (1999). Mechanisms contributing to fluid-flow-induced Ca2+ mobilization in articular chondrocytes. *J Cell Physiol* **180,** 402-408.

Yellowley CE, Jacobs CR, Li Z, Zhou Z & Donahue HJ. (1997). Effects of fluid flow on intracellular calcium in bovine articular chondrocytes. *The American journal of physiology* **273,** C30-36.

Yoo JU, Barthel TS, Nishimura K, Solchaga L, Caplan AI, Goldberg VM & Johnstone B. (1998). The chondrogenic potential of human bone-marrow-derived mesenchymal progenitor cells. *J Bone Joint Surg Am* **80,** 1745-1757.

Yun K & Im SH. (2007). Lef1 regulates COX-2 transcription in chondrocytes. *Biochem Biophys Res Commun* **364,** 270-275.

Zemmyo M, Meharra EJ, Kuhn K, Creighton-Achermann L & Lotz M. (2003). Accelerated, aging-dependent development of osteoarthritis in alpha1 integrin-deficient mice. *Arthritis Rheum* **48,** 2873-2880.

Zhang M, Wang JJ & Chen YJ. (2006). Effects of mechanical pressure on intracellular calcium release channel and cytoskeletal structure in rabbit mandibular condylar chondrocytes. *Life Sci* **78,** 2480-2487.

Zhong J, Eliceiri B, Stupack D, Penta K, Sakamoto G, Quertermous T, Coleman M, Boudreau N & Varner JA. (2003). Neovascularization of ischemic tissues by gene delivery of the extracellular matrix protein Del-1. *J Clin Invest* **112,** 30-41.

Zou H, Wieser R, Massague J & Niswander L. (1997). Distinct roles of type I bone morphogenetic protein receptors in the formation and differentiation of cartilage. *Genes Dev* **11,** 2191-2203.

Zwicky R & Baici A. (2000). Cytoskeletal architecture and cathepsin B trafficking in human articular chondrocytes. *Histochem Cell Biol* **114,** 363-372.